

PROJECT ADMINISTRATION DATA SHEET



ORIGINAL



REVISION NO. _____

Project No. E-21-636GTRI/~~STT~~DATE 6 / 8 / 83Project Director: G. K. Huddleston~~School~~/LabElect. Engr.Sponsor: U. S. Army Missile Command; Redstone Arsenal, AL 35898Type Agreement: Delivery Order No. 0015 under BOA DAAH01-83-D-A013 (OCA File #82)Award Period: From 5/12/83 To 9/30/83 (Performance) 11/30/83 (Reports)

Sponsor Amount:

This ChangeTotal to DateEstimated: \$ 25,080\$ 25,080Funded: \$ 25,080\$ 25,080Cost Sharing Amount: \$ NoneCost Sharing No: N/ATitle: Radome Design and Boresight Error Measurement Simulation

ADMINISTRATIVE DATA

OCA Contact

William F. BrownExt. 4820

1) Sponsor Technical Contact:

2) Sponsor Admin/Contractual Matters:

Dr. M. M. HallumMr. Thomas A. BryantSystems Simulation & Dev. DirectorateOffice of Naval ResearchUS Army Missile CommandRoom 206, O'Keefe Bldg.US Army Missile LaboratoryGeorgia Institute of TechnologyAttn: DRSMI-RDFAtlanta, Georgia 30332Redstone Arsenal, AL 35898Defense Priority Rating: DO-A2Military Security Classification: Unclassified (general
(or) Company/Industrial Proprietary: scope of work)

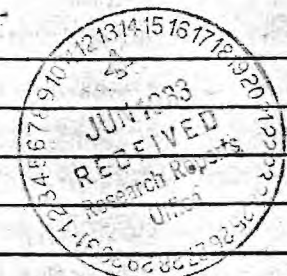
RESTRICTIONS

See Attached Gov't Supplemental Information Sheet for Additional Requirements.

Travel: Foreign travel must have prior approval - Contact OCA in each case. Domestic travel requires sponsor

approval where total will exceed greater of \$500 or 125% of approved proposal budget category. See additional re
strictions on re-budgeting travel funds: (2) C-2 (f) (page 4 of basic agreement)
Equipment: Title vests with (1) B-2 (c) (page 3 of basic agreement)Government; except that items costing less than \$1,000 vest with GIT if prior approval to
purchase is obtained from the Contracting Officer

COMMENTS:



COPIES TO:

Project Director
Research Administrative Network
Research Property Management
AccountingProcurement/EES Supply Services
Research Security Services
Reports Coordinator (OCA)
Research Communications (2)GTRI
Library
Project File
Other I. Newton

SPONSORED PROJECT TERMINATION/CLOSEOUT SHEET

N-B&F
SR410

Date January 4, 1984

Project No. E-21-636

School/~~ECR~~ EE

Includes Subproject No.(s) _____

Project Director(s) Dr. G.K. Huddleston

GTRI / ~~ECR~~

Sponsor U.S. Army Missile Command; Redstone Arsenal, AL

Title Radome Design and Boresight Error Measurement Simulation

Effective Completion Date: 9/30/83 (Performance) 11/30/83 (Reports)

Grant/Contract Closeout Actions Remaining: (Del. Order #0015 under MICOM BOA)

☐ None

☒ Final Invoice or Final Fiscal Report

☐ Closing Documents

☒ Final Report of Inventions

☒ Govt. Property Inventory & Related Certificate

☒ Classified Material Certificate

☐ Other _____

Continues Project No. _____

Continued by Project No. _____

COPIES TO:

Project Director
Research Administrative Network
Research Property Management
Accounting
Procurement/EES Supply Services
Research Security Services
Reports Coordinator (OCA)
Legal Services

Library
GTRI
Research Communications (2)
Project File
Other _____



GEORGIA INSTITUTE OF TECHNOLOGY
SCHOOL OF ELECTRICAL ENGINEERING
ATLANTA, GEORGIA 30332

TELEPHONE: (404) 894- 2948

July 7, 1983

Dr. M. M. Hallum
DRSMI-RDF
Redstone Arsenal, AL., 35898

Subject: Monthly Technical Report on D.O. #0016/BOA
DAAH01-83-D-A013, Georgia Tech Project E21-636,
for the Period 6/1/83 - 6/30/83.

Dear Sir:

The ambient design of a research ablative radome has been completed to the extent needed by the manufacturer to complete the fabrication. Design data has been delivered to Steve Risner (DRSMI-RLA).

Efforts during the next reporting period will be directed to simulation of the boresight error measurement facility to identify and quantify measurement errors.

Approximately 40 man-hours have been expended on this project.

Respectfully submitted,

Gene K. Huddleston
Associate Professor

GKH:sr

cc: Tom Bryant, ONR
OCA (2)
File

GEORGIA INSTITUTE OF TECHNOLOGY

PRINCIPAL INVESTIGATOR G K HUDDLESTON

ACCOUNT NO. E-21-636

STATUS AT END OF MAY 1983

DEPARTMENT ELEC ENG

SPONSOR ARMY DCASR

GRANT/CONTRACT NUMBER *DAAAHD1-83-D-A013/001

RESTRICTED FUND RF-41163

EFFECTIVE DATE 5-12-83

EXPIRATION DATE 6-30-83

	MONTH	FISCAL YEAR	TOTAL CONTRACT
COMPUTER			
BUDGET			679.00
EXPENDED	.00	.00	.00
ENCUMBERED	.00	.00	.00
FREE BALANCE			679.00
OVERHEAD			
BUDGET			8,042.00
EXPENDED	.00	.00	.00
FREE BALANCE			8,042.00
TOTAL			
BUDGET			25,080.00
EXPENDED	.00	.00	.00
ENCUMBERED	.00	.00	.00
FREE BALANCE			25,080.00

RATE OF 47.2 BASE OF 4

PRINCIPAL INVESTIGATOR G K HUDDLESTON

STATUS AT END OF MAY 1983

SPONSOR ARMY DCASR

GRANT/CONTRACT NUMBER *DAAAHD1-83-D-A013/001

EFFECTIVE DATE 5-12-83

ACCOUNT NO. E-21-636

DEPARTMENT ELEC ENG

RESTRICTED FUND RF-41163

EXPIRATION DATE 6-30-83

	MONTH	FISCAL	YEAR	TOTAL CONTRACT
PERSONAL SERVICES				
BUDGET				12,618.00
EXPENDED	.00		.00	.00
ENCUMBERED	.00		.00	.00
FREE BALANCE				12,618.00
FRINGE BENEFITS				
BUDGET				2,650.00
EXPENDED	.00		.00	.00
ENCUMBERED	.00		.00	.00
FREE BALANCE				2,650.00
MATERIALS AND SUPPLIES				
BUDGET				275.00
EXPENDED	.00		.00	.00
ENCUMBERED	.00		.00	.00
FREE BALANCE				275.00
TRAVEL				
BUDGET				816.00
EXPENDED	.00		.00	.00
ENCUMBERED	.00		.00	.00
FREE BALANCE				816.00
TOTAL DIRECT CHARGES				
BUDGET				16,359.00
EXPENDED	.00		.00	.00
ENCUMBERED	.00		.00	.00
FREE BALANCE				16,359.00



GEORGIA INSTITUTE OF TECHNOLOGY
SCHOOL OF ELECTRICAL ENGINEERING
ATLANTA, GEORGIA 30332

TELEPHONE: (404) 894- 2948

August 1, 1983

Dr. M. M. Hallum
DRSMI-RDF
Redstone Arsenal, Alabama, 35898

Subject: Monthly Technical Report on D.O. #0016/BOA
DAAH01-83-D-A013, Georgia Tech Project E21-636,
for the Period 7/1/83 - 7/31/83

Dear Sir:

Computer-aided simulation of the boresight error measurement facility has been done. Technical data and findings have been delivered to Steve Risner (DRSMI-RLA). The data was also discussed during meetings with Ken Letson and yourself on July 18, 1983.

Efforts during the next reporting period will be directed toward the analysis and design of a SCFS radome. Improvements in the boresight error measurement facility will also be addressed.

Radome analysis programs were delivered to Steve Risner on July 18 for use on a VAX computing system.

Approximately 110 man-hours have been expended on this project.

Respectfully submitted,

Gene K. Huddleston
Associate Professor

GKH:sr

GEORGIA INSTITUTE OF TECHNOLOGY

PAGE 03

PRINCIPAL INVESTIGATOR G K HUDDLESTON

ACCOUNT NO. E-21-638

STATUS AT END OF JUNE 1983

DEPARTMENT ELEC ENG

SPONSOR ARMY-DCASR

GRANT/CONTRACT NUMBER *DAAH01-83-D-A013/0015

RESTRICTED FUND RF-41163

EFFECTIVE DATE 5-12-83

EXPIRATION DATE 6-30-83

MONTH FISCAL YEAR TOTAL CONTRACT

PERSONAL SERVICES

BUDGET			12,618.00
EXPENDED	.00	.00	.00
ENCUMBERED	.00	.00	.00
FREE BALANCE			12,618.00

FRINGE BENEFITS

BUDGET			2,650.00
EXPENDED	.00	.00	.00
ENCUMBERED	.00	.00	.00
FREE BALANCE			2,650.00

MATERIALS AND SUPPLIES

BUDGET			275.00
EXPENDED	.00	.00	.00
ENCUMBERED	.00	.00	.00
FREE BALANCE			275.00

TRAVEL

BUDGET			816.00
EXPENDED	.00	.00	.00
ENCUMBERED	.00	.00	.00
FREE BALANCE			816.00

TOTAL DIRECT CHARGES

BUDGET			16,359.00
EXPENDED	.00	.00	.00
ENCUMBERED	.00	.00	.00
FREE BALANCE			16,359.00

GEORGIA INSTITUTE OF TECHNOLOGY

PAGE 01

PRINCIPAL INVESTIGATOR G K HUDDLESTON

ACCOUNT NO. E-21-638

STATUS AT END OF JUNE 1983

DEPARTMENT ELEC ENG

SPONSOR ARMY-DCASR

GRANT/CONTRACT NUMBER *DAAHO1-83-D-A013/0015

RESTRICTED FUND RF-41163

EFFECTIVE DATE 5-12-83

EXPIRATION DATE 6-30-83

	MONTH	FISCAL YEAR	TOTAL CONTRACT
COMPUTER			

BUDGET			679.00
EXPENDED	.00	.00	.00
ENCUMBERED	.00	.00	.00
FREE BALANCE			679.00

OVERHEAD

BUDGET			8,042.00
EXPENDED	.00	.00	.00
FREE BALANCE			8,042.00

RATE OF 47.2 BASE OF 4

TOTAL

BUDGET			25,080.00
EXPENDED	.00	.00	.00
ENCUMBERED	.00	.00	.00
FREE BALANCE			25,080.00



GEORGIA INSTITUTE OF TECHNOLOGY
SCHOOL OF ELECTRICAL ENGINEERING
ATLANTA, GEORGIA 30332

TELEPHONE: (404) 894- 2948

September 7, 1983

Dr. M. M. Hallum
DRSMI-RDF
Redstone Arsenal, AL., 35898

Subject: Monthly Technical Report on D.O. 0015/BOA
DAAH01-83-D-A013, Georgia Tech Project E-21-636,
for the period 8/1/83 - 8/31/83.

Dear Sir:

Efforts during this reporting period have been directed to improving the model used for the antenna in the random analysis, to running additional design data for the ablative radome, and to making modifications on the one-point boresight error computation.

Efforts during the next reporting period will be directed to the design of the SCFS radome.

Expenditures through August 31 should total approximately \$15,888, including travel and computer costs. Approximately 270 man-hours have been expended on this project.

Respectfully,

Gene K. Huddleston,
Associate Professor

GKH:sr

PRINCIPAL INVESTIGATOR G K HUDDLESTON

ACCOUNT NO. E-21-636

STATUS AT END OF JULY 1983

DEPARTMENT ELEC ENG

SPONSOR ARMY-DCASR

GRANT/CONTRACT NUMBER *DAAH01-83-D-A013/0015

RESTRICTED FUND RF-41163

EFFECTIVE DATE 5-12-83

EXPIRATION DATE 9-30-83

PERSONAL SERVICES MONTH FISCAL YEAR TOTAL CONTRACT

BUDGET			12,618.00
EXPENDED	.00	.00	.00
ENCUMBERED	.00	.00	.00
FREE BALANCE			12,618.00

FRINGE BENEFITS

BUDGET			2,650.00
EXPENDED	.00	.00	.00
ENCUMBERED	.00	.00	.00
FREE BALANCE			2,650.00

MATERIALS AND SUPPLIES

BUDGET			275.00
EXPENDED	37.30	37.30	37.30
ENCUMBERED	.00	.00	.00
FREE BALANCE			237.70

TRAVEL

BUDGET			816.00
EXPENDED	.00	.00	.00
ENCUMBERED	460.00	460.00	460.00
FREE BALANCE			356.00

TOTAL DIRECT CHARGES

BUDGET			16,359.00
EXPENDED	37.30	37.30	37.30
ENCUMBERED	460.00	460.00	460.00
FREE BALANCE			15,861.70

PRINCIPAL INVESTIGATOR G K HUDDLESTON

ACCOUNT NO. E-21-838

STATUS AT END OF JULY 1983

DEPARTMENT ELEC ENG

SPONSOR ARMY-DCASR

GRANT/CONTRACT NUMBER *DAAH01-83-D-A013/0015

RESTRICTED FUND RF-41163

EFFECTIVE DATE 5-12-83

EXPIRATION DATE 9-30-83

	MONTH	FISCAL YEAR	TOTAL CONTRACT
COMPUTER			

BUDGET			679.00
EXPENDED	.00	.00	.00
ENCUMBERED	.00	.00	.00
FREE BALANCE			679.00

OVERHEAD

BUDGET			8,042.00	
EXPENDED	18.43	18.43	18.43	RATE OF 49.4 BASE OF 4
ENCUMBERED	227.24	227.24	227.24	
FREE BALANCE			7,796.33	

TOTAL

BUDGET			25,080.00
EXPENDED	55.73	55.73	55.73
ENCUMBERED	687.24	687.24	687.24
FREE BALANCE			24,337.03

GEORGIA INSTITUTE OF TECHNOLOGY

PROJECT EXPENDITURE & BUDGET REPORT

PRINCIPAL INVESTIGATOR G K HUDDLESTON

ACCOUNT NO. E-21-638

TRANSACTIONS FOR JULY 1983

DEPARTMENT ELEC ENG

DESCRIPTION	REQ	S VOUCHER	CODE	ENCUMBRANCES	EXPENDITURES
MATERIALS AND SUPPLIES					
PHOTO LAB CHG 7/83	406	1	175	74350	37.30
TOTAL				.00	37.30
TRAVEL					
G K HUDDLESTON	1	Z		64000	460.00
TOTAL				460.00	.00
OVERHEAD					
TOTAL				227.24	18.43
MONTHLY TOTAL				687.24	55.73



GEORGIA INSTITUTE OF TECHNOLOGY
SCHOOL OF ELECTRICAL ENGINEERING
ATLANTA, GEORGIA 30332

TELEPHONE: (404) 894-2948

October 10, 1983

Dr. M. M. Hallum
DRSMI-RDF
Redstone Arsenal, AL 35898

Subject: Monthly Technical Report on D.O.0015/BOA
DAAH01-83-D-A013, Georgia Tech Project
E21-636, for the period 9/1/83 - 9/30/83.

Dear Sir:

The efforts reported earlier to compile additional design data on the ablative radome and to initiate the design of a SCFS radome have been completed. The results of these efforts were reported to you during my visit with you and others on 28-29 September 1983.

All tasks specified under the statement of work have been completed. A final report is being prepared (draft due 25 October).

Expenditures through September 30 should total approximately \$24,169. This figure includes \$573 for travel expenses and \$509 for computer charges. Approximately 420 man-hours have been expended on this project.

Respectfully,

Gene K. Huddleston
Associate Professor

GKH:sr

GEORGIA INSTITUTE OF TECHNOLOGY

PROJECT EXPENDITURE & BUDGET REPORT

PRINCIPAL INVESTIGATOR G K HUDDLESTON

ACCOUNT NO.

E-21-636

TRANSACTIONS FOR AUGUST 1983

DEPARTMENT

ELEC ENG

DESCRIPTION	REQ	S	VOUCHER	CODE	ENCUMBRANCES	EXPENDITURES
PERSONAL SERVICES						
HUDDLESTON, GENEK				51110		5,844.66
ENCUMBRANCE ADJUSTMNT		P		51110	8,766.99	
MONTHLY PAYROLL		P		51110	-5,844.66	
TOTAL					2,922.33	5,844.66
FRINGE BENEFITS						
AUG 83 SPON BENE			P 999999	52024		1,373.50
TOTAL					.00	1,373.50
TRAVEL						
HUDDLESTON, GENE K	1	O	80105	64010		113.52
HUDDLESTON, GENE K	1	O	80105	64015		117.72
HUDDLESTON, GENE K	1	O	80105	64035		2.33
HUDDLESTON, GENE K	1	O	80105	64000	-460.00	
TOTAL					-460.00	233.57
OVERHEAD						
TOTAL						
TOTAL	RATE OF	49.4%	BASE OF	4	1,216.39	3,681.15
MONTHLY TOTAL					3,678.72	11,132.88

PRINCIPAL INVESTIGATOR G K HUDDLESTON

ACCOUNT NO.

E-21-636

STATUS AT END OF AUGUST 1983

DEPARTMENT

ELEC ENG

SPONSOR ARMY-DCASR

GRANT/CONTRACT NUMBER *DAAHO1-83-D-AO13/OO15

RESTRICTED FUND RF-41163

EFFECTIVE DATE 5-12-83

EXPIRATION DATE 9-30-83

	MONTH	FISCAL YEAR	TOTAL CONTRACT
PERSONAL SERVICES			

BUDGET			12,181.00
EXPENDED	5,844.66	5,844.66	5,844.66
ENCUMBERED	2,922.33	2,922.33	2,922.33
FREE BALANCE			3,414.01

FRINGE BENEFITS

BUDGET			2,862.00
EXPENDED	1,373.50	1,373.50	1,373.50
ENCUMBERED	.00	.00	.00
FREE BALANCE			1,488.50

MATERIALS AND SUPPLIES

BUDGET			275.00
EXPENDED	.00	37.30	37.30
ENCUMBERED	.00	.00	.00
FREE BALANCE			237.70

TRAVEL

BUDGET			816.00
EXPENDED	233.57	233.57	233.57
ENCUMBERED	-460.00	.00	.00
FREE BALANCE			582.43

TOTAL DIRECT CHARGES

BUDGET			16,134.00
EXPENDED	7,451.73	7,489.03	7,489.03
ENCUMBERED	2,462.33	2,922.33	2,922.33
FREE BALANCE			5,722.64

GEORGIA INSTITUTE OF TECHNOLOGY

PAGE 02

PRINCIPAL INVESTIGATOR G K HUDDLESTON

ACCOUNT NO. E-21-636

STATUS AT END OF AUGUST 1983

DEPARTMENT ELEC ENG

SPONSOR ARMY-DCASR

GRANT/CONTRACT NUMBER *DAAH01-83-D-A013/0015

RESTRICTED FUND RF-41163

EFFECTIVE DATE 5-12-83

EXPIRATION DATE 9-30-83

	MONTH	FISCAL YEAR	TOTAL CONTRACT
COMPUTER			

BUDGET			652.00
EXPENDED	.00	.00	.00
ENCUMBERED	.00	.00	.00
FREE BALANCE			652.00

OVERHEAD

BUDGET			8,294.00	
EXPENDED	3,681.15	3,699.58	3,699.58	RATE OF 49.4 BASE OF 4
ENCUMBERED	1,216.39	1,443.63	1,443.63	
FREE BALANCE			3,150.79	

TOTAL

BUDGET			25,080.00
EXPENDED	11,132.88	11,188.61	11,188.61
ENCUMBERED	3,678.72	4,365.96	4,365.96
FREE BALANCE			9,525.43

GEORGIA INSTITUTE OF TECHNOLOGY

PROJECT EXPENDITURE & BUDGET REPORT

PRINCIPAL INVESTIGATOR G K HUDDLESTON

ACCOUNT NO. E-21-636

TRANSACTIONS FOR SEPTEMBER 1983

DEPARTMENT ELEC ENG

DESCRIPTION	REQ	S	VOUCHER	CODE	ENCUMBRANCES	EXPENDITURES
PERSONAL SERVICES						
HUDDLESTON, GENEK				51110		6,336.33
ENCUMBRANCE ADJSTMNT		P		51110	3,414.00	
MONTHLY PAYROLL		P		51110	-6,336.33	
TOTAL					-2,922.33	6,336.33
FRINGE BENEFITS						
SEP 83 SPON BENE		P	999999	52024		1,489.04
TOTAL					.00	1,489.04
TRAVEL						
CORPORATE, TRAVEL	2	O	95431	64025		172.00
CORPORATE, TRAVEL	2	O	95431	64000	-172.00	
G K HUDDLESTON	2	Z		64000	415.00	
TOTAL					243.00	172.00
COMPUTER						
CYBER COMP 9-83		I	1024	76020		440.55
TOTAL					.00	440.55
OVERHEAD						
TOTAL					-1,323.59	4,168.33
MONTHLY TOTAL					-4,002.92	12,606.25

RATE OF 49.4% BASE OF 4

GEORGIA INSTITUTE OF TECHNOLOGY

PRINCIPAL INVESTIGATOR G K HUDDLESTON

ACCOUNT NO. E-21-638

STATUS AT END OF SEPTEMBER 1983

DEPARTMENT ELEC ENG

SPONSOR ARMY-DCASR

GRANT/CONTRACT NUMBER *DAAH01-83-D-A013/0015

RESTRICTED FUND RF-41163

EFFECTIVE DATE 5-12-83

EXPIRATION DATE 9-30-83

	MONTH	FISCAL YEAR	TOTAL CONTRACT
PERSONAL SERVICES			
BUDGET			12,181.00
EXPENDED	6,336.33	12,180.99	12,180.99
ENCUMBERED	-2,922.33	.00	.00
FREE BALANCE			.01
FRINGE BENEFITS			
BUDGET			2,862.00
EXPENDED	1,489.04	2,862.54	2,862.54
ENCUMBERED	.00	.00	.00
FREE BALANCE			-.54
MATERIALS AND SUPPLIES			
BUDGET			275.00
EXPENDED	.00	37.30	37.30
ENCUMBERED	.00	.00	.00
FREE BALANCE			237.70
TRAVEL			
BUDGET			816.00
EXPENDED	172.00	405.57	405.57
ENCUMBERED	243.00	243.00	243.00
FREE BALANCE			167.43
TOTAL DIRECT CHARGES			
BUDGET			16,134.00
EXPENDED	7,997.37	15,486.40	15,486.40
ENCUMBERED	-2,679.33	243.00	243.00
FREE BALANCE			404.60

GEORGIA INSTITUTE OF TECHNOLOGY

PRINCIPAL INVESTIGATOR G K HUDDLESTON

ACCOUNT NO. E-21-636

STATUS AT END OF SEPTEMBER 1983

DEPARTMENT ELEC ENG

SPONSOR ARMY-DCASR

GRANT/CONTRACT NUMBER *DAAH01-83-D-A013/0015

RESTRICTED FUND RF-41163

EFFECTIVE DATE 5-12-83

EXPIRATION DATE 9-30-83

COMPUTER MONTH FISCAL YEAR TOTAL CONTRACT

BUDGET			652.00
EXPENDED	440.55	440.55	440.55
ENCUMBERED	.00	.00	.00
FREE BALANCE			211.45

OVERHEAD

BUDGET			8,294.00	
EXPENDED	4,168.33	7,867.91	7,867.91	RATE OF 49.4 BASE OF 4
ENCUMBERED	-1,323.59	120.04	120.04	
FREE BALANCE			306.05	

TOTAL

BUDGET			25,080.00	
EXPENDED	12,606.25	23,794.86	23,794.86	THIS ACCOUNT IS 96.3 EXPENDED
ENCUMBERED	-4,002.92	363.04	363.04	
FREE BALANCE			922.10	

PRINCIPAL INVESTIGATOR G K HUDDLESTON

ACCOUNT NO.

E-21-638

TRANSACTIONS FOR		DECEMBER 1983	
1	12/1/83	12/1/83	12/1/83
2	12/2/83	12/2/83	12/2/83
3	12/3/83	12/3/83	12/3/83
4	12/4/83	12/4/83	12/4/83
5	12/5/83	12/5/83	12/5/83
6	12/6/83	12/6/83	12/6/83
7	12/7/83	12/7/83	12/7/83
8	12/8/83	12/8/83	12/8/83
9	12/9/83	12/9/83	12/9/83
10	12/10/83	12/10/83	12/10/83
11	12/11/83	12/11/83	12/11/83
12	12/12/83	12/12/83	12/12/83
13	12/13/83	12/13/83	12/13/83
14	12/14/83	12/14/83	12/14/83
15	12/15/83	12/15/83	12/15/83
16	12/16/83	12/16/83	12/16/83
17	12/17/83	12/17/83	12/17/83
18	12/18/83	12/18/83	12/18/83
19	12/19/83	12/19/83	12/19/83
20	12/20/83	12/20/83	12/20/83
21	12/21/83	12/21/83	12/21/83
22	12/22/83	12/22/83	12/22/83
23	12/23/83	12/23/83	12/23/83
24	12/24/83	12/24/83	12/24/83
25	12/25/83	12/25/83	12/25/83
26	12/26/83	12/26/83	12/26/83
27	12/27/83	12/27/83	12/27/83
28	12/28/83	12/28/83	12/28/83
29	12/29/83	12/29/83	12/29/83
30	12/30/83	12/30/83	12/30/83
31	12/31/83	12/31/83	12/31/83

DEPARTMENT

ELEC ENG

DESCRIPTION

REQ**S. VOUCHER****CODE**

ENCUMBRANCES

EXPENDITURES

MATERIALS AND SUPPLIES

PHOTO LAB CHG 12/83

3314

I

2530

74350

158.40

TOTAL

.00

158.40

OVERHEAD

TOTAL**RATE OF**

49.4%

BASE OF 4

:00

78.25

MONTHLY

TOTAL

.00

236.65

PRINCIPAL INVESTIGATOR G K HUDDLESTON

ACCOUNT NO. E-21-826

STATUS AT END OF DECEMBER 1983

DEPARTMENT ELEC ENG

SPONSOR ARMY-DCASR

GRANT/CONTRACT NUMBER *DAAH01-83-D-A013/0015

RESTRICTED FUND RF-41163

EFFECTIVE DATE 5-12-83

EXPIRATION DATE 9-30-83

	MONTH	FISCAL YEAR	TOTAL CONTRACT
--	-------	-------------	----------------

PERSONAL SERVICES

BUDGET			12,181.00
EXPENDED	.00	12,180.99	12,180.99
ENCUMBERED	.00	.00	.00
FREE BALANCE			.01

FRINGE BENEFITS

BUDGET			2,862.00
EXPENDED	.00	2,862.54	2,862.54
ENCUMBERED	.00	.00	.00
FREE BALANCE			-.54

MATERIALS AND SUPPLIES

BUDGET			275.00
EXPENDED	158.40	211.74	211.74
ENCUMBERED	.00	.00	.00
FREE BALANCE			63.26

TRAVEL

BUDGET			816.00
EXPENDED	.00	585.23	585.23
ENCUMBERED	.00	.00	.00
FREE BALANCE			230.77

TOTAL DIRECT CHARGES

BUDGET			16,134.00
EXPENDED	158.40	15,840.50	15,840.50
ENCUMBERED	.00	.00	.00
FREE BALANCE			293.50

PRINCIPAL INVESTIGATOR G K HUDDLESTON

ACCOUNT NO. E-21-836

STATUS AT END OF DECEMBER 1983

DEPARTMENT ELEC ENG

SPONSOR ARMY-DCASR

GRANT/CONTRACT NUMBER *DAAH01-83-D-A013/0015

RESTRICTED FUND RF-41183

EFFECTIVE DATE 5-12-83

EXPIRATION DATE 9-30-83

COMPUTER MONTH FISCAL YEAR TOTAL CONTRACT

BUDGET			852.00
EXPENDED	.00	509.45	509.45
ENCUMBERED	.00	.00	.00
FREE BALANCE			142.55

OVERHEAD

BUDGET			8,294.00	
EXPENDED	78.25	8,076.87	8,076.87	RATE OF 49.4 BASE OF 4
ENCUMBERED	.00	.00	.00	
FREE BALANCE			217.13	

TOTAL

BUDGET			25,080.00	
EXPENDED	236.65	24,426.82	24,426.82	THIS ACCOUNT IS 97.4 EXPENDED
ENCUMBERED	.00	.00	.00	
FREE BALANCE			653.18	



GEORGIA INSTITUTE OF TECHNOLOGY
SCHOOL OF ELECTRICAL ENGINEERING
ATLANTA, GEORGIA 30332

TELEPHONE: (404) 894-2948

October 26, 1983

Dr. M. M. Hallum
DRSMI-RDF
Redstone Arsenal, AL 35898

Subject: Draft Final Report on D.O. 0015/BOA
DAAH01-83-D-A-013, Georgia Tech Project E-21-636,
Covering the Period 5/12/83 through 9/30/83

Dear Sir:

Enclosed please find two (2) copies of the subject report for your review and approval.

The final report is due on 30 November 1983.

Sincerely,

Gene K. Huddleston
Associate Professor

GKH:sr

Encls (as stated)

**RADOME DESIGN AND
BORESIGHT ERROR MEASUREMENT SIMULATION**

Final Technical Report on Project E-21-636

By

Gene K. Huddleston
School of Electrical Engineering
Georgia Institute of Technology
Atlanta, Georgia 30332

For

M. M. Hallum
U.S. Army Missile Command
DRSMI-RDF
Redstone Arsenal, AL 35898

Under

Delivery Order 0015

DAAH01-83-D-A013

November 1983

FOREWORD

This report was prepared by the School of Electrical Engineering, Georgia Institute of Technology, Atlanta, Georgia, under Delivery Order 0015 of BOA DAH001-83-D-A013. The report author is Gene K. Huddleston, Associate Professor, School of Electrical Engineering.

The work was performed for the U.S. Army Missile Command under the direction of M. M. Hallum (DRSMI-RDF), K. N. Letson (-RLA), and Steven P. Risner (-RLA).

This report was submitted on November 30, 1983.

The views, opinions, and/or findings contained in this report are those of the author and should not be construed as an official Department of the Army position, policy, or decision, unless so designated by other documentation.

TABLE OF CONTENTS

	<u>Page</u>
FOREWORD	i
1. INTRODUCTION AND SUMMARY.....	1
2. ABLATIVE AND CERAMIC RADOME DESIGN.....	3
2.1 Introduction.....	3
2.2 Flat Panel Analysis.....	5
2.3 Ablative Radome Analysis for Uniform Wall Thickness.....	6
2.4 Ablative Radome with Tapered Wall Thickness.....	6
2.5 Fused Silica Radome Design.....	8
3. BORESIGHT ERROR MEASUREMENT SIMULATION.....	9
3.1 Introduction.....	9
3.2 BSE Algorithms.....	11
3.3 Effects of Distance.....	14
3.4 Effects of Reflections.....	16
3.5 Effects of Frequency.....	16
4. CONCLUSIONS AND RECOMMENDATIONS.....	17
4.1 Ablative and Ceramic Radomes.....	17
4.2 BSE Measurement Simulation.....	17
REFERENCES.....	19
APPENDIX A - FLAT PANEL ANALYSIS RESULTS.....	21
APPENDIX B - UNIFORM ABLATIVE RADOME PERFORMANCE.....	29
APPENDIX C - TAPERED ABLATIVE RADOME PERFORMANCE.....	37
APPENDIX D - TAPERED SUBSTRATE RADOME PERFORMANCE.....	45
APPENDIX E - FUSED SILICA RADOME PERFORMANCE.....	53
APPENDIX F - EFFECTS OF DISTANCE ON BSE ALGORITHMS.....	61
APPENDIX G - EFFECTS ON REFLECTIONS ON BSE ALGORITHMS.....	69
APPENDIX H - EFFECTS OF FREQUENCY ON BSE ALGORITHMS.....	77

CHAPTER 1

INTRODUCTION AND SUMMARY

This report describes the electrical design of an ablative and a ceramic radome for a supersonic microwave seeker application. In addition, the results of a computer simulation of the effects of the anechoic chamber environment on boresight error measurements are presented.

Chapter 2 describes the electrical design of tangent ogive ($L/D = 3$) ablative radome consisting of a load-bearing substrate material ($\epsilon_r = 4.50$, $\tan\delta = .008$) and a fibre-loaded Teflon ablator outer layer ($\epsilon_r = 2.45$, $\tan\delta = .003$). The computed electrical performance of both flat dielectric panels and full scale radomes indicate that the optimum ablative radome design with respect to boresight error slope consists of a thick substrate and a thin ablator. The best performance would be obtained with a half-wave wall of the single substrate material; the optimum two-layer structure is a compromise between the half-wave wall and the ablation requirements.

Boresight error slopes (BSES) less than 5% and radome transmission loss less than 0.6 dB are predicted for the optimum ablative radome configuration consisting of .600" substrate and .060" (uniform) ablator thicknesses. To provide for ablation during flight so as to reach this optimum design at the terminal phase, a tapered ablator (.110" at the tip and .070" at the base of the radome) can be provided having initial BSES < 11% and loss less than 0.6 dB. Hence, a .05" tapered change in ablator thickness results in a change in maximum BSES from 11% to 5%.

The design of a comparable fused silica radome is also described in Chapter 2. Designs having uniform wall thickness and an asymmetrical wall thickness design are examined. The ceramic radome design work is not complete.

Chapter 3 describes the results of a computer simulation of a radome boresight error measurement facility. The simulation quantifies the effects of reflections from the anechoic chamber boundaries, the effects of frequency drifts during measurement, and the effects of separation distance between the source antenna and the radome/antenna combination under test (RAUT).

Measurement results are simulated for three BSE measurement techniques: null seeker, offset 1-point method, and a two-point method. All three methods are more sensitive to the distance of separation than to reflections. The two-point method gives approximately the same results as the null seeker. All three methods show significant sensitivity to even small (1%) frequency changes.

The simulation results also show that the offset 1-point method of BSE measurement yields widely varying results and is deemed unsuitable for use. A modified (non-offset) 1-point method of measurement does yield results comparable to the null seeker for large separation distance and no reflections; however, the performance of the modified 1-point method has not been fully studied.

CHAPTER 2

ABLATIVE AND CERAMIC RADOME DESIGN

2.1 Introduction

The geometry of the optimum ablative radome design is shown in Figure 2-1. The placement of the antenna, and its radiating characteristics, are also indicated. A metal rain cap is located at a distance of 45.42" from the radome base as indicated by the large tic mark extending above the horizontal axis. The location of the bulkhead is indicated by the other vertical tic mark at 5.32".

Several design constraints were imposed:

(1) The outer shape of the radome was specified as a tangent ogive with base diameter $D_{OS} = 16.00"$ and radius of curvature $R_{OS} = 148.03"$.

(2) The radome wall thickness could not exceed 0.75" lest the antenna would not gimbal.

(3) The minimum substrate thickness was 0.35" for structural rigidity and strength.

(4) The minimum ablator thickness must be compatible with expected ablation during flight ($\sim 0.045"$ maximum) and manufacturing techniques.

The ablative radome design of Figure 2-1 was arrived at by examining the plane wave transmission properties of several two-layer flat panel designs. From these data, the basic two-layer radome wall design was selected for further refinement using a three-dimensional computer-aided radome analysis [1]. The radome design parameters consisted of substrate and ablator thicknesses at a single frequency. The designs were compared on the basis of boresight error slope (BSES), assuming reasonable (< 1.0 dB) transmission loss. The effects of tapered ablator thickness were also studied.

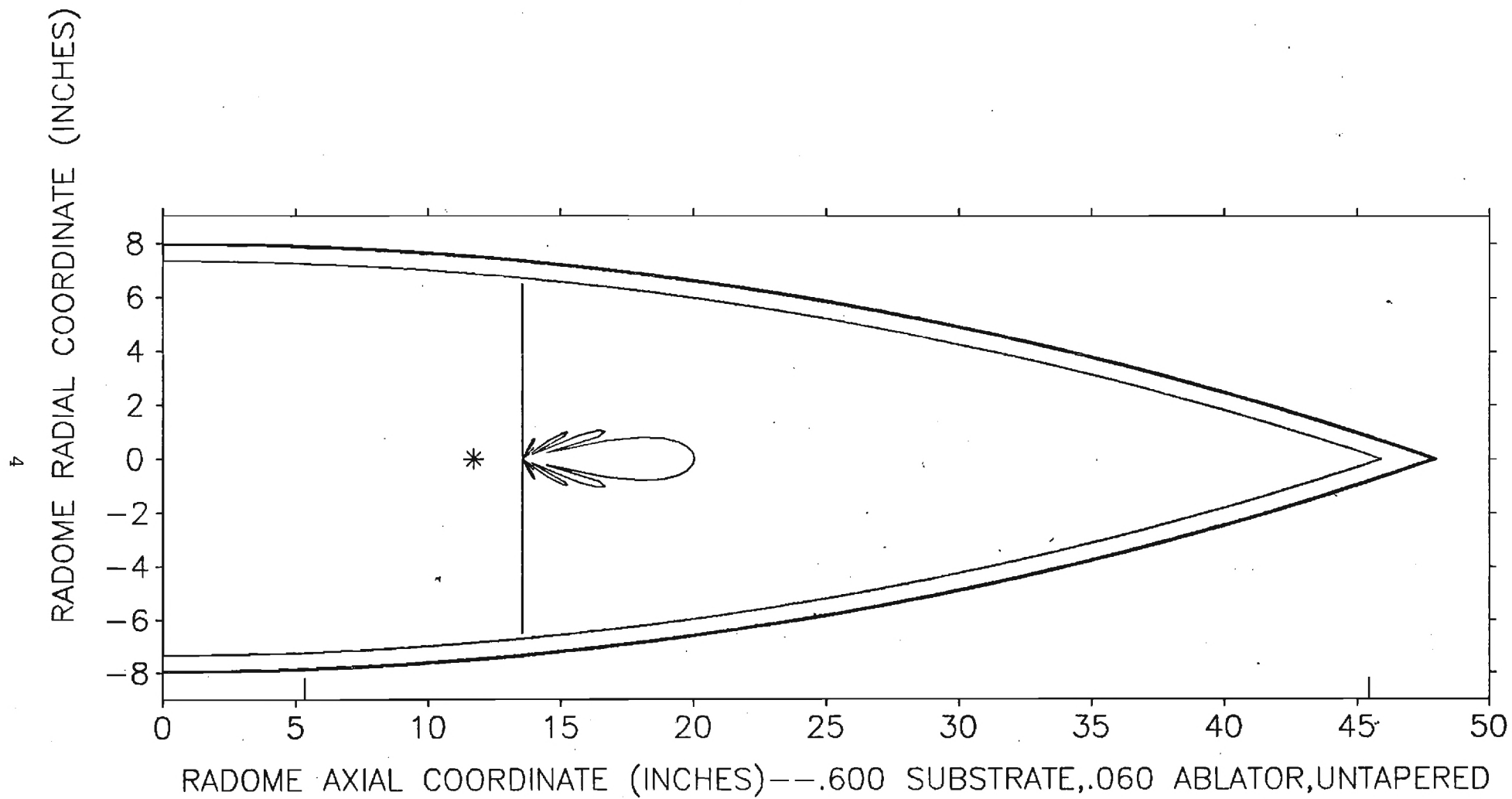


Figure 2-1. Ablative Radome Geometry.

Preliminary performance data for three fused silica radome designs are present in the last section.

2.2 Flat Panel Analysis

The plane wave transmission properties of the two-layer flat panels are shown in Appendix A. Substrate ($\epsilon_r = 4.50$, $\tan\delta = .008$) thicknesses range from 0.25" to 0.600". The ablator thicknesses are shown in each legend. The lefthand ordinate (goes with upper set of curves) is power transmittance for perpendicular polarization (always worse than for the incident electric-field parallel to the plane of incidence). The abscissa is angle of incidence. The righthand ordinate (lower set of curves) is delta insertion phase delay; i.e., $\Delta_{IPD} = IPD_{\perp} - IPD_{\parallel}$.

The flat panel design criteria used were: (1) transmittance greater than 80% over the range of incidence angles expected in the radome; (2) $\Delta_{IPD} \approx 0$ over the same range.

For the tangent ogive shape of Figure 2-1, the largest incidence angle encountered is approximately 72° as determined by drawing a ray normal to the center of the aperture antenna to the tip of the radome. The angle between the ray and the normal to the inner wall is the incidence angle. The lowest angle of incidence is determined by gimbaling the aperture to the expected limit and measuring the normal ray incidence angle on the radome wall. This approximate estimating procedure yields a range of $30^\circ < \theta_i < 72^\circ$.

Examination of the data in Appendix A shows that the thicker substrate designs yield better transmittance and Δ_{IPD} performance. The performance would be best for a 1/2-wave wall of substrate only (.622" @ $\theta_D = 72^\circ$). But it is not possible to conclude from the flat panel results if the 0.550" substrate design will yield better radome BSES performance than the 0.600" substrate design; hence, the need for the following 3-D radome analysis.

2.3 Ablative Radome Analysis for Uniform Wall Thickness

The computed radome performance for five combinations of substrate and ablator thicknesses are shown in Appendix B. Data for both pitch and yaw planes are shown. The ordinates of interest are boresight error slope (BSES), boresight error (BSE), and gain. The abscissa in every case is radome gimbal angle. The legend identifies the five different designs.

Examination of the data in Appendix B clearly reveals that the optimum ablative radome design has a substrate thickness of 0.600" and ablator thickness of 0.060".

2.4 Ablative Radome with Tapered Wall Thickness

The computed performance of six ablative radome designs having tapered wall thickness are presented in Appendix C. The optimum design (designated hereafter as Design 1) is also shown as the standard of comparison. The performance of a over-dimensioned prototype design (Design 0) from which the optimum design and any tapered designs will be machined is also shown.

The tapered designs considered are further identified in Table 2-1. The thickness taper is linear with respect to the axial radome coordinate. The first thickness given in the table is the thickness in the layer at the base of the radome; the second thickness is the thickness of the layer at the tip. Only one thickness is given for the uniform thickness. Table 2-1 also identifies the three fused silica radome designs to be discussed later.

The ablator of Design 6 is tapered to be thicker at the tip as anticipated at the initial point of flight. Design A shows the performance at a later time in flight -- and approaches the optimum design performance (Design 1). Design D shows what happens to the performance if the ablator thickness erodes to zero at the tip.

TABLE 2-1. Identification of Radome Designs

Design No.	Base Diameter	THICKNESS		Remarks
		Substrate Base/Tip	Ablator Base/Tip	
0	16.10	.690	.110	First Delivered Prototype
1	16.00	.600	.060	Optimum Design
6	16.02	.600	.070/.110	Tapered Ablator
A	16.004	.600	.062/.070	Tapered Ablator
D	16.00	.600	.060/.000	Tapered Ablator
E	16.00	.600/.620	.060/.000	Tapered Ablator & Substrate
F	16.00	.600/.640	.060/.000	Tapered Ablator & Substrate
G	16.00	.600/.660	.060/.000	Tapered Ablator & Substrate

H	16.00	.730	0.	Fused Silica Blank
I	16.00	.710	0.	Thinner Wall
J	16.00	Tailored	0.	Tailored SiO ₂

Appendix D shows the effects on radome performance caused by tapering the substrate material for the case where the ablator has eroded to zero thickness at the tip. Designs 1 and D are shown for reference. These data merely show that substrate thickness taper can also be used as a degree of freedom in the design process.

2.5 Fused Silica Radome Design

Computed performance data for three fused silica radome designs are shown in Appendix E. Ablative Designs 0 and 1 are also shown for reference.

Design H is the fused silica "blank" as received from the manufacturer. It would be rough machined to a wall thickness of $0.73" \pm .010"$. Its performance is closer to the optimum ablator performance than the other two SiO_2 designs.

Making the SiO_2 wall thickness thinner (Design I) does not help.

An asymmetrical wall thickness prescription (Design J) does not help the performance of the fused silica radome, where the average wall thickness is approximately $0.67"$.

The design of the fused silica radome is not complete.

CHAPTER 3

BORESIGHT ERROR MEASUREMENT SIMULATION

3.1 Introduction

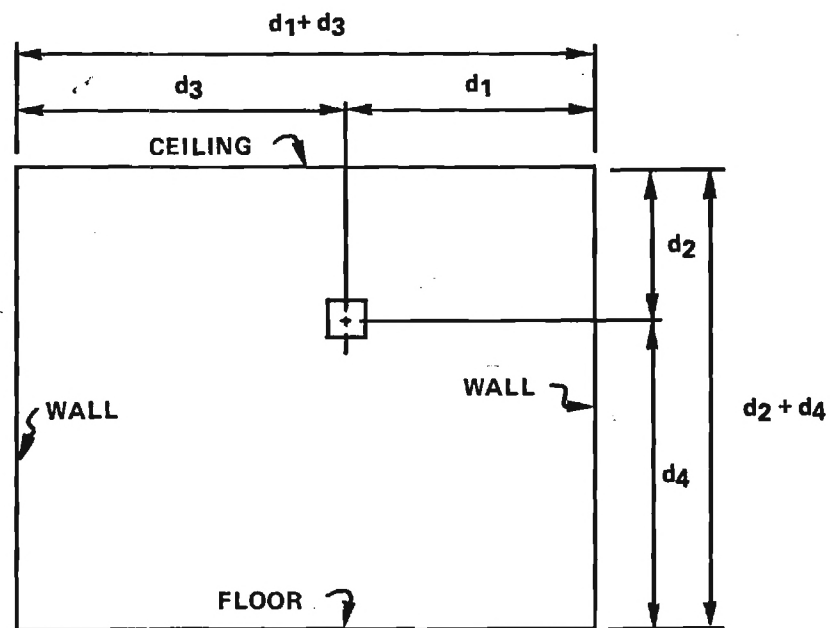
A computer-aided simulation of the boresight error measurement procedure and facility was carried out to quantify the effects of separation distance, wave reflections from anechoic chamber boundaries, and frequency drifts.

The 3-D radome analysis program used earlier to design the ablative and ceramic radomes was modified to include the near-field and reflection effects as illustrated in Figure 3-1(b). Waves emanate from the source antenna in the directions indicated by the rays (one arrowhead). These direct rays impinge on the radome as shown. Note that the angles of incidence on the radome wall for these rays are different than those of a true plane wave (horizontal rays).

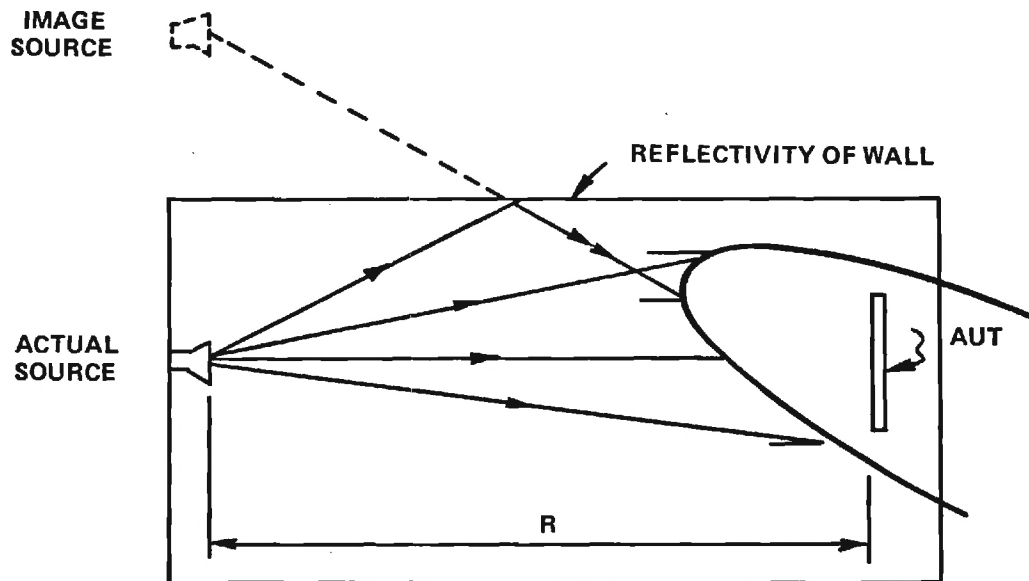
Some of the rays emanating from the source antenna strike the walls, floor, and ceiling of the chamber and are reflected onto the radome. These reflections can be conveniently included using image sources, one for each boundary of the chamber (4 total). Each image is mirrored into the associated boundary and is given strength E' with respect to the actual source strength E_0 according to

$$\frac{E'}{E_0} = 10^{(-R_{dB}/20.)} \quad (3-1)$$

where R_{dB} is the reflectivity of the chamber wall in decibels. The reflectivity is assumed to be independent of incidence angle.



(a) VIEW OF SOURCE ANTENNA AT FAR END OF CHAMBER.



(b) TOP VIEW OF CHAMBER SHOWING ONE IMAGE SOURCE.

FIGURE 3 - 1

GEOMETRY OF BORESIGHT ERROR
MEASUREMENT SIMULATION.

3.2 BSE Algorithms

Three BSE measurement procedures or algorithms were simulated: null seeker, offset 1-point method, and 2-point method. In the null seeker method, the computation is done such that the source is moved around until nulls are obtained in each Δ/ϵ signal channel of the monopulse antenna. The direction to the source when it is in the null position is defined as the boresight error.

Figure 3-2 shows tracking functions computed for the radome/antenna combination under test (RAUT), where the tracking functions in elevation and azimuth are defined by

$$f_{EL} \triangleq \text{Im} \left\{ \frac{\Delta_{EL}}{\sum} \right\} \quad (3-2a)$$

$$f_{AZ} \triangleq \text{Im} \left\{ \frac{\Delta_{AZ}}{\sum} \right\} \quad (3-2b)$$

Four computed tracking functions are shown in Figure 3-2 as indicated on each graph. The tracking functions are graphed versus the angle θ from boresight in a diagonal plane defined by $x_A = y_A$ in antenna coordinates. Without the radome, f_{EL} and f_{AZ} are almost identical so that only one solid graph is shown for both functions. When the radome is placed over the antenna and aligned with the true antenna boresight (Pitch = 0° , Yaw = 0°), the tracking functions are slightly different as indicated by the $AZ(0^\circ, 0^\circ)$ and $EL(0^\circ, 0^\circ)$ graphs. Note also that the slopes of these functions (monopulse error slope MES) are different but are approximately equal to the MES of the antenna without the radome. Finally, the offset dash graph $EL(6^\circ, 0^\circ)$ of Figure 3-2 shows the elevation tracking function when the radome is pitched up by 6° ; f_{AZ} is essentially the same as for the $(0^\circ, 0^\circ)$ case.

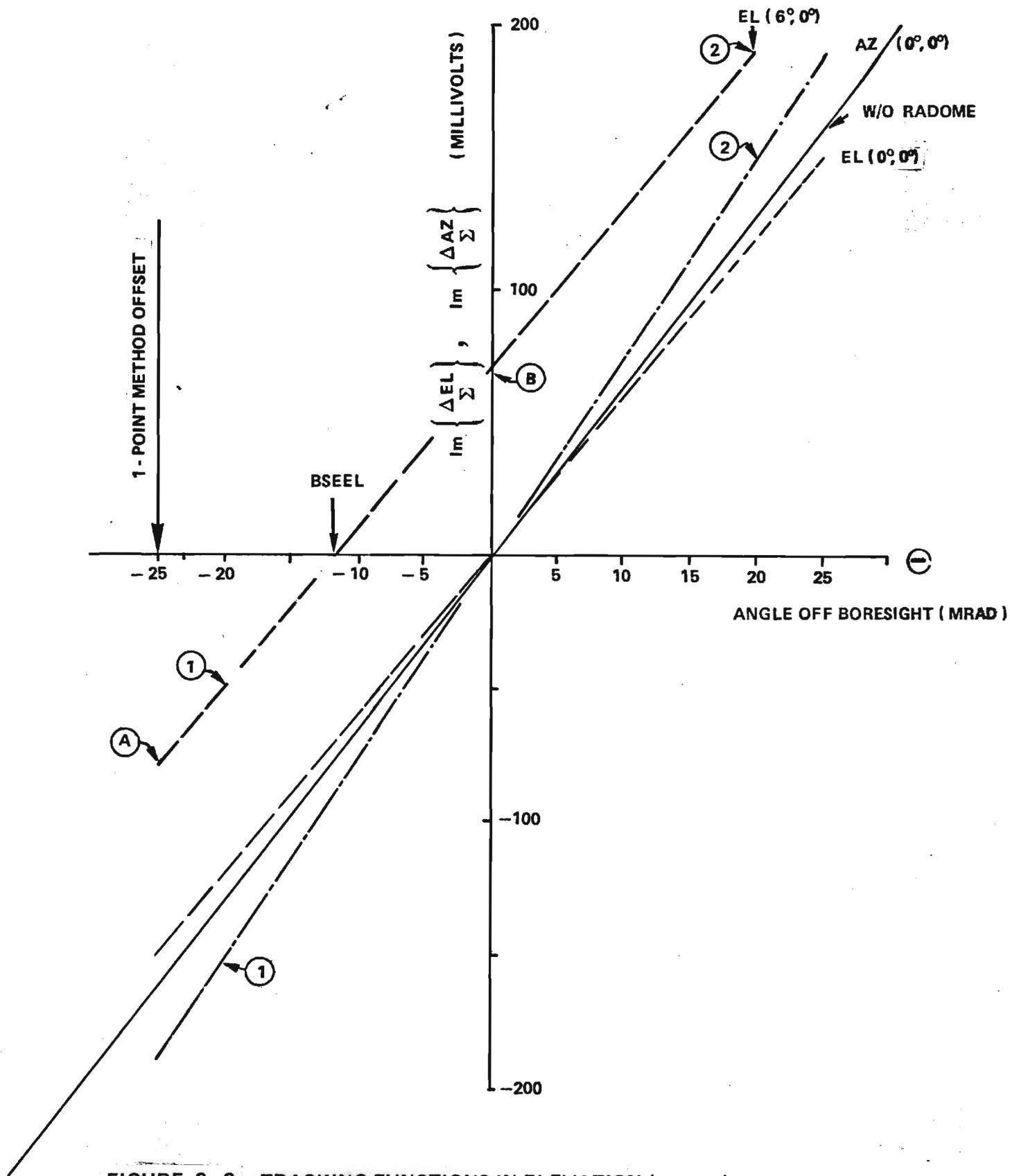


FIGURE 3 - 2. TRACKING FUNCTIONS IN ELEVATION (- - -) AND AZIMUTH (- . -) PLANES WITH AND WITHOUT (—) RADOME FOR (0.,0.) ORIENTATION.

The BSE algorithms can be explained using the $EL(6^\circ, 0^\circ)$ graph of Figure 3-2. The null seeker algorithm finds the zero-crossing of the tracking functions f_{EL} and f_{AZ} : $f_{EL} = 0$ at -11.5 mrad; $f_{AZ} = 0$ at 0 mrad in Figure 3-2. The 2-point method uses the values of each tracking function computed at only two points at ± 20 mrad to generate a linear estimate of each tracking function, and, hence, an estimate of where the zero crossings occur.

The offset 1-point method uses the value of each tracking function as measured at the angle-off-boresight of -25 mrad. This single value (Point A in Figure 3-2), combined with the MES yields the following linear tracking model

$$f_{EL} = MES_{EL} \theta_{EL} + B_{EL} \quad (3-3)$$

where the ordinate intercept B_{EL} is given in terms of the measured tracking function at the known angle $\theta = -25$ mrad by

$$B_{EL} = f_{EL}(\theta - 25 \text{ mrad}) - MES_{EL}(-25 \text{ mrad}) \quad (3-4)$$

The zero-crossing, or BSE_{EL} , is then obtained by setting Eqn. (3-3) equal to zero and solving for θ_{EL} ; i.e.,

$$\theta_{EL} = \frac{f_{EL}(\theta - 25 \text{ mrad})}{MES_{EL}} = BSE_{EL} \quad (3-4)$$

A similar treatment holds for the azimuth tracking function.

The on-axis 1-point method of BSE measurement or computation uses the single value of the tracking function obtained when the target (source) is located on the true boresight of the antenna. The value of f_{EL} is indicated by Point B in Figure 3-2. The boresight error is then given by Eqn. (3-4).

In both 1-point methods, the monopulse error slope that should correctly be used is the slope of the tracking function for that particular radome orientation. In practice, the true slope is not used; instead, the MES of the antenna without the radome is used in Eqn. (3-4). The significance of this source of error is investigated in the following presentation of the BSE measurement simulation.

A comparison of the results obtained in the simulation of the three BSE algorithms is shown in Figure 3-3 for scan of the radome in the pitch plane. A true plane wave (source at $R = \infty$) was incident on the radome, and no reflections from the chamber boundaries were allowed ($R_{dB} > 100$ dB). The graphs show excellent agreement between the null seeker and 2-point methods. Discrepancies are noted for the 1-point method. In what follows, the null seeker results for $R = \infty$ and no reflections are considered to be the true data.

3.3 Effects of Distance

The effects of the distance R of separation between the source antenna and the monopulse seeker AUT are presented in Appendix F for each BSE algorithm. Distances of $R = 20'$, $30'$, $40'$, and $R = \infty$ are used. No reflections are included.

The simulation results of Appendix F indicate that the distance of separation is a significant source of error in BSE measurements. For example, for a 20' separation, a maximum error of 5 mrad is observed using the null seeker or 2-point method. Oscillatory errors are observed using the offset 1-point method. The errors in gain (radome loss) are minor for all three methods.

The antenna used in the simulation has a value of $D^2/\lambda = 71.6$. The 20' separation corresponds to $3.35 D^2/\lambda$. The radome value of $L_1^2/\lambda = 558$ yields only $0.43 L_1^2/\lambda$ for the 20' separation. (The radome length L_1 used is the radome length from the gimbal point to the tip.) These considerations indi-

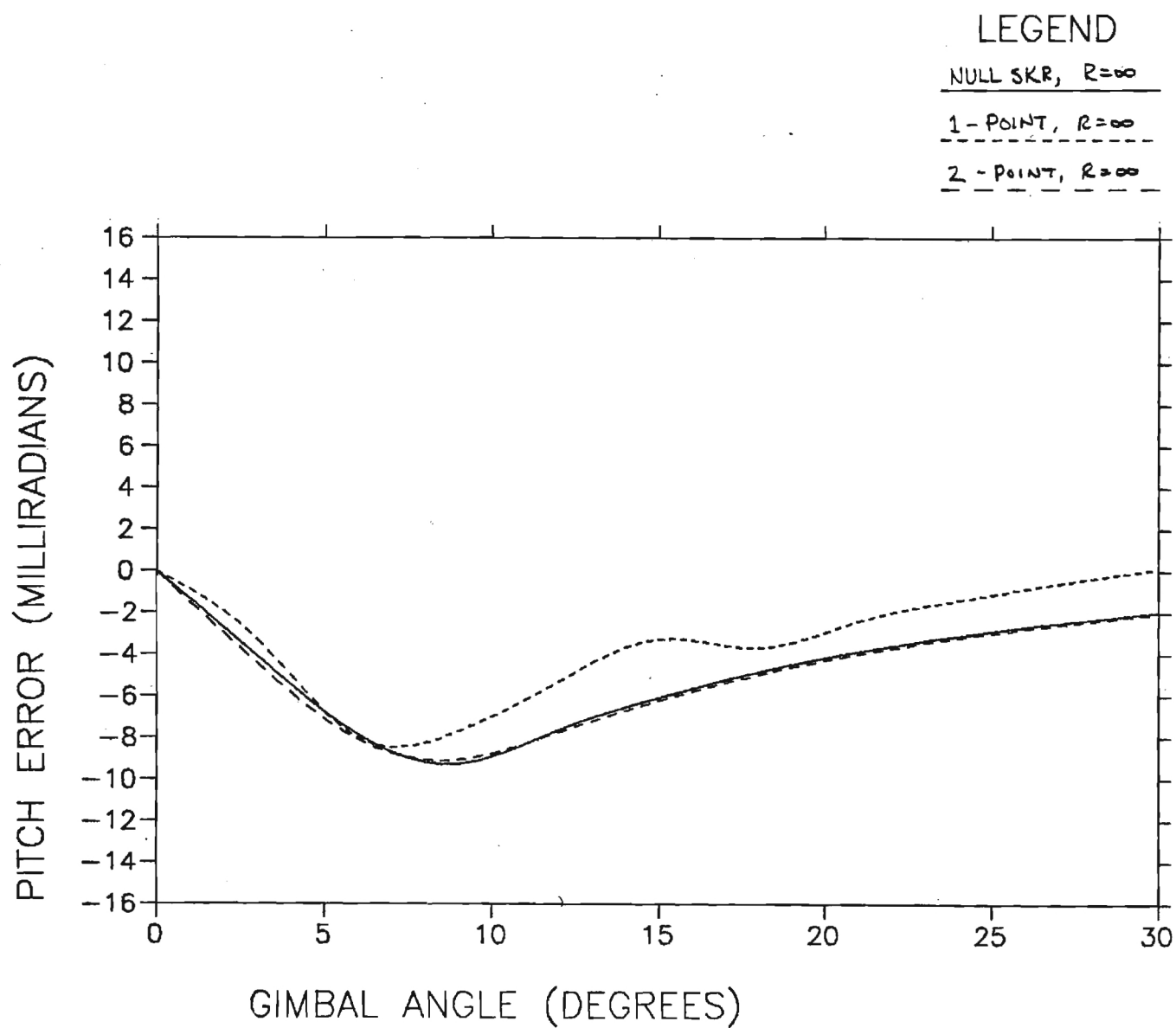


Figure 3-3. Comparisons of Boresight Errors Computed Using Three Different Algorithms.

cate that any rules of thumb for separation distance in BSE measurements should utilize radome length rather than antenna diameter.

3.4 Effects of Reflections

The effects of wave reflections from the anechoic chamber walls, floor, and ceiling are presented in graphical form in Appendix G. Only the 20' separation distance was considered since it corresponds roughly to the length of the chamber of interest. Chamber reflectivities of 20 dB, 30 dB, and 100 dB were considered.

The BSE data in Appendix G shows that the 2-point method is least sensitive to reflections, and that the offset 1-point method is the most sensitive. And in some instances the reflections tend to compensate for the 20' separation distance!

The gain data in Appendix F shows that chamber reflections have a significant effect on this parameter.

3.5 Effects of Frequency

The simulation was performed to determine the effects of small ($\pm 1\%$) frequency drifts on measured BSE for the case of $R = 30'$ separation and reflectivity of 30 dB. The computed results are presented in Appendix H for all three BSE algorithms.

The data in Appendix H show that small frequency drifts are a significant source of error in BSE measurements. Therefore, frequency-stabilized (phase locked) sources should be used.

CHAPTER 4

CONCLUSIONS AND RECOMMENDATIONS

4.1 Ablative and Ceramic Radomes

Ablative radomes consisting of a load-bearing fibreglas substrate and a thin fibre-loaded Teflon ablator layer can be designed to have electrical performance comparable to what can be expected for ceramic radomes; however, the change in boresight error slope caused by ablation can be significant, and this effect must be taken into account in the radome design.

The investigation of the ceramic radome is not complete, and no conclusions can be drawn concerning the advantages of asymmetrical wall thickness. It is recommended that this work be completed, including an investigation of the effects of asymmetrical aerodynamic heating on BSE.

4.2 BSE Measurement Simulation

The computer-aided simulation shows that separation distance, reflections, and frequency drifts are all significant sources of error in BSE measurements. Also, the results obtained depend on the algorithm or procedure used to compute or measure BSE. The offset 1-point method yields the most variable results and is deemed unsuitable for use. The on-axis 1-point method has not been fully studied, and it is recommended that this be done using the simulation already developed.

REFERENCES

1. G. K. Huddleston, H. L. Bassett, and J. M. Newton, "Computer Aided Radome Analysis Based on Geometrical Optics and Lorentz Reciprocity," Final Report on AFOSR-77-3469, Vol. 2 of 4, February 1980.

APPENDIX A
FLAT PANEL ANALYSIS RESULTS

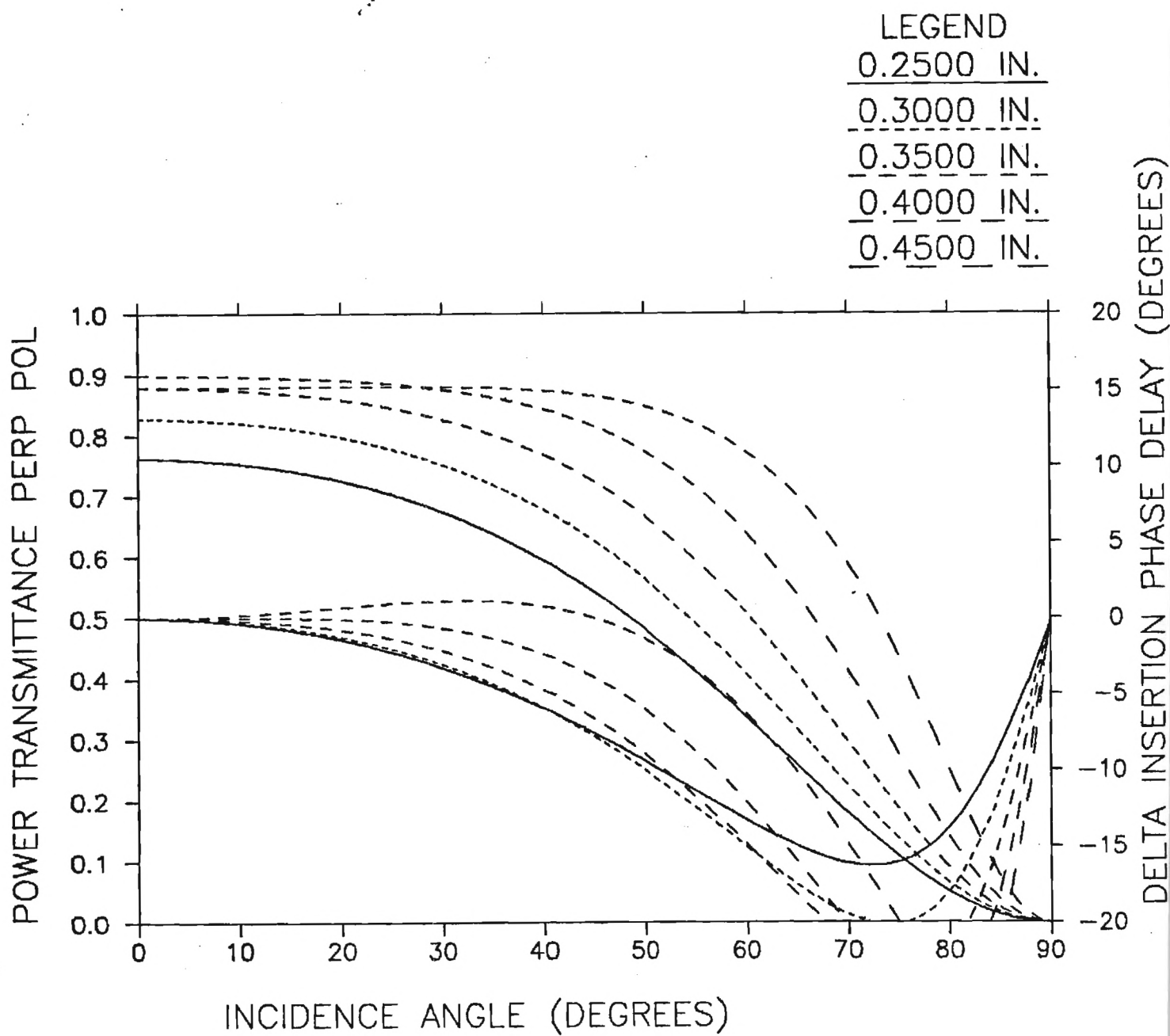


Figure A-1. Substrate Thickness = 0.25".

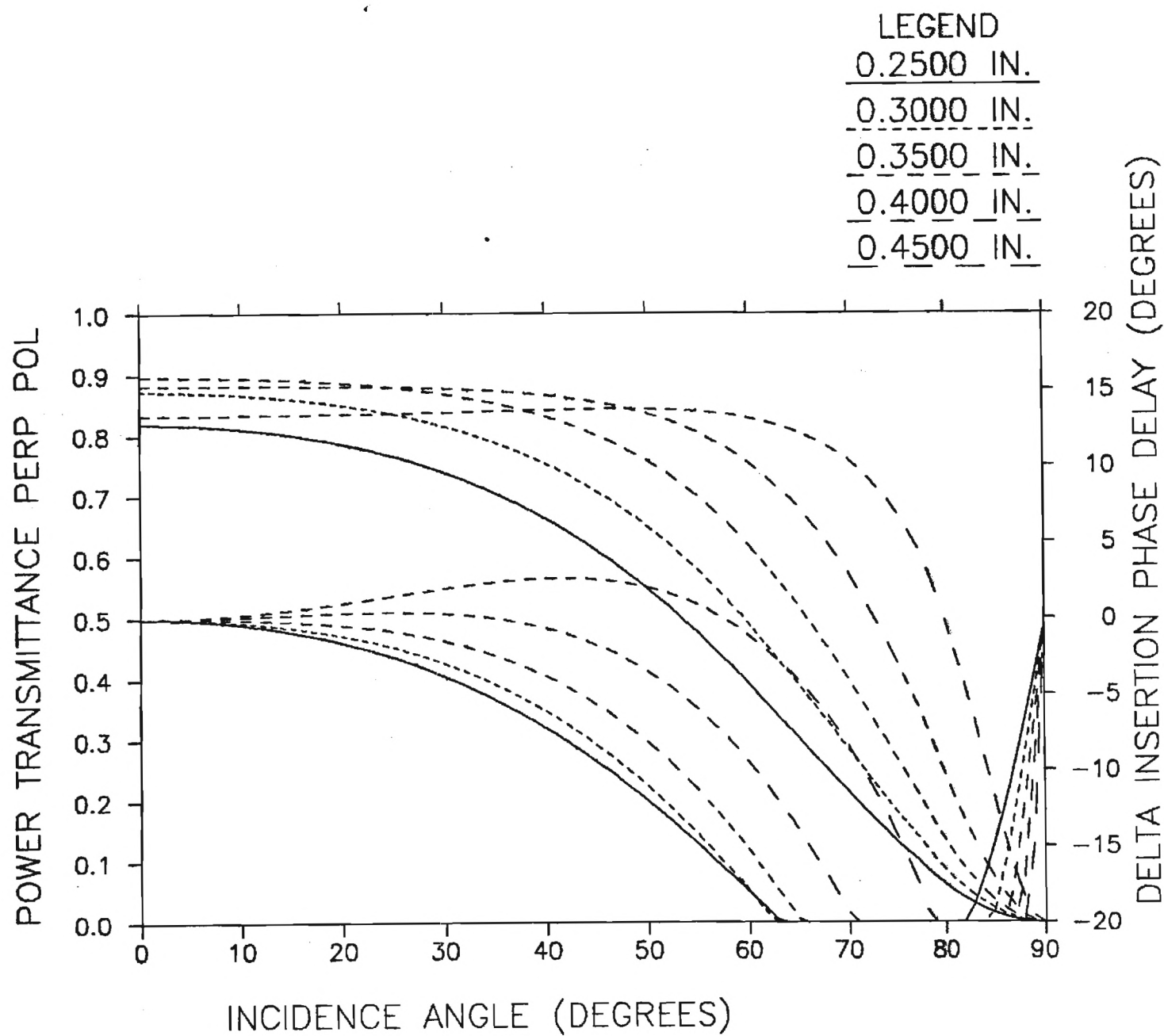


Figure A-2. Substrate Thickness = 0.30".

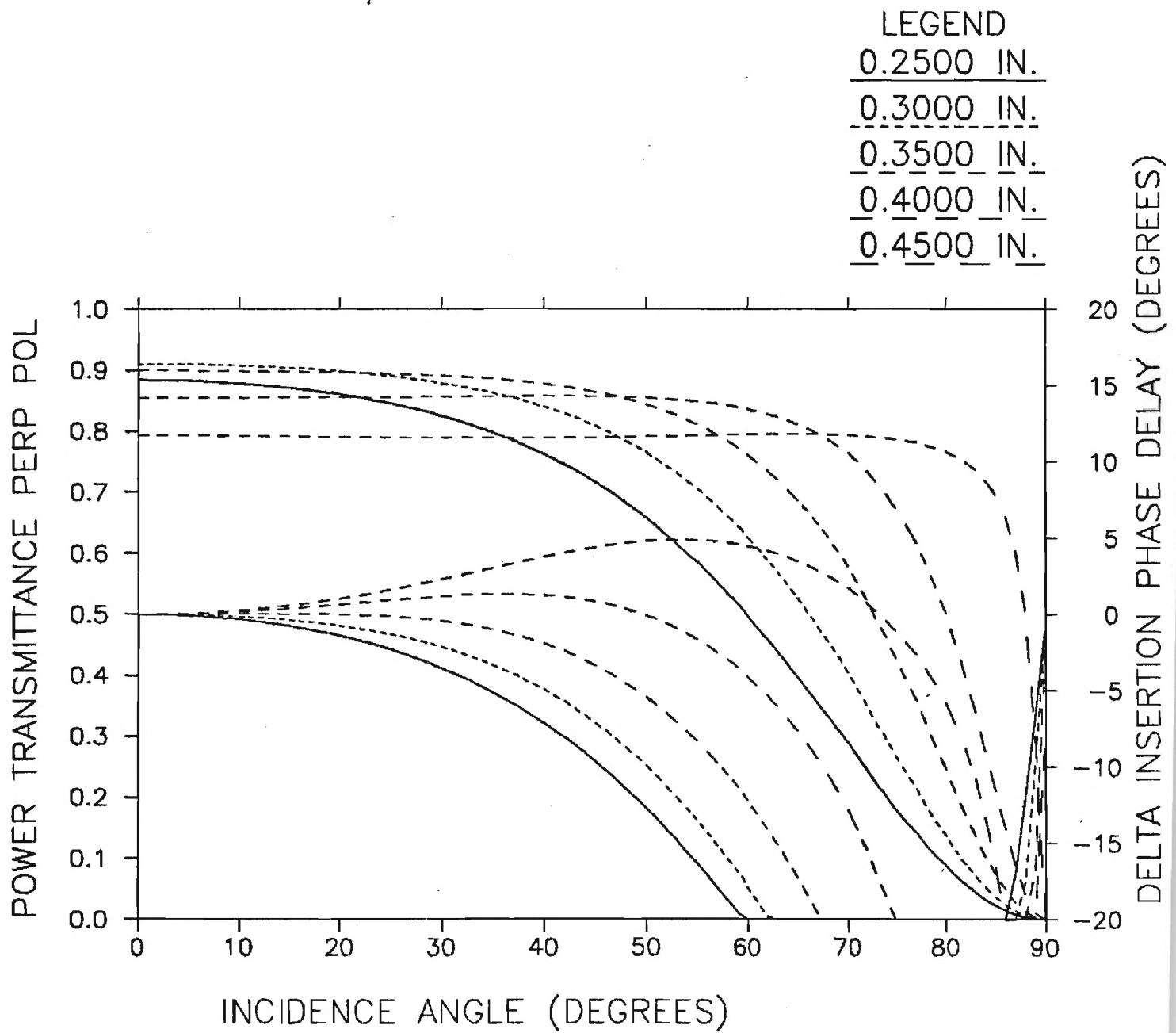


Figure A-3. Substrate Thickness = 0.35".

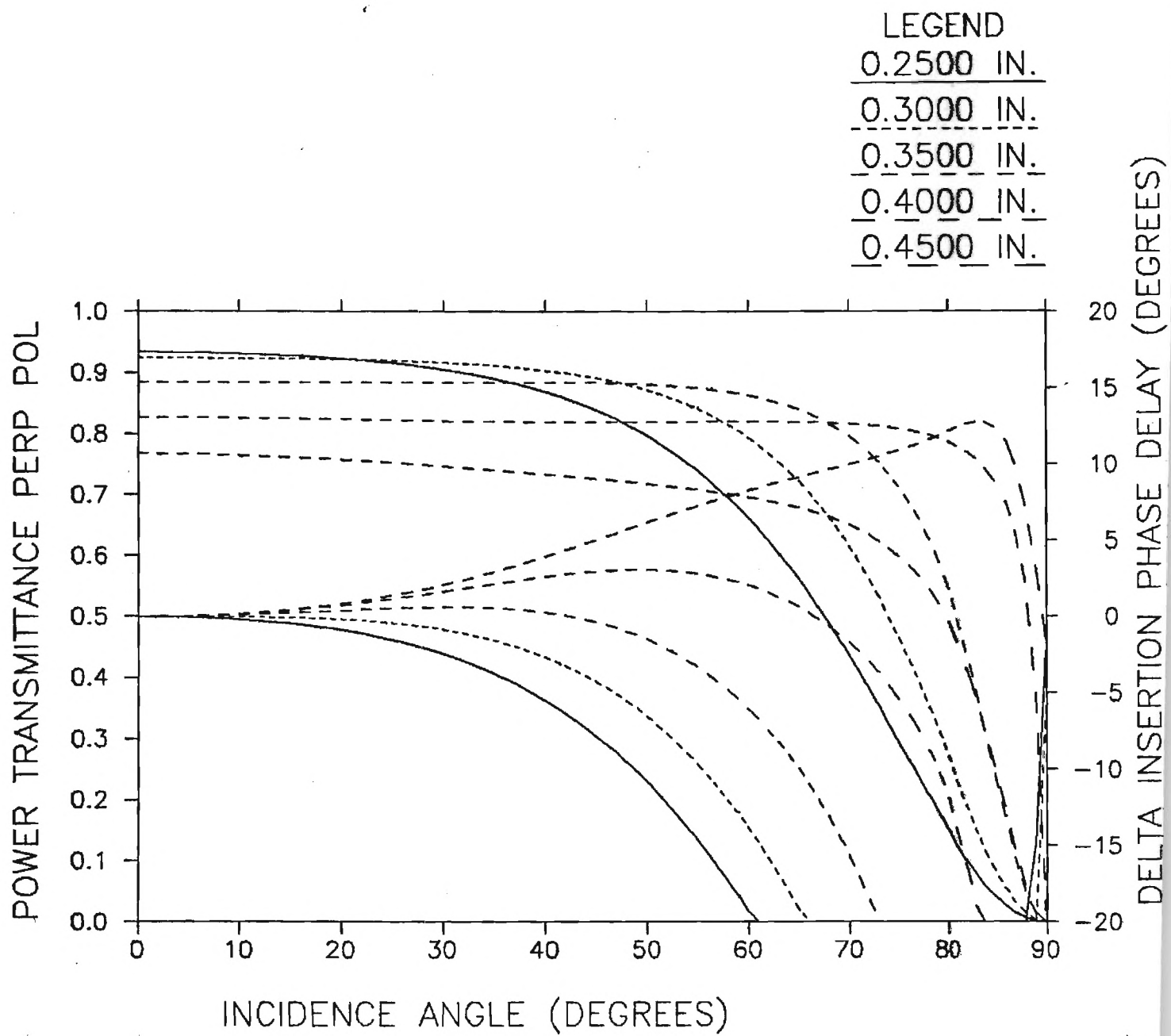


Figure A-4. Substrate Thickness = 0.40".

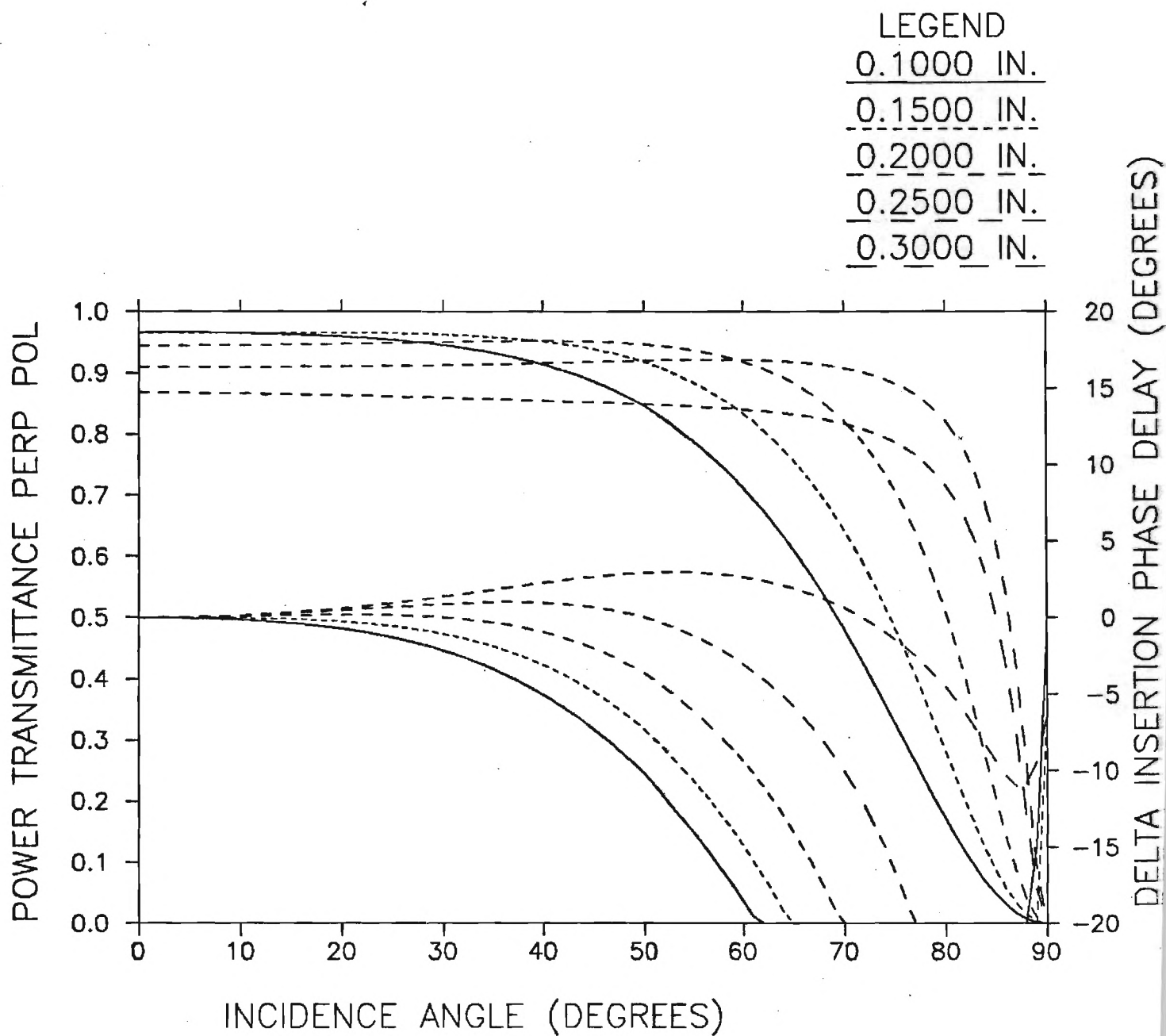


Figure A-5. Substrate Thickness = 0.50".

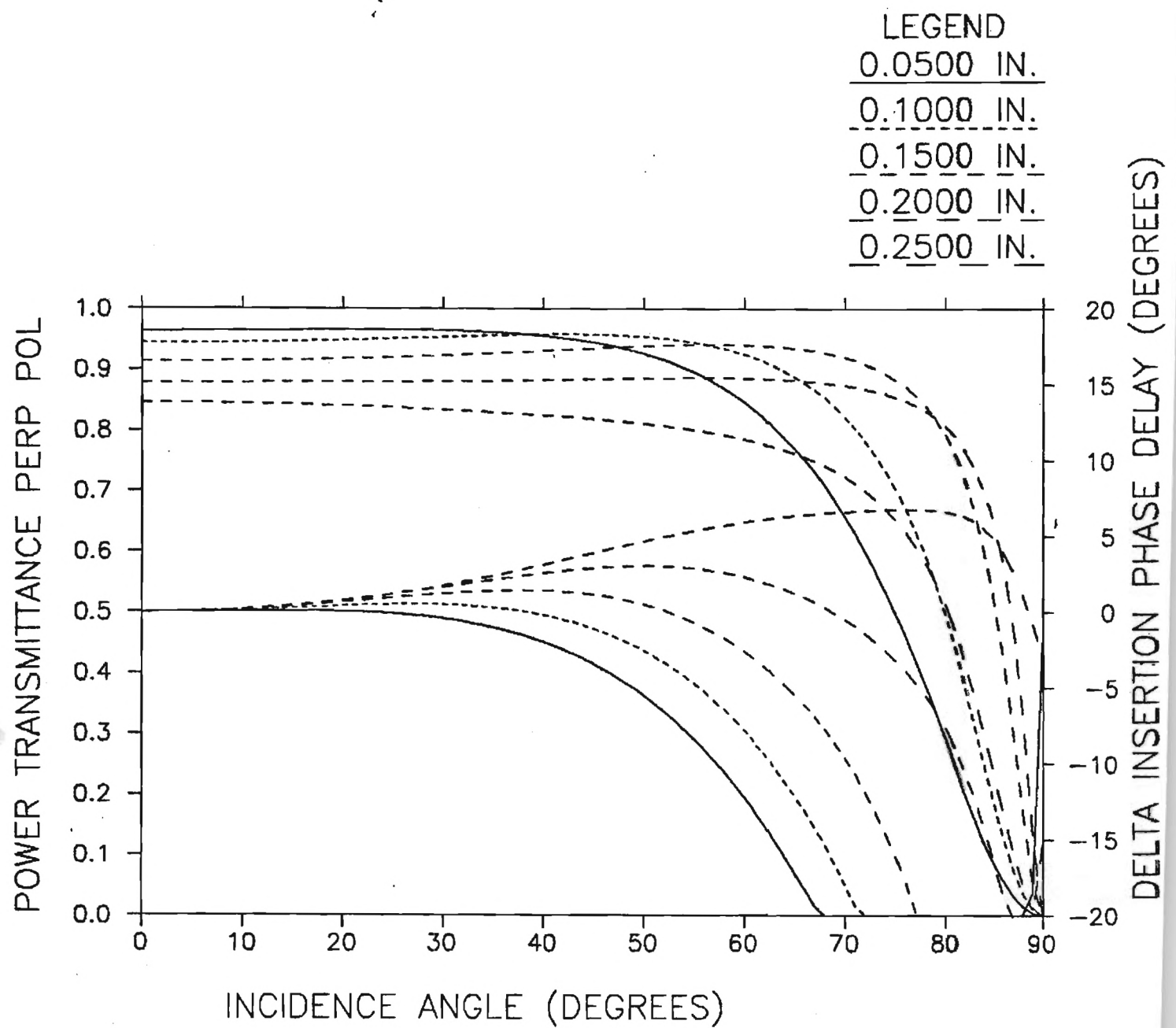


Figure A-6. Substrate Thickness = 0.55".

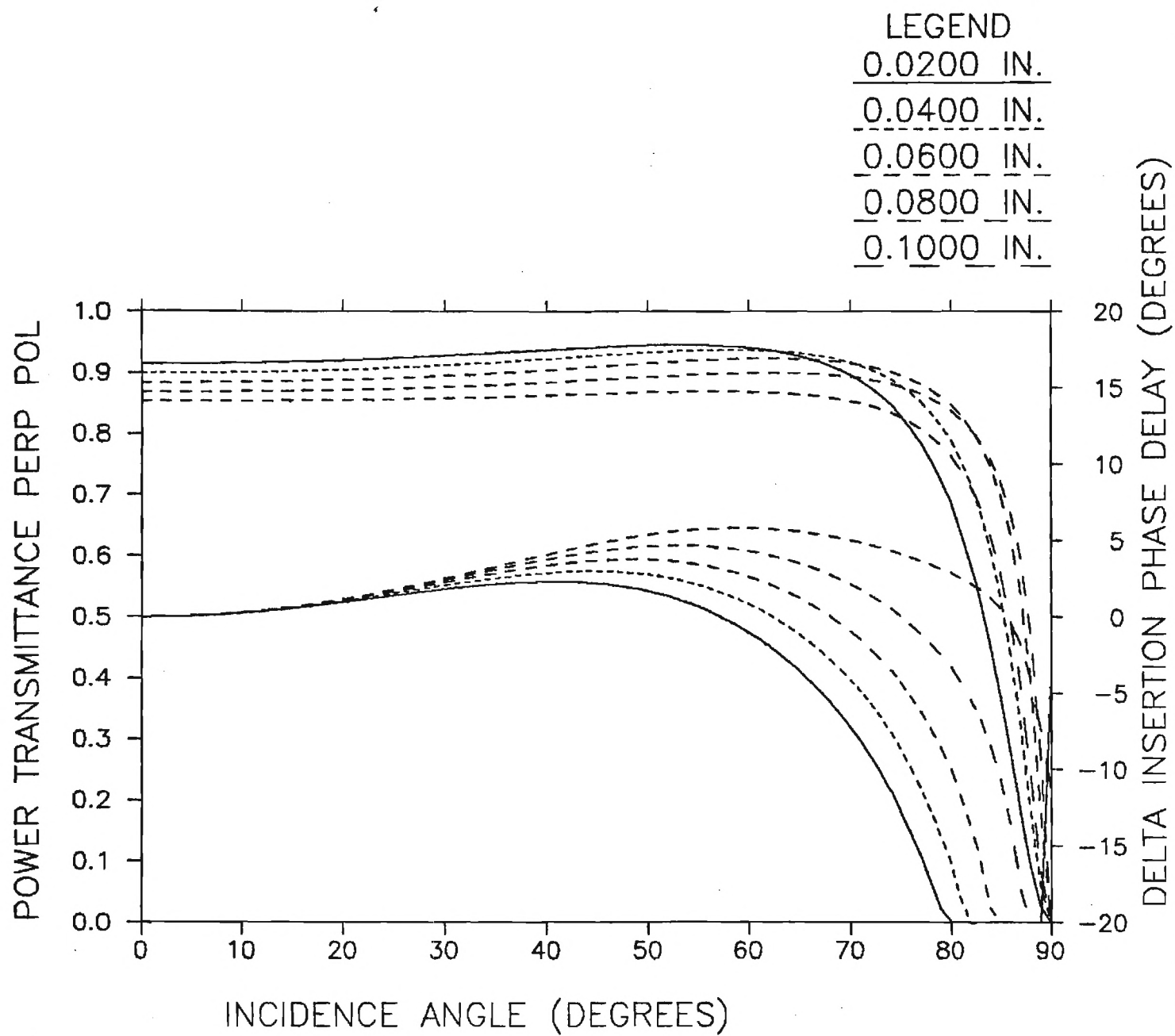


Figure A-7. Substrate Thickness = 0.60".

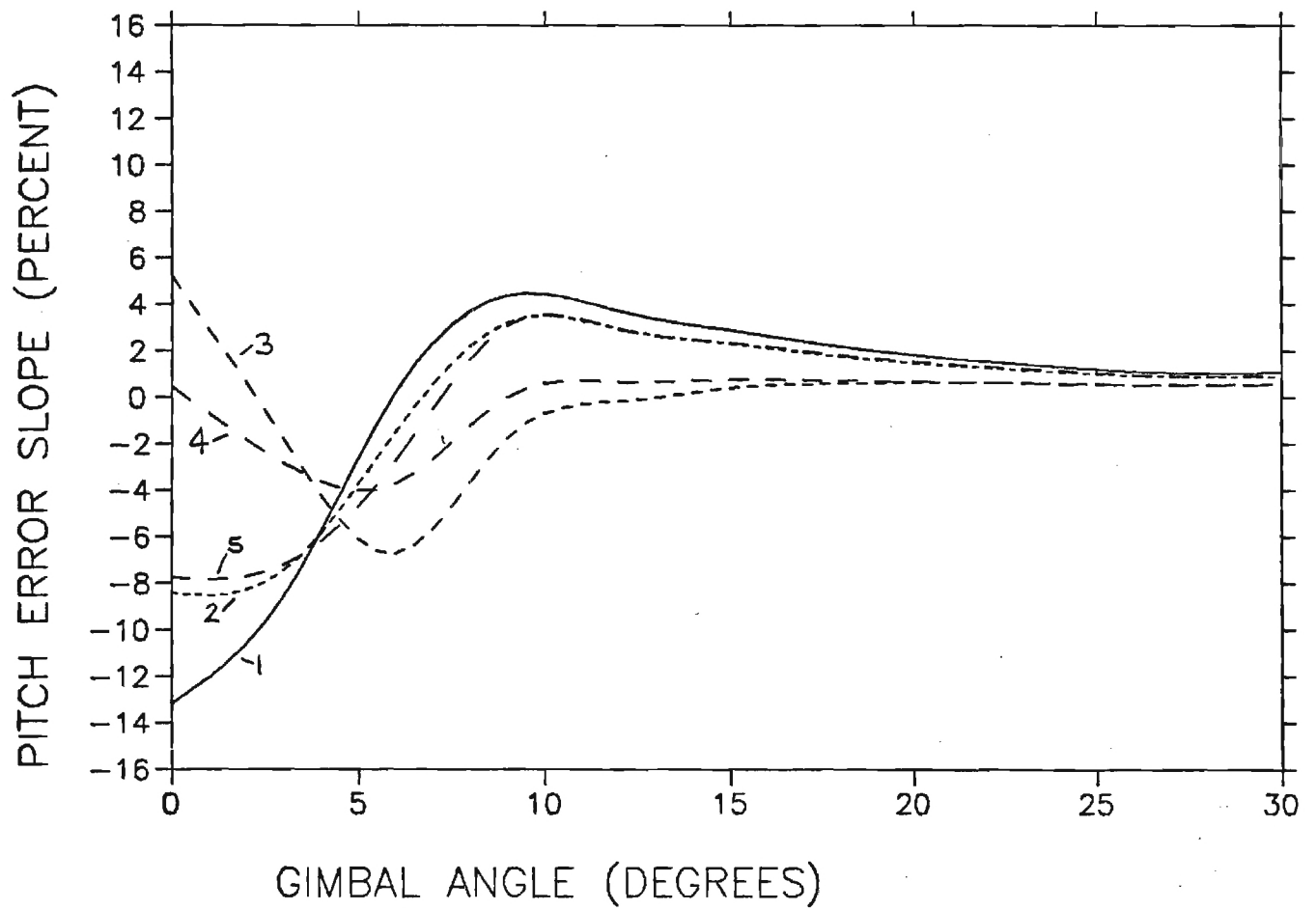
APPENDIX B

UNIFORM ABLATIVE RADOME PERFORMANCE

SUBSTRATE ABLATOR

LEGEND

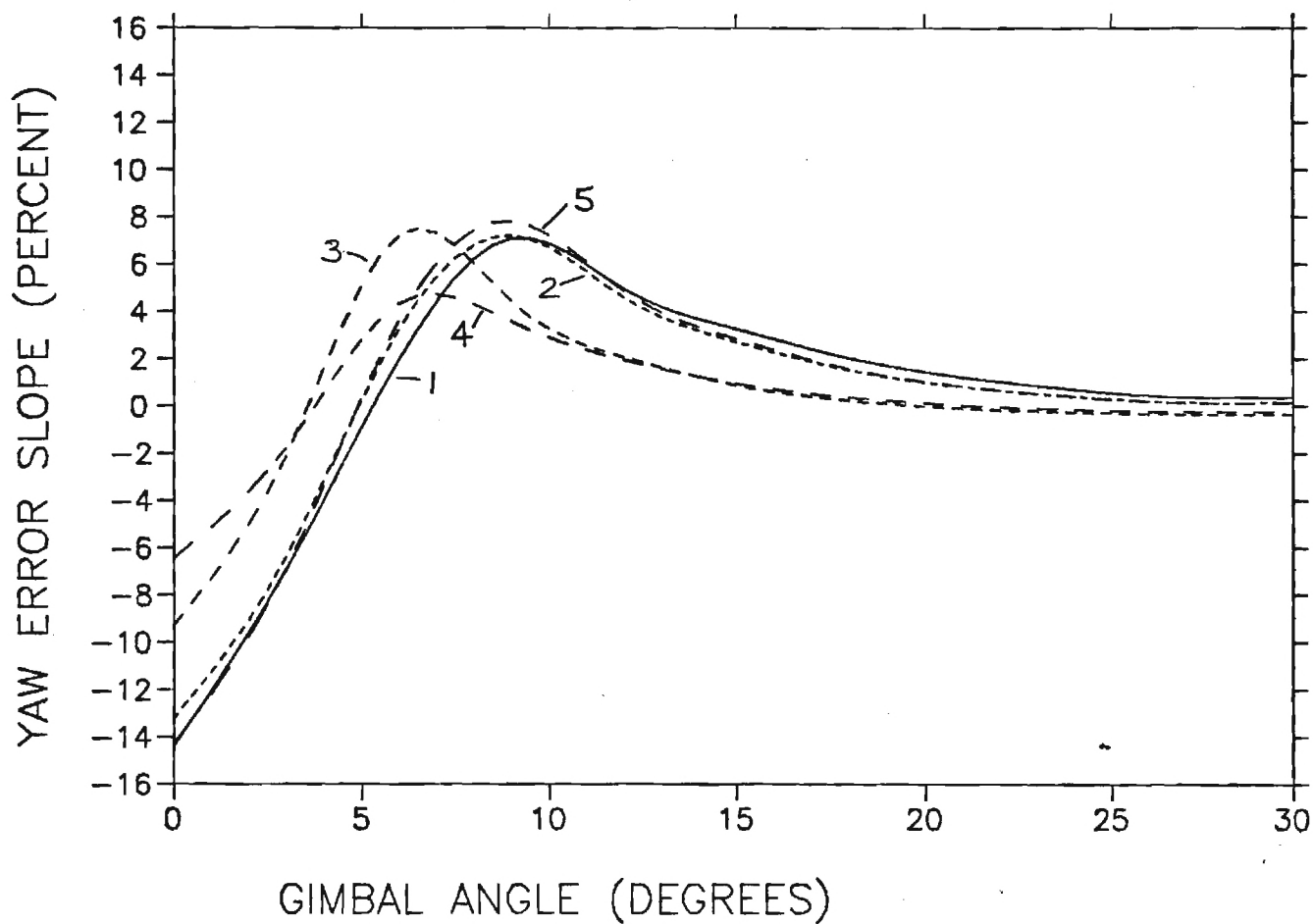
1	.350"	.400"
2	.550"	.150"
3	.550"	.200"
4	.600"	.060"
5	.500"	.250"



SUB. ABLATOR

LEGEND

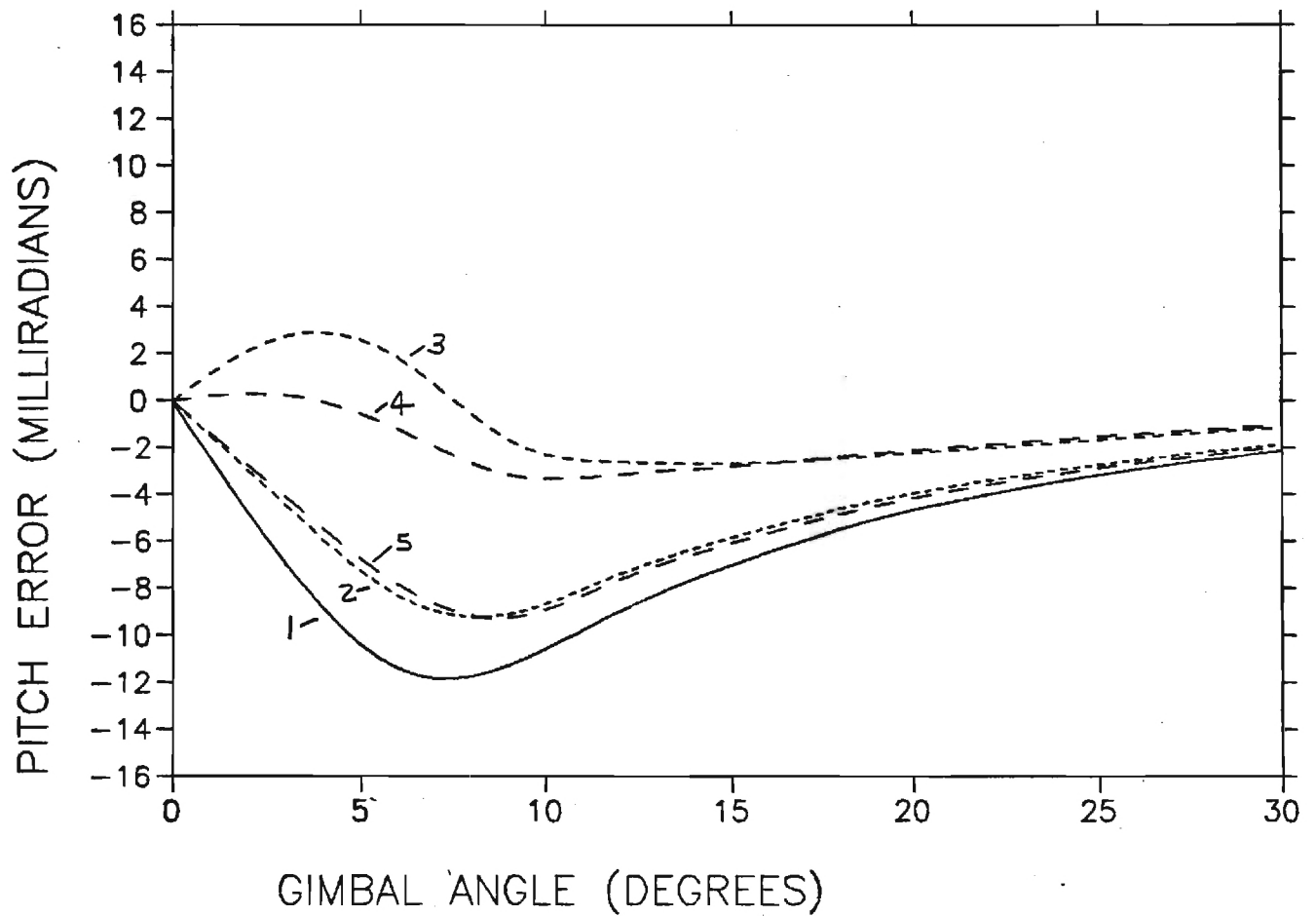
1	<u>.350"</u>	<u>.400"</u>
2	<u>.550"</u>	<u>.150"</u>
3	<u>.550"</u>	<u>.200"</u>
4	<u>.600"</u>	<u>.060"</u>
5	<u>.500"</u>	<u>.250"</u>



SUB. ABLATOR

LEGEND

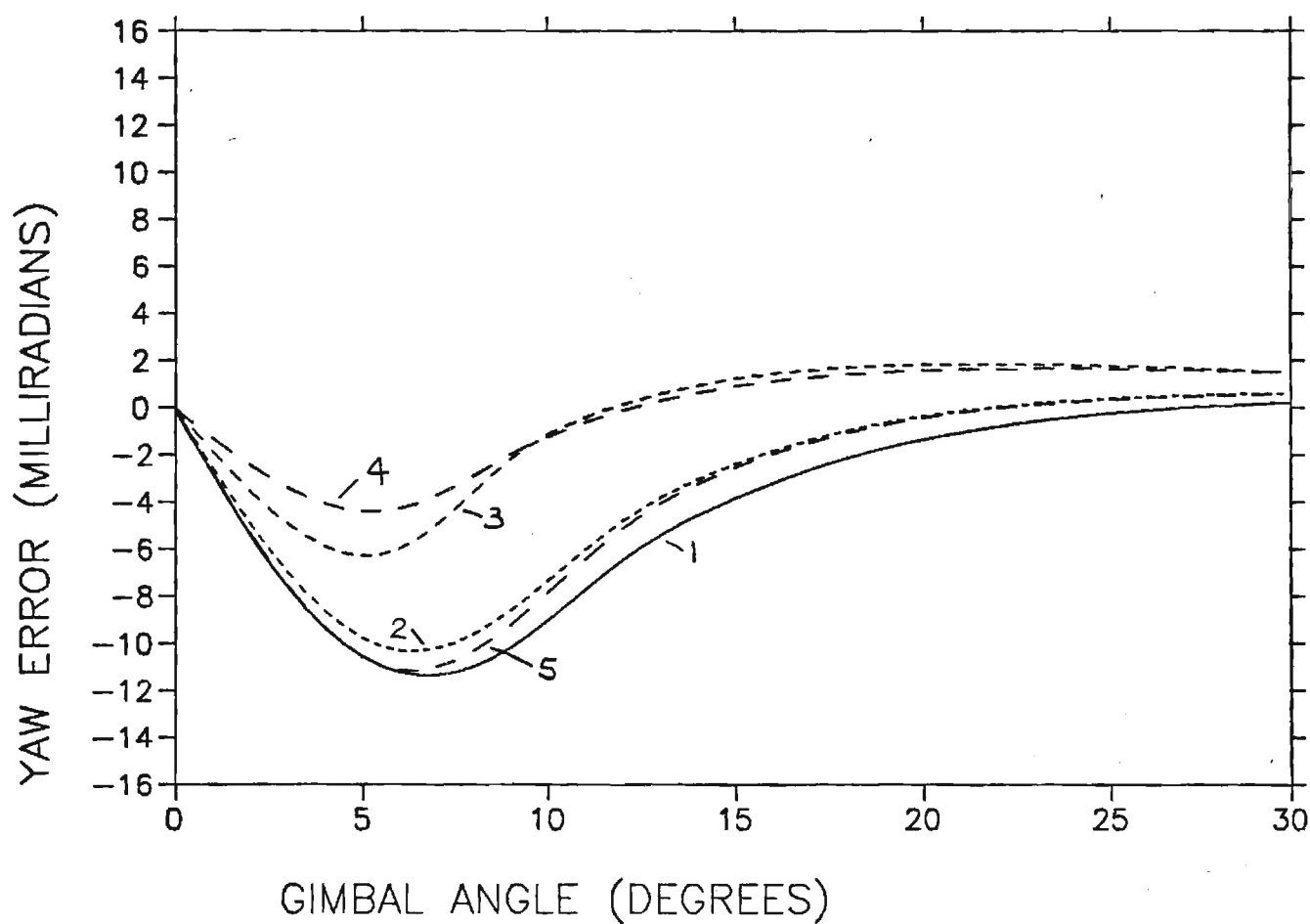
1	<u>.350"</u>	<u>.400"</u>
2	<u>.550"</u>	<u>.150"</u>
3	<u>.550"</u>	<u>.200"</u>
4	<u>.600"</u>	<u>.060"</u>
5	<u>.500"</u>	<u>.250"</u>



SUB. ABLATOR

LEGEND

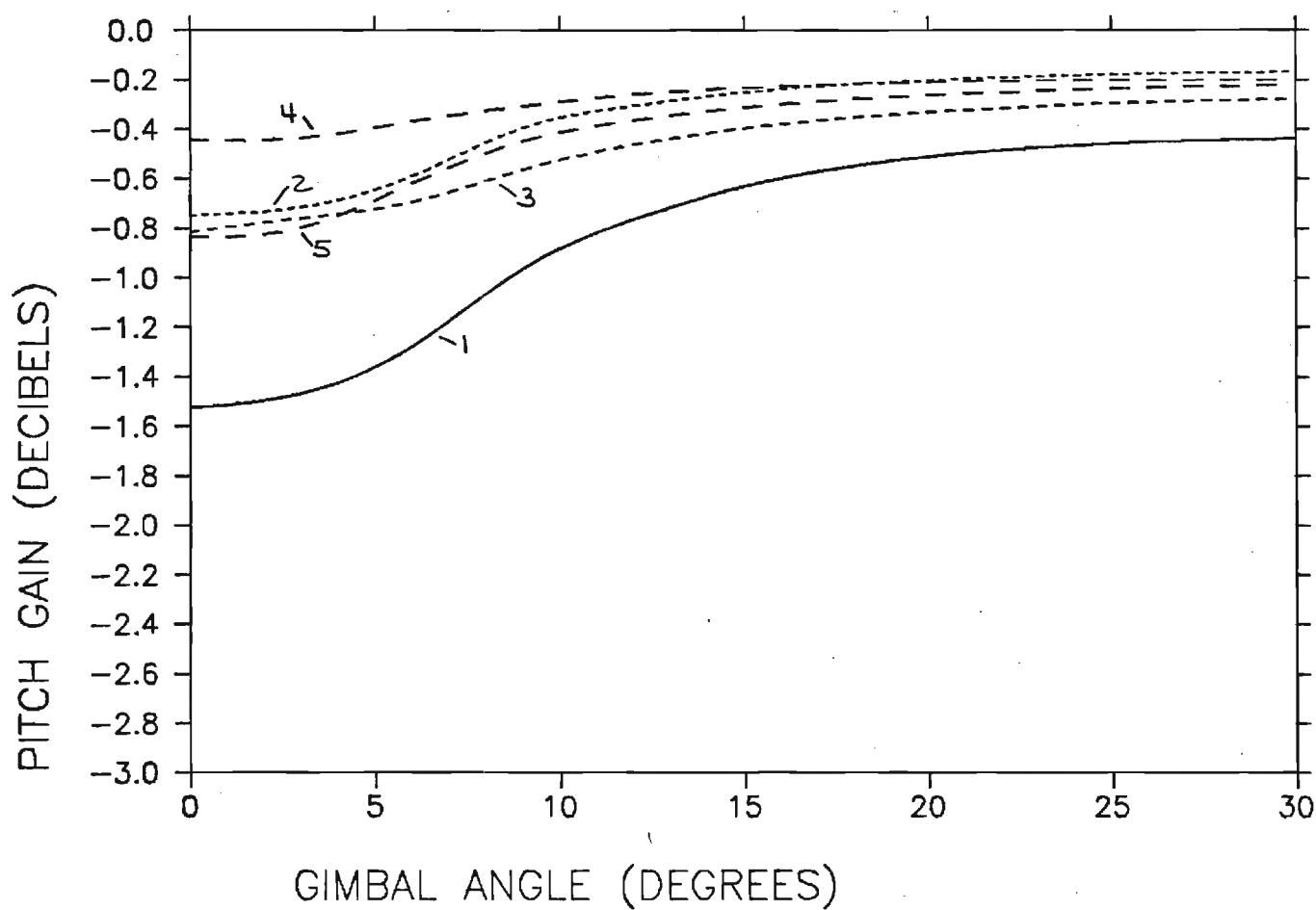
1	<u>.350"</u>	<u>.400"</u>
2	<u>.550"</u>	<u>.150"</u>
3	<u>.550"</u>	<u>.200"</u>
4	<u>.600"</u>	<u>.060"</u>
5	<u>.500"</u>	<u>.250"</u>



SUB. ABLATOR

LEGEND

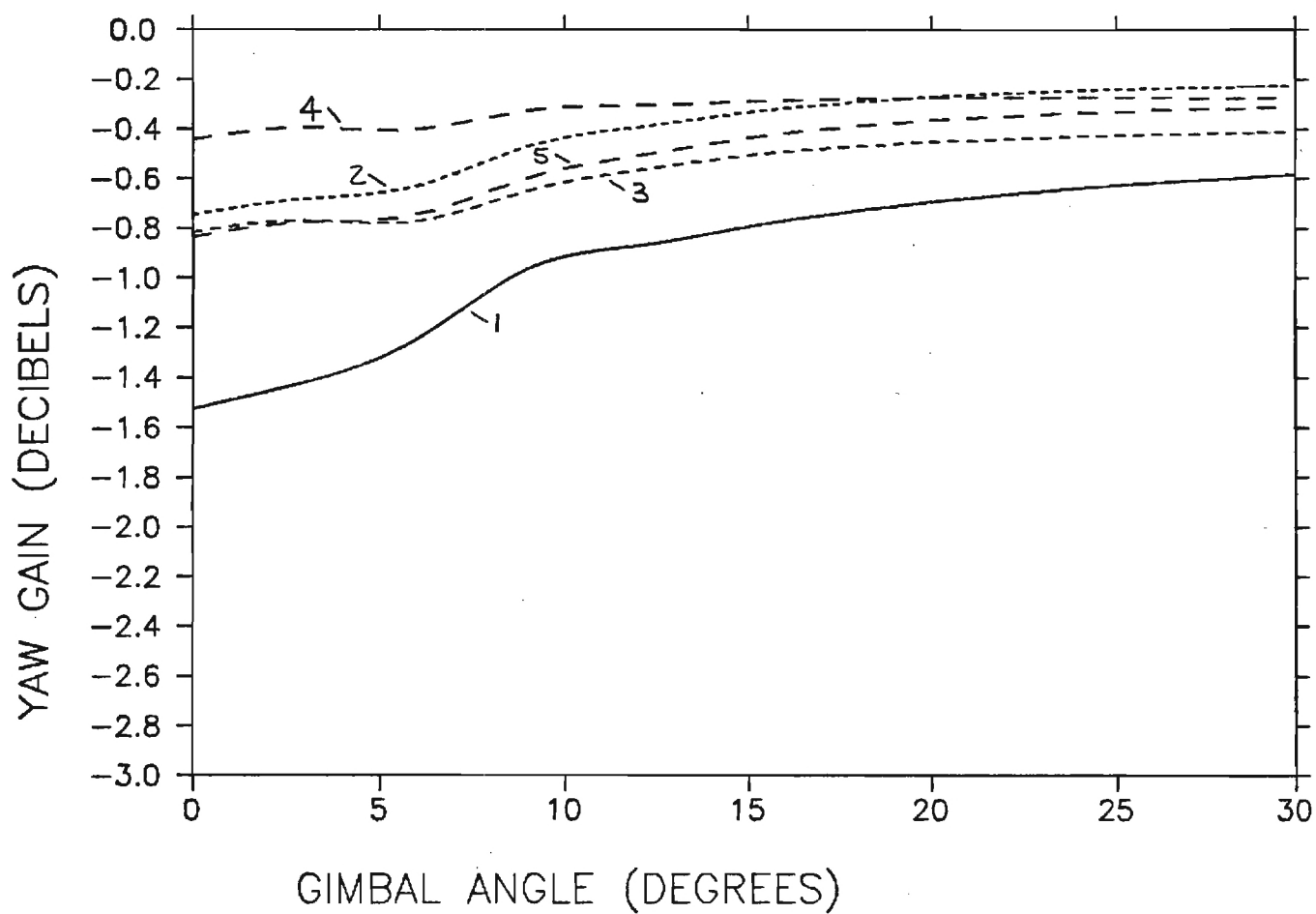
1	<u>.350"</u>	<u>.400"</u>
2	<u>.550"</u>	<u>.150"</u>
3	<u>.550"</u>	<u>.200"</u>
4	<u>.600"</u>	<u>.060"</u>
5	<u>.500"</u>	<u>.250"</u>



SUB. ABLATOR

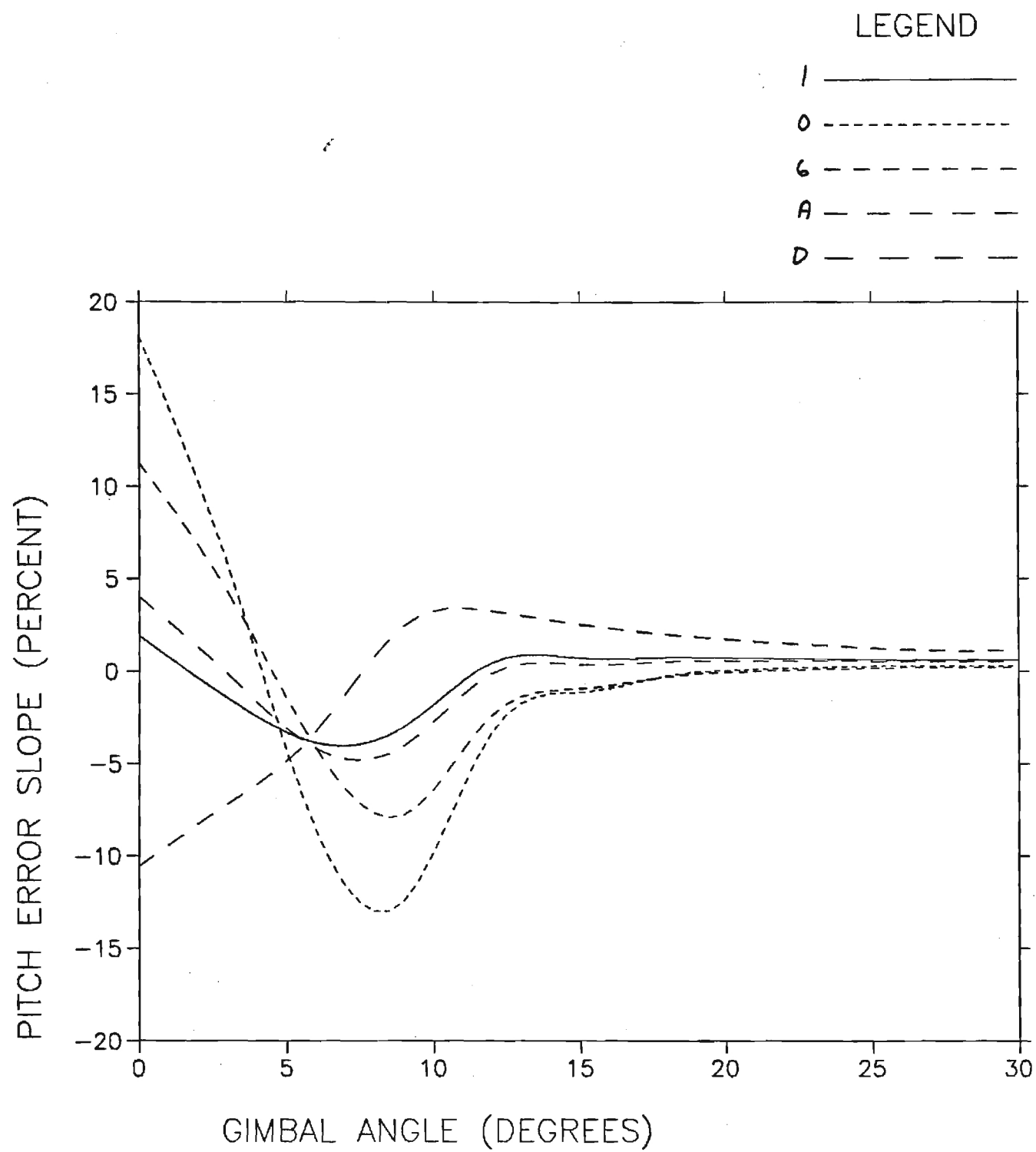
LEGEND

1	.350"	.400"
2	.550"	.150"
3	.550"	.200"
4	.600"	.060"
5	.500"	.250"



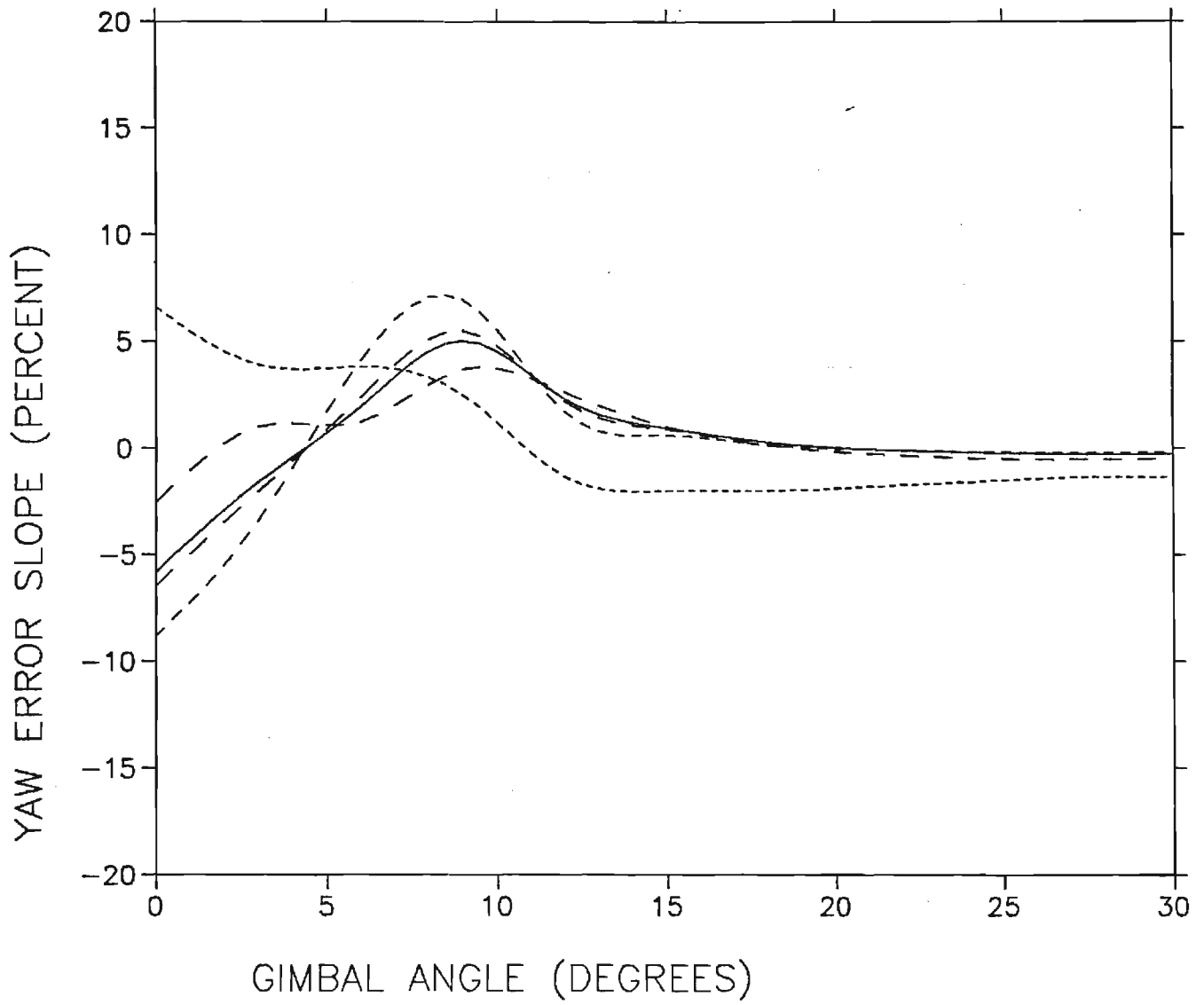
APPENDIX C

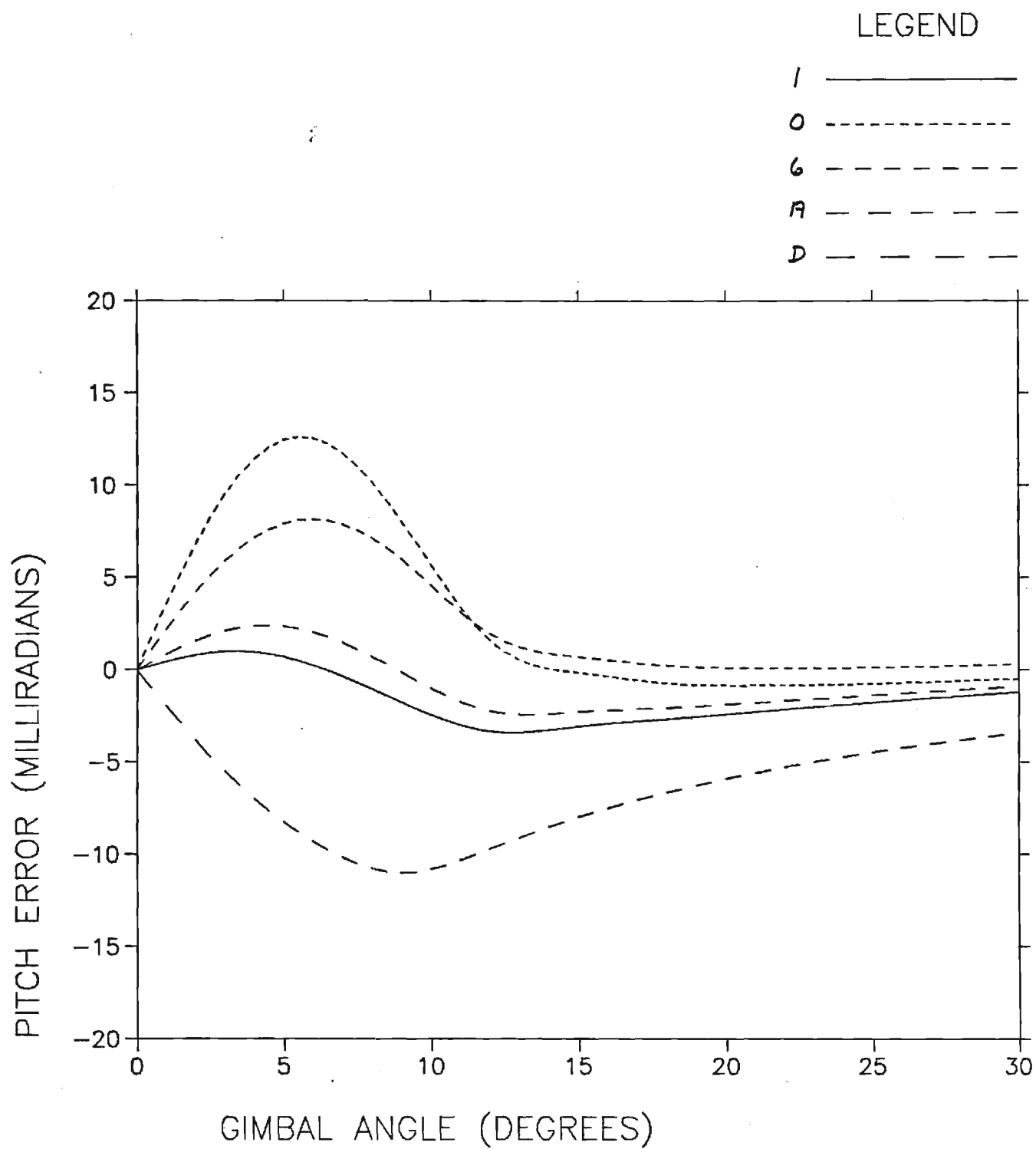
TAPERED ABLATOR RADOME PERFORMANCE

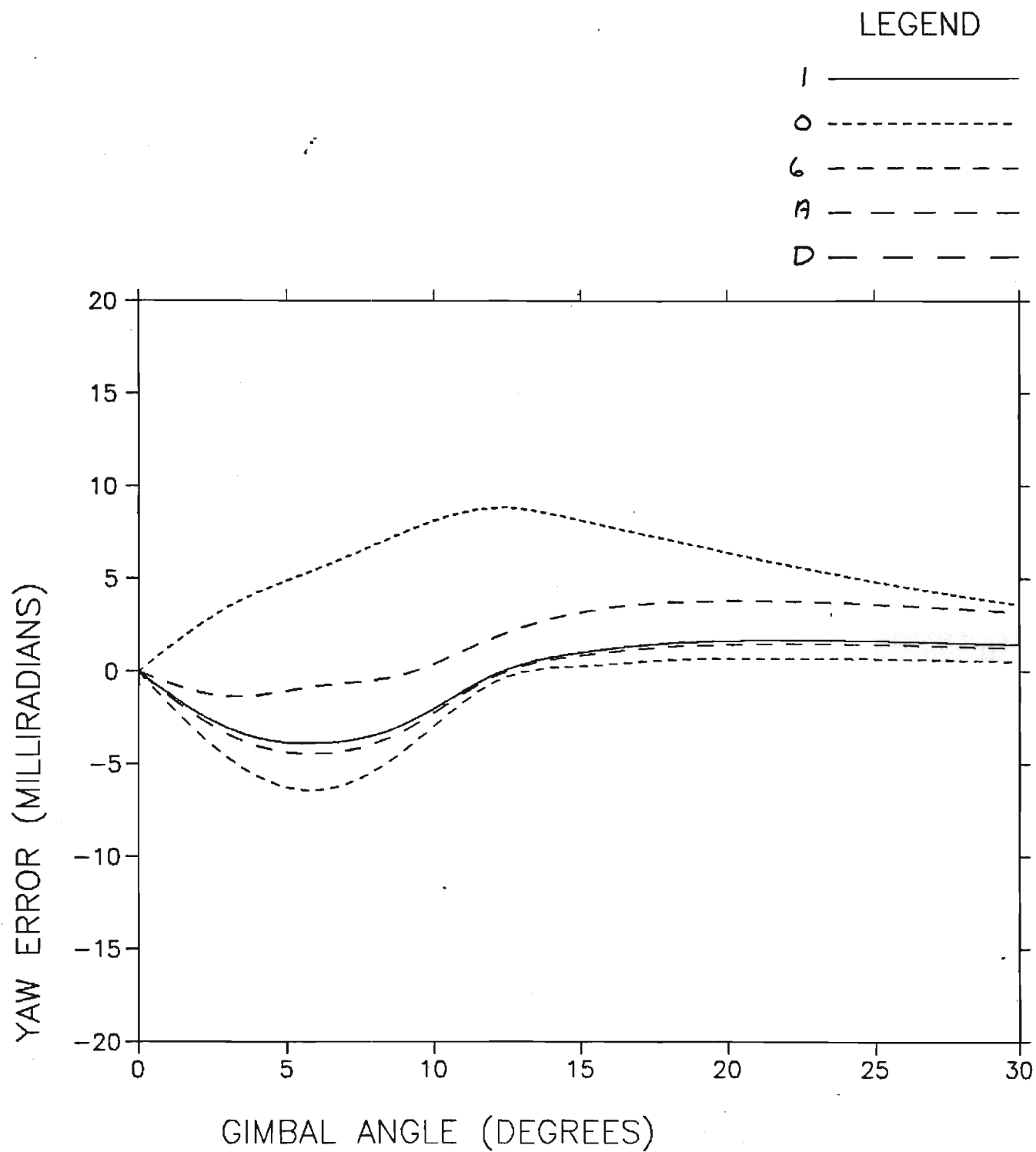


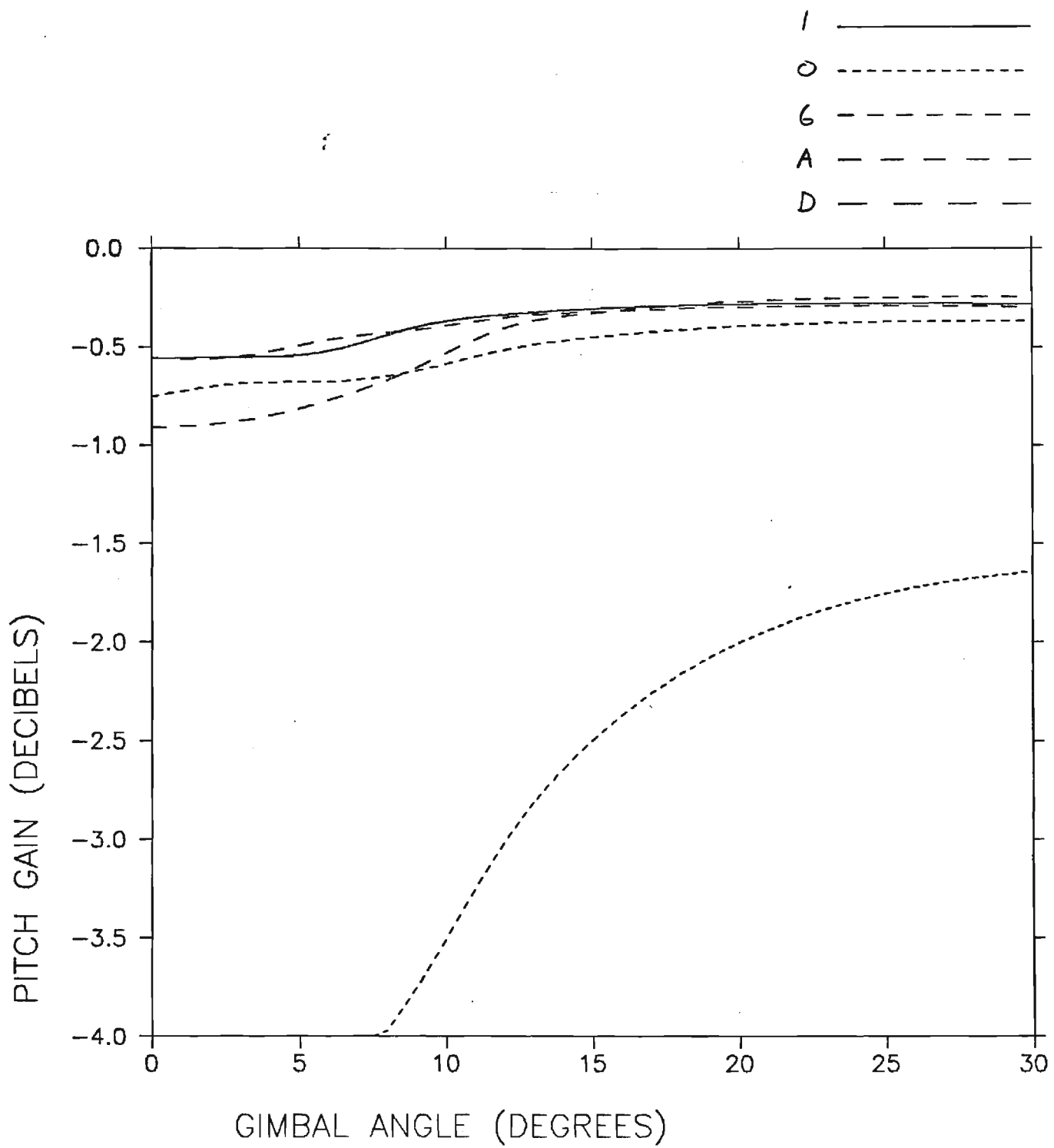
LEGEND

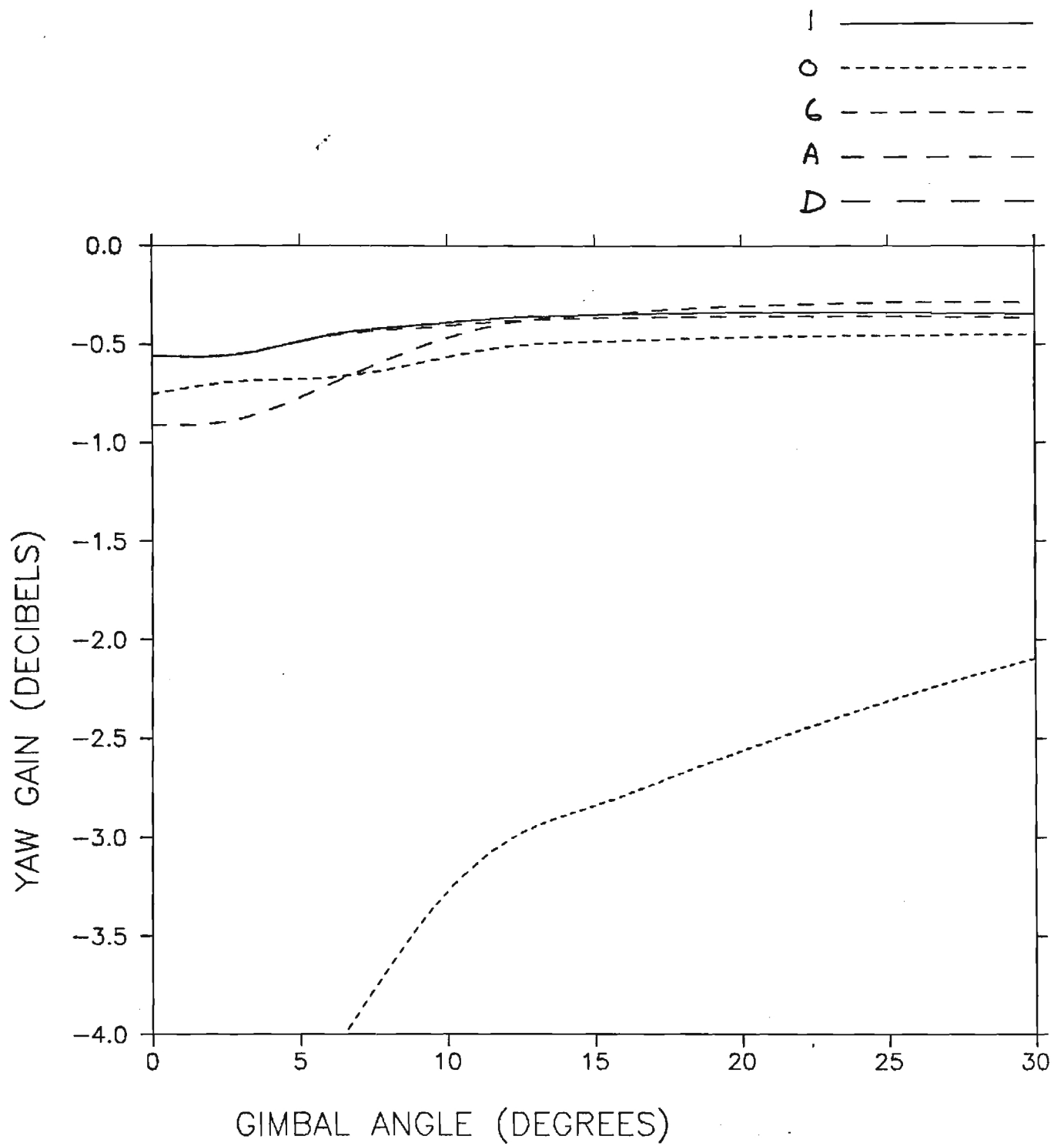
- I —————
- O - - - - -
- 6 - - - - -
- A - - - - -
- D - - - - -









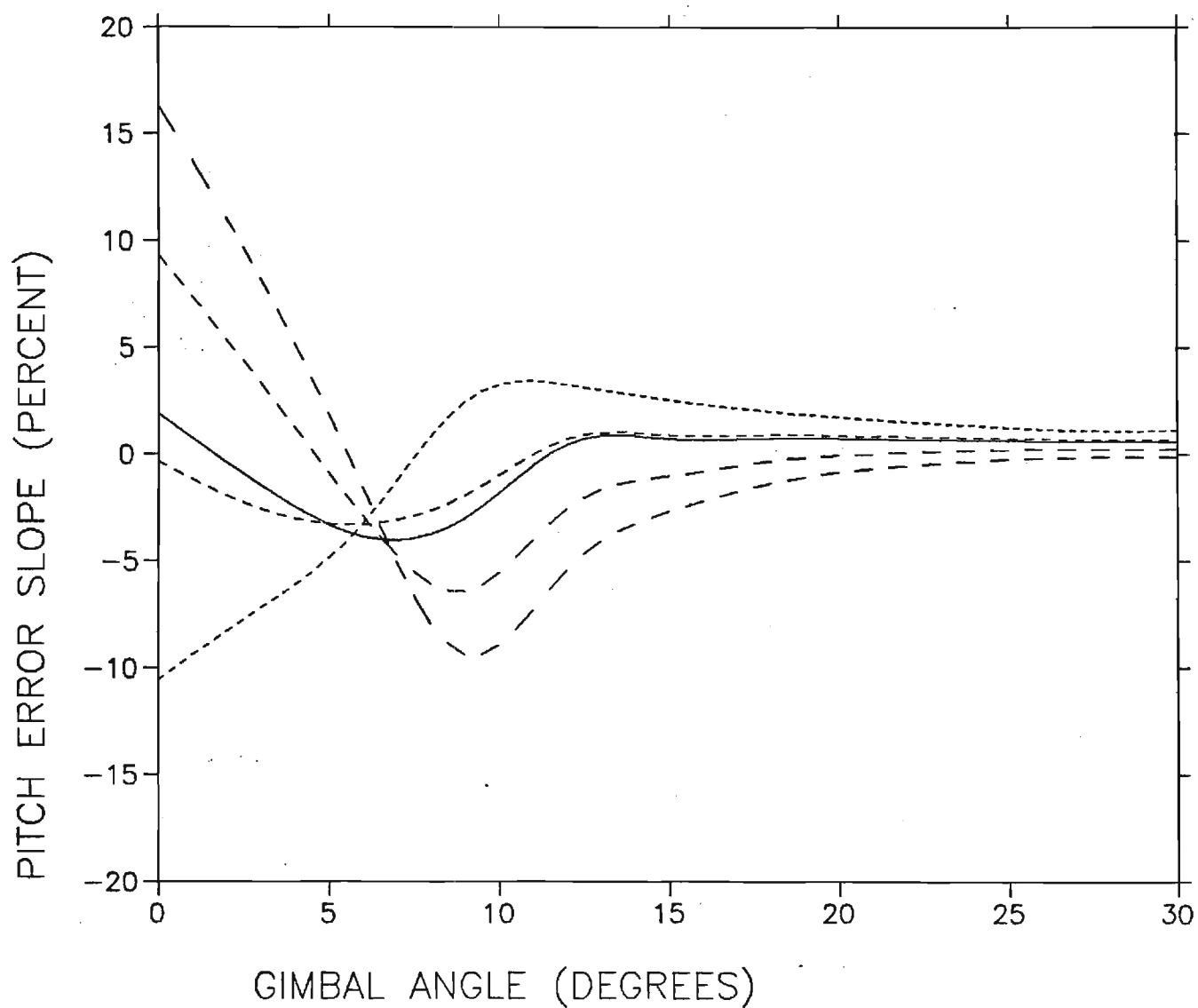


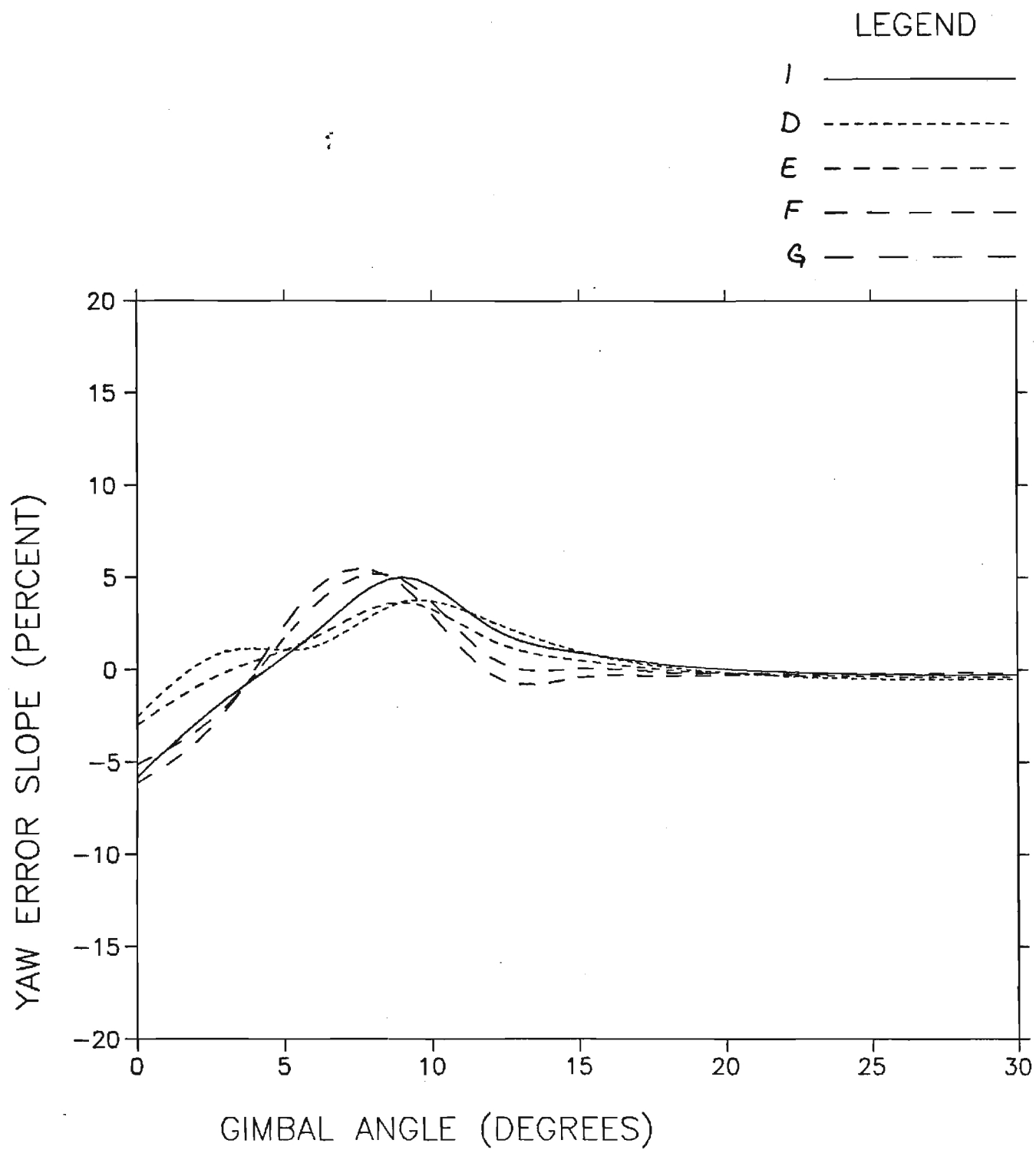
APPENDIX D

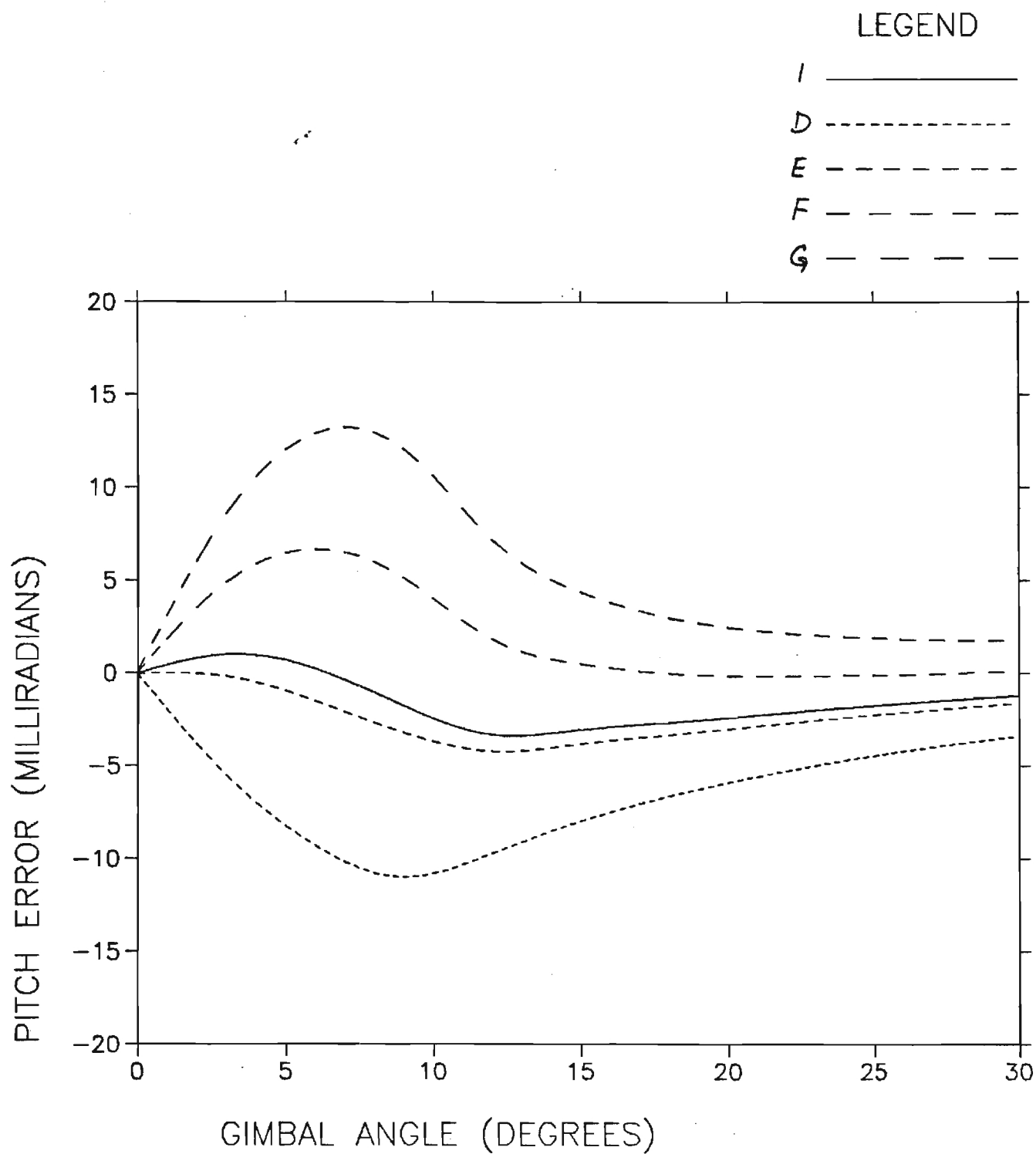
TAPERED SUBSTRATE RADOME PERFORMANCE

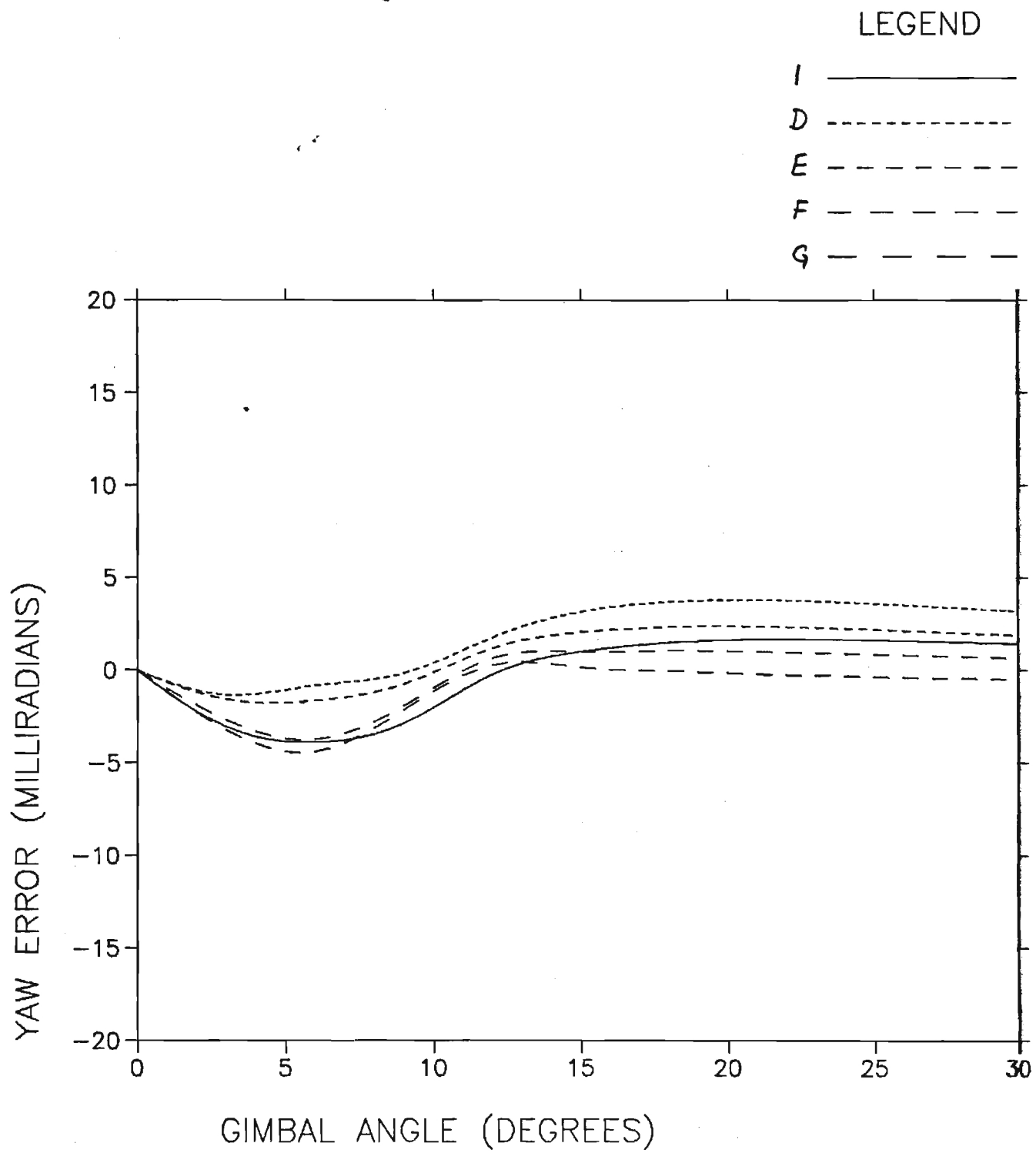
LEGEND

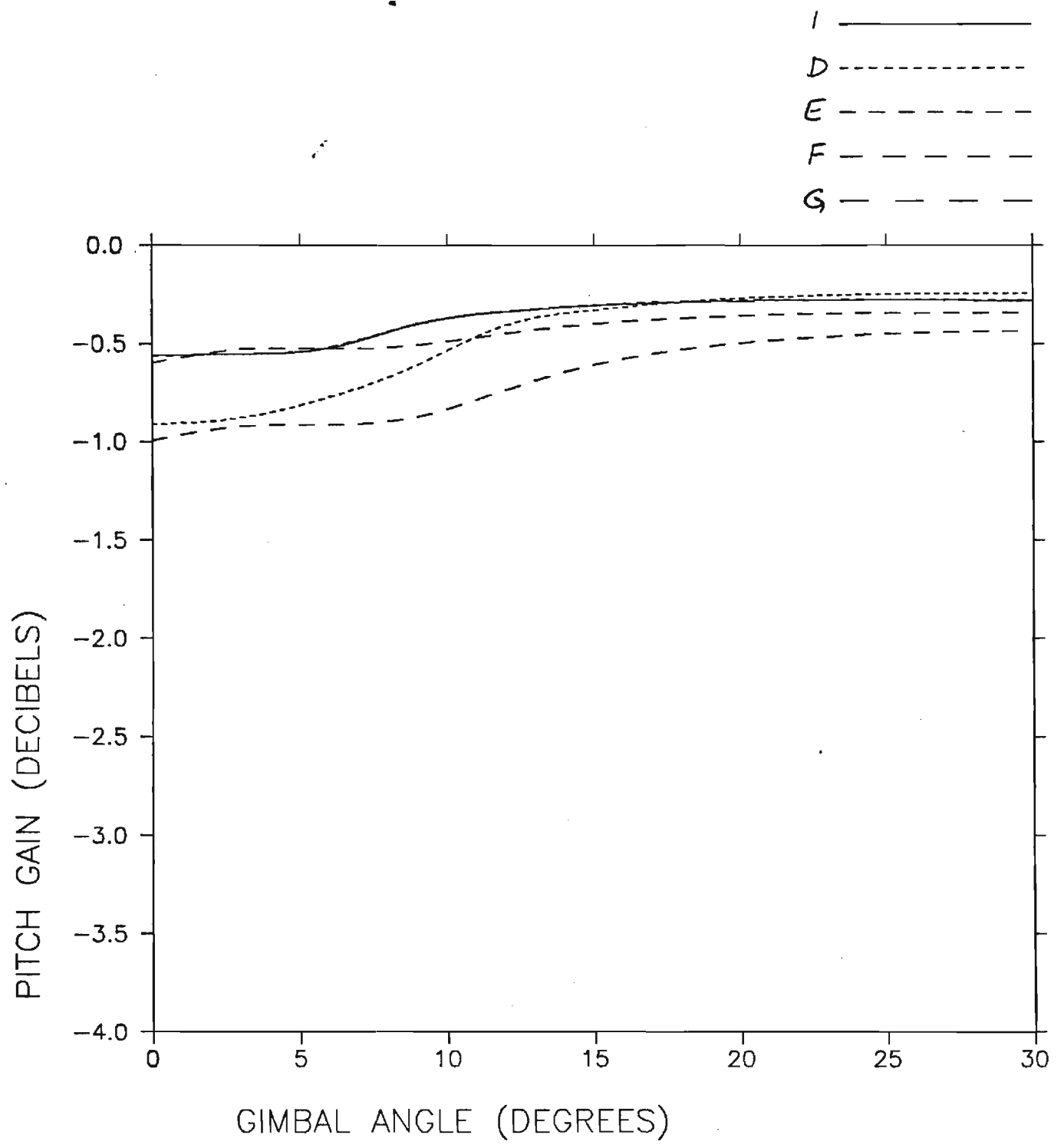
I —————
D - - - - -
E - - - - -
F - - - - -
G - - - - -

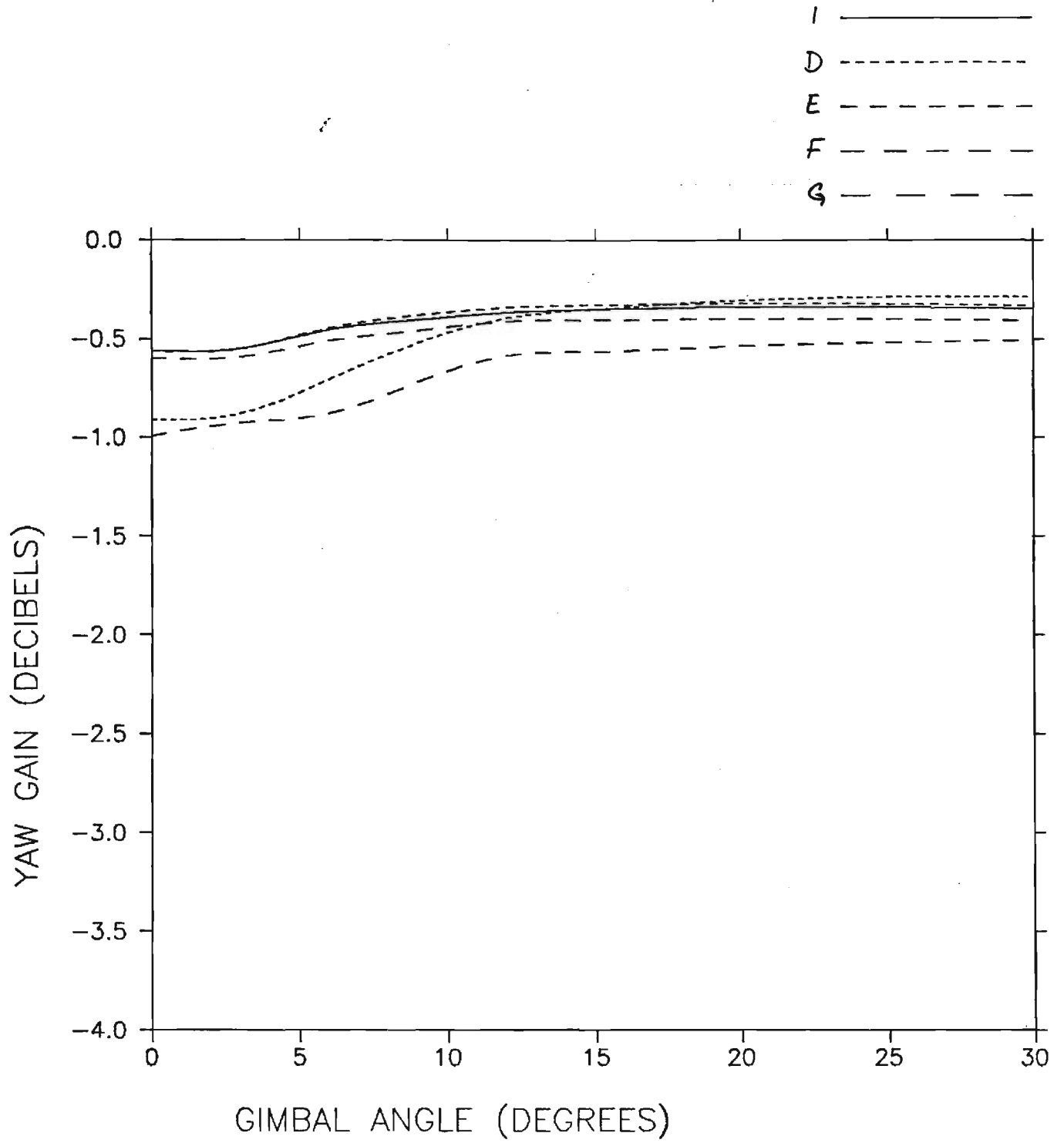






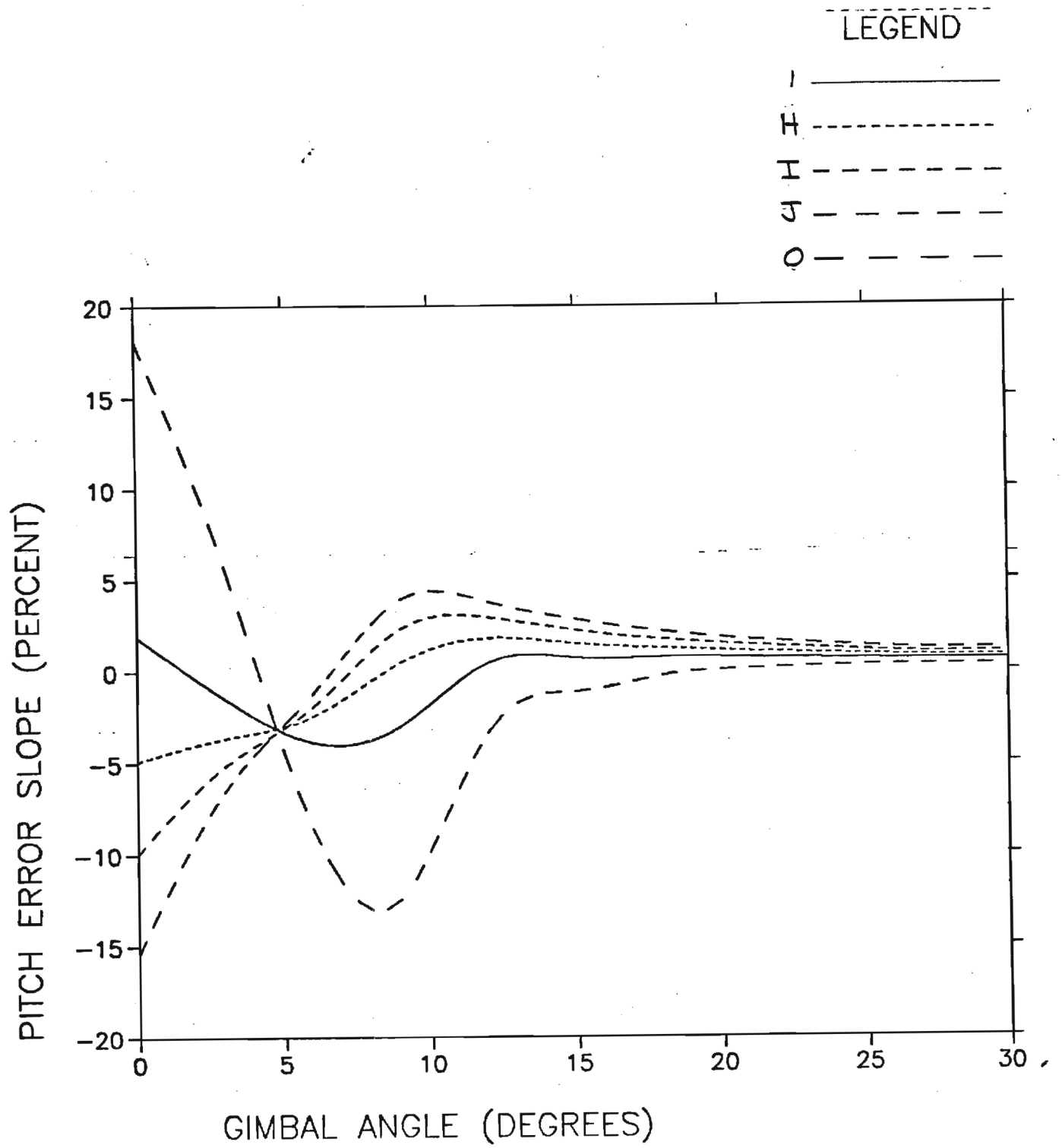


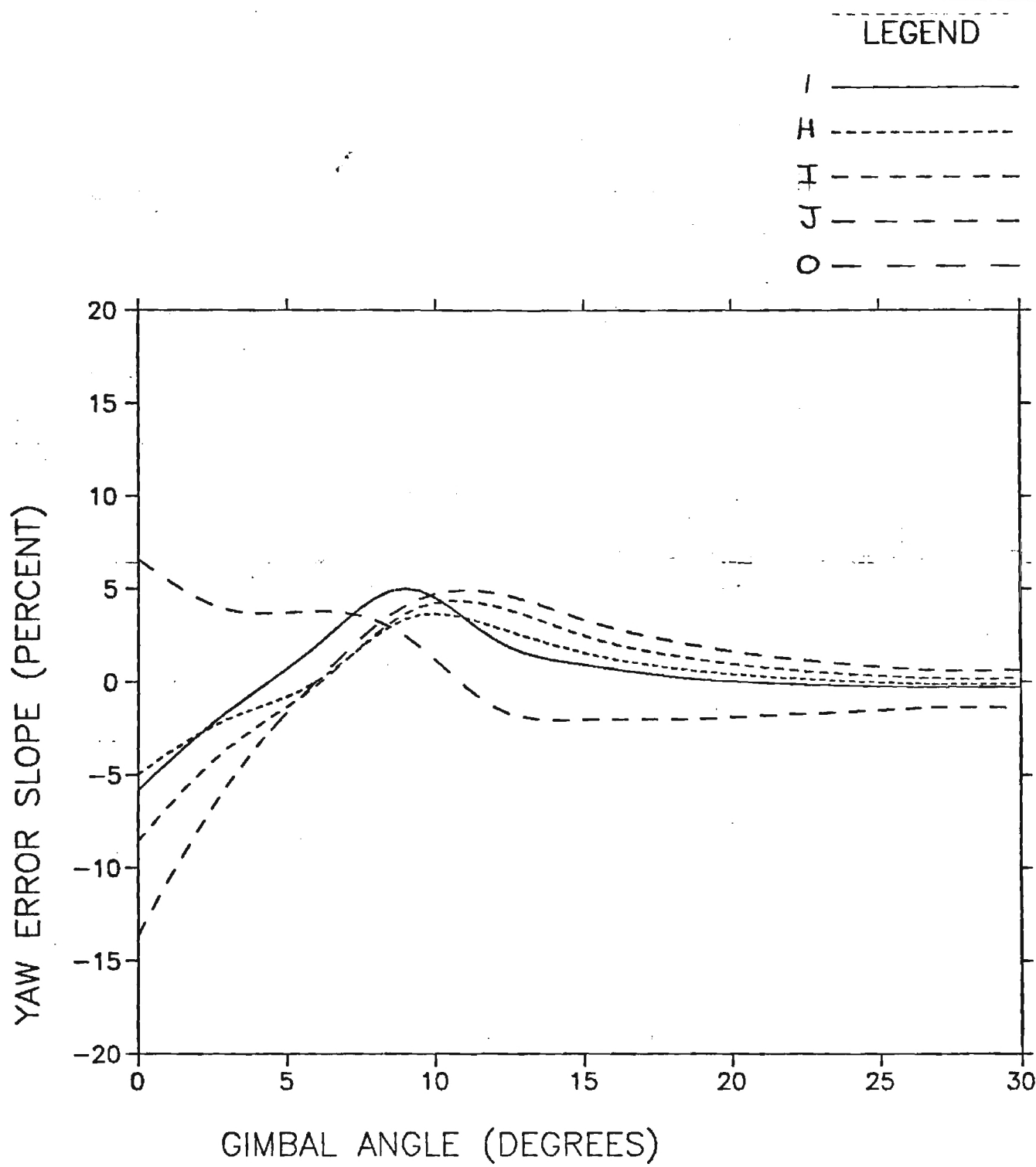


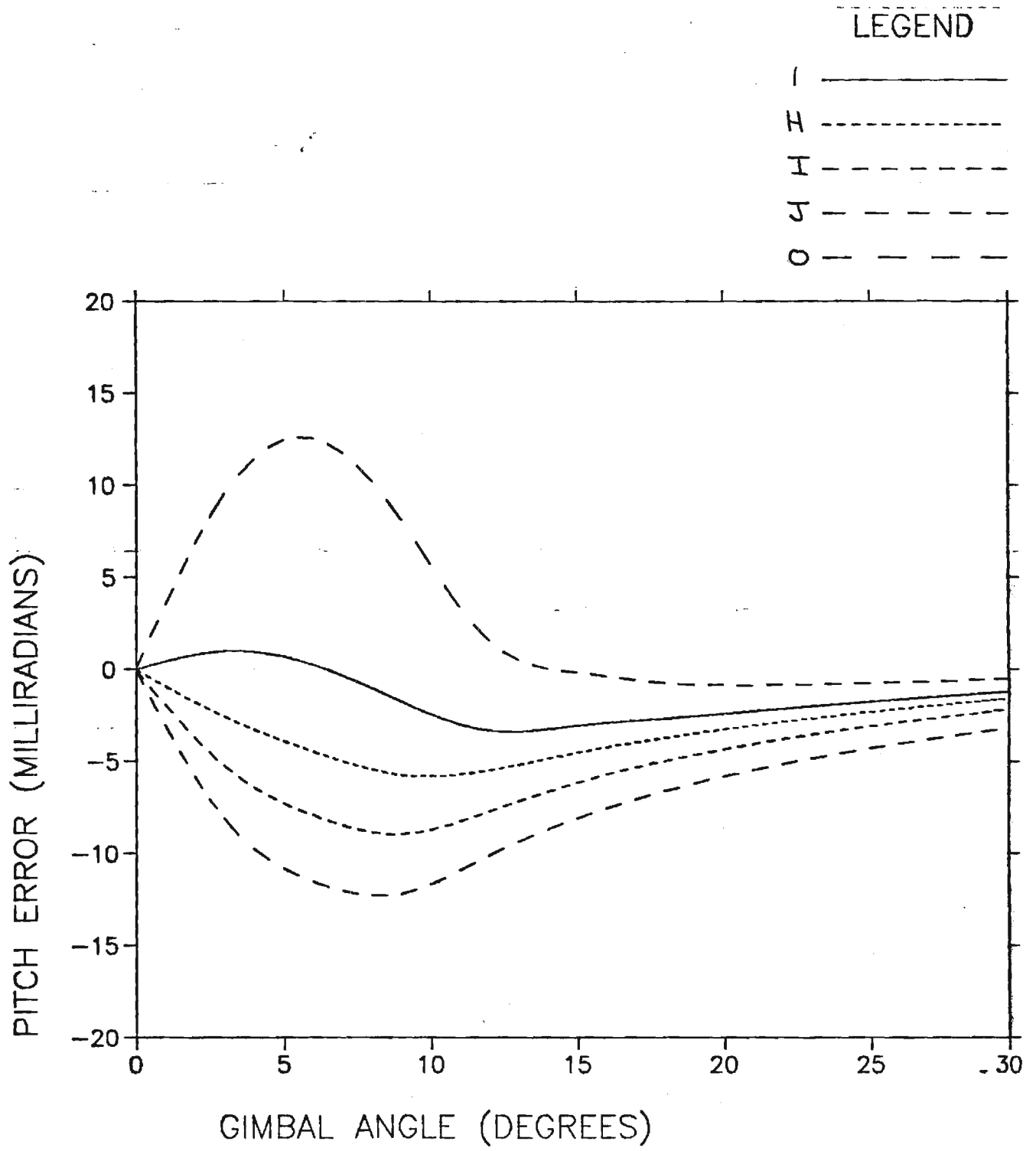


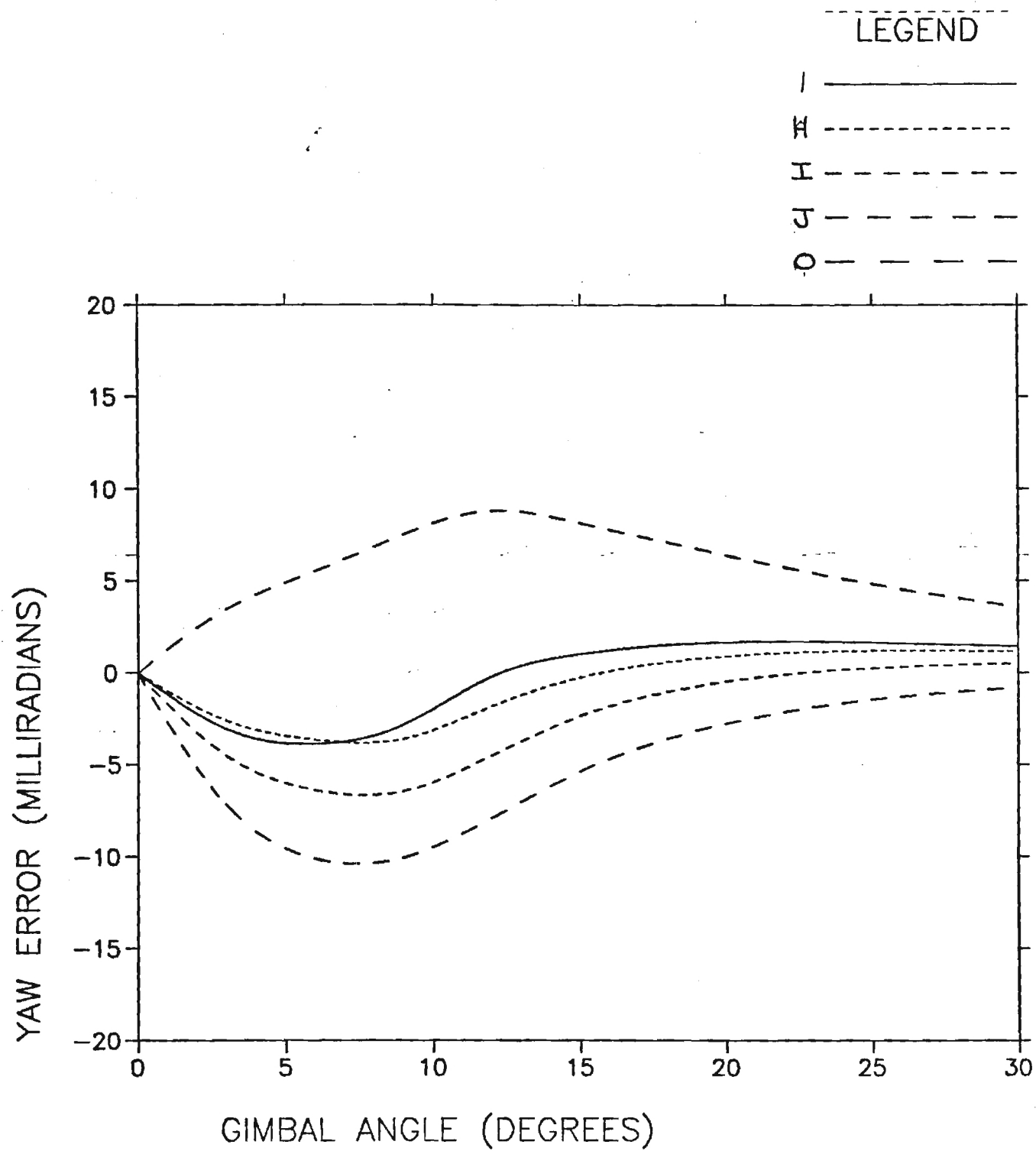
APPENDIX E

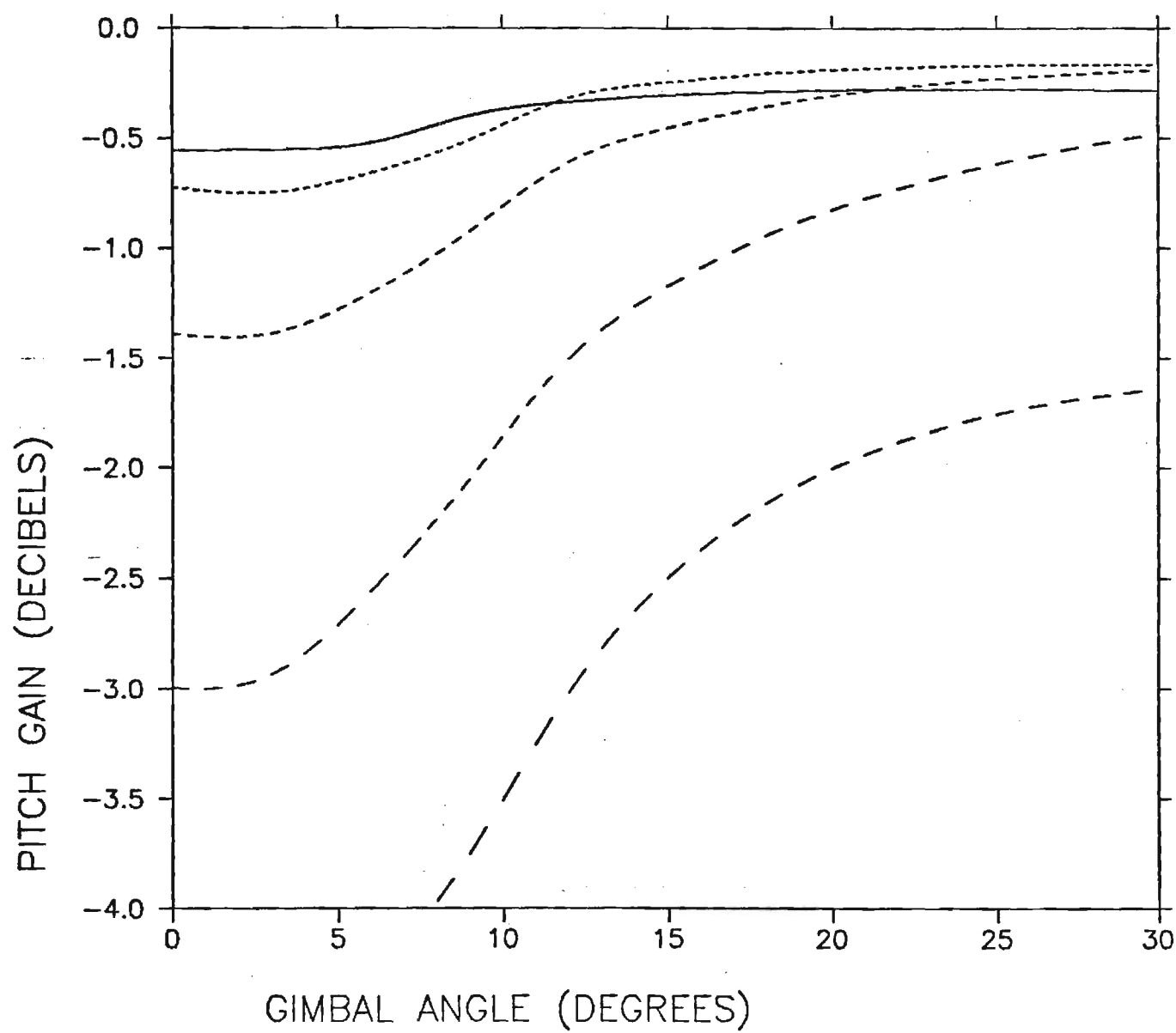
FUSED SILICA RADOME PERFORMANCE

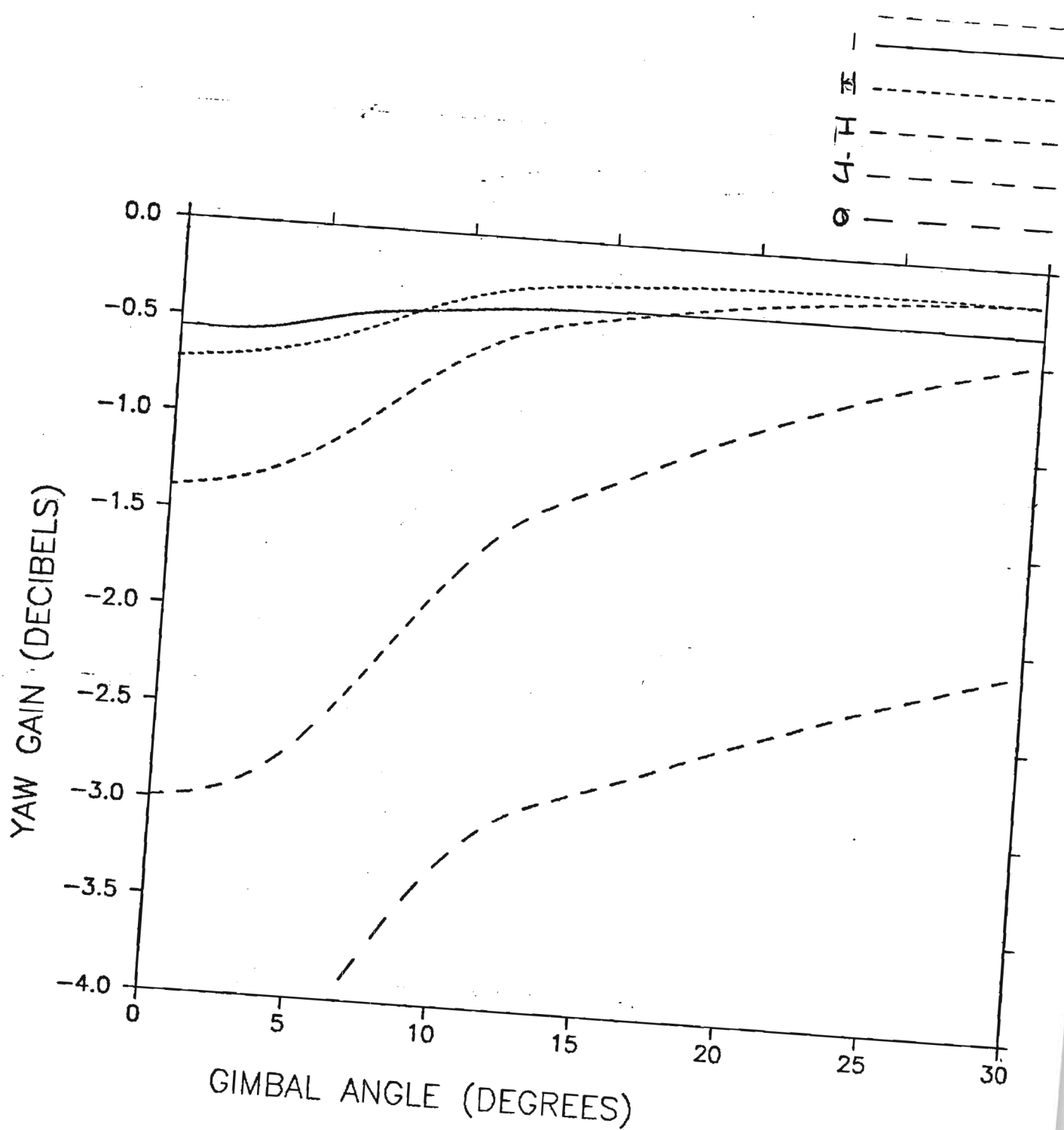










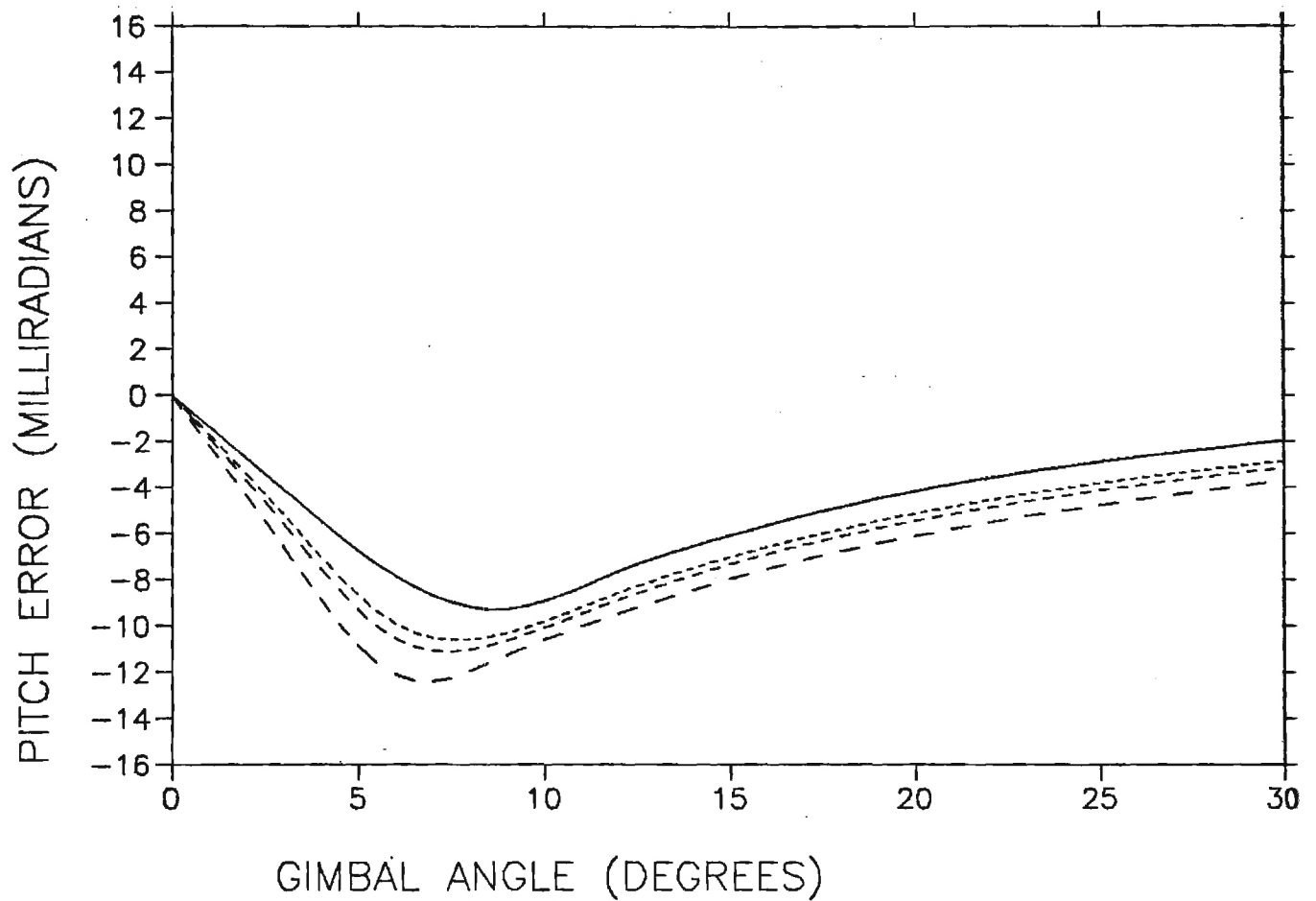


APPENDIX F

EFFECTS OF DISTANCE ON BSE ALGORITHMS

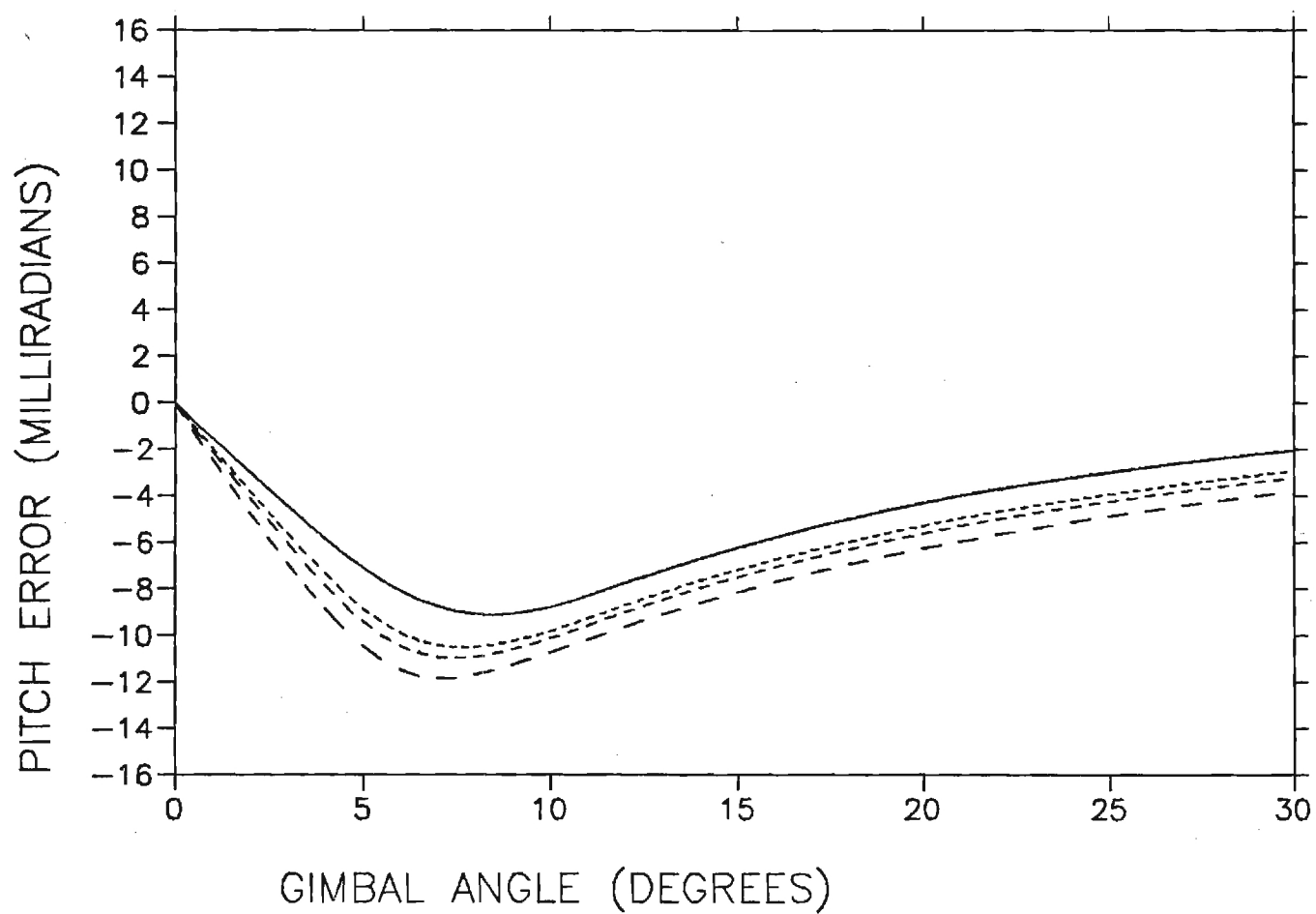
LEGEND

NULL SKR, $R=\infty$
 " $R=40'$, 100dB
 " $R=30'$, 100dB
 " $R=20'$, 100dB



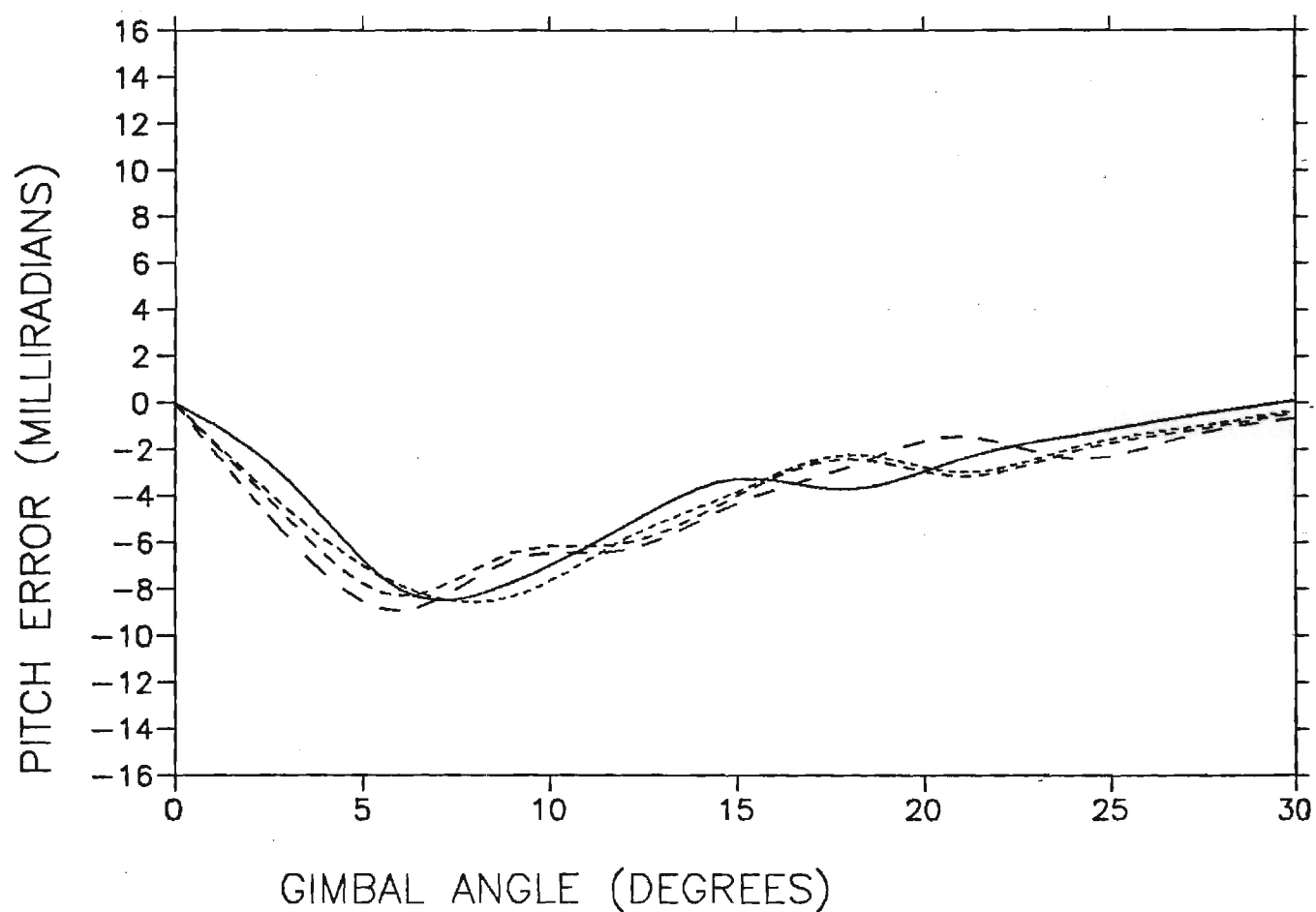
LEGEND

2-POINT, $R=\infty$
 " $R=40'$, 100dB
 --- 30'
 --- 20'



LEGEND

1-POINT, $R=\infty$
 " $R=40'$, 100dB
 " $R=30'$, 100dB
 " $R=20'$, 100dB



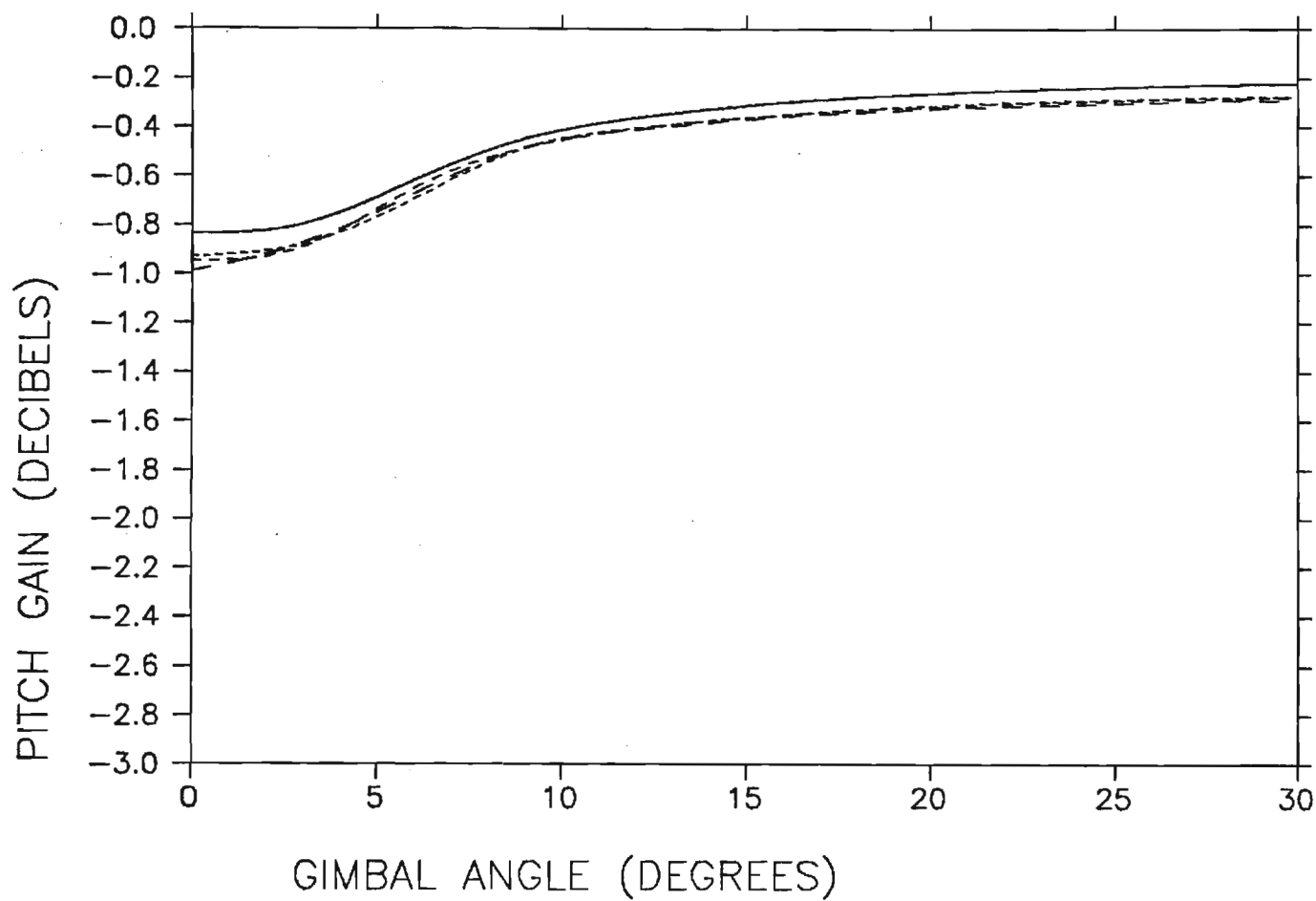
LEGEND

NULL SKIR, $R=\infty$

" $R=40'$, 100dB

" $R=30'$, 100dB

" $R=20'$, 100dB



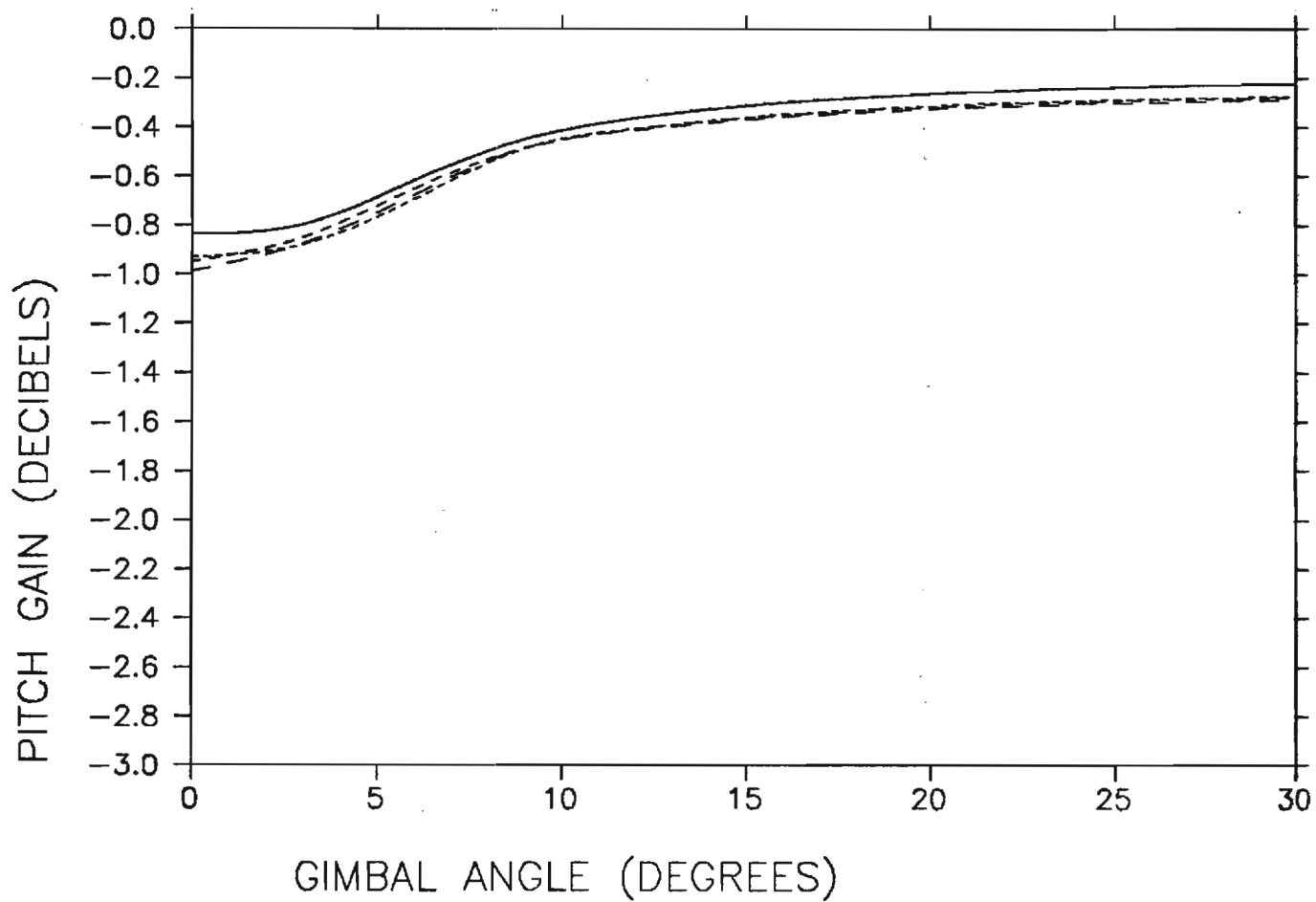
LEGEND

2-Point, $R=\infty$

" 100dB, $R=40'$

 $R=30'$

 $R=20'$



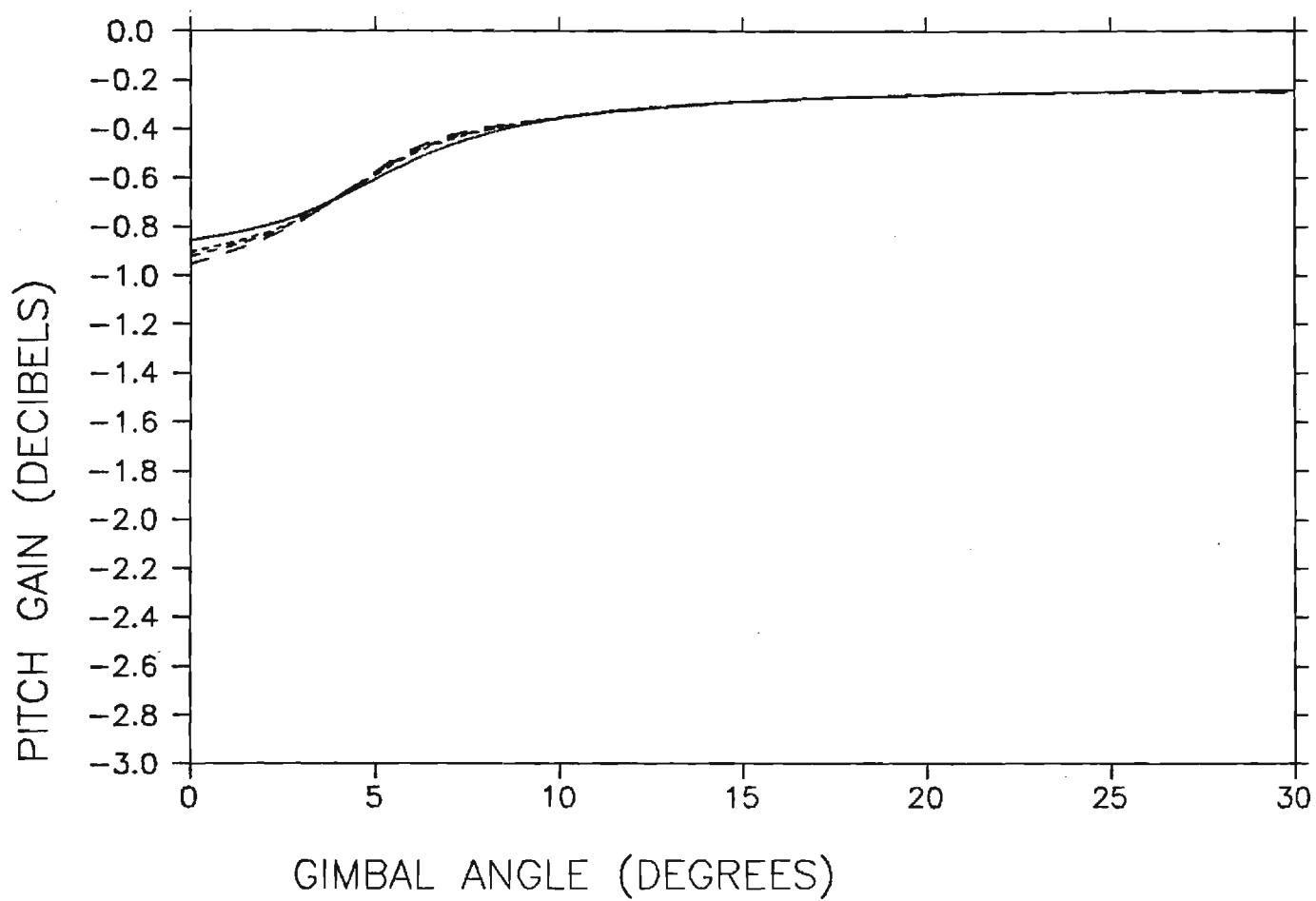
LEGEND

1-Point, $R=\infty$

" $R=40'$, 100dB

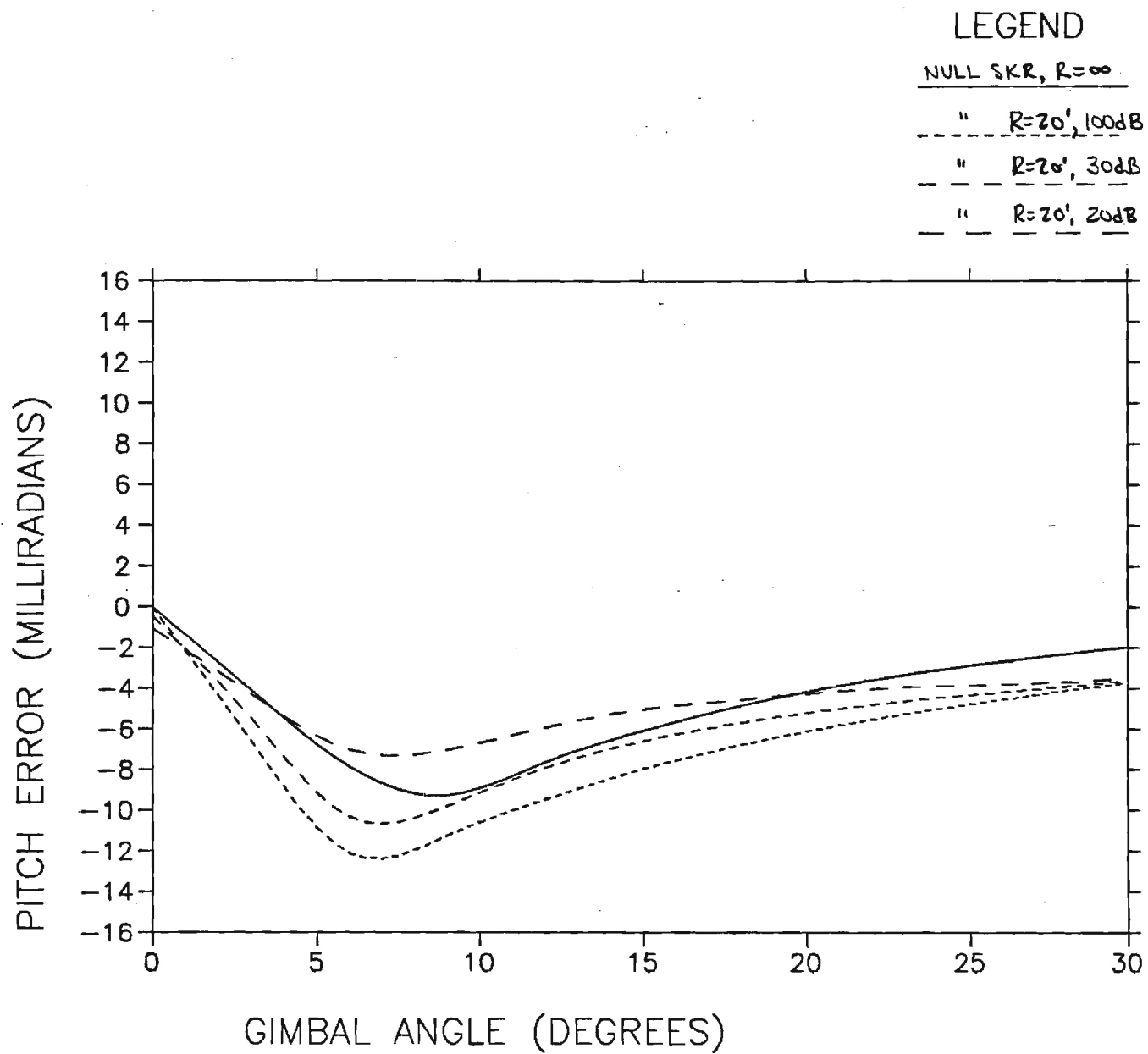
" $R=30'$, 100dB

" $R=20'$, 100dB



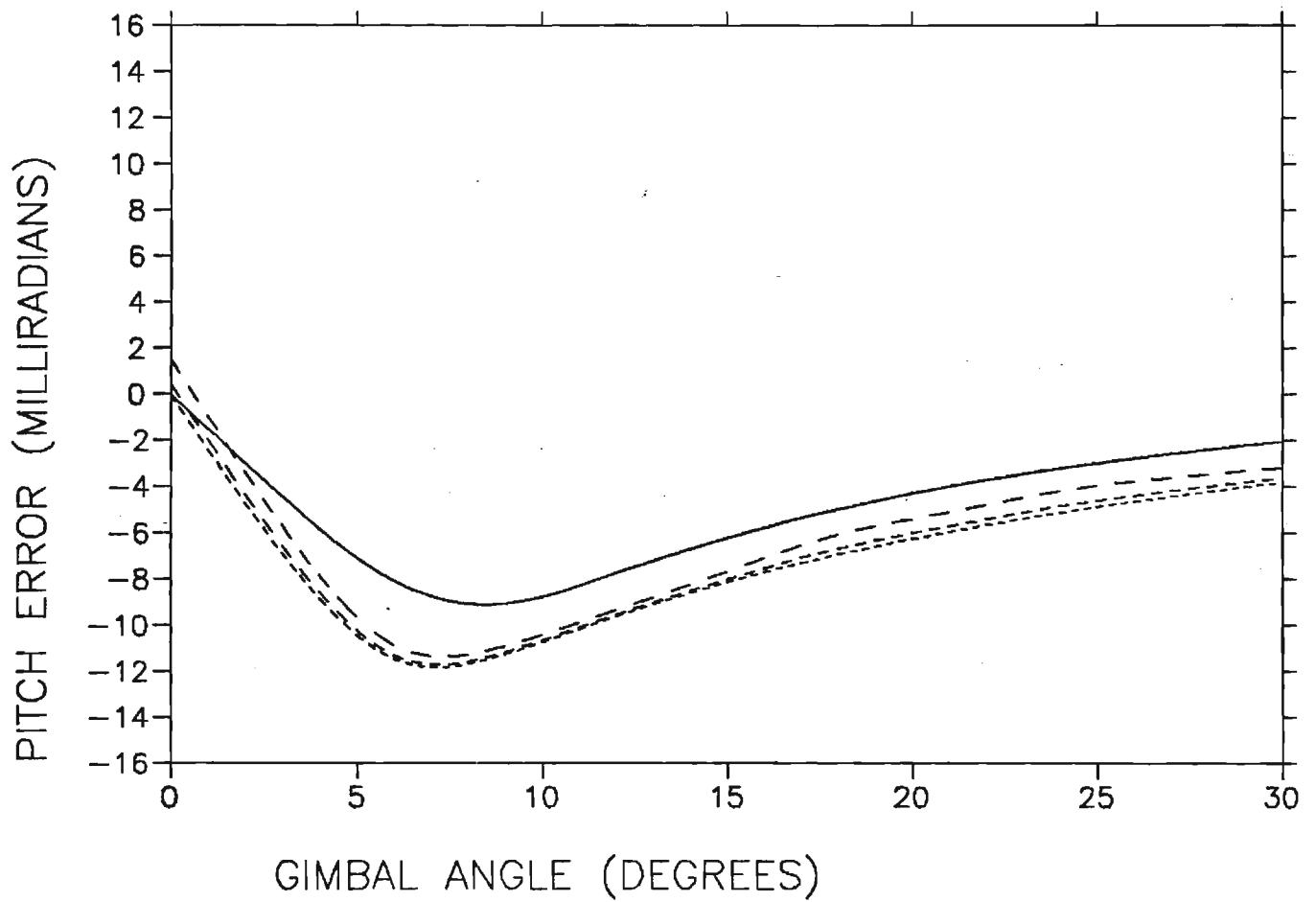
APPENDIX G

EFFECTS OF REFLECTIONS ON BSE ALGORITHMS



LEGEND

Z-POINT, $R=\infty$
" $R=20'$, 100dB
 $R=20'$, 30dB
 $R=20'$, 20dB



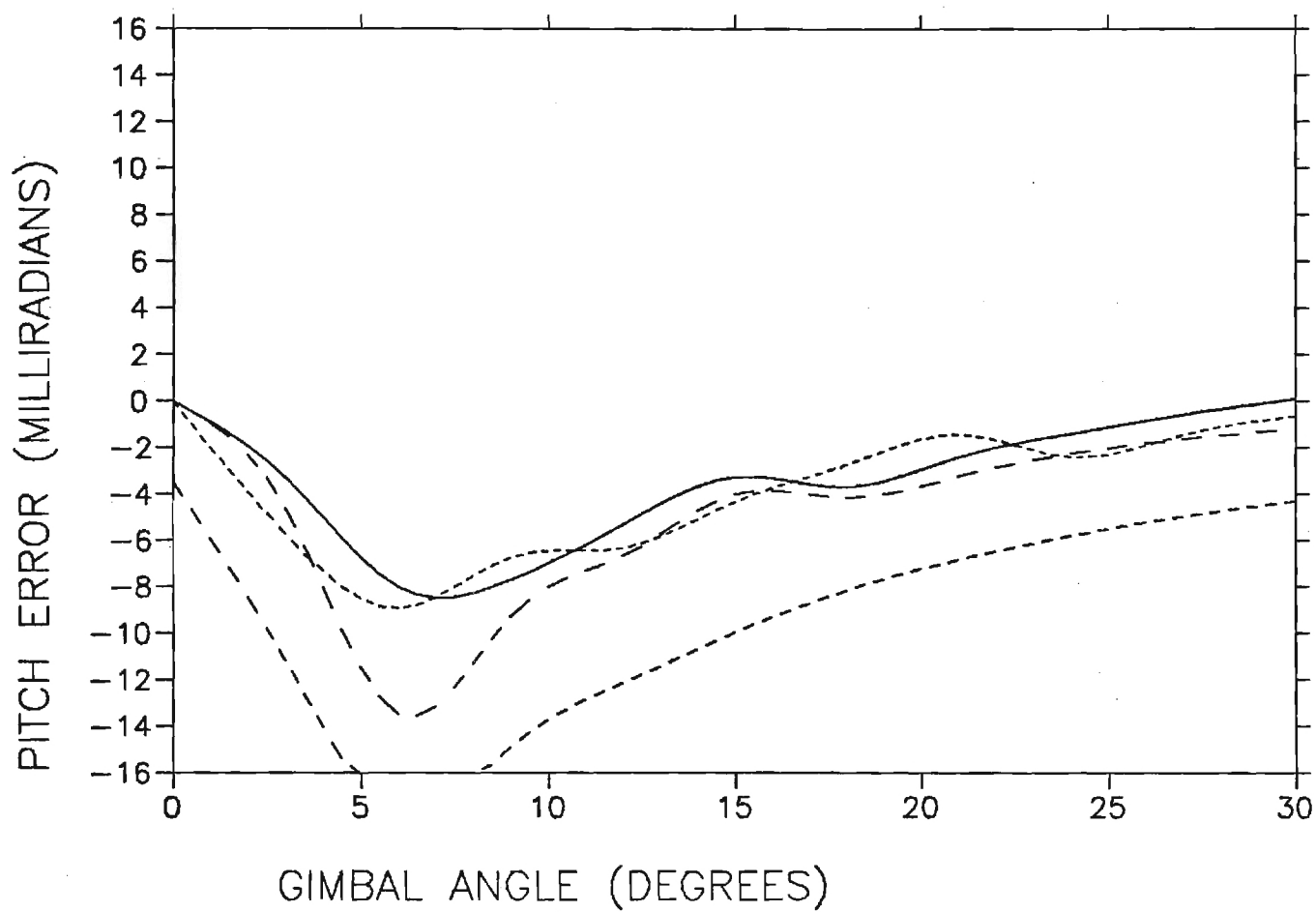
LEGEND

1-POINT, $R=\infty$

1-POINT, $R=20'$, 100dB

1-POINT, $R=20'$, 30dB

" $R=20'$, 20dB



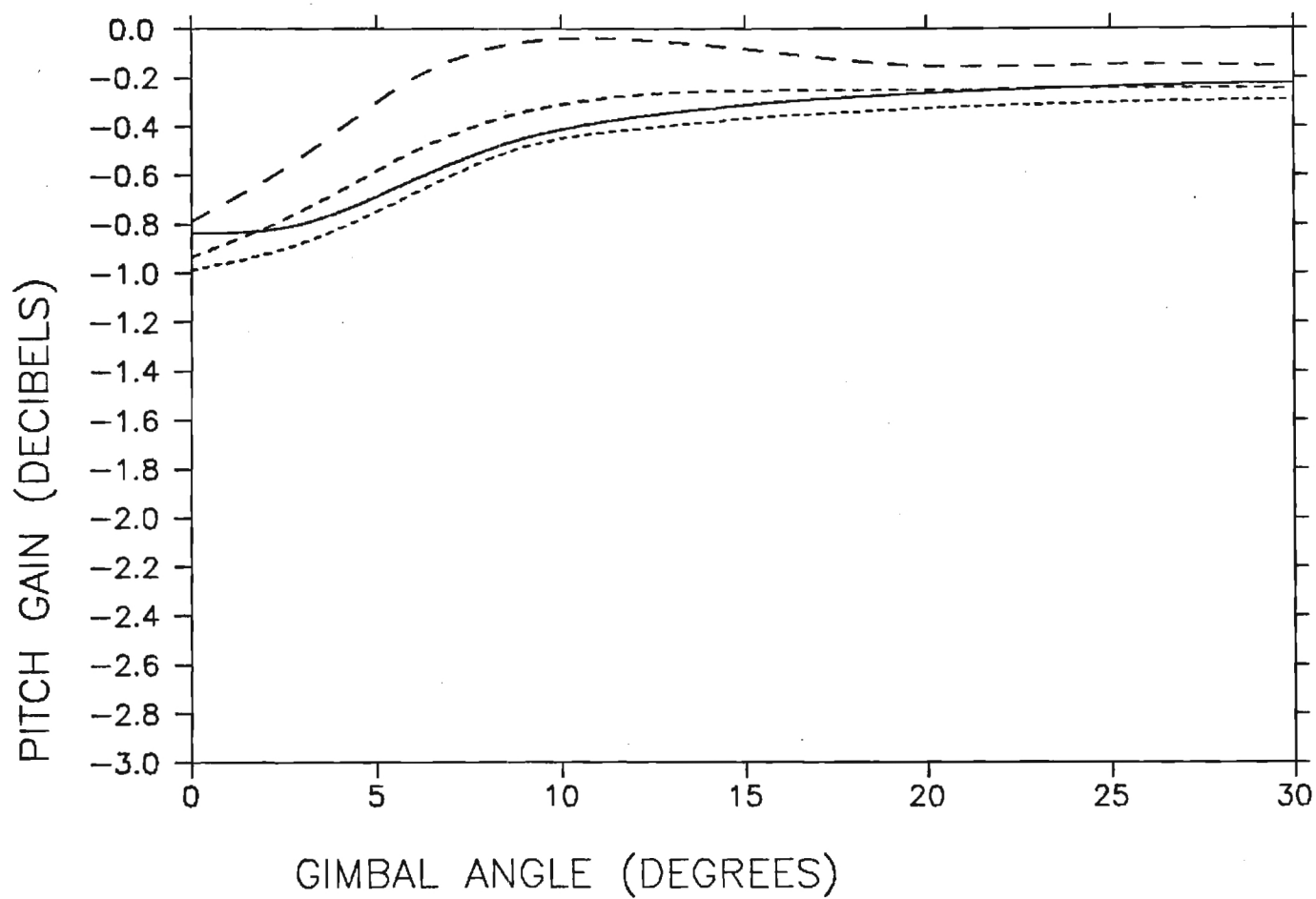
LEGEND

NULL SKR, $R=\infty$

" $R=20'$, 100dB

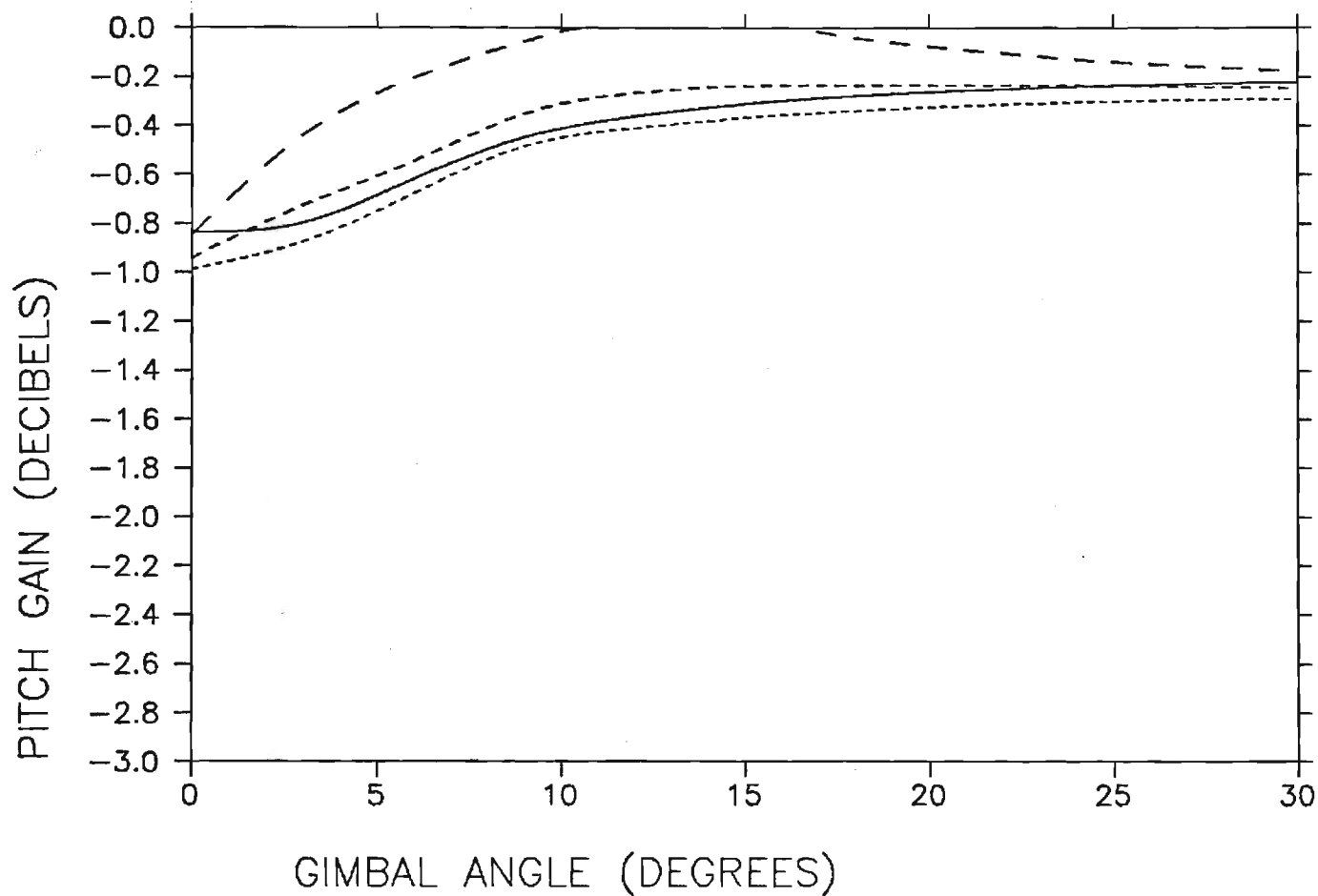
" $R=20'$, 30dB

" $R=20'$, 20dB



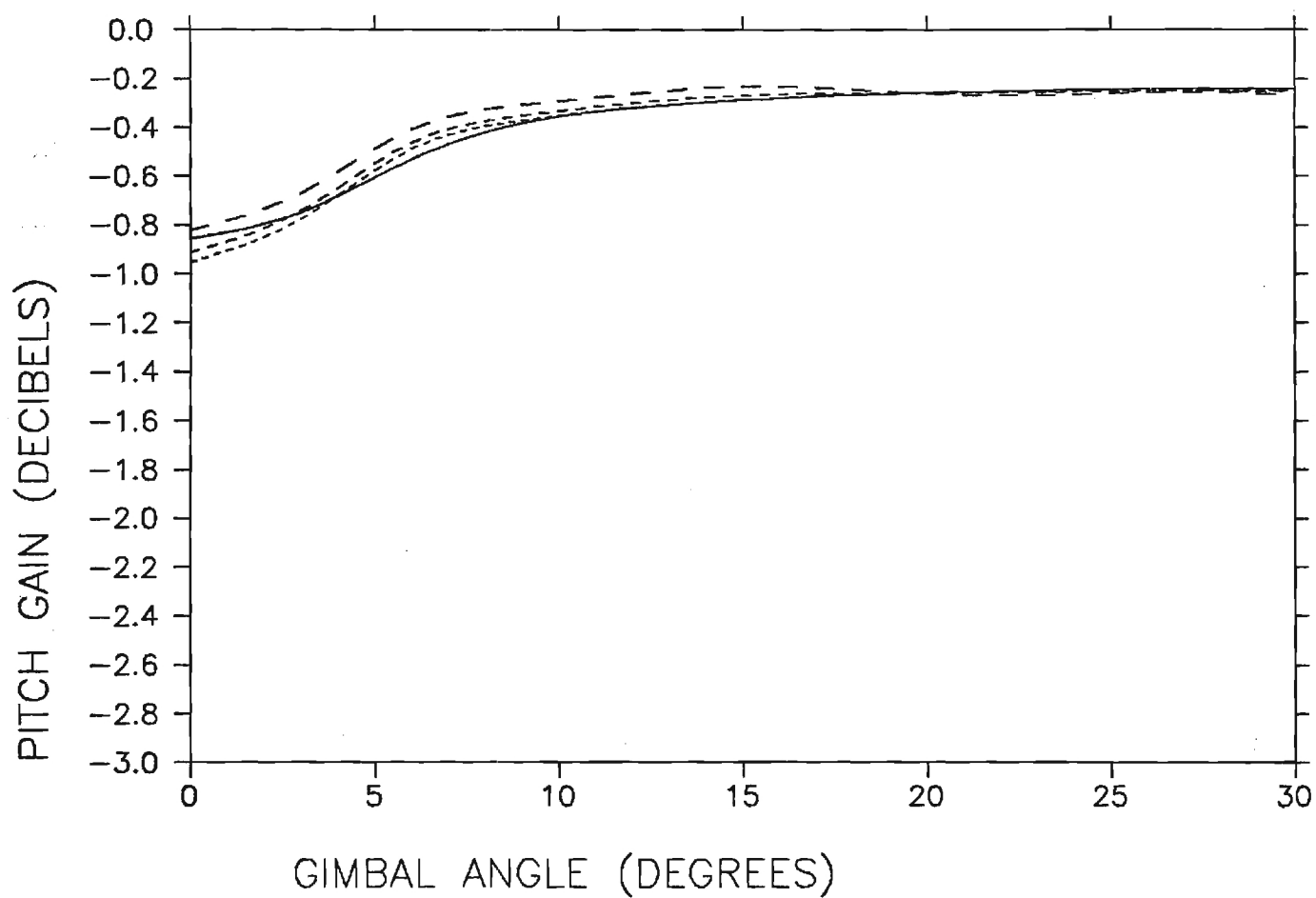
LEGEND

Z-Point, R=∞	
" R=20', 100dB	
" " 30dB	
" " 20dB	



LEGEND

- 1-Point, $R=\infty$
- " $R=20'$, 100dB
- " $R=20'$, 30dB
- " $R=20'$, 20dB



APPENDIX H

EFFECTS ON FREQUENCY ON BSE ALGORITHMS

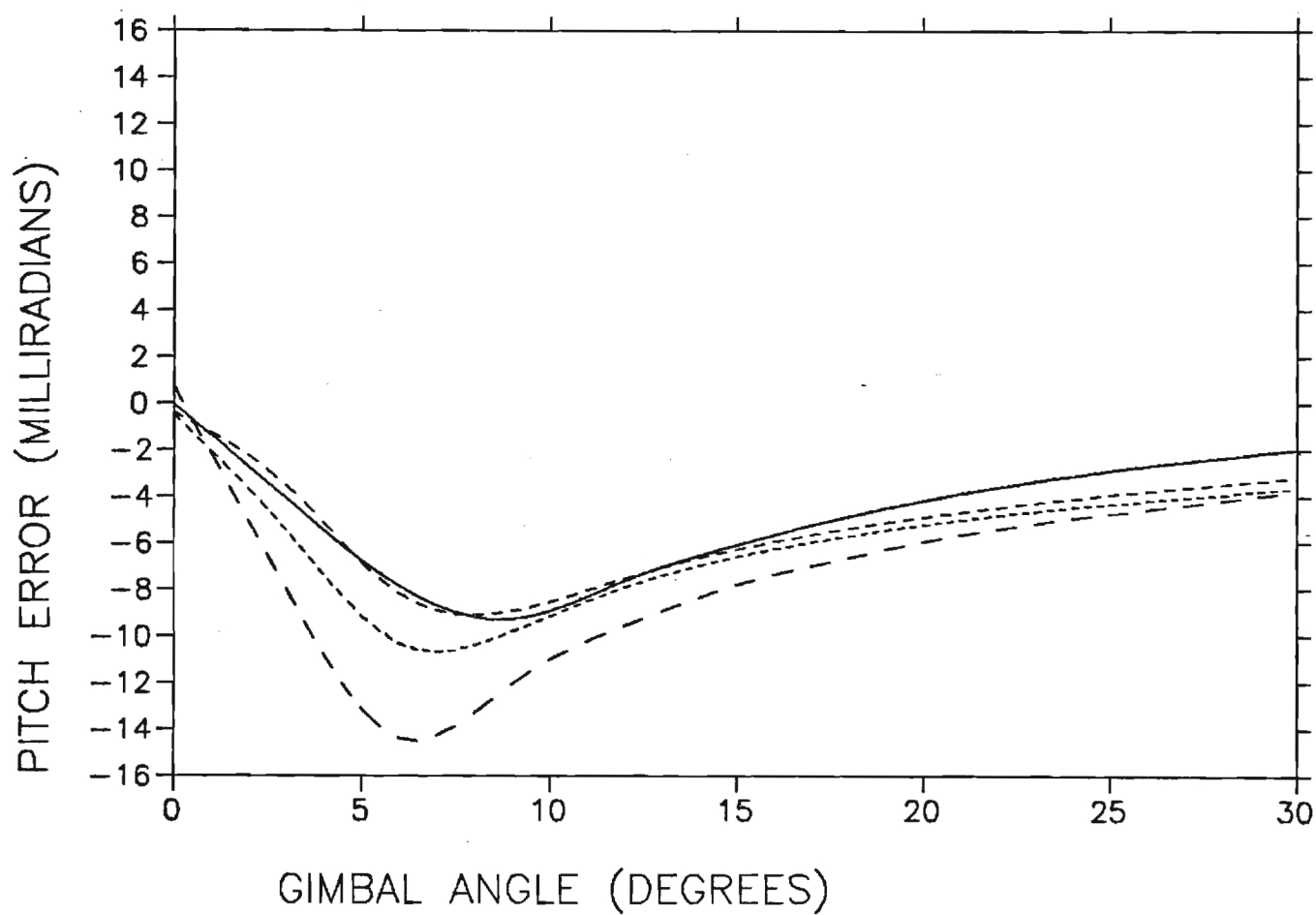
LEGEND

NULL SKR, $R=\infty$, f_0

$R=20''$, 30dB, f_0

 " 1.01 f_0

 " .99 f_0



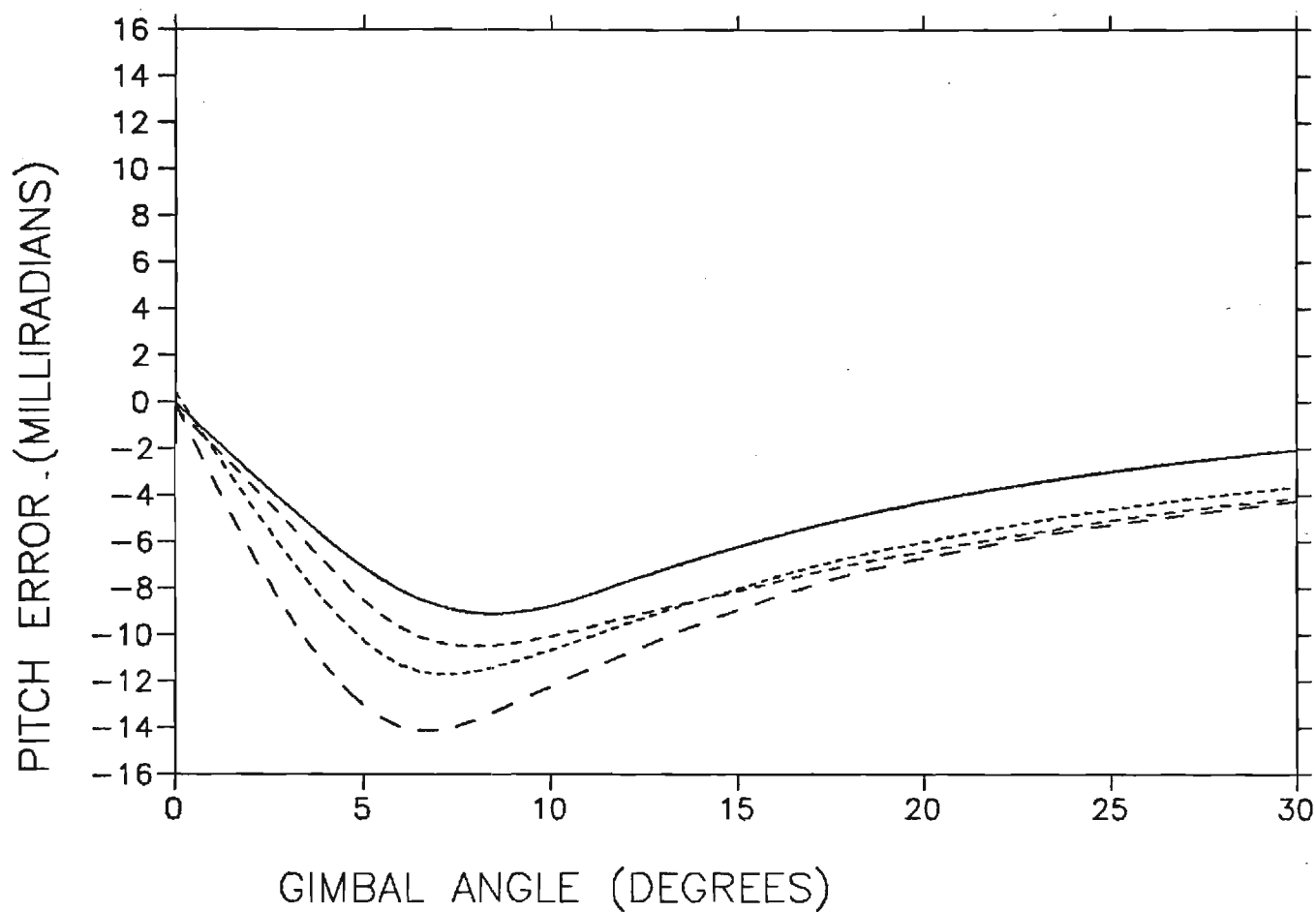
LEGEND

2-Point, $R=\infty$, f_0

" $R=20', 30dB, f_0$

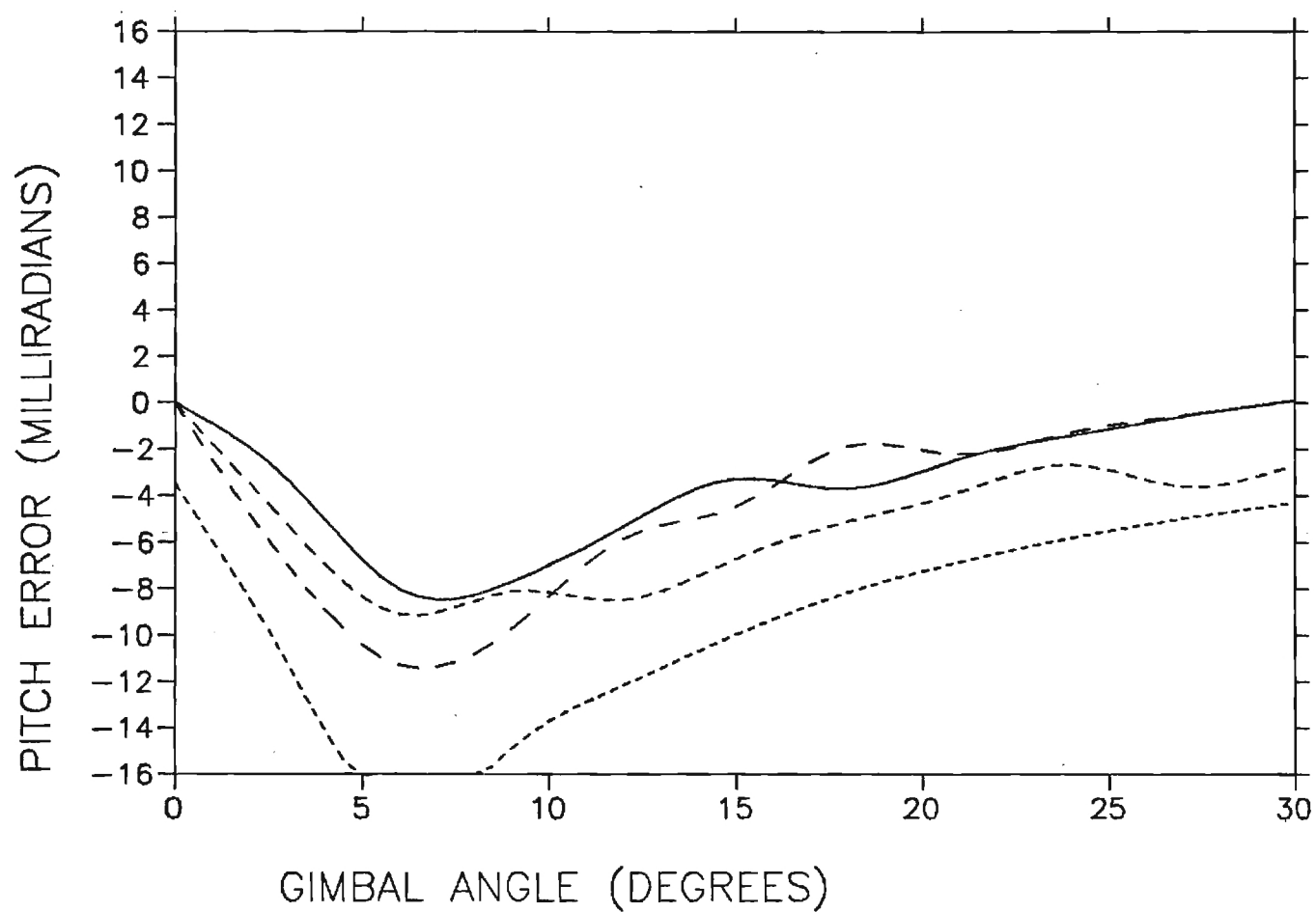
" $1.01f_0$

" $.99f_0$



LEGEND

1-Point, $R=\infty$, f_0
 " $R=20'$, $300B$, f_0
 " $1.01f_0$
 " $.99f_0$



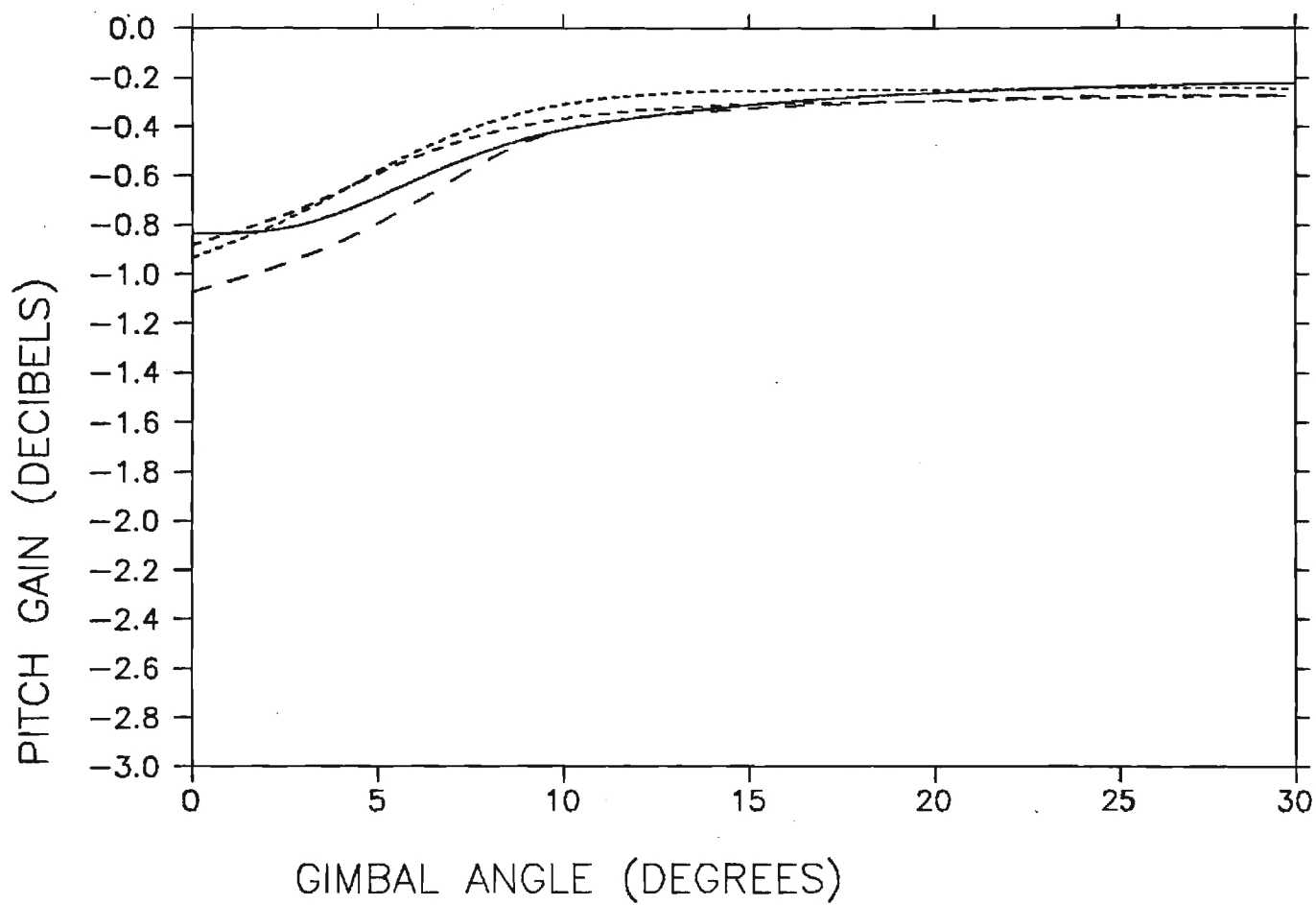
LEGEND

NULLSKR, $R=\infty$, f_0

" $R=20'$, 30dB, f_0

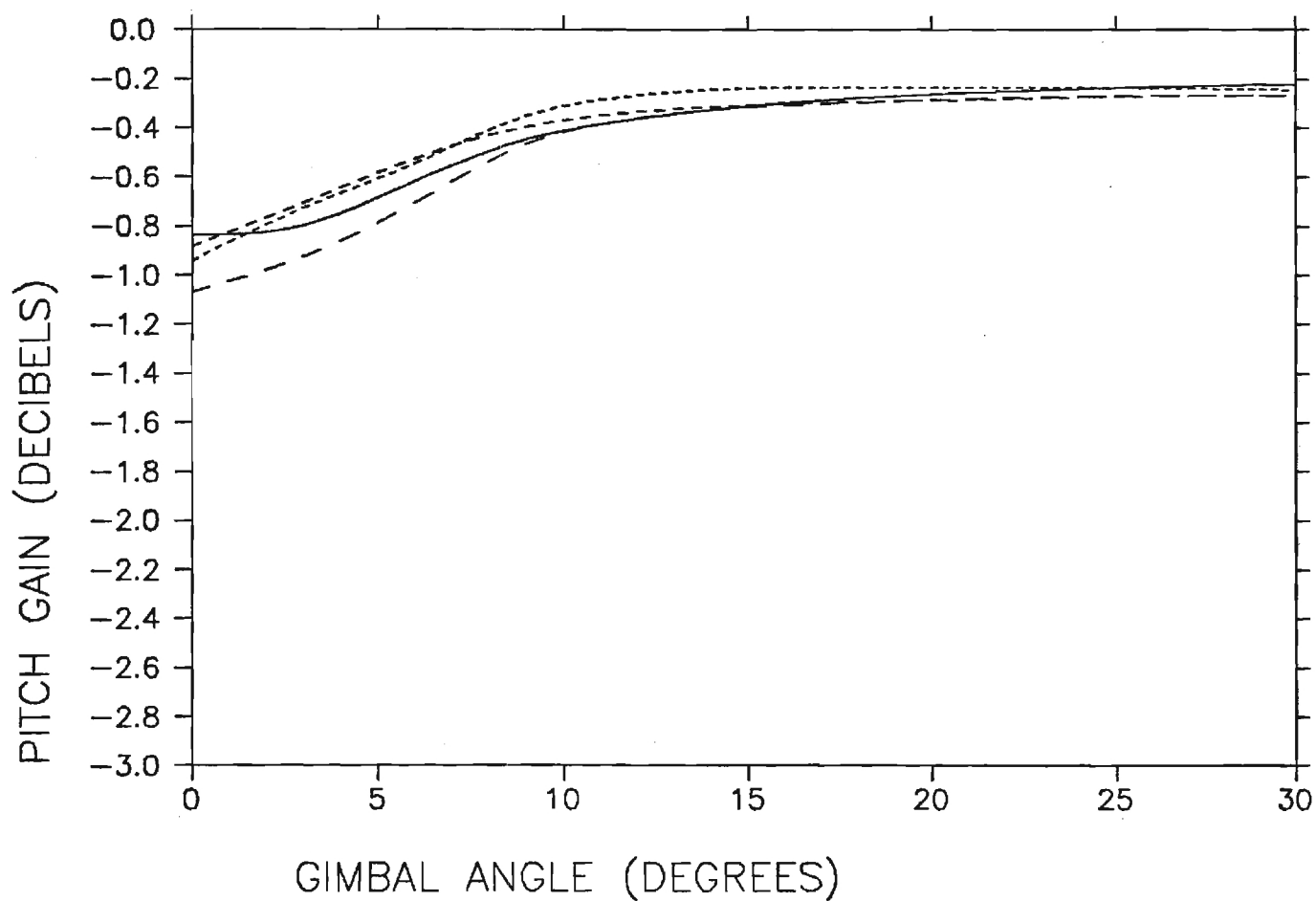
" $1.01 f_0$

" $.99 f_0$



LEGEND

Z-Point, $R=\infty$, f_0
" $R=20'$, 3dB, f_0
" 1.01 f_0
" .99 f_0



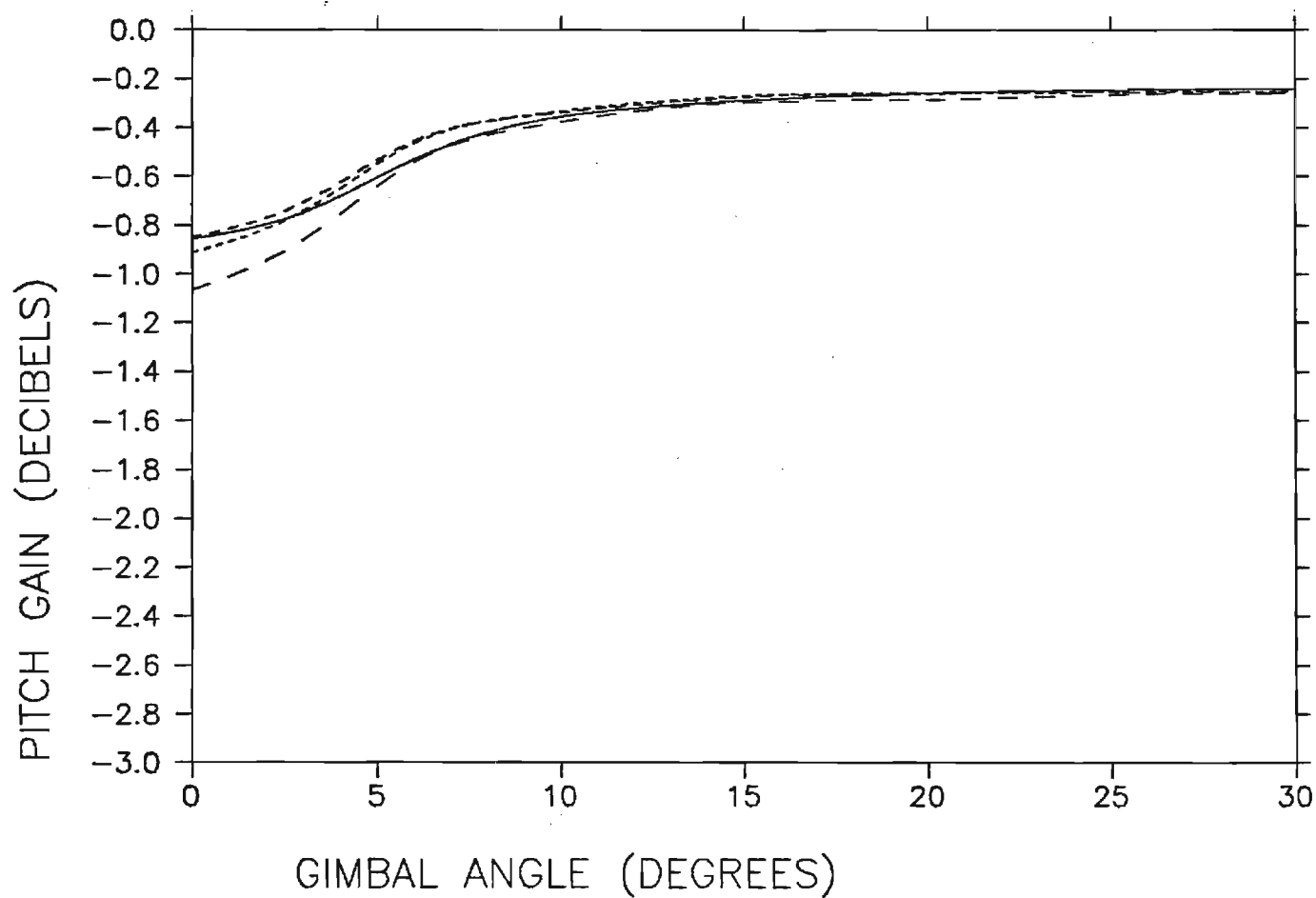
LEGEND

1-Point, $R=\infty$, f_0

" $R=20'$, $30dB$, f_0

" $1.01 f_0$

" $.99 f_0$



Final Technical Report

RADOME DESIGN AND BORESIGHT ERROR MEASUREMENT SIMULATION

By

Gene K. Huddleston

Submitted to

U. S. ARMY MISSILE LABORATORY

DRSMI-RDF

REDSTONE ARSENAL, ALABAMA 35898

Under

Delivery Order No. 0015

Prime Contract DAAH01-83-D-A013

Georgia Tech Project E21-636

November 1983

GEORGIA INSTITUTE OF TECHNOLOGY

A Unit of the University System of Georgia

Engineering Experiment Station

Atlanta, Georgia 30332



1983



The views, opinions, and/or findings contained in this report are those of the authors and should not be construed as an official Department of the Army position, policy, or decision, unless so designated by other documentation.

REPORT DOCUMENTATION PAGE		READ INSTRUCTIONS BEFORE COMPLETING FORM
1. REPORT NUMBER	2. GOVT ACCESSION NO.	3. RECIPIENT'S CATALOG NUMBER
4. TITLE (and Subtitle) Radome Design and Boresight Error Measurement Simulation		5. TYPE OF REPORT & PERIOD COVERED Final Report 5/12/83 - 9/30/83
		6. PERFORMING ORG. REPORT NUMBER E21-636
7. AUTHOR(s) G. K. Huddleston		8. CONTRACT OR GRANT NUMBER(s) DAAH01-83-D-A013
9. PERFORMING ORGANIZATION NAME AND ADDRESS School of Electrical Engineering Georgia Institute of Technology Atlanta, Georgia, 30332		10. PROGRAM ELEMENT, PROJECT, TASK AREA & WORK UNIT NUMBERS Delivery Order 0015
11. CONTROLLING OFFICE NAME AND ADDRESS DRSMI-RDF Redstone Arsenal, Alabama, 35898		12. REPORT DATE November 1983
		13. NUMBER OF PAGES
14. MONITORING AGENCY NAME & ADDRESS (if different from Controlling Office)		15. SECURITY CLASS. (of this report) Unclassified
		15a. DECLASSIFICATION/DOWNGRADING SCHEDULE
16. DISTRIBUTION STATEMENT (of this Report)		
17. DISTRIBUTION STATEMENT (of the abstract entered in Block 20, if different from Report)		
18. SUPPLEMENTARY NOTES		
19. KEY WORDS (Continue on reverse side if necessary and identify by block number) Radome analysis; ablative radomes; boresight error		
20. ABSTRACT (Continue on reverse side if necessary and identify by block number) The design of an ablative radome for supersonic missile seeker applications at microwave frequencies is described. The results of a computer simulation of three boresight error measurement methods are also presented.		

**RADOME DESIGN AND
BORESIGHT ERROR MEASUREMENT SIMULATION**

Final Technical Report on Project E-21-636

By

Gene K. Huddleston
School of Electrical Engineering
Georgia Institute of Technology
Atlanta, Georgia 30332

For

M. M. Hallum
U.S. Army Missile Command
DRSMI-RDF
Redstone Arsenal, AL 35898

Under

Delivery Order 0015

DAAH01-83-D-A013

November 1983

FOREWORD

This report was prepared by the School of Electrical Engineering, Georgia Institute of Technology, Atlanta, Georgia, under Delivery Order 0015 of BOA DAH001-83-D-A013. The report author is Gene K. Huddleston, Associate Professor, School of Electrical Engineering.

The work was performed for the U.S. Army Missile Command under the direction of M. M. Hallum (DRSMI-RDF), K. N. Letson (-RLA), and Steven P. Risner (-RLA).

This report was submitted on November 30, 1983.

The views, opinions, and/or findings contained in this report are those of the author and should not be construed as an official Department of the Army position, policy, or decision, unless so designated by other documentation.

TABLE OF CONTENTS

	<u>Page</u>
FOREWORD	i
1. INTRODUCTION AND SUMMARY.....	1
2. ABLATIVE AND CERAMIC RADOME DESIGN.....	3
2.1 Introduction.....	3
2.2 Flat Panel Analysis.....	5
2.3 Ablative Radome Analysis for Uniform Wall Thickness.....	6
2.4 Ablative Radome with Tapered Wall Thickness.....	6
2.5 Fused Silica Radome Design.....	8
3. BORESIGHT ERROR MEASUREMENT SIMULATION.....	9
3.1 Introduction.....	9
3.2 BSE Algorithms.....	11
3.3 Effects of Distance.....	14
3.4 Effects of Reflections.....	16
3.5 Effects of Frequency.....	16
4. CONCLUSIONS AND RECOMMENDATIONS.....	17
4.1 Ablative and Ceramic Radomes.....	17
4.2 BSE Measurement Simulation.....	17
REFERENCES.....	19
APPENDIX A - FLAT PANEL ANALYSIS RESULTS.....	21
APPENDIX B - UNIFORM ABLATIVE RADOME PERFORMANCE.....	29
APPENDIX C - TAPERED ABLATIVE RADOME PERFORMANCE.....	37
APPENDIX D - TAPERED SUBSTRATE RADOME PERFORMANCE.....	45
APPENDIX E - FUSED SILICA RADOME PERFORMANCE.....	53
APPENDIX F - EFFECTS OF DISTANCE ON BSE ALGORITHMS.....	61
APPENDIX G - EFFECTS ON REFLECTIONS ON BSE ALGORITHMS.....	69
APPENDIX H - EFFECTS OF FREQUENCY ON BSE ALGORITHMS.....	77

CHAPTER 1

INTRODUCTION AND SUMMARY

This report describes the electrical design of an ablative and a ceramic radome for a supersonic microwave seeker application. In addition, the results of a computer simulation of the effects of the anechoic chamber environment on boresight error measurements are presented.

Chapter 2 describes the electrical design of tangent ogive ($L/D = 3$) ablative radome consisting of a load-bearing substrate material ($\epsilon_r = 4.50$, $\tan\delta = .008$) and a fibre-loaded Teflon ablator outer layer ($\epsilon_r = 2.45$, $\tan\delta = .003$). The computed electrical performance of both flat dielectric panels and full scale radomes indicate that the optimum ablative radome design with respect to boresight error slope consists of a thick substrate and a thin ablator. The best performance would be obtained with a half-wave wall of the single substrate material; the optimum two-layer structure is a compromise between the half-wave wall and the ablation requirements.

Boresight error slopes (BSES) less than 5% and radome transmission loss less than 0.6 dB are predicted for the optimum ablative radome configuration consisting of .600" substrate and .060" (uniform) ablator thicknesses. To provide for ablation during flight so as to reach this optimum design at the terminal phase, a tapered ablator (.110" at the tip and .070" at the base of the radome) can be provided having initial BSES < 11% and loss less than 0.6 dB. Hence, a .05" tapered change in ablator thickness results in a change in maximum BSES from 11% to 5%.

The design of a comparable fused silica radome is also described in Chapter 2. Designs having uniform wall thickness and an asymmetrical wall thickness design are examined. The ceramic radome design work is not complete.

Chapter 3 describes the results of a computer simulation of a radome boresight error measurement facility. The simulation quantifies the effects of reflections from the anechoic chamber boundaries, the effects of frequency drifts during measurement, and the effects of separation distance between the source antenna and the radome/antenna combination under test (RAUT).

Measurement results are simulated for three BSE measurement techniques: null seeker, offset 1-point method, and a two-point method. All three methods are more sensitive to the distance of separation than to reflections. The two-point method gives approximately the same results as the null seeker. All three methods show significant sensitivity to even small (1%) frequency changes.

The simulation results also show that the offset 1-point method of BSE measurement yields widely varying results and is deemed unsuitable for use. A modified (non-offset) 1-point method of measurement does yield results comparable to the null seeker for large separation distance and no reflections; however, the performance of the modified 1-point method has not been fully studied.

CHAPTER 2

ABLATIVE AND CERAMIC RADOME DESIGN

2.1 Introduction

The geometry of the optimum ablative radome design is shown in Figure 2-1. The placement of the antenna, and its radiating characteristics, are also indicated. A metal rain cap is located at a distance of 45.42" from the radome base as indicated by the large tic mark extending above the horizontal axis. The location of the bulkhead is indicated by the other vertical tic mark at 5.32".

Several design constraints were imposed:

(1) The outer shape of the radome was specified as a tangent ogive with base diameter $D_{OS} = 16.00"$ and radius of curvature $R_{OS} = 148.03"$.

(2) The radome wall thickness could not exceed 0.75" lest the antenna would not gimbal.

(3) The minimum substrate thickness was 0.35" for structural rigidity and strength.

(4) The minimum ablator thickness must be compatible with expected ablation during flight (~ 0.045" maximum) and manufacturing techniques.

The ablative radome design of Figure 2-1 was arrived at by examining the plane wave transmission properties of several two-layer flat panel designs. From these data, the basic two-layer radome wall design was selected for further refinement using a three-dimensional computer-aided radome analysis [1]. The radome design parameters consisted of substrate and ablator thicknesses at a single frequency. The designs were compared on the basis of boresight error slope (BSES), assuming reasonable (< 1.0 dB) transmission loss. The effects of tapered ablator thickness were also studied.

RADOME RADIAL COORDINATE (INCHES)

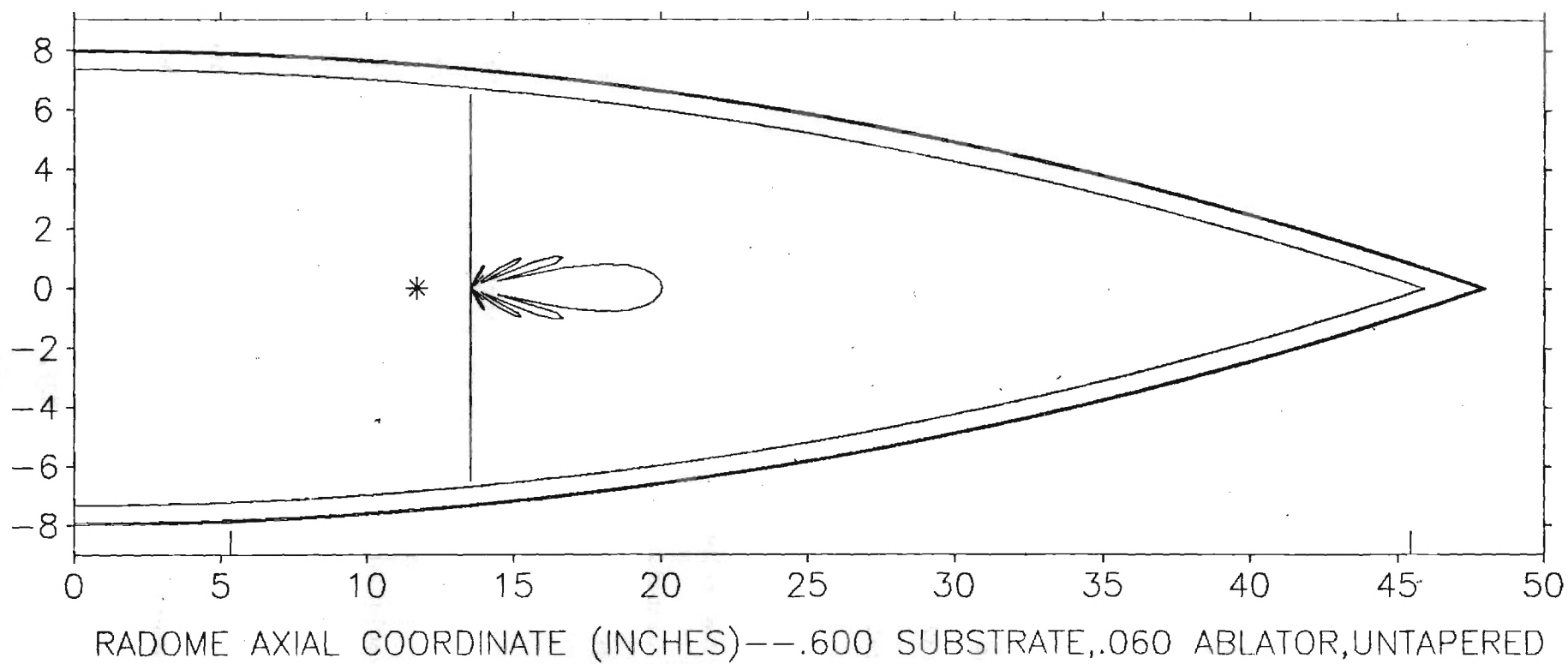


Figure 2-1. Ablative Radome Geometry.

Preliminary performance data for three fused silica radome designs are present in the last section.

2.2 Flat Panel Analysis

The plane wave transmission properties of the two-layer flat panels are shown in Appendix A. Substrate ($\epsilon_r = 4.50$, $\tan\delta = .008$) thicknesses range from 0.25" to 0.600". The ablator thicknesses are shown in each legend. The lefthand ordinate (goes with upper set of curves) is power transmittance for perpendicular polarization (always worse than for the incident electric-field parallel to the plane of incidence). The abscissa is angle of incidence. The righthand ordinate (lower set of curves) is delta insertion phase delay; i.e., $\Delta_{IPD} = IPD_{\perp} - IPD_{\parallel}$.

The flat panel design criteria used were: (1) transmittance greater than 80% over the range of incidence angles expected in the radome; (2) $\Delta_{IPD} \approx 0$ over the same range.

For the tangent ogive shape of Figure 2-1, the largest incidence angle encountered is approximately 72° as determined by drawing a ray normal to the center of the aperture antenna to the tip of the radome. The angle between the ray and the normal to the inner wall is the incidence angle. The lowest angle of incidence is determined by gimbaling the aperture to the expected limit and measuring the normal ray incidence angle on the radome wall. This approximate estimating procedure yields a range of $30^\circ < \theta_i < 72^\circ$.

Examination of the data in Appendix A shows that the thicker substrate designs yield better transmittance and Δ_{IPD} performance. The performance would be best for a 1/2-wave wall of substrate only (.622" @ $\theta_D = 72^\circ$). But it is not possible to conclude from the flat panel results if the 0.550" substrate design will yield better radome BSES performance than the 0.600" substrate design; hence, the need for the following 3-D radome analysis.

2.3 Ablative Radome Analysis for Uniform Wall Thickness

The computed radome performance for five combinations of substrate and ablator thicknesses are shown in Appendix B. Data for both pitch and yaw planes are shown. The ordinates of interest are boresight error slope (BSES), boresight error (BSE), and gain. The abscissa in every case is radome gimbal angle. The legend identifies the five different designs.

Examination of the data in Appendix B clearly reveals that the optimum ablative radome design has a substrate thickness of 0.600" and ablator thickness of 0.060".

2.4 Ablative Radome with Tapered Wall Thickness

The computed performance of six ablative radome designs having tapered wall thickness are presented in Appendix C. The optimum design (designated hereafter as Design 1) is also shown as the standard of comparison. The performance of a over-dimensioned prototype design (Design 0) from which the optimum design and any tapered designs will be machined is also shown.

The tapered designs considered are further identified in Table 2-1. The thickness taper is linear with respect to the axial radome coordinate. The first thickness given in the table is the thickness in the layer at the base of the radome; the second thickness is the thickness of the layer at the tip. Only one thickness is given for the uniform thickness. Table 2-1 also identifies the three fused silica radome designs to be discussed later.

The ablator of Design 6 is tapered to be thicker at the tip as anticipated at the initial point of flight. Design A shows the performance at a later time in flight -- and approaches the optimum design performance (Design 1). Design D shows what happens to the performance if the ablator thickness erodes to zero at the tip.

TABLE 2-1. Identification of Radome Designs

<u>Design No.</u>	<u>Base Diameter</u>	<u>THICKNESS</u>		<u>Remarks</u>
		<u>Substrate Base/Tip</u>	<u>Ablator Base/Tip</u>	
0	16.10	.690	.110	First Delivered Prototype
1	16.00	.600	.060	Optimum Design
6	16.02	.600	.070/.110	Tapered Ablator
A	16.004	.600	.062/.070	Tapered Ablator
D	16.00	.600	.060/.000	Tapered Ablator
E	16.00	.600/.620	.060/.000	Tapered Ablator & Substrate
F	16.00	.600/.640	.060/.000	Tapered Ablator & Substrate
G	16.00	.600/.660	.060/.000	Tapered Ablator & Substrate

H	16.00	.730	0.	Fused Silica Blank
I	16.00	.710	0.	Thinner Wall
J	16.00	Tailored	0.	Tailored SiO ₂

Appendix D shows the effects on radome performance caused by tapering the substrate material for the case where the ablator has eroded to zero thickness at the tip. Designs 1 and D are shown for reference. These data merely show that substrate thickness taper can also be used as a degree of freedom in the design process.

2.5 Fused Silica Radome Design

Computed performance data for three fused silica radome designs are shown in Appendix E. Ablative Designs 0 and 1 are also shown for reference.

Design H is the fused silica "blank" as received from the manufacturer. It would be rough machined to a wall thickness of $0.73" \pm .010"$. Its performance is closer to the optimum ablator performance than the other two SiO_2 designs.

Making the SiO_2 wall thickness thinner (Design I) does not help.

An asymmetrical wall thickness prescription (Design J) does not help the performance of the fused silica radome, where the average wall thickness is approximately $0.67"$.

The design of the fused silica radome is not complete.

CHAPTER 3

BORESIGHT ERROR MEASUREMENT SIMULATION

3.1 Introduction

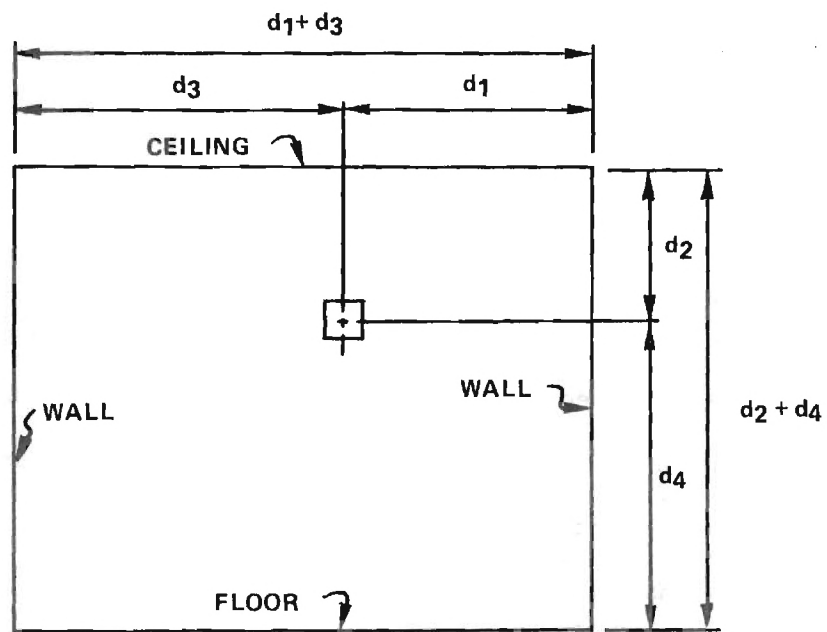
A computer-aided simulation of the boresight error measurement procedure and facility was carried out to quantify the effects of separation distance, wave reflections from anechoic chamber boundaries, and frequency drifts.

The 3-D radome analysis program used earlier to design the ablative and ceramic radomes was modified to include the near-field and reflection effects as illustrated in Figure 3-1(b). Waves emanate from the source antenna in the directions indicated by the rays (one arrowhead). These direct rays impinge on the radome as shown. Note that the angles of incidence on the radome wall for these rays are different than those of a true plane wave (horizontal rays).

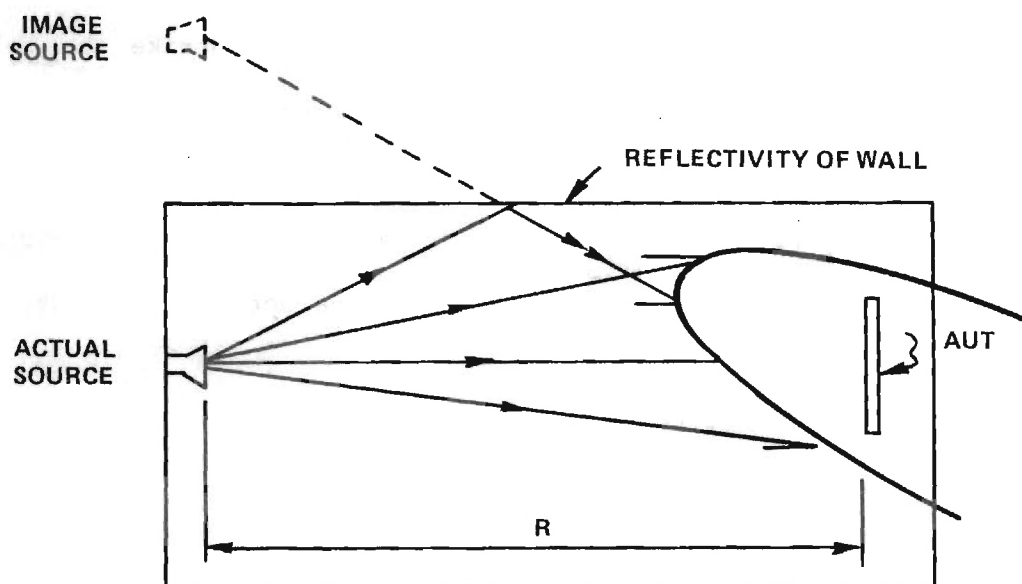
Some of the rays emanating from the source antenna strike the walls, floor, and ceiling of the chamber and are reflected onto the radome. These reflections can be conveniently included using image sources, one for each boundary of the chamber (4 total). Each image is mirrored into the associated boundary and is given strength E' with respect to the actual source strength E_0 according to

$$\frac{E'}{E_0} = 10^{(-R_{dB}/20.)} \quad (3-1)$$

where R_{dB} is the reflectivity of the chamber wall in decibels. The reflectivity is assumed to be independent of incidence angle.



(a) VIEW OF SOURCE ANTENNA AT FAR END OF CHAMBER.



(b) TOP VIEW OF CHAMBER SHOWING ONE IMAGE SOURCE.

FIGURE 3 - 1 GEOMETRY OF BORESIGHT ERROR MEASUREMENT SIMULATION.

3.2 BSE Algorithms

Three BSE measurement procedures or algorithms were simulated: null seeker, offset 1-point method, and 2-point method. In the null seeker method, the computation is done such that the source is moved around until nulls are obtained in each Δ/ϵ signal channel of the monopulse antenna. The direction to the source when it is in the null position is defined as the boresight error.

Figure 3-2 shows tracking functions computed for the radome/antenna combination under test (RAUT), where the tracking functions in elevation and azimuth are defined by

$$f_{EL} \triangleq \text{Im} \left\{ \frac{\Delta_{EL}}{\sum} \right\} \quad (3-2a)$$

$$f_{AZ} \triangleq \text{Im} \left\{ \frac{\Delta_{AZ}}{\sum} \right\} \quad (3-2b)$$

Four computed tracking functions are shown in Figure 3-2 as indicated on each graph. The tracking functions are graphed versus the angle θ from boresight in a diagonal plane defined by $x_A = y_A$ in antenna coordinates. Without the radome, f_{EL} and f_{AZ} are almost identical so that only one solid graph is shown for both functions. When the radome is placed over the antenna and aligned with the true antenna boresight (Pitch = 0° , Yaw = 0°), the tracking functions are slightly different as indicated by the $AZ(0^\circ, 0^\circ)$ and $EL(0^\circ, 0^\circ)$ graphs. Note also that the slopes of these functions (monopulse error slope MES) are different but are approximately equal to the MES of the antenna without the radome. Finally, the offset dash graph $EL(6^\circ, 0^\circ)$ of Figure 3-2 shows the elevation tracking function when the radome is pitched up by 6° ; f_{AZ} is essentially the same as for the $(0^\circ, 0^\circ)$ case.

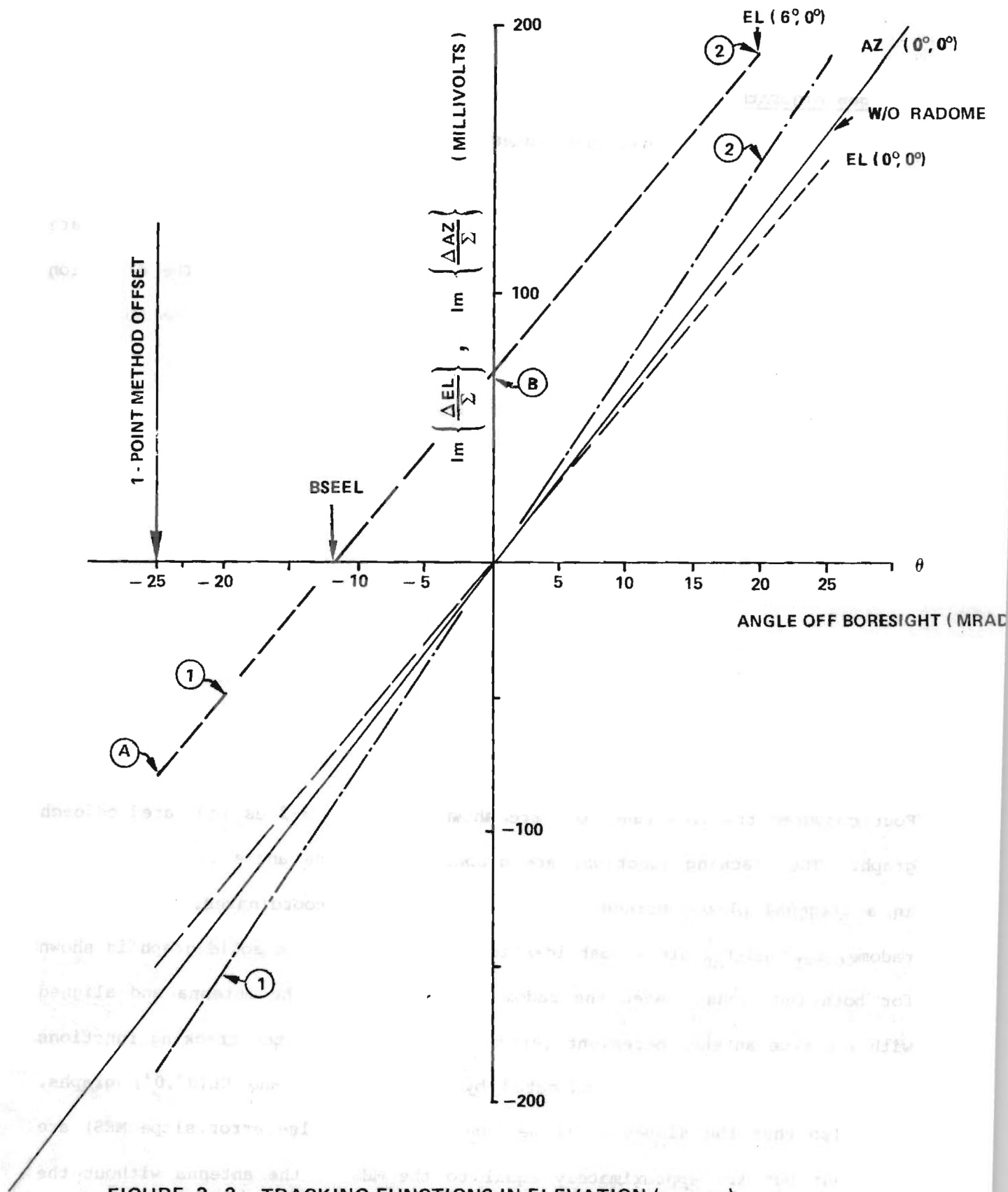


FIGURE 3-2. TRACKING FUNCTIONS IN ELEVATION (---) AND AZIMUTH (—) PLANES WITH AND WITHOUT (—) RADOME FOR (0,0) ORIENTATION.

The BSE algorithms can be explained using the $EL(6^\circ, 0^\circ)$ graph of Figure 3-2. The null seeker algorithm finds the zero-crossing of the tracking functions f_{EL} and f_{AZ} : $f_{EL} = 0$ at -11.5 mrad; $f_{AZ} = 0$ at 0 mrad in Figure 3-2. The 2-point method uses the values of each tracking function computed at only two points at ± 20 mrad to generate a linear estimate of each tracking function, and, hence, an estimate of where the zero crossings occur.

The offset 1-point method uses the value of each tracking function as measured at the angle-off-boresight of -25 mrad. This single value (Point A in Figure 3-2), combined with the MES yields the following linear tracking model

$$f_{EL} = MES_{EL} \theta_{EL} + B_{EL} \quad (3-3)$$

where the ordinate intercept B_{EL} is given in terms of the measured tracking function at the known angle $\theta = -25$ mrad by

$$B_{EL} = f_{EL}(\theta - 25 \text{ mrad}) - MES_{EL}(-25 \text{ mrad}) \quad (3-4)$$

The zero-crossing, or BSE_{EL} , is then obtained by setting Eqn. (3-3) equal to zero and solving for θ_{EL} ; i.e.,

$$\theta_{EL} = \frac{f_{EL}(\theta - 25 \text{ mrad})}{MES_{EL}} = BSE_{EL} \quad (3-4)$$

A similar treatment holds for the azimuth tracking function.

The on-axis 1-point method of BSE measurement or computation uses the single value of the tracking function obtained when the target (source) is located on the true boresight of the antenna. The value of f_{EL} is indicated by Point B in Figure 3-2. The boresight error is then given by Eqn. (3-4).

In both 1-point methods, the monopulse error slope that should correctly be used is the slope of the tracking function for that particular radome orientation. In practice, the true slope is not used; instead, the MES of the antenna without the radome is used in Eqn. (3-4). The significance of this source of error is investigated in the following presentation of the BSE measurement simulation.

A comparison of the results obtained in the simulation of the three BSE algorithms is shown in Figure 3-3 for scan of the radome in the pitch plane. A true plane wave (source at $R = \infty$) was incident on the radome, and no reflections from the chamber boundaries were allowed ($R_{dB} > 100$ dB). The graphs show excellent agreement between the null seeker and 2-point methods. Discrepancies are noted for the 1-point method. In what follows, the null seeker results for $R = \infty$ and no reflections are considered to be the true data.

3.3 Effects of Distance

The effects of the distance R of separation between the source antenna and the monopulse seeker AUT are presented in Appendix F for each BSE algorithm. Distances of $R = 20'$, $30'$, $40'$, and $R = \infty$ are used. No reflections are included.

The simulation results of Appendix F indicate that the distance of separation is a significant source of error in BSE measurements. For example, for a 20' separation, a maximum error of 5 mrad is observed using the null seeker or 2-point method. Oscillatory errors are observed using the offset 1-point method. The errors in gain (radome loss) are minor for all three methods.

The antenna used in the simulation has a value of $D^2/\lambda = 71.6$. The 20' separation corresponds to $3.35 D^2/\lambda$. The radome value of $L_1^2/\lambda = 558$ yields only $0.43 L_1^2/\lambda$ for the 20' separation. (The radome length L_1 used is the radome length from the gimbal point to the tip.) These considerations indi-

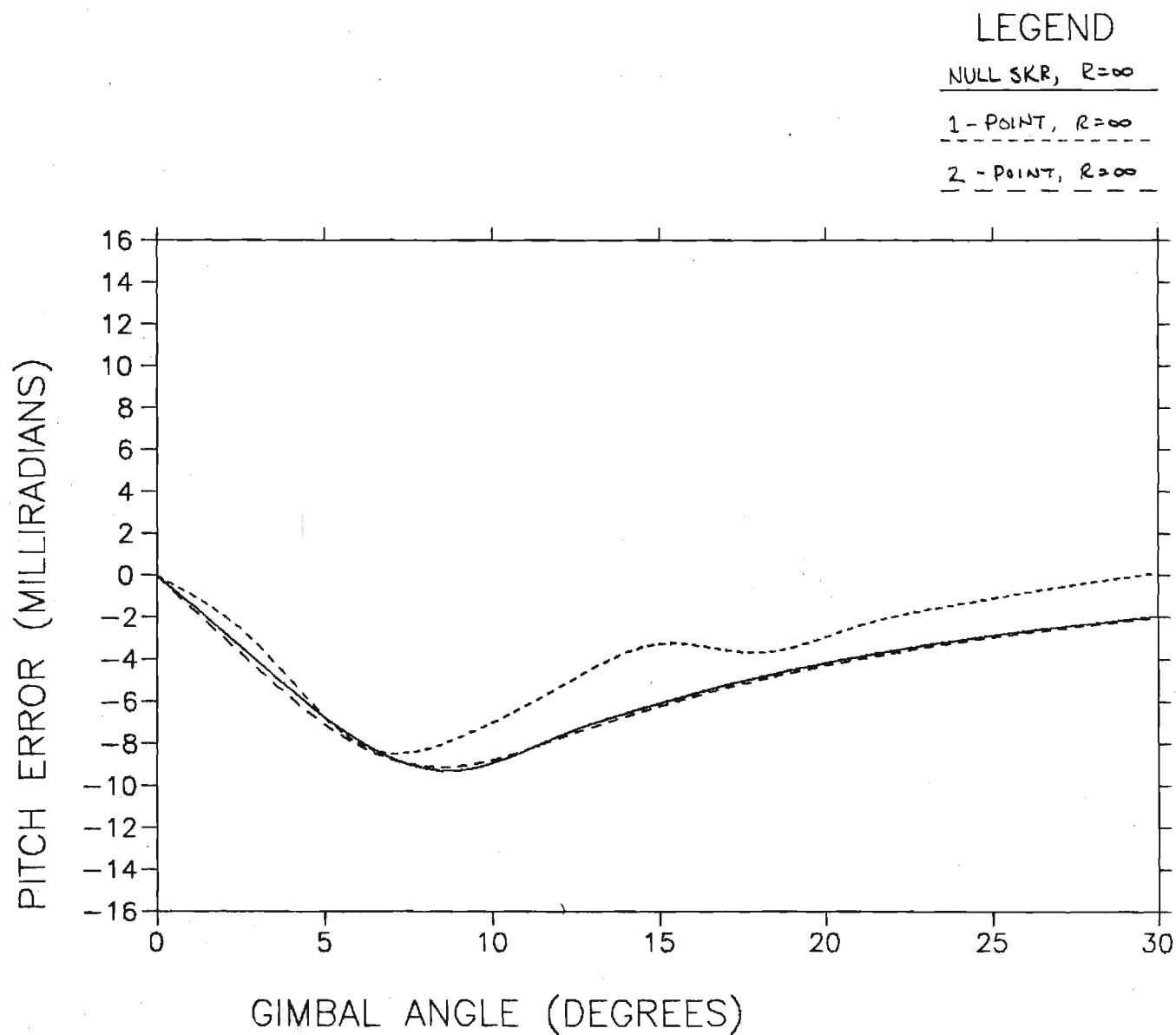


Figure 3-3. Comparisons of Boresight Errors Computed Using Three Different Algorithms.

cate that any rules of thumb for separation distance in BSE measurements should utilize radome length rather than antenna diameter.

3.4 Effects of Reflections

The effects of wave reflections from the anechoic chamber walls, floor, and ceiling are presented in graphical form in Appendix G. Only the 20' separation distance was considered since it corresponds roughly to the length of the chamber of interest. Chamber reflectivities of 20 dB, 30 dB, and 100 dB were considered.

The BSE data in Appendix G shows that the 2-point method is least sensitive to reflections, and that the offset 1-point method is the most sensitive. And in some instances the reflections tend to compensate for the 20' separation distance!

The gain data in Appendix F shows that chamber reflections have a significant effect on this parameter.

3.5 Effects of Frequency

The simulation was performed to determine the effects of small ($\pm 1\%$) frequency drifts on measured BSE for the case of $R = 30'$ separation and reflectivity of 30 dB. The computed results are presented in Appendix H for all three BSE algorithms.

The data in Appendix H show that small frequency drifts are a significant source of error in BSE measurements. Therefore, frequency-stabilized (phase locked) sources should be used.

CHAPTER 4

CONCLUSIONS AND RECOMMENDATIONS

4.1 Ablative and Ceramic Radomes

Ablative radomes consisting of a load-bearing fibreglas substrate and a thin fibre-loaded Teflon ablator layer can be designed to have electrical performance comparable to what can be expected for ceramic radomes; however, the change in boresight error slope caused by ablation can be significant, and this effect must be taken into account in the radome design.

The investigation of the ceramic radome is not complete, and no conclusions can be drawn concerning the advantages of asymmetrical wall thickness. It is recommended that this work be completed, including an investigation of the effects of asymmetrical aerodynamic heating on BSE.

4.2 BSE Measurement Simulation

The computer-aided simulation shows that separation distance, reflections, and frequency drifts are all significant sources of error in BSE measurements. Also, the results obtained depend on the algorithm or procedure used to compute or measure BSE. The offset 1-point method yields the most variable results and is deemed unsuitable for use. The on-axis 1-point method has not been fully studied, and it is recommended that this be done using the simulation already developed.

REFERENCES

1. G. K. Huddleston, H. L. Bassett, and J. M. Newton, "Computer Aided Radome Analysis Based on Geometrical Optics and Lorentz Reciprocity," Final Report on AFOSR-77-3469, Vol. 2 of 4, February 1980.

APPENDIX A

FLAT PANEL ANALYSIS RESULTS

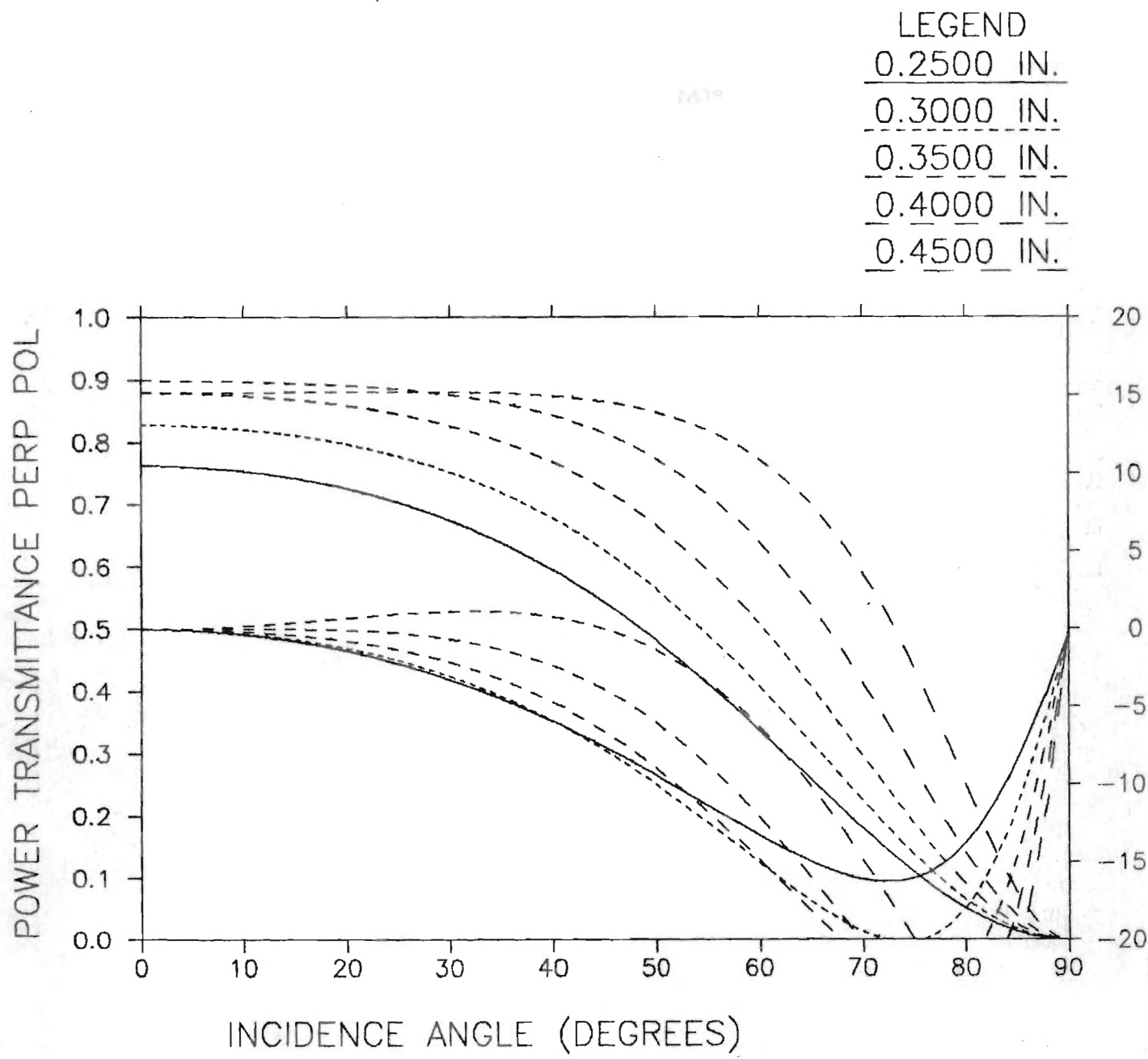


Figure A-1. Substrate Thickness = 0.25".

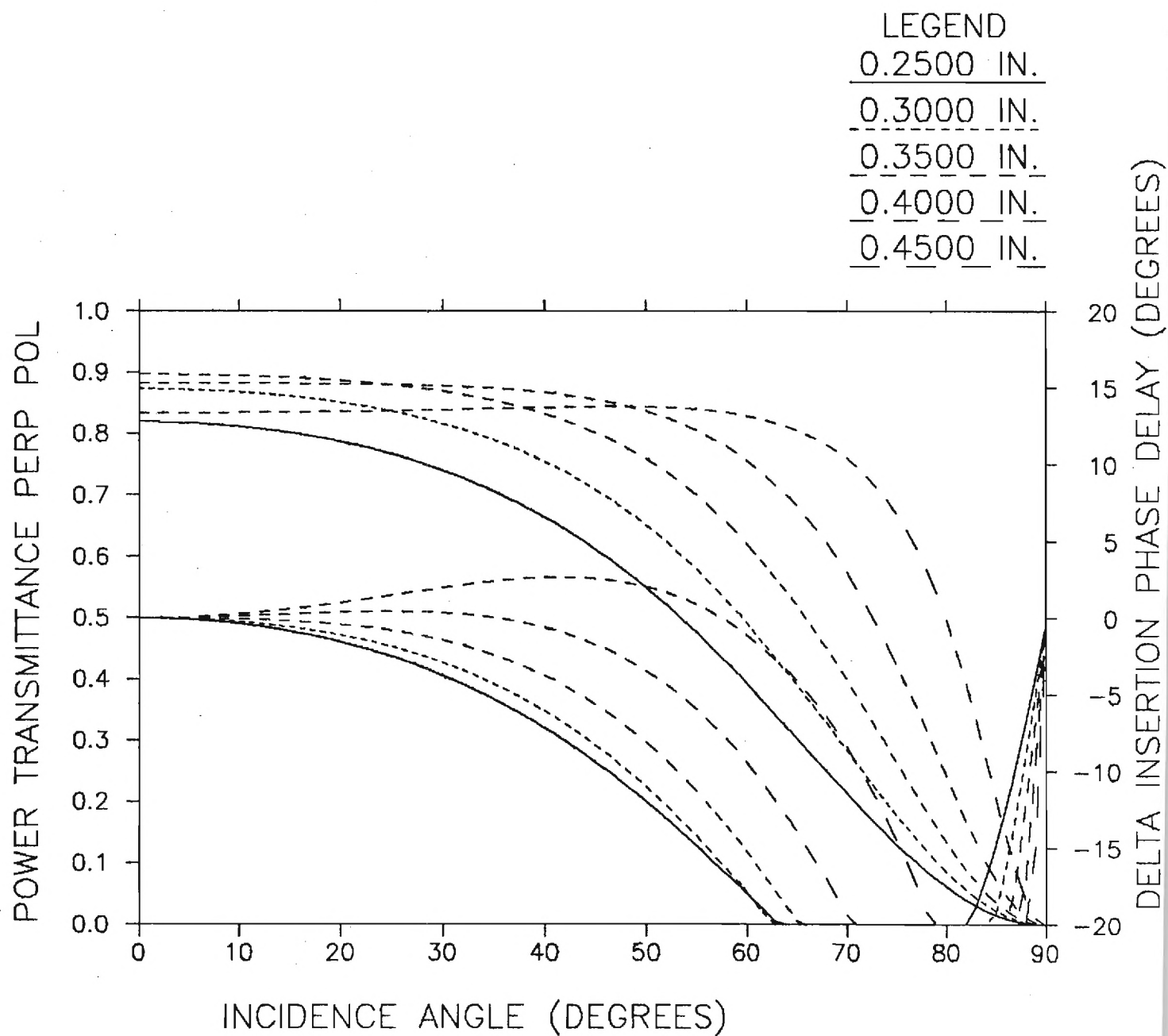


Figure A-2. Substrate Thickness = 0.30".

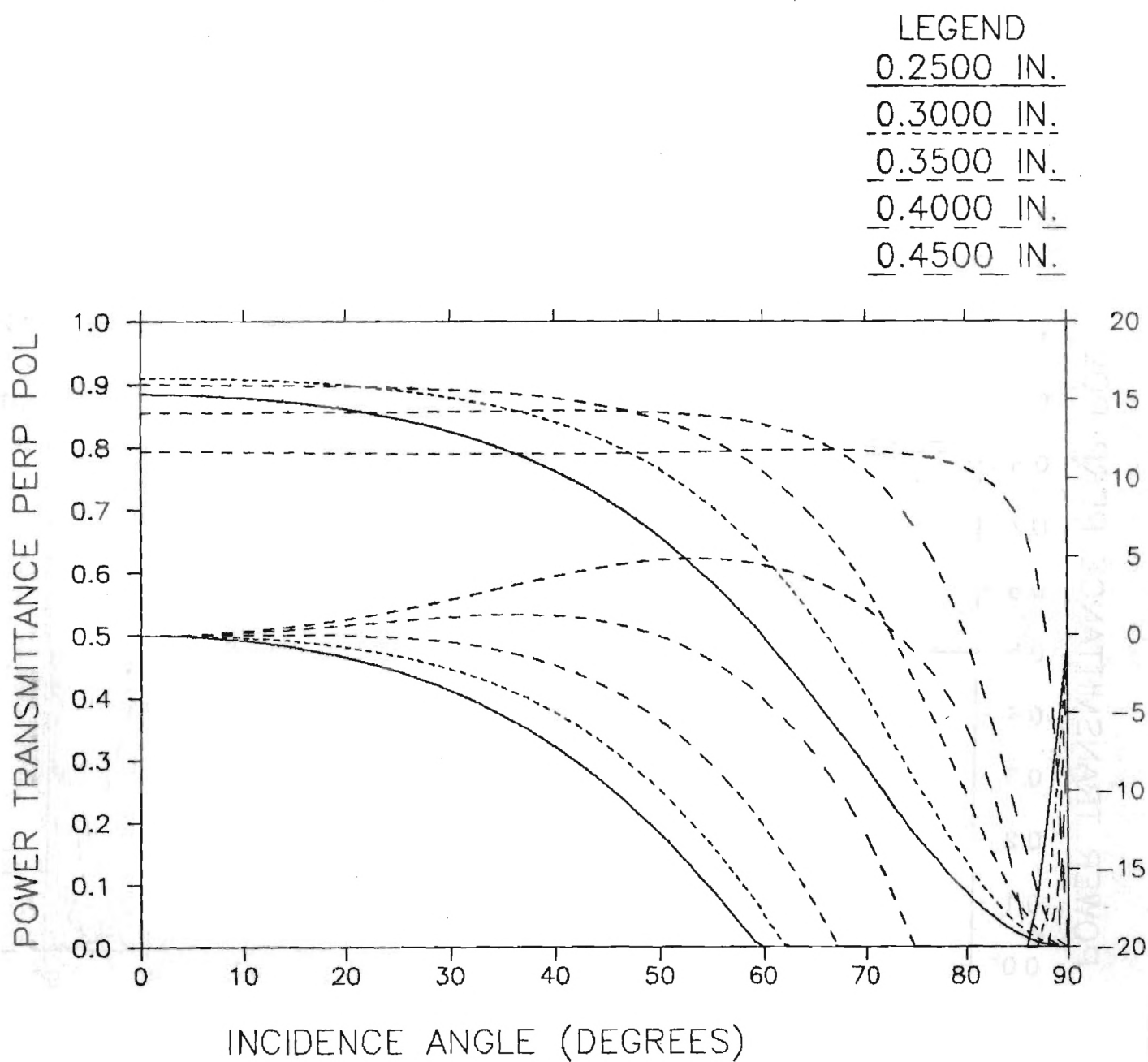


Figure A-3. Substrate Thickness = 0.35".

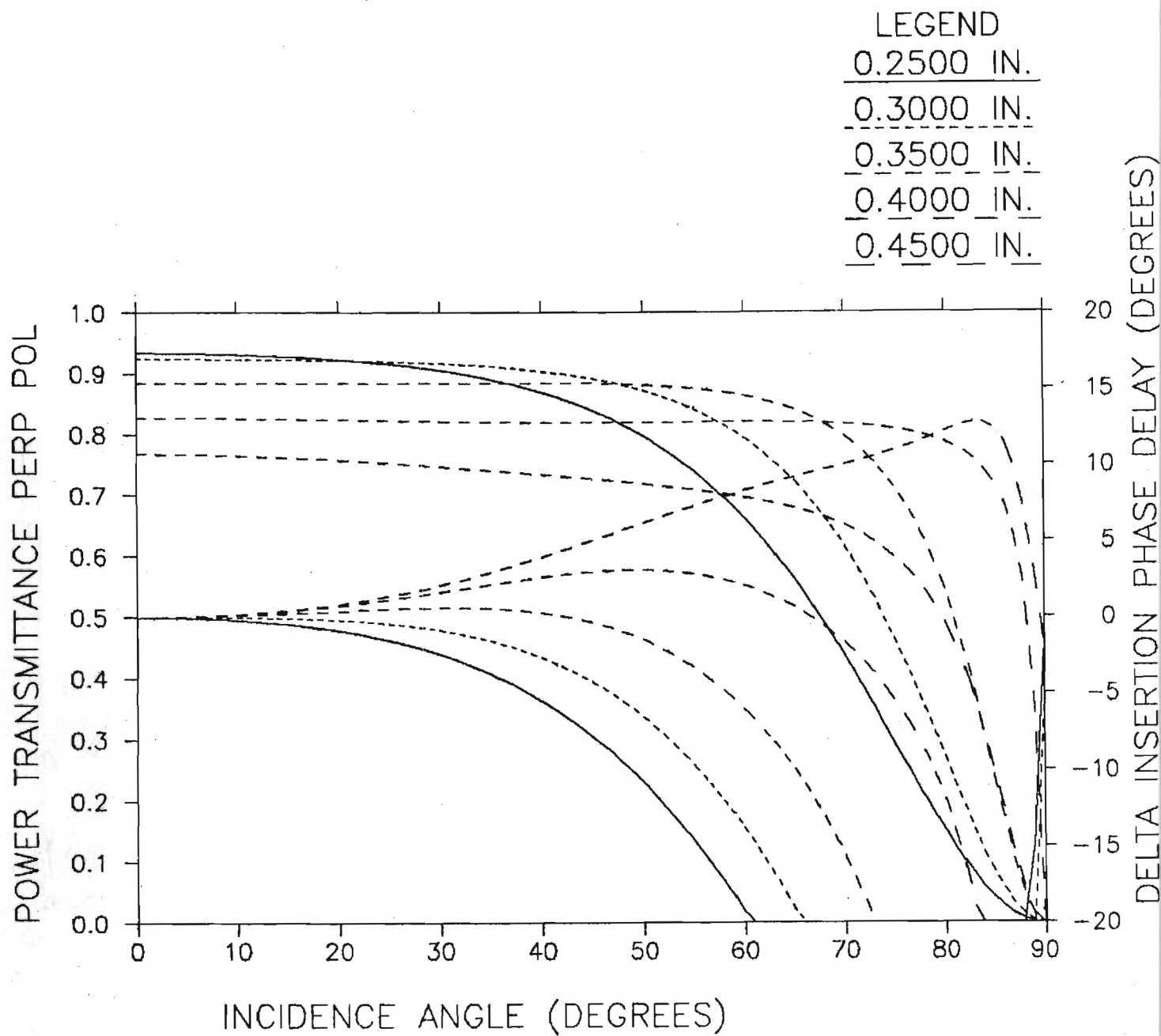


Figure A-4. Substrate Thickness = 0.40".

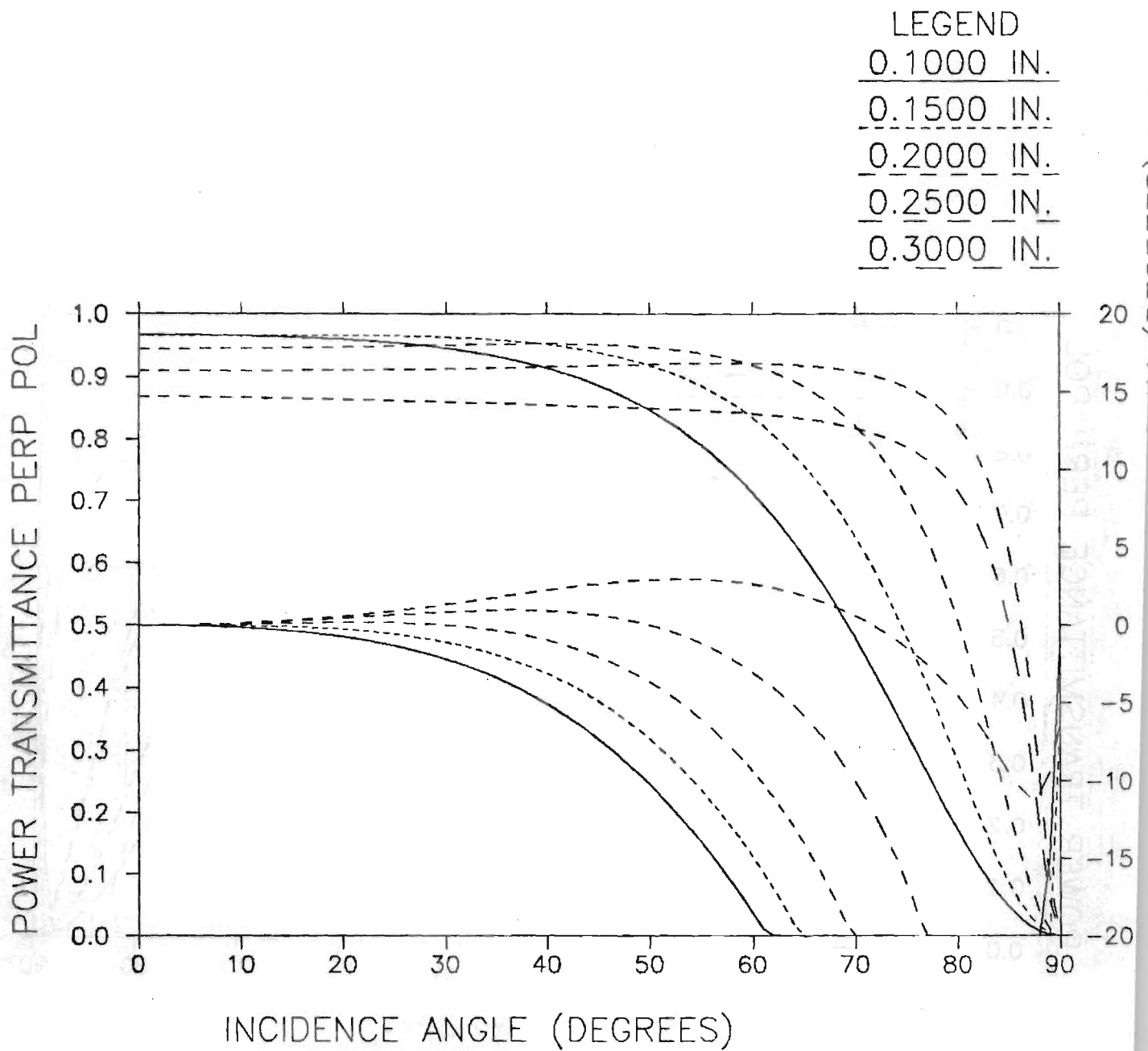


Figure A-5. Substrate Thickness = 0.50".

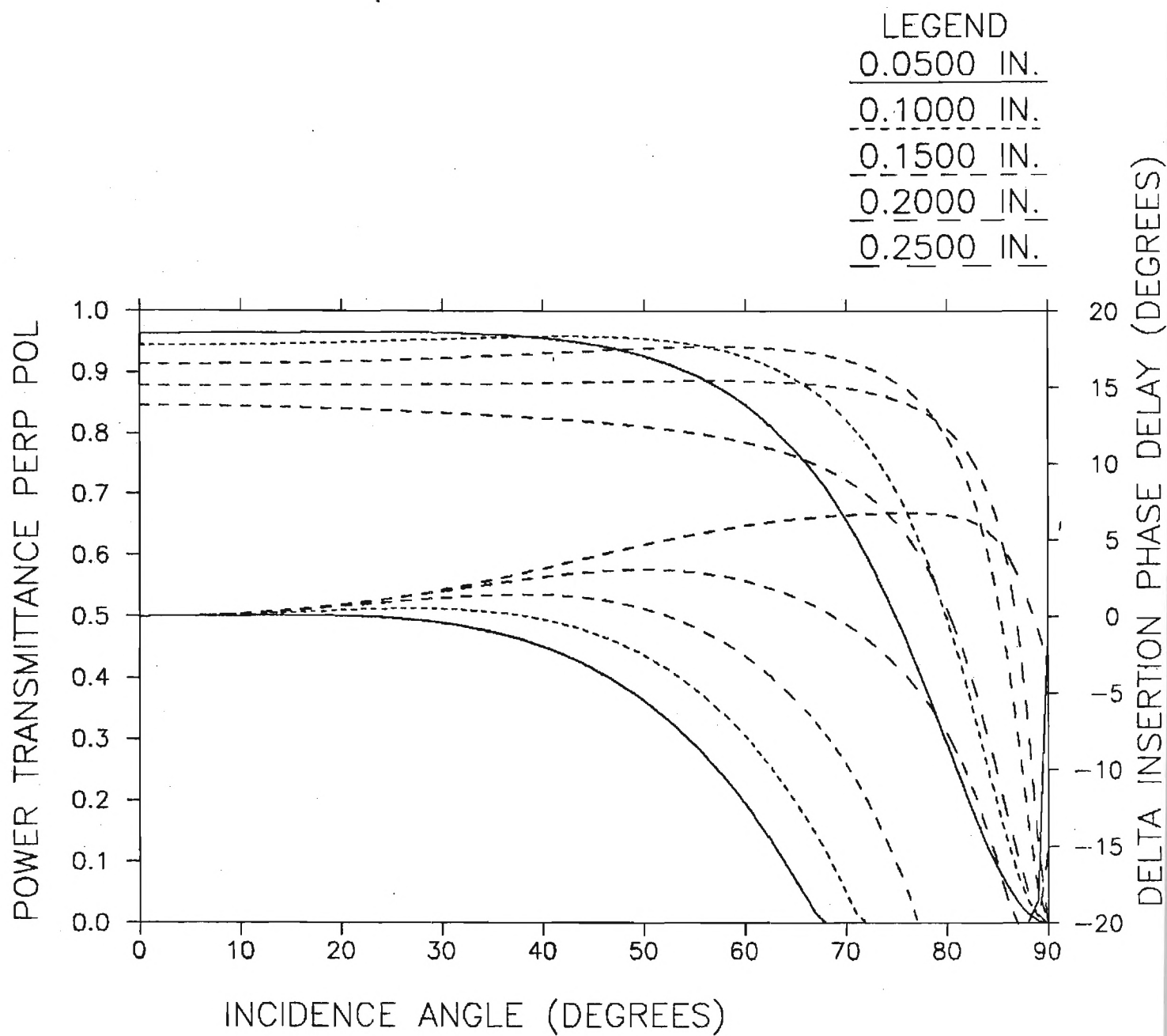


Figure A-6. Substrate Thickness = 0.55".

LEGEND

0.0200 IN.

0.0400 IN.

0.0600 IN.

0.0800 IN.

0.1000 IN.

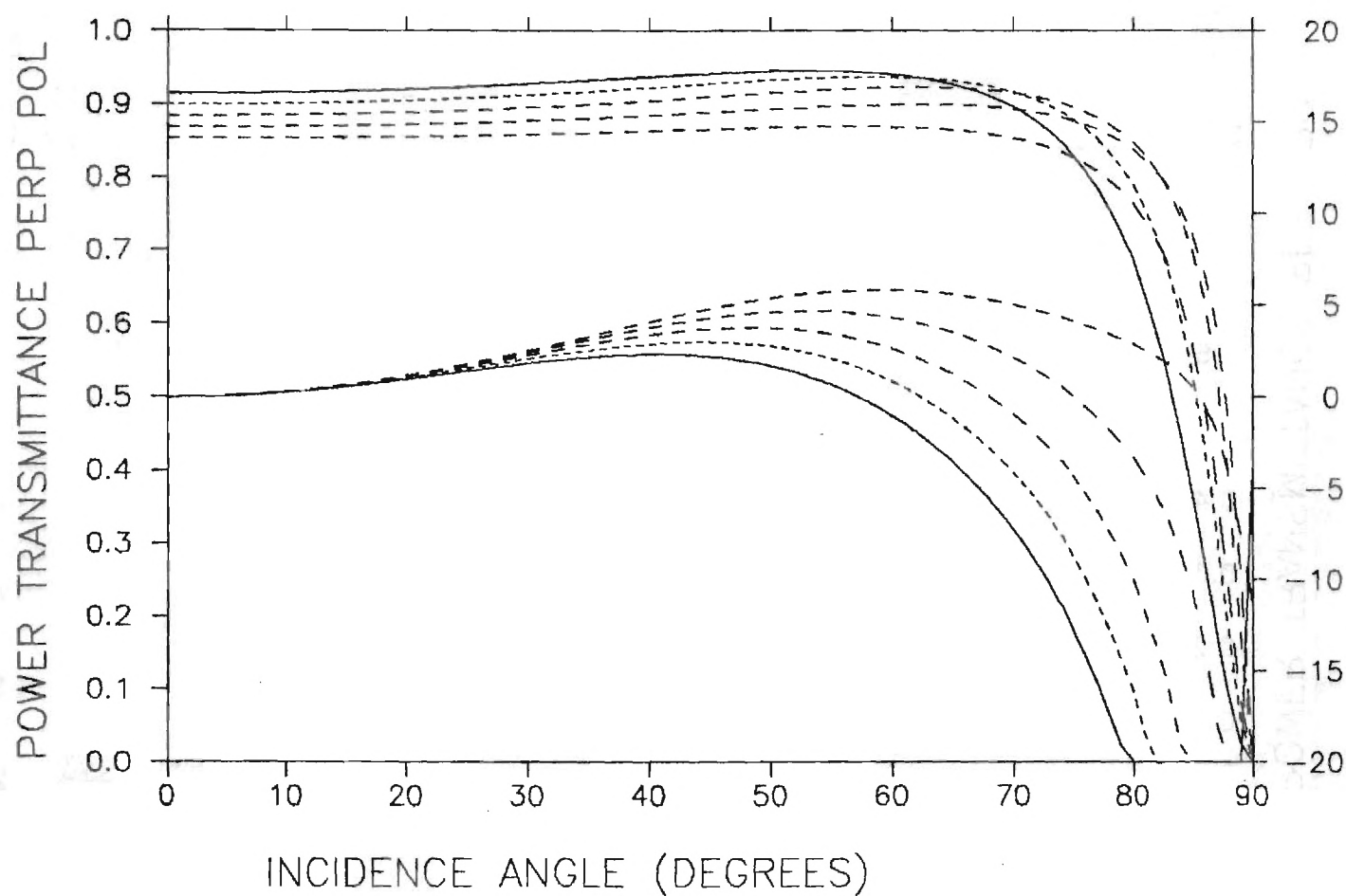


Figure A-7. Substrate Thickness = 0.60".

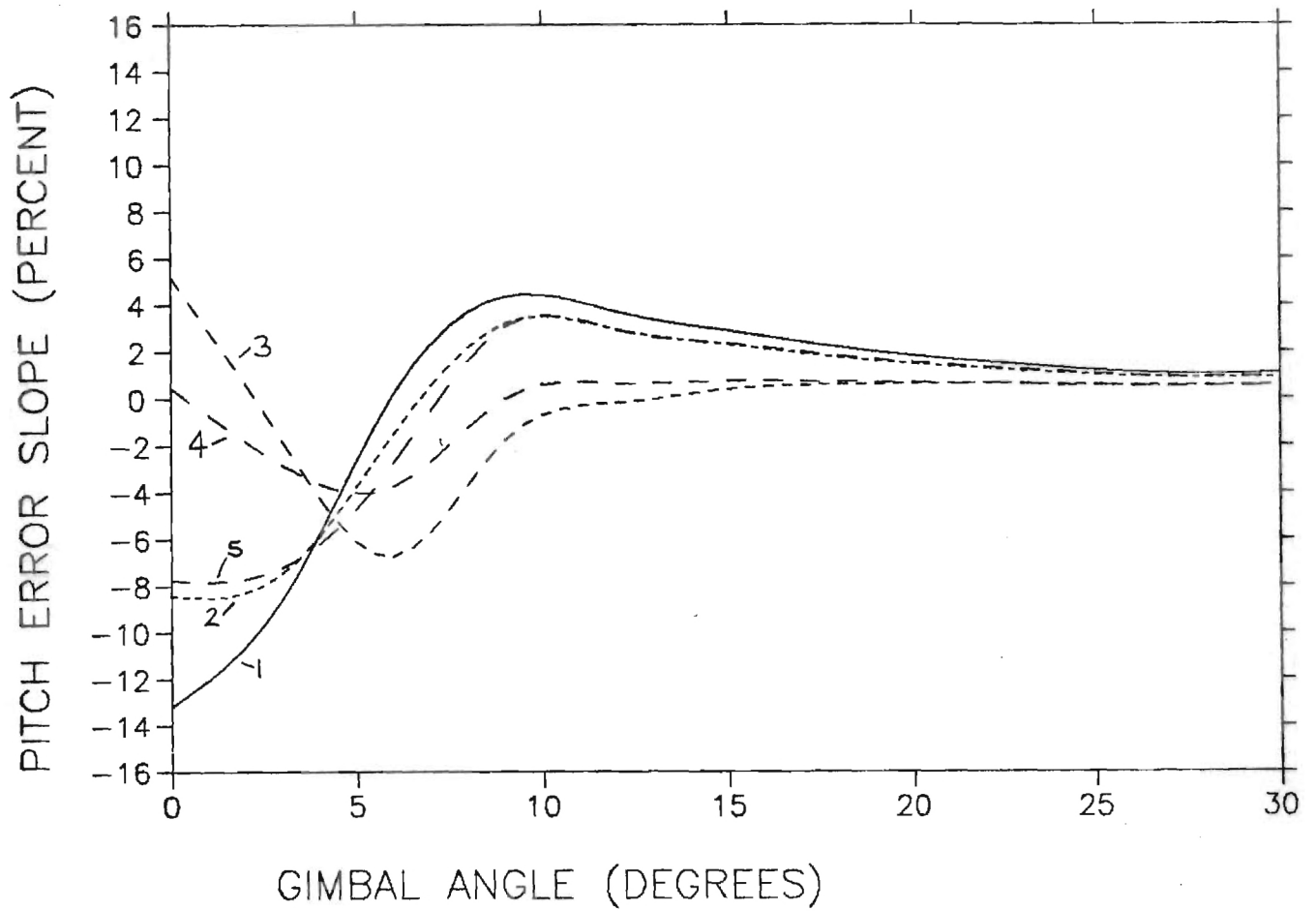
APPENDIX B

UNIFORM ABLATIVE RADOME PERFORMANCE

SUBSTRATE ABLATOR

LEGEND

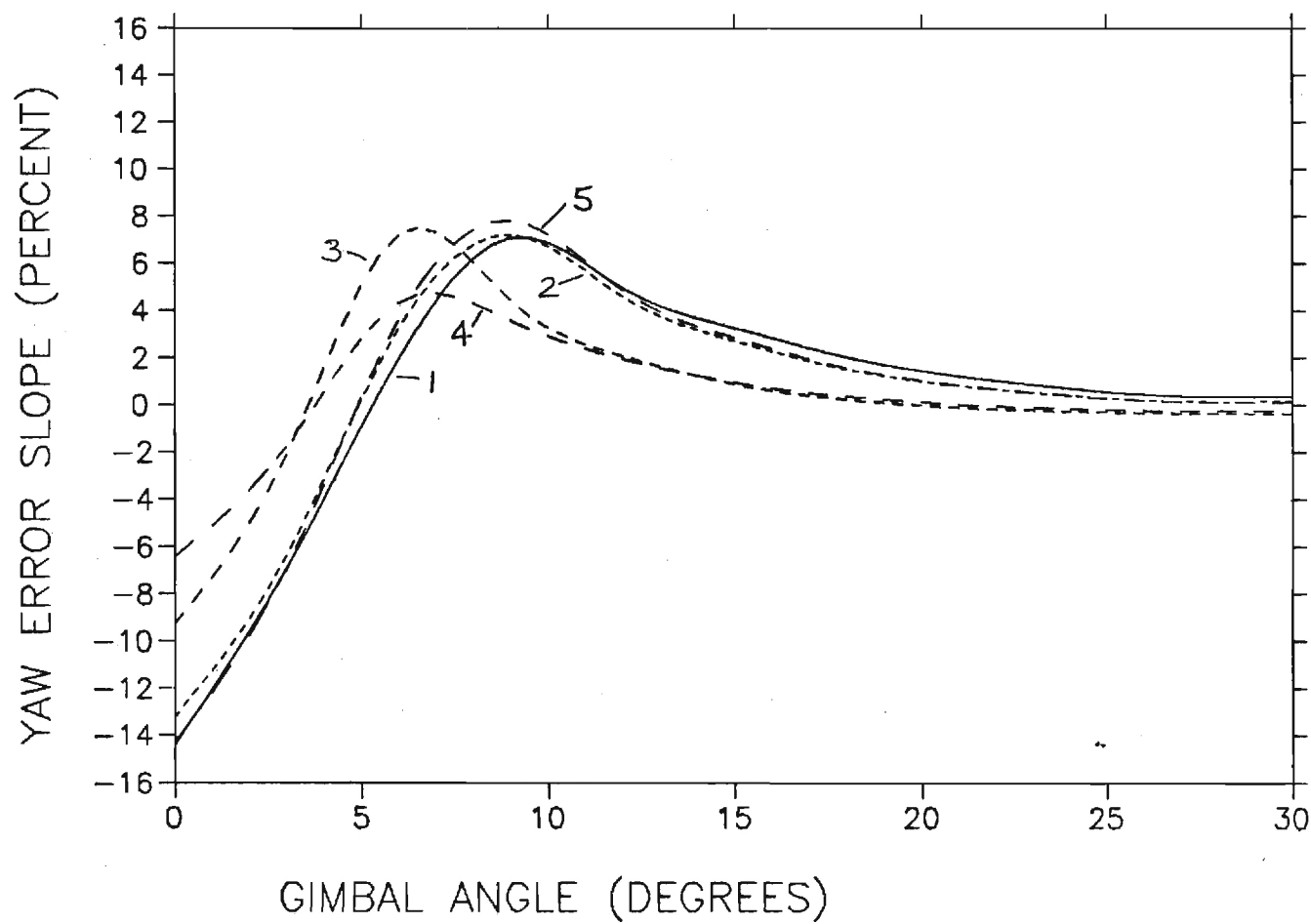
1	.350"	.400"
2	.550"	.150"
3	.550"	.200"
4	.600"	.060"
5	.500"	.250"



SUB. ABLATOR

LEGEND

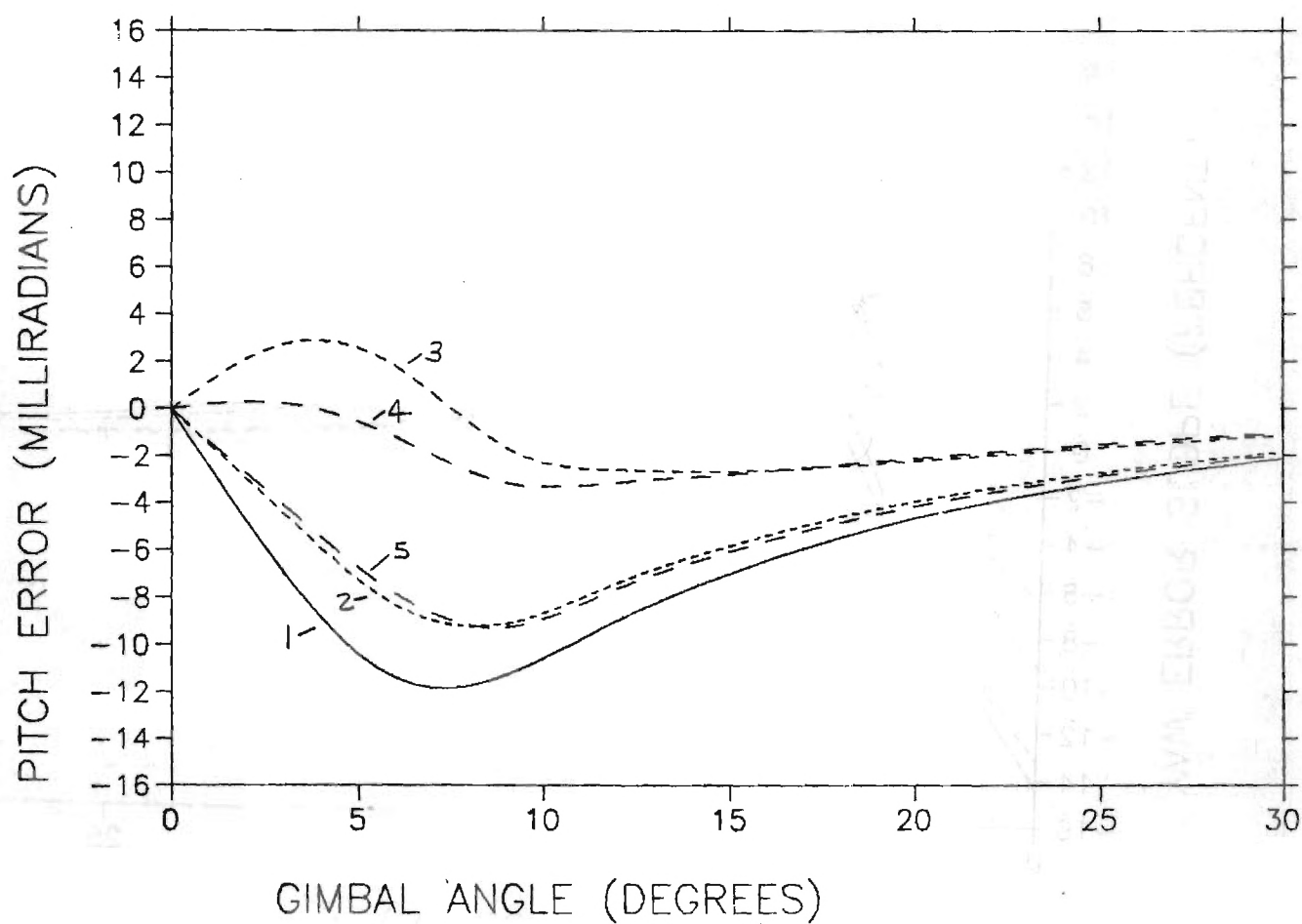
1	<u>.350"</u>	<u>.400"</u>
2	<u>.550"</u>	<u>.150"</u>
3	<u>.550"</u>	<u>.200"</u>
4	<u>.600"</u>	<u>.060"</u>
5	<u>.500"</u>	<u>.250"</u>



SUB. ABLATOR

LEGEND

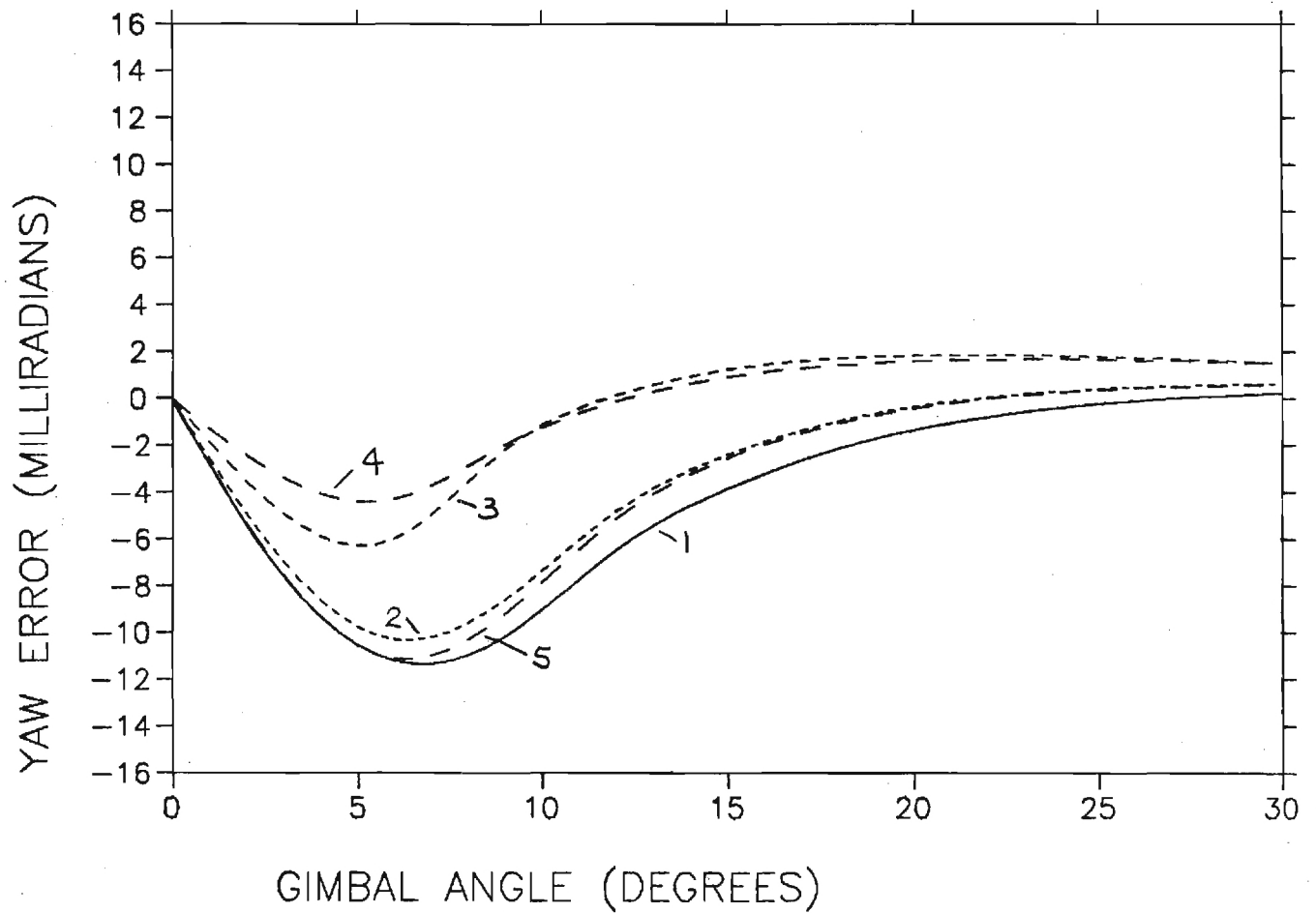
1	<u>.350"</u>	<u>.400"</u>
2	<u>.550"</u>	<u>.150"</u>
3	<u>.550"</u>	<u>.200"</u>
4	<u>.600"</u>	<u>.060"</u>
5	<u>.500"</u>	<u>.250"</u>



SUB. ABLATOR

LEGEND

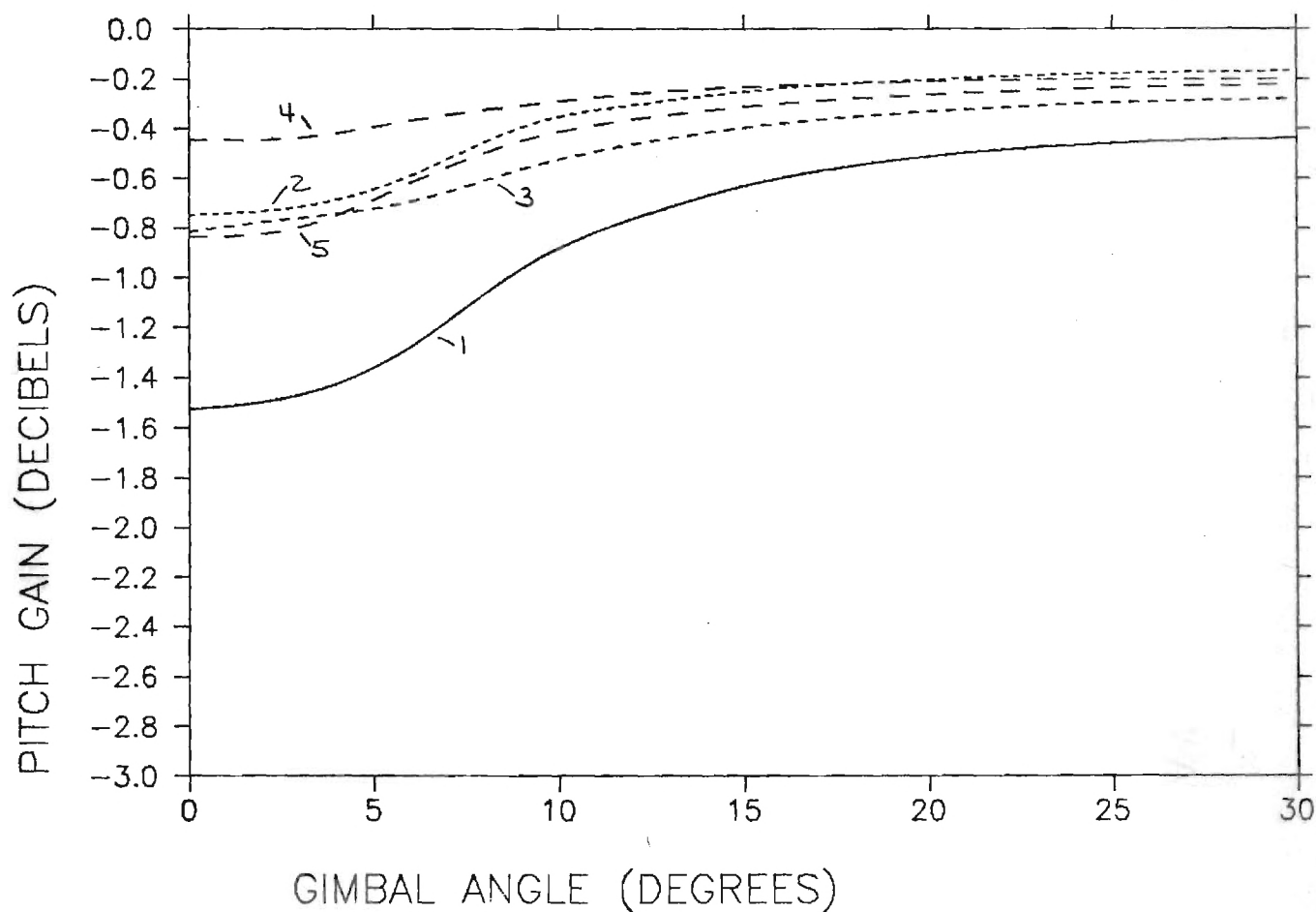
1	<u>.350"</u>	<u>.400"</u>
2	<u>.550"</u>	<u>.150"</u>
3	<u>.550"</u>	<u>.200"</u>
4	<u>.600"</u>	<u>.060"</u>
5	<u>.500"</u>	<u>.250"</u>



SUB. ABLATOR

LEGEND

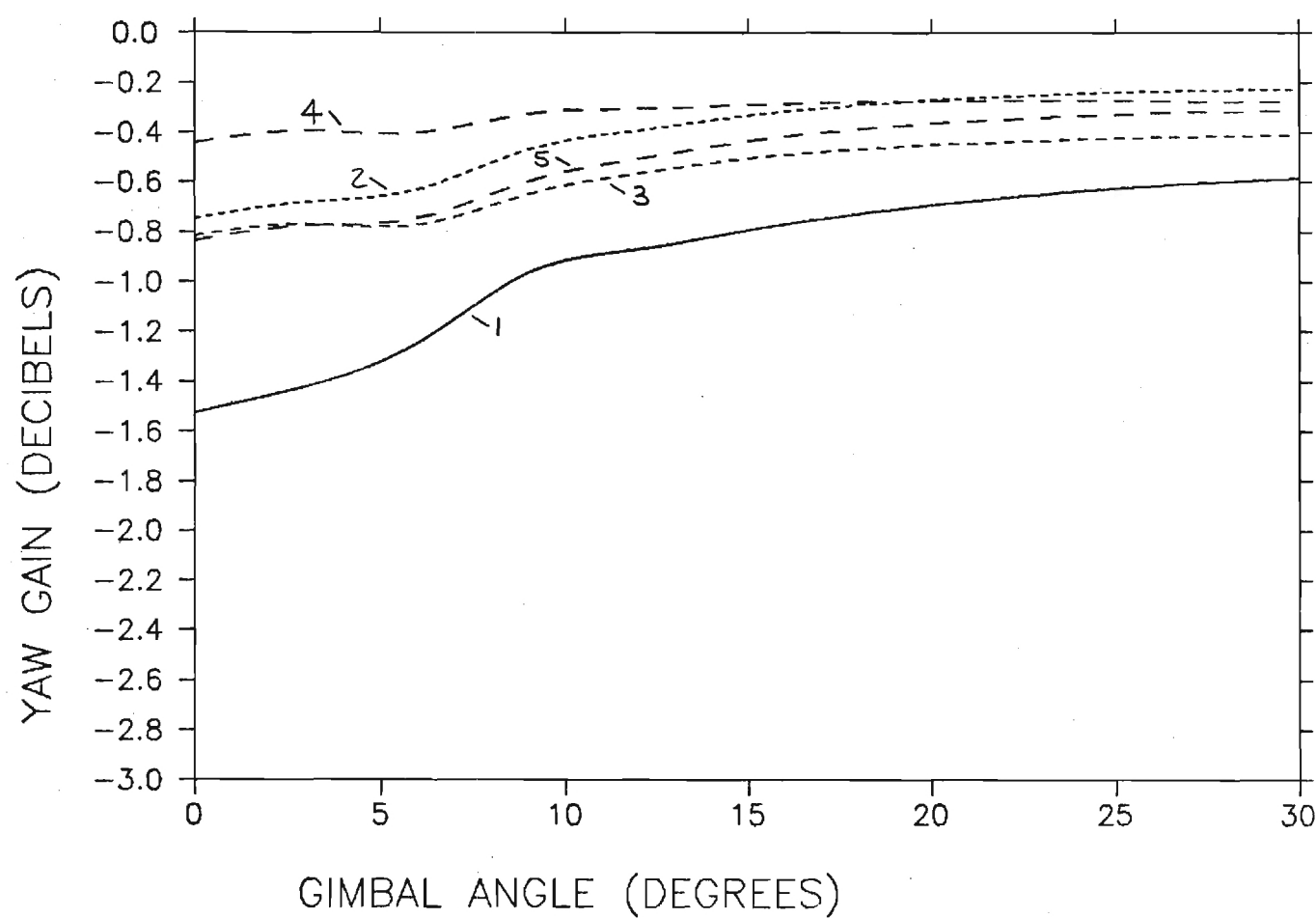
1	<u>.350"</u>	<u>.400"</u>
2	<u>.550"</u>	<u>.150"</u>
3	<u>.550"</u>	<u>.200"</u>
4	<u>.600"</u>	<u>.060"</u>
5	<u>.500"</u>	<u>.250"</u>



SUB. ABLATOR

LEGEND

1	.350"	.400"
2	.550"	.150"
3	.550"	.200"
4	.600"	.060"
5	.500"	.250"



ЯОТЯІІА

ЯОТЯІІА

ЯОТЯІІА

ЯОТЯІІА

ЯОТЯІІА

ЯОТЯІІА

ЯОТЯІІА

ЯОТЯІІА

ЯОТЯІІА

ЯОТЯІІА

ЯОТЯІІА

ЯОТЯІІА

ЯОТЯІІА

ЯОТЯІІА

ЯОТЯІІА

ЯОТЯІІА

ЯОТЯІІА

ЯОТЯІІА

ЯОТЯІІА

ЯОТЯІІА

ЯОТЯІІА

ЯОТЯІІА

ЯОТЯІІА

ЯОТЯІІА

ЯОТЯІІА

ЯОТЯІІА

ЯОТЯІІА

ЯОТЯІІА

ЯОТЯІІА

ЯОТЯІІА

ЯОТЯІІА

ЯОТЯІІА

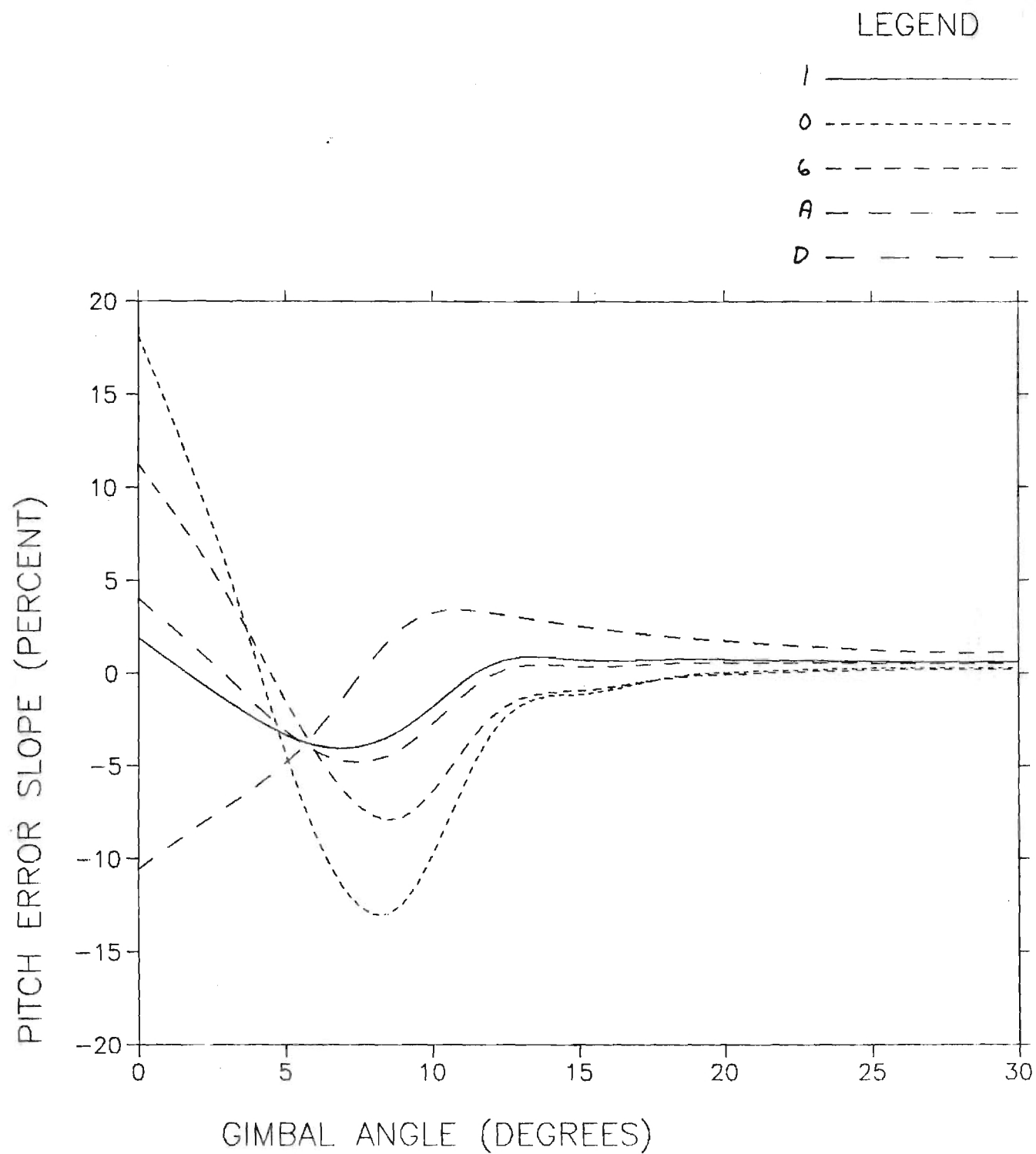
ЯОТЯІІА

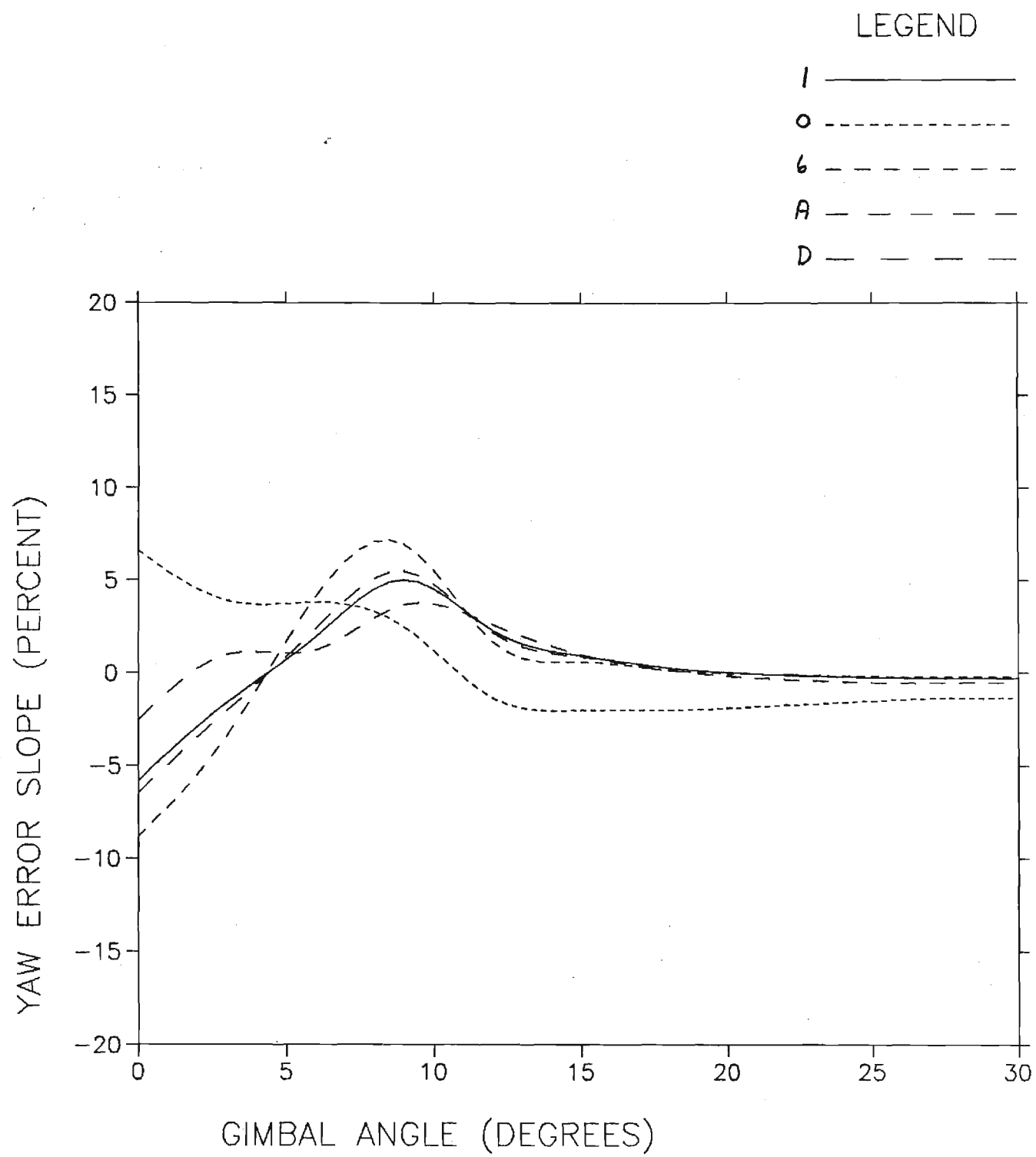
ЯОТЯІІА

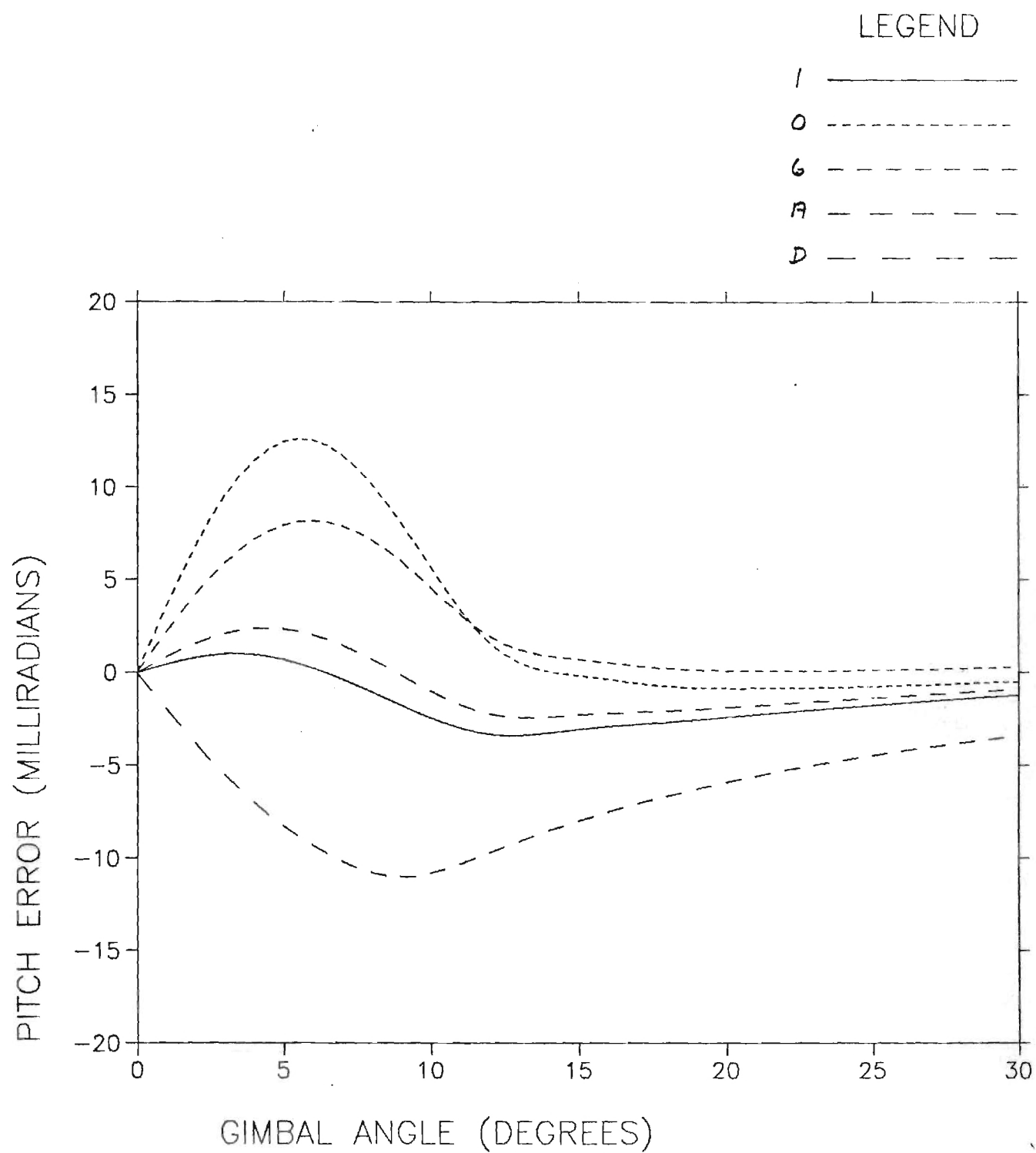
ЯОТЯІІА

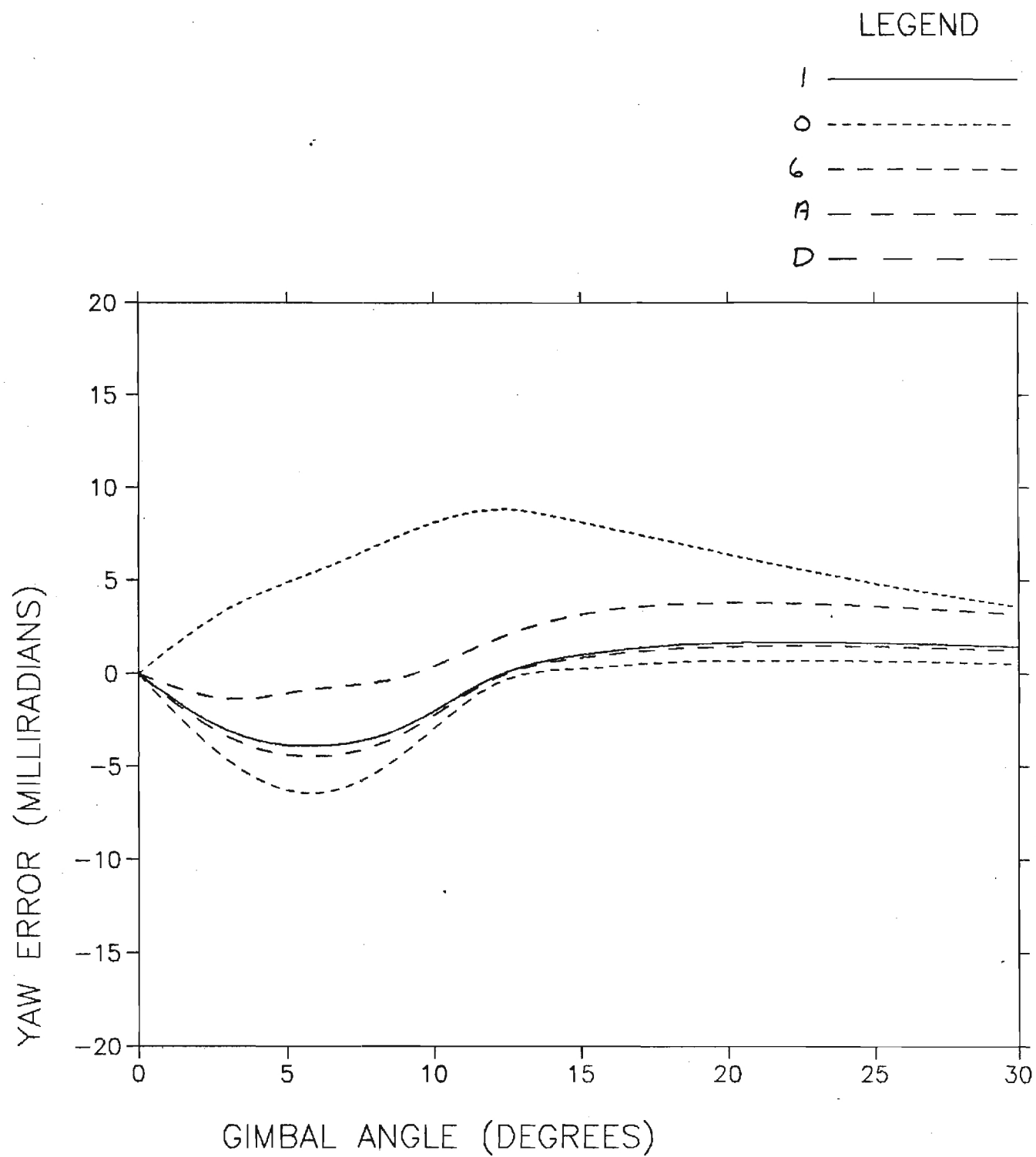
APPENDIX C

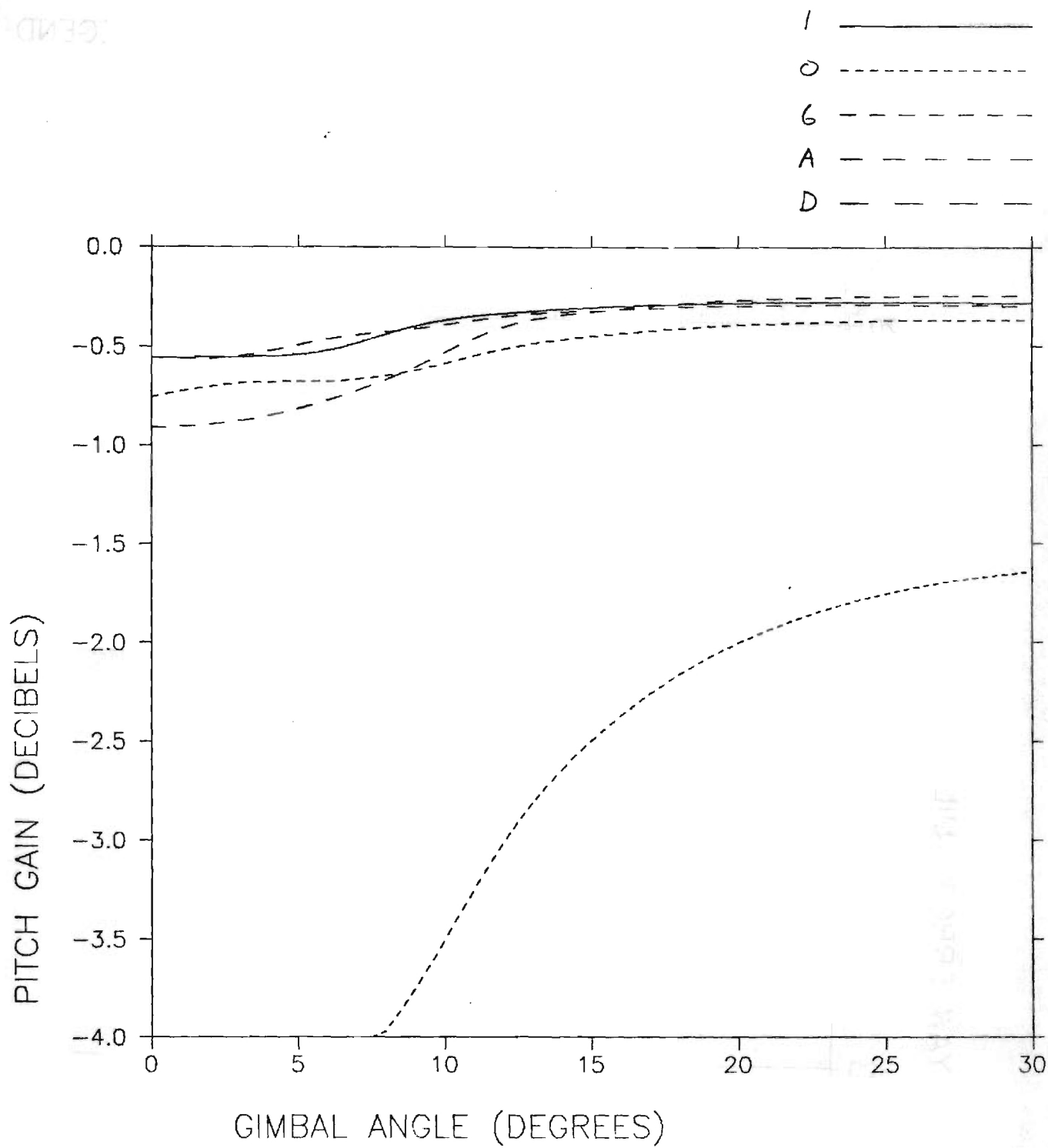
TAPERED ABLATOR RADOME PERFORMANCE

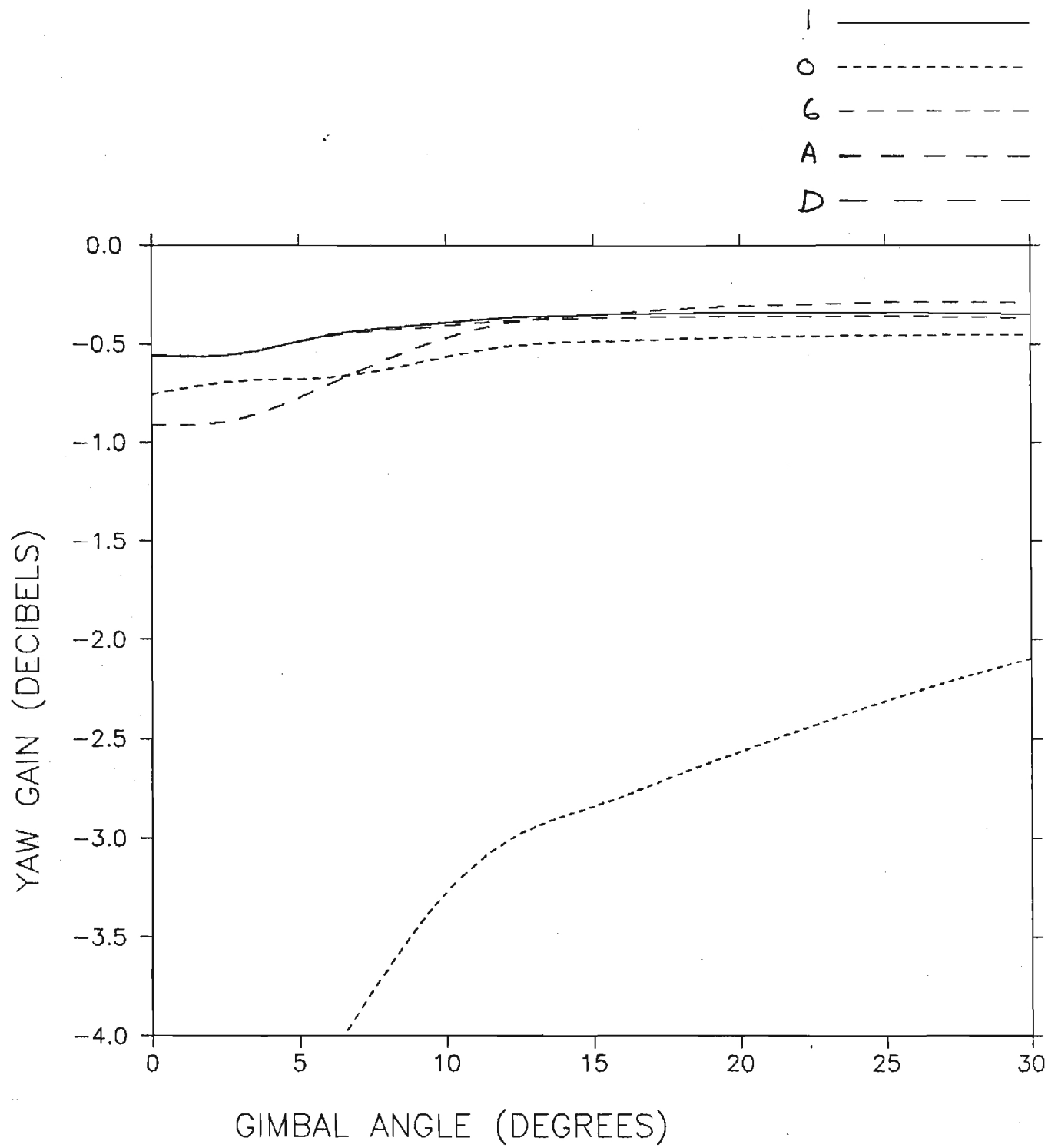








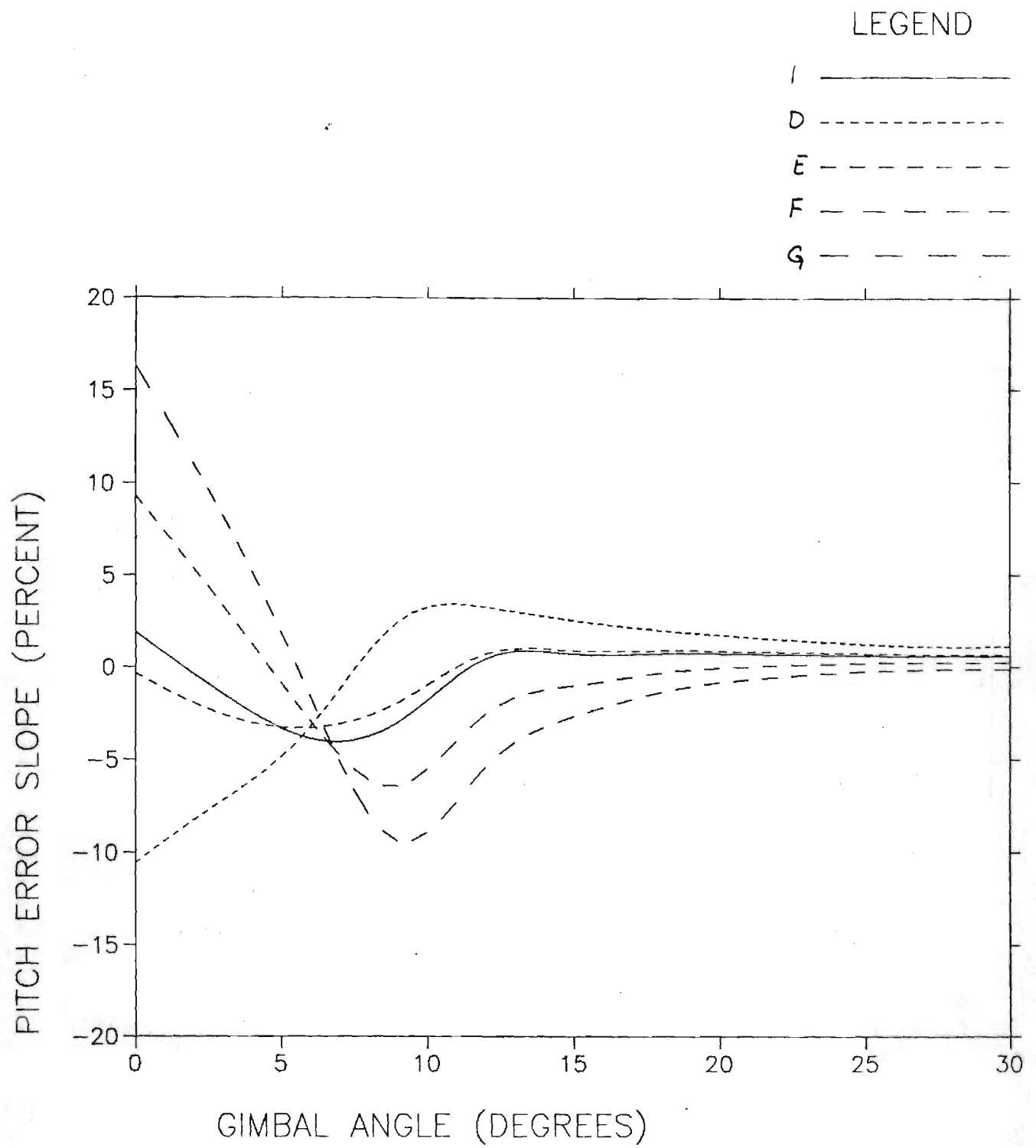






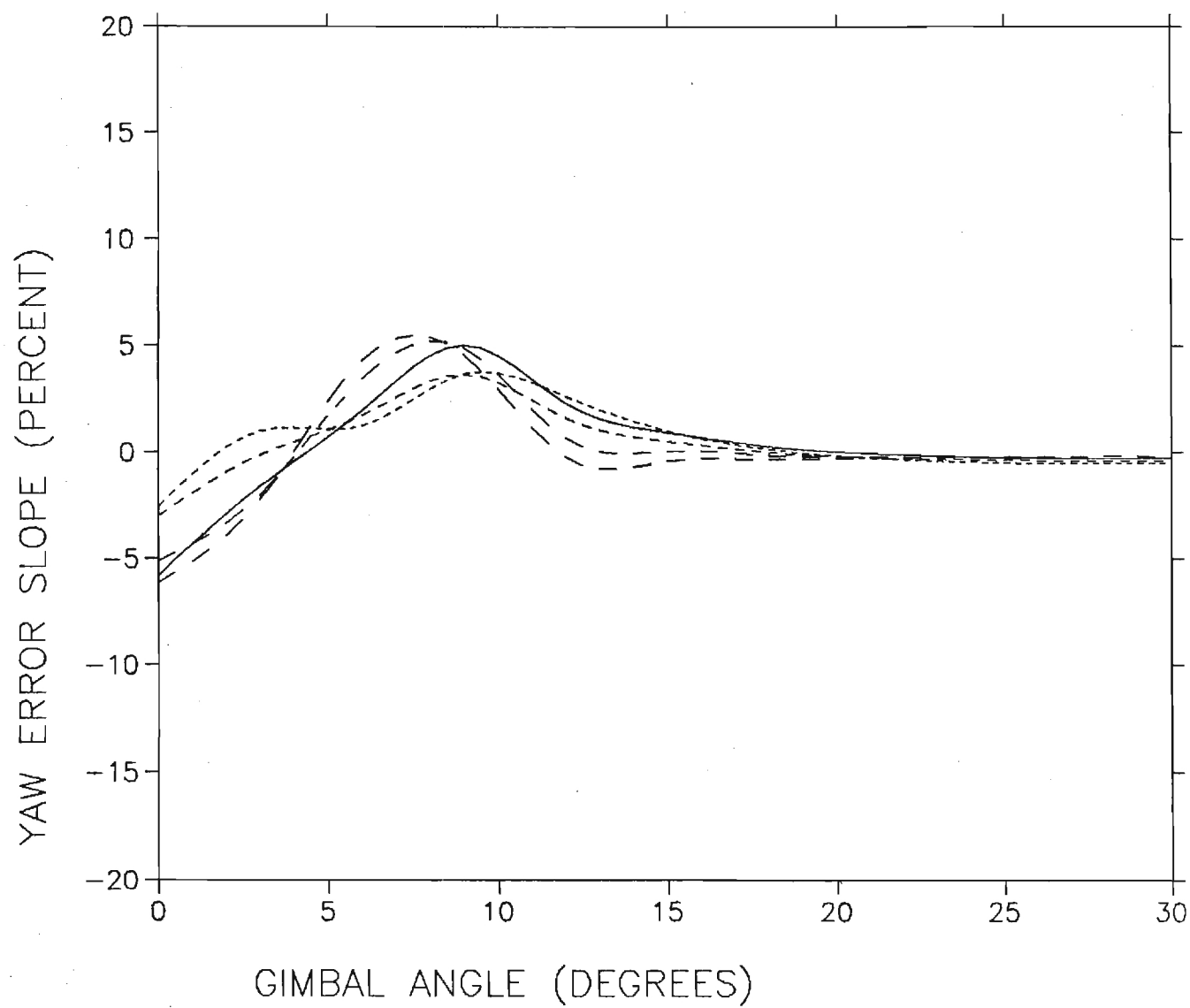
APPENDIX D

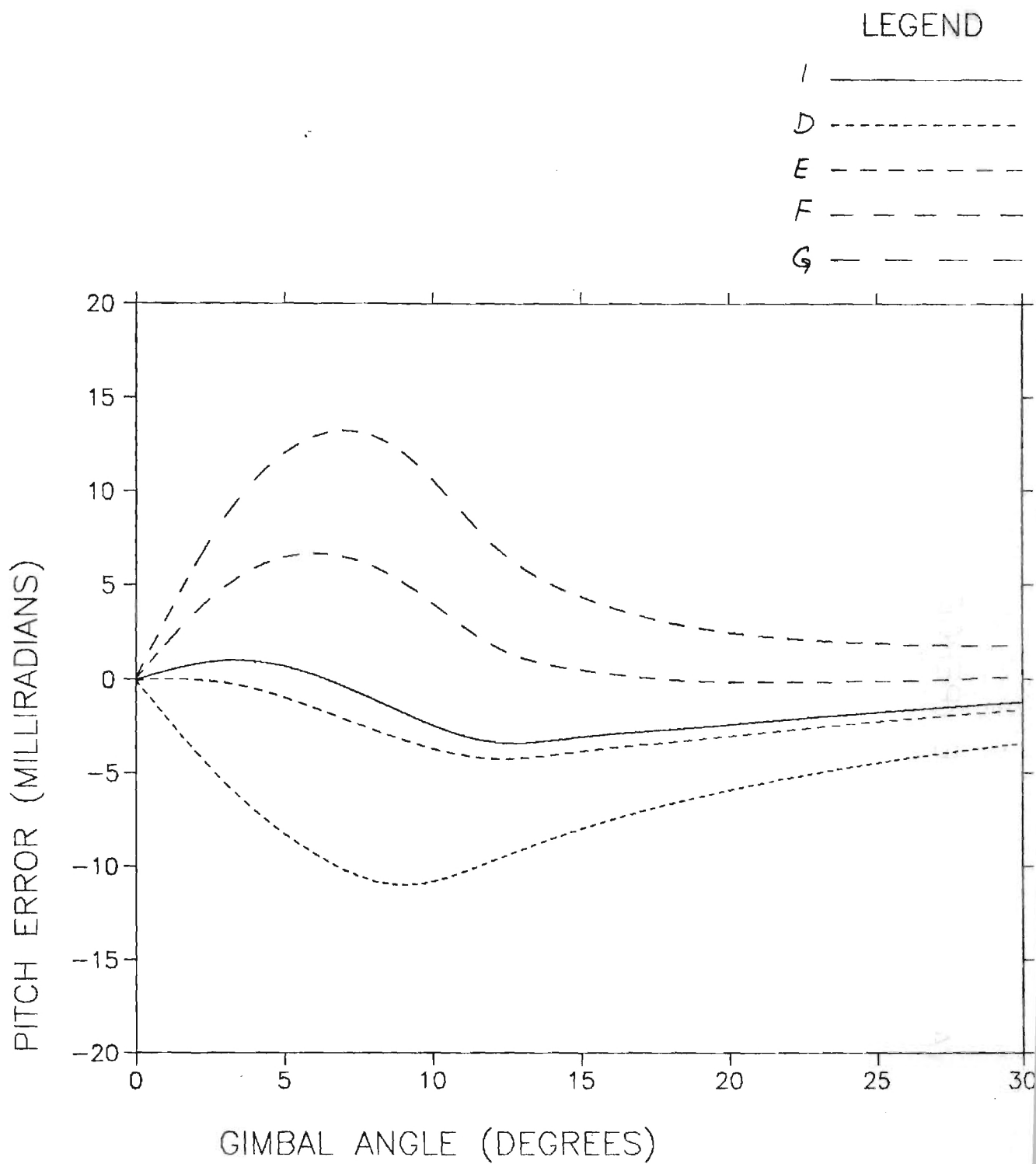
TAPERED SUBSTRATE RADOME PERFORMANCE

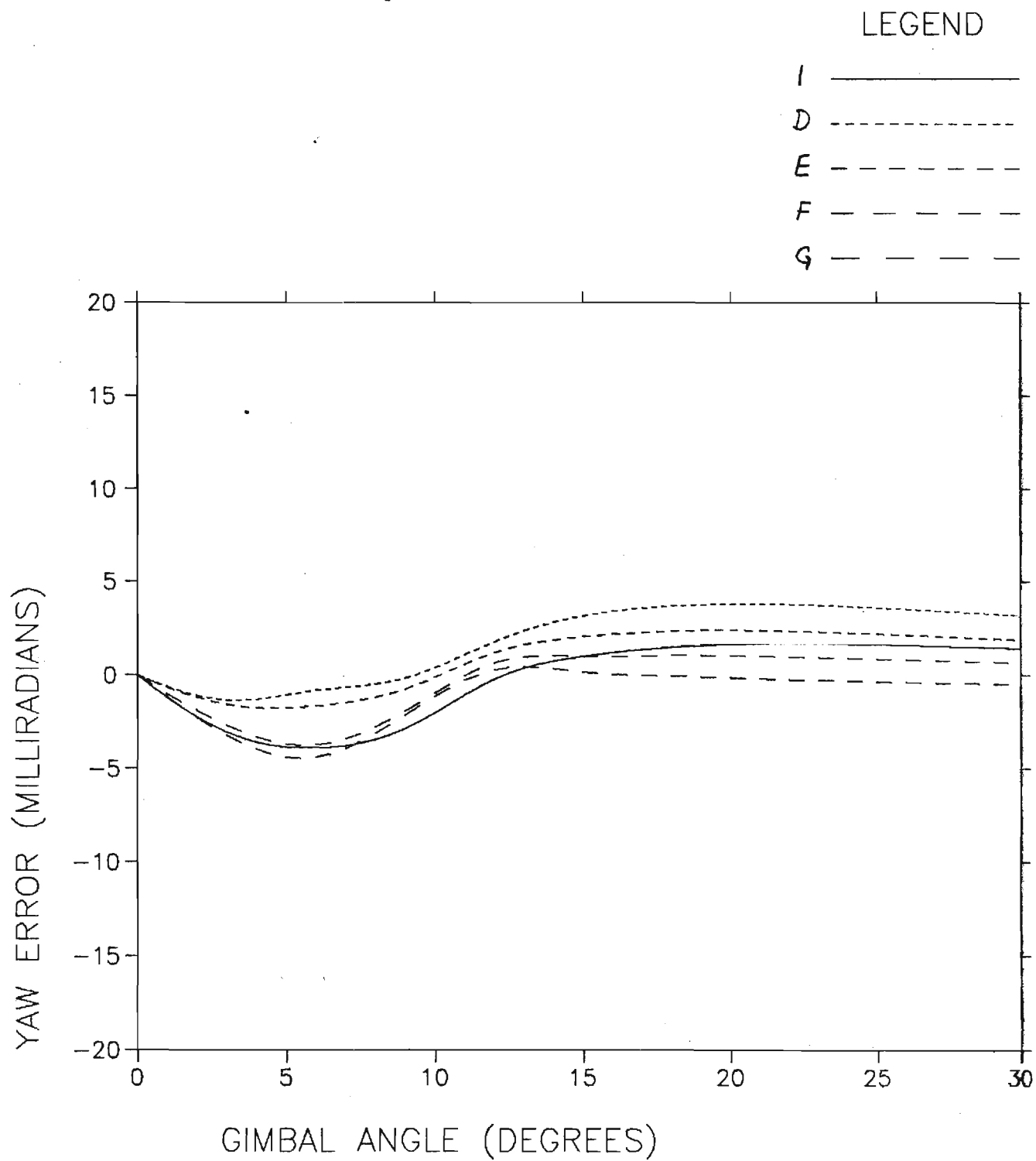


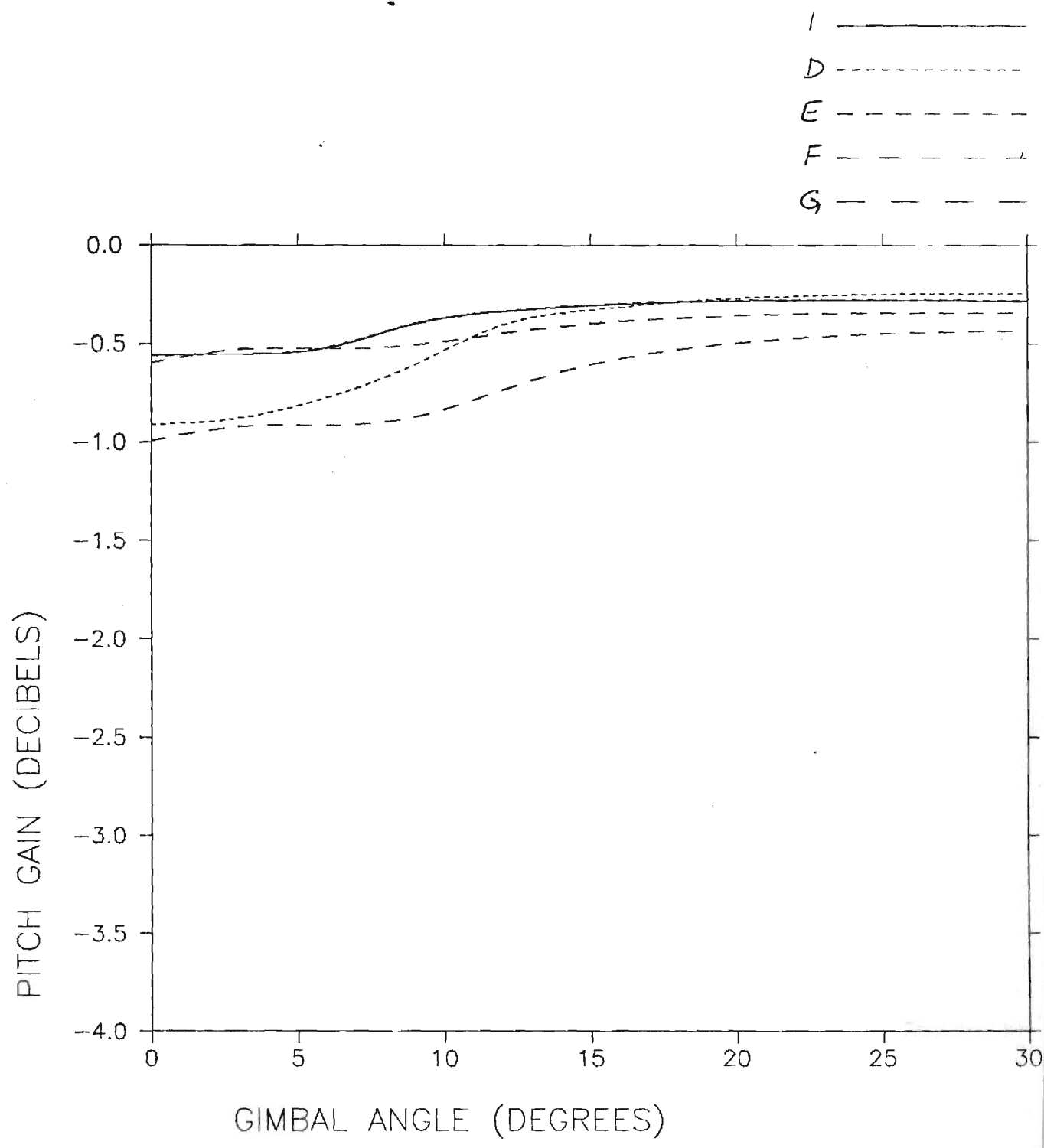
LEGEND

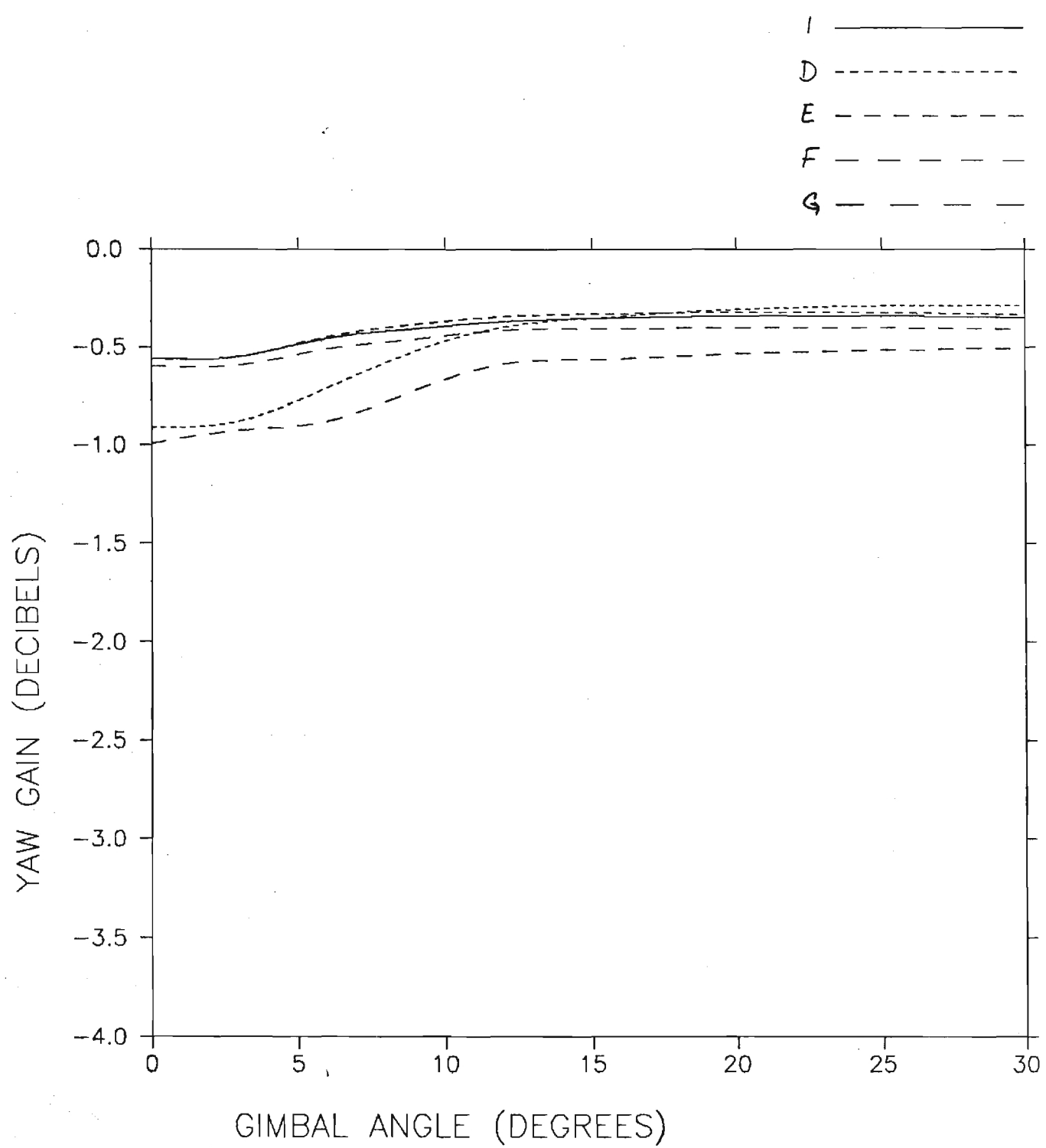
I —————
D - - - - -
E - - - - -
F - - - - -
G - - - - -





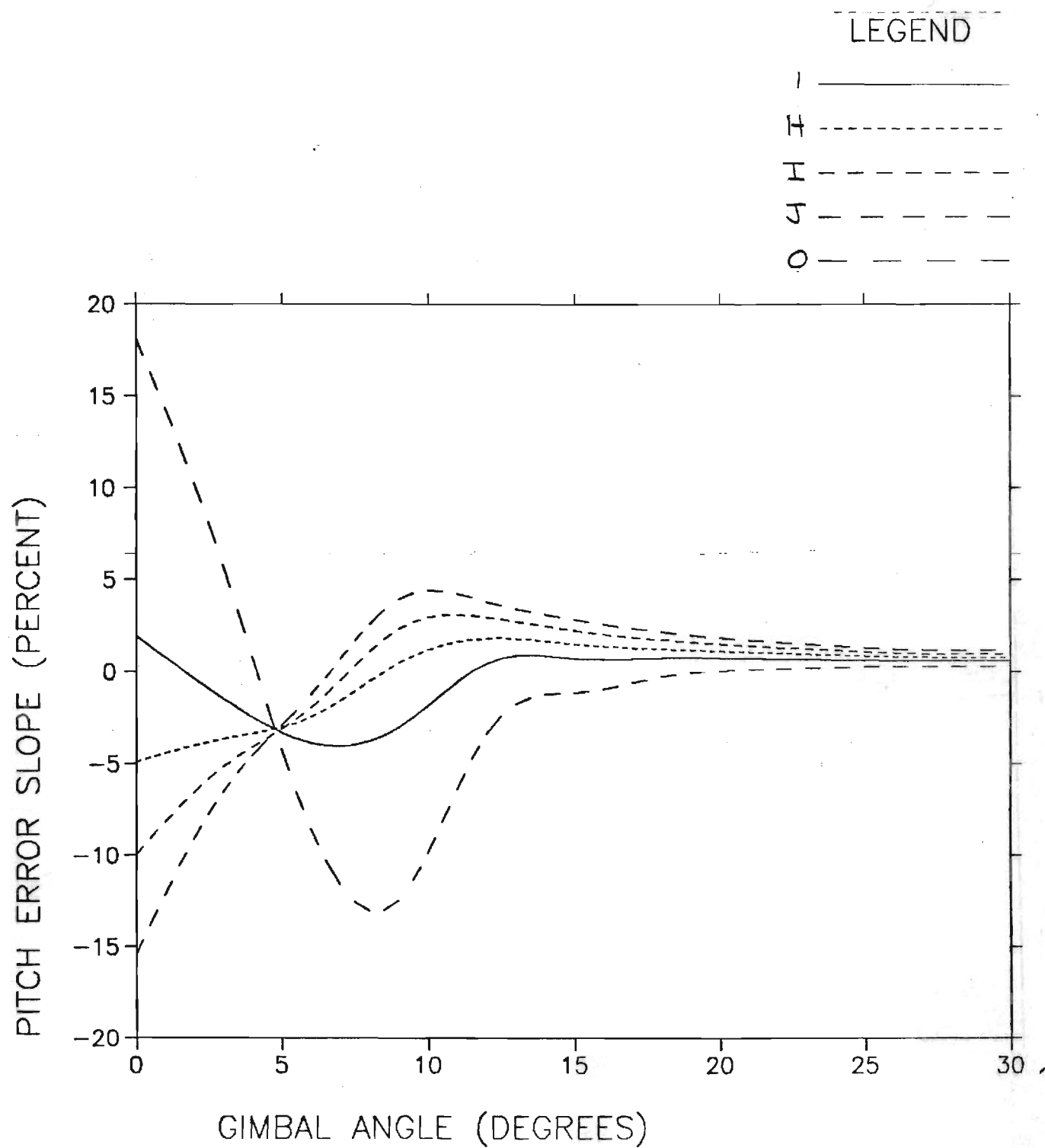


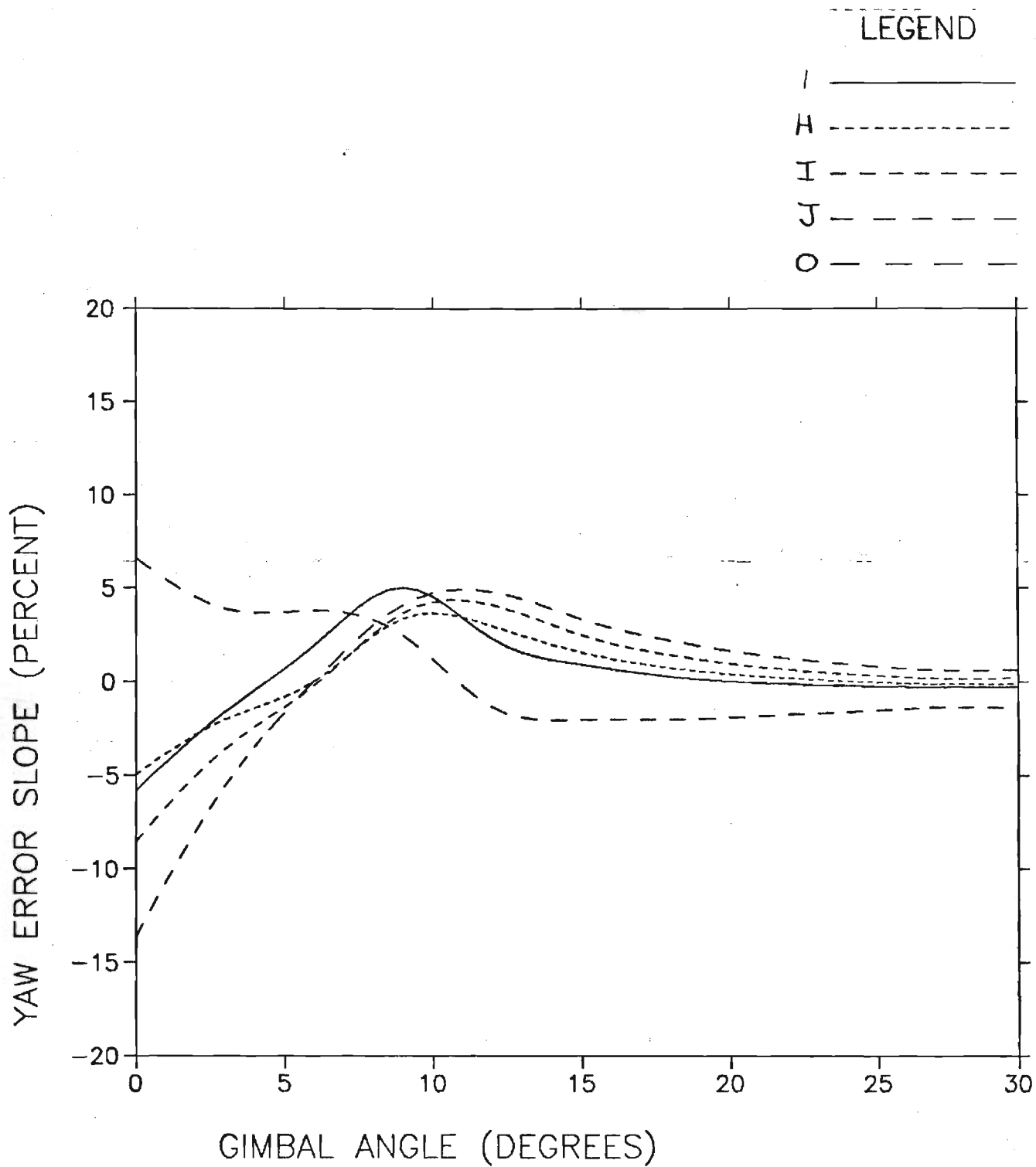


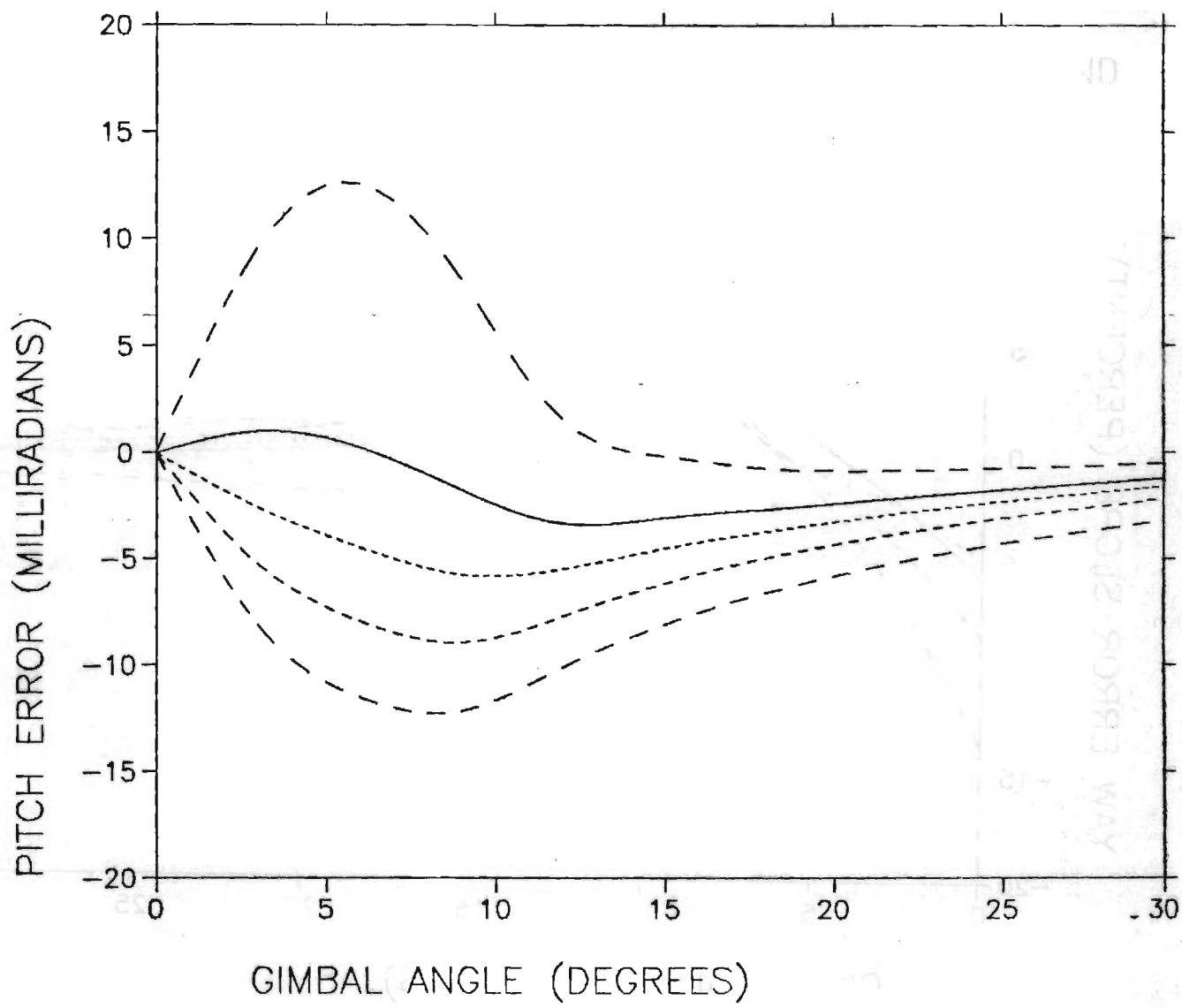


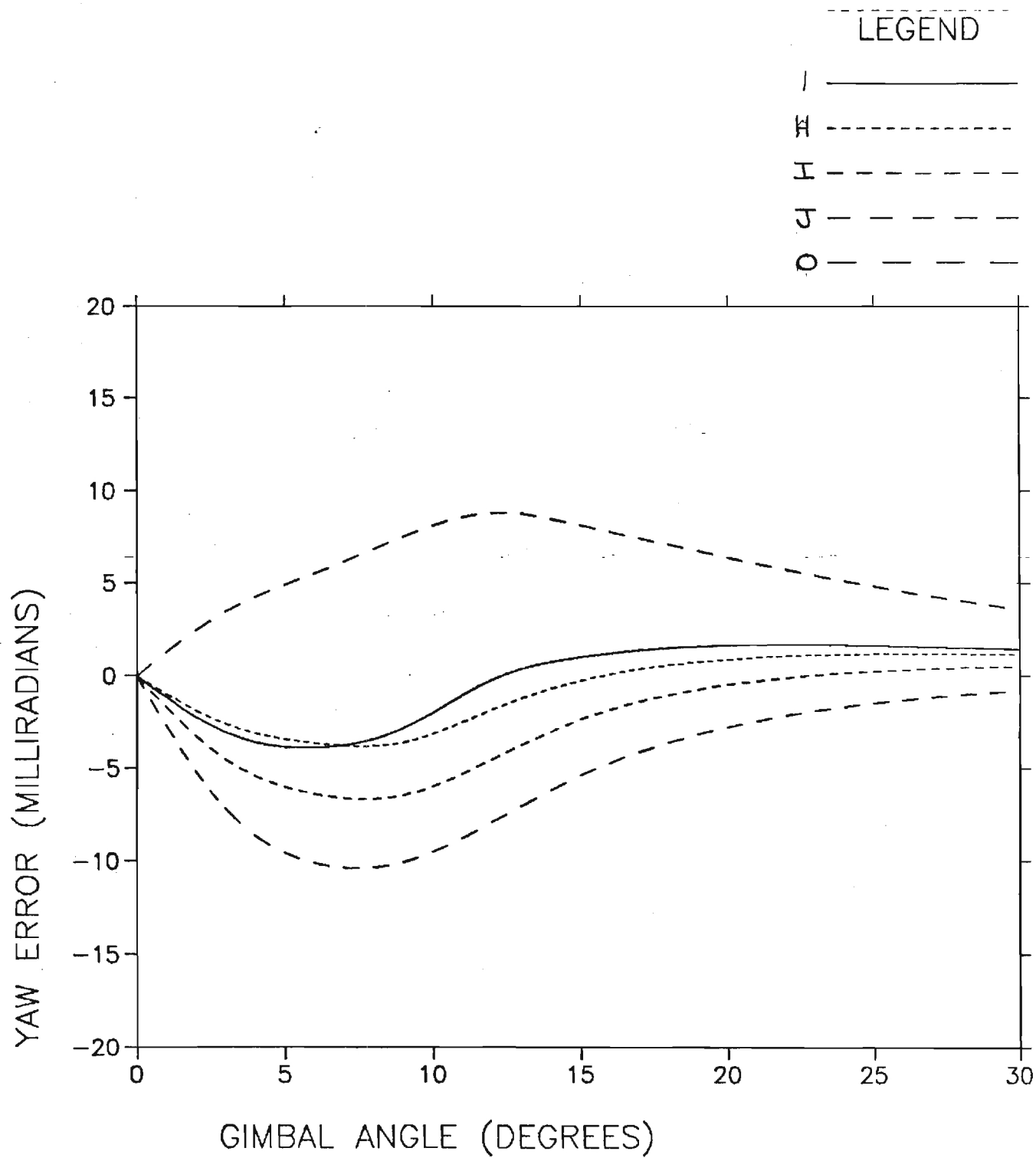
APPENDIX E

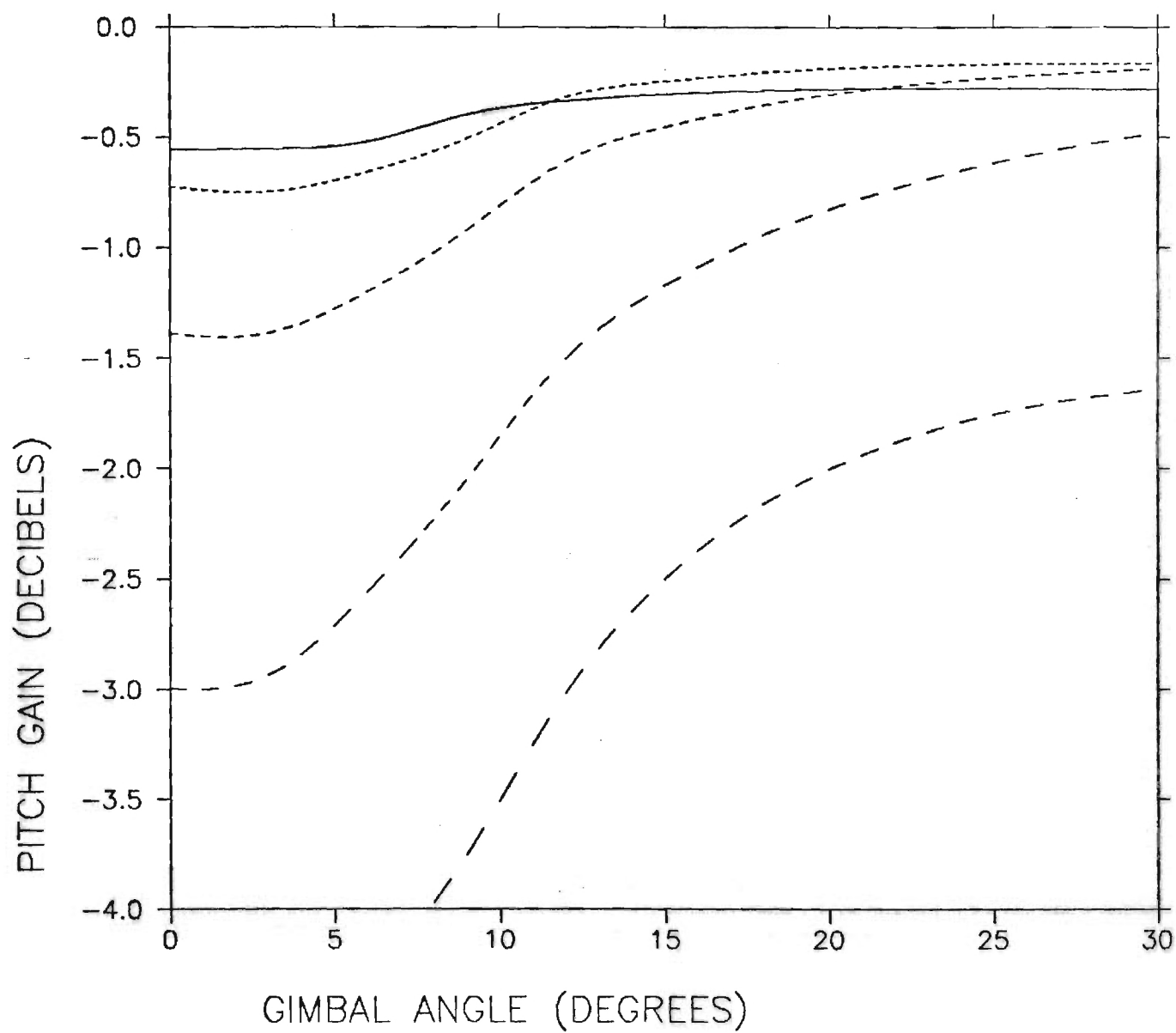
FUSED SILICA RADOME PERFORMANCE

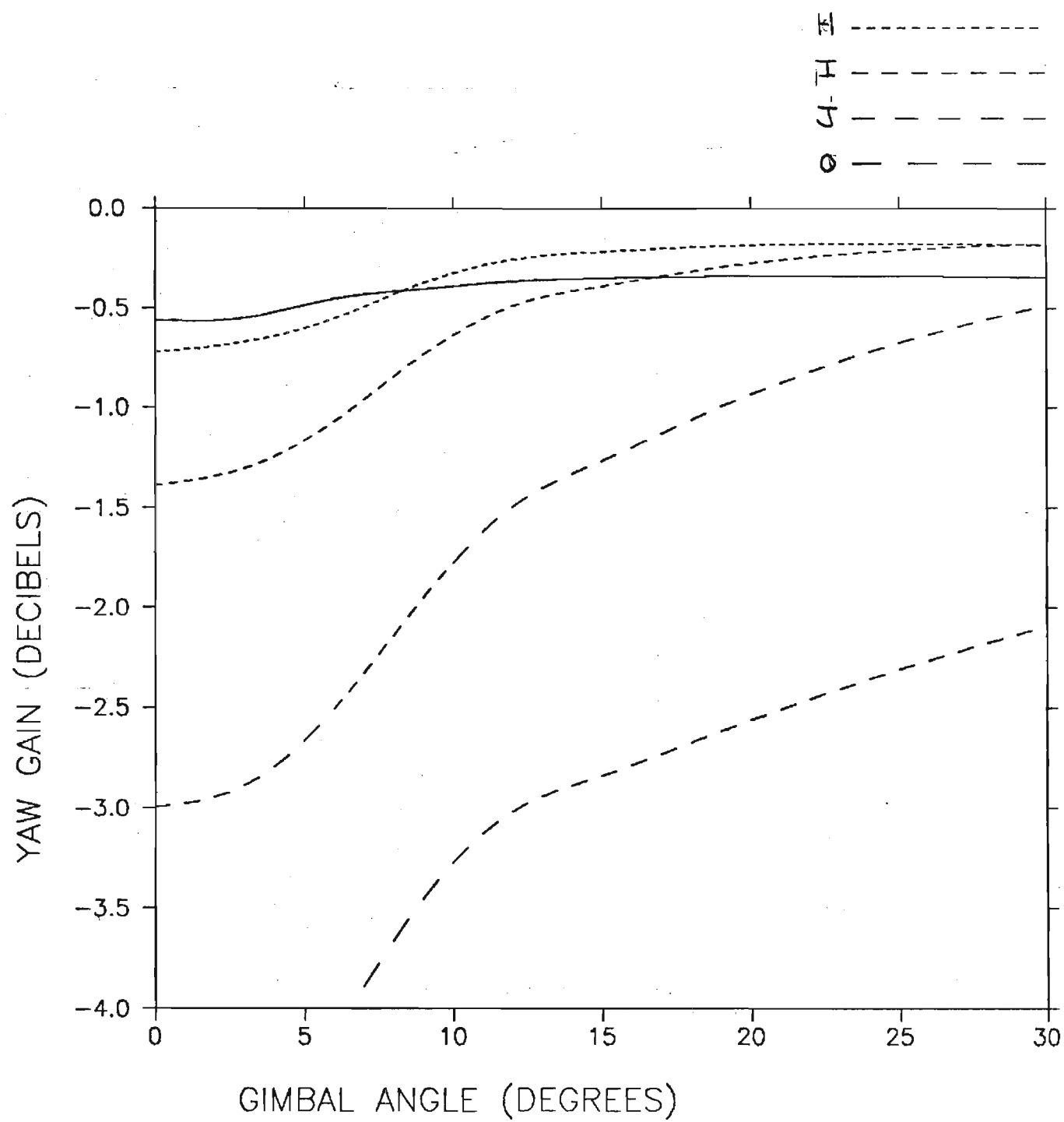












APPENDIX F

EFFECTS OF DISTANCE ON BSE ALGORITHMS

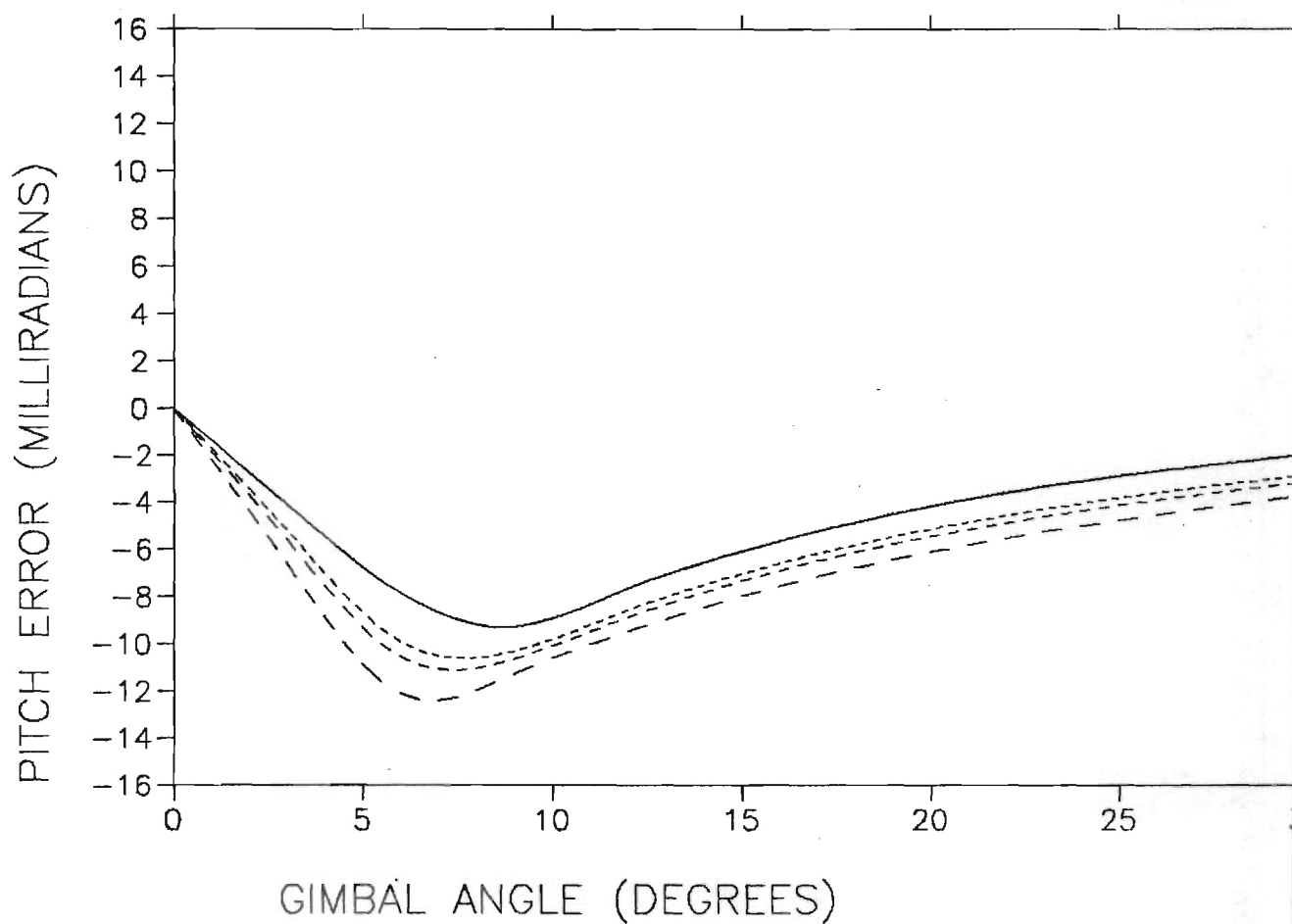
LEGEND

NULL SKR, $R=\infty$

" $R=40'$, 100dB

" $R=30'$, 100dB

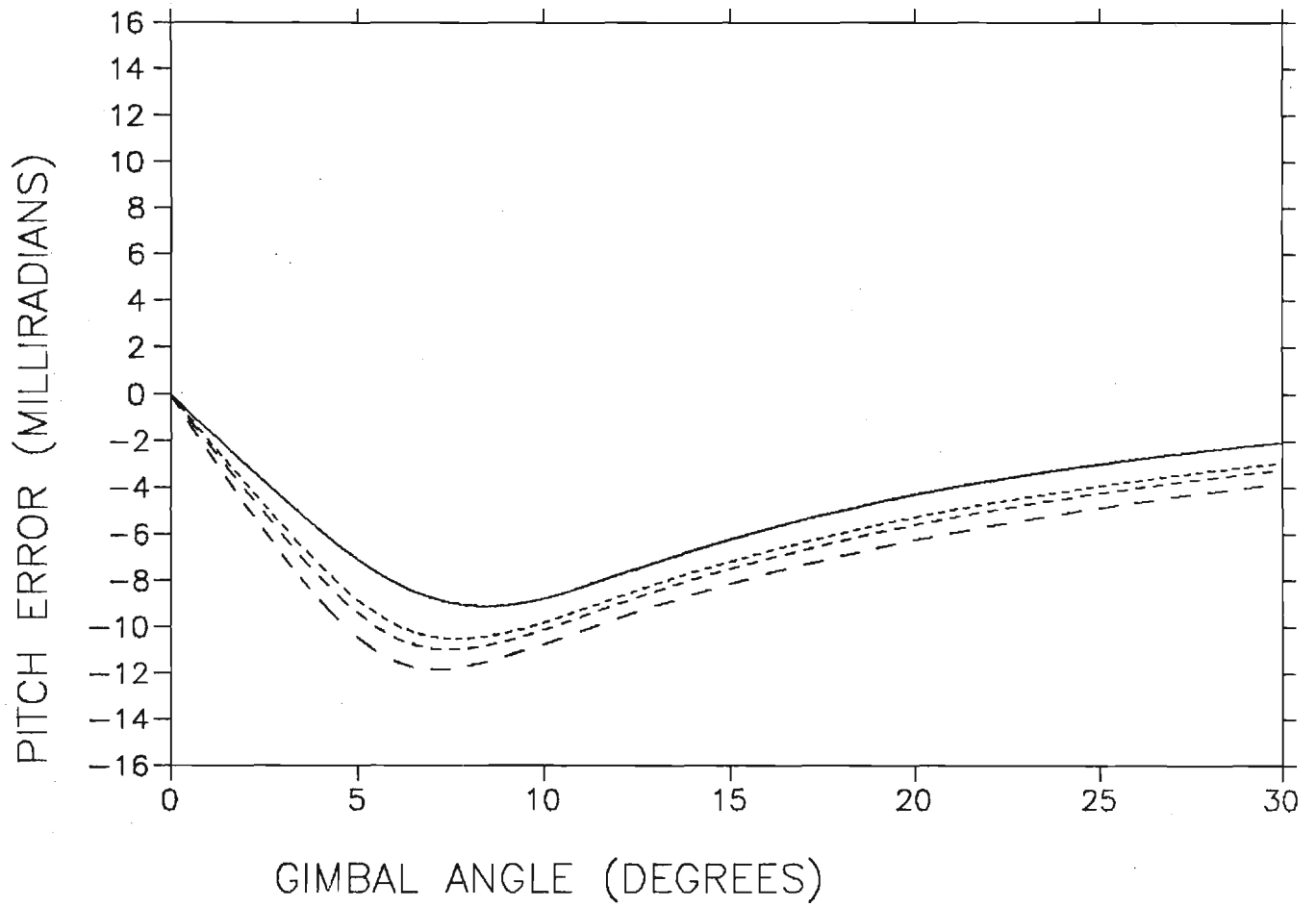
" $R=20'$, 100dB



PITCH FGHZ, LET2, 20 FT, 100DBREF, 16X16 AUT, .500 SUB., .250 ABL. 7-17-83

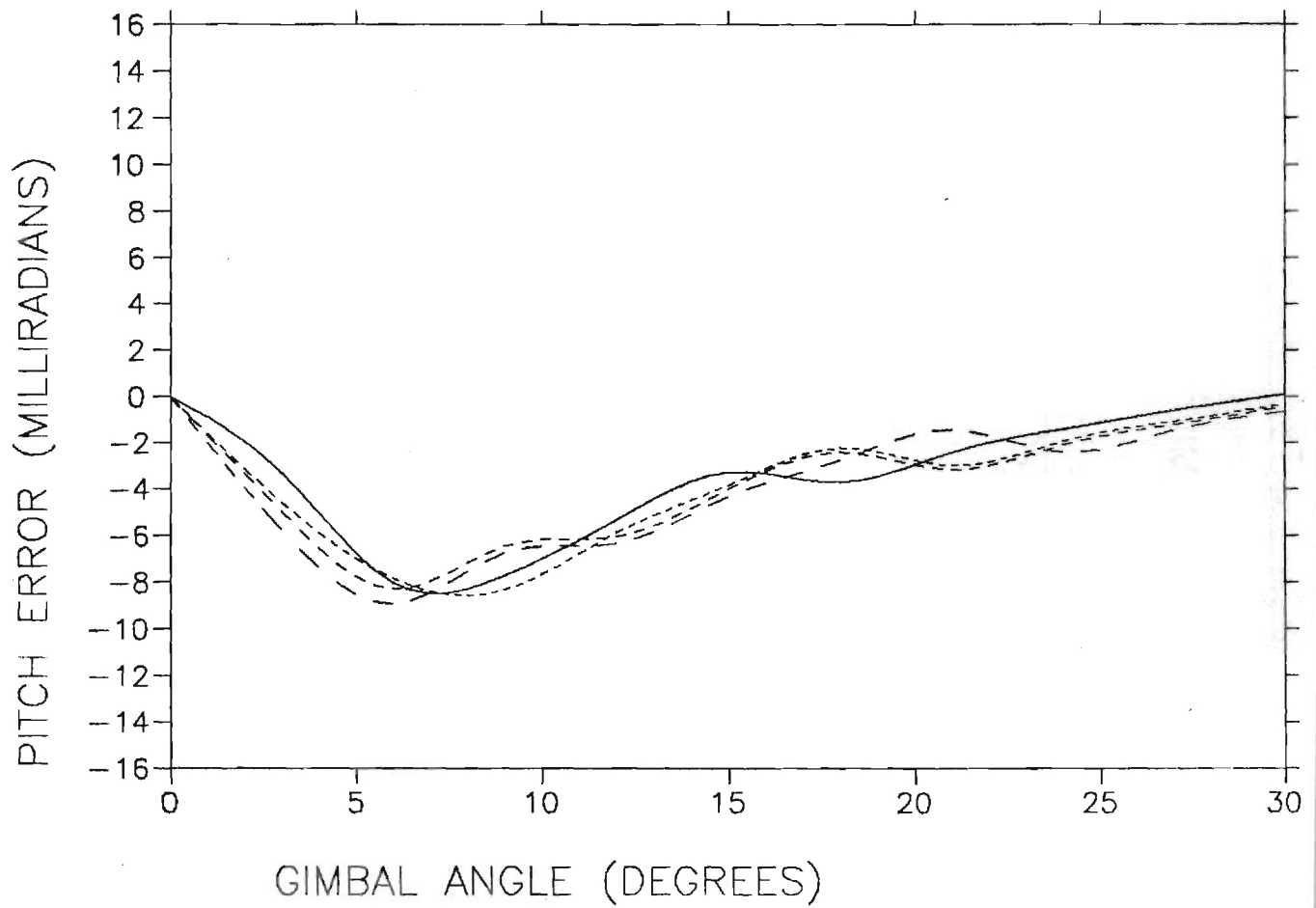
LEGEND

2-POINT, $R=\infty$
 " $R=40'$, 100dB
 " $30'$
 " $20'$



LEGEND

- 1-POINT, $R=\infty$
- " $R=46'$, 100dB
- " $R=30'$, 100dB
- " $R=20'$, 100dB



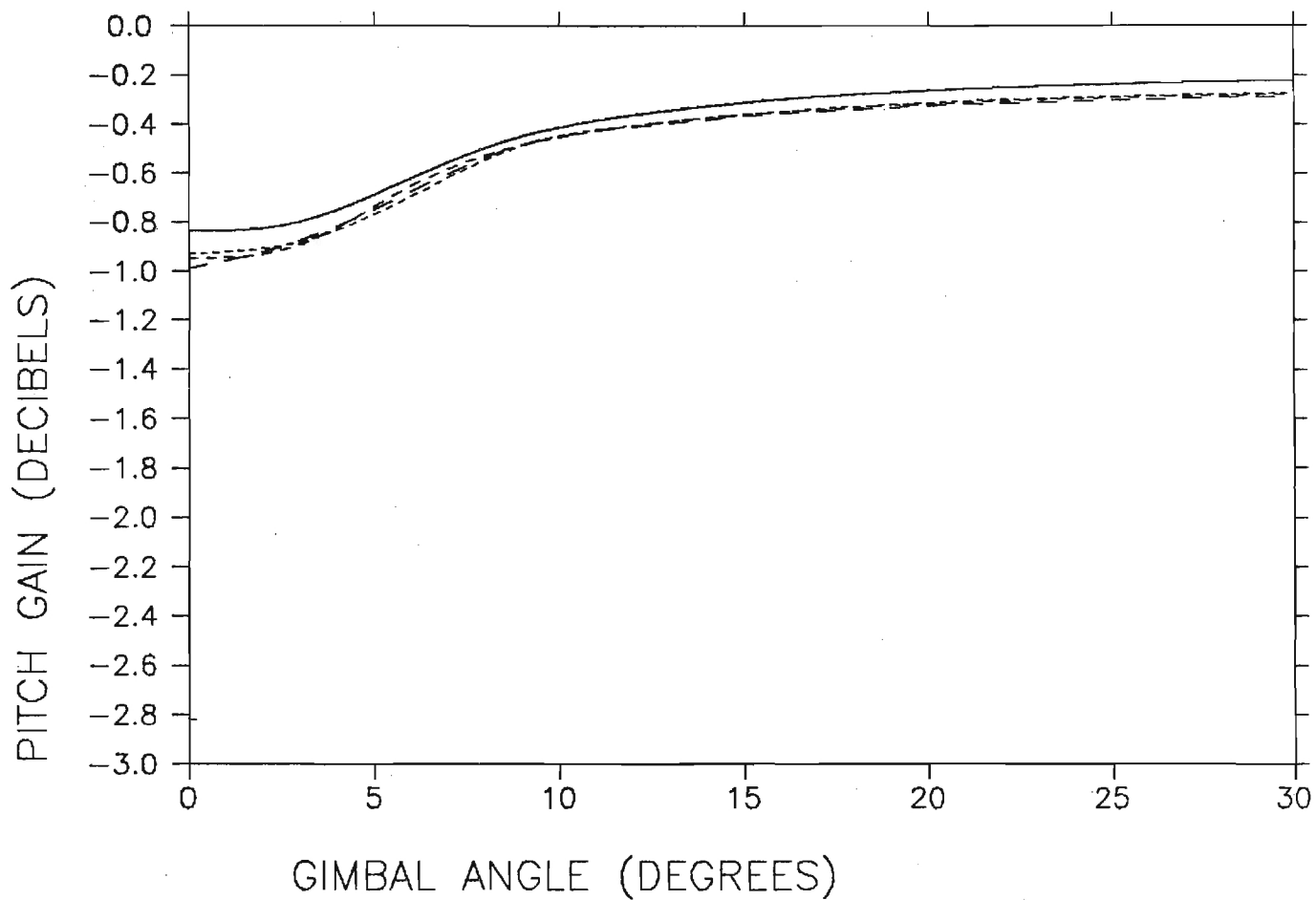
LEGEND

NULL SKIR, $R=\infty$

" $R=40'$, 100dB

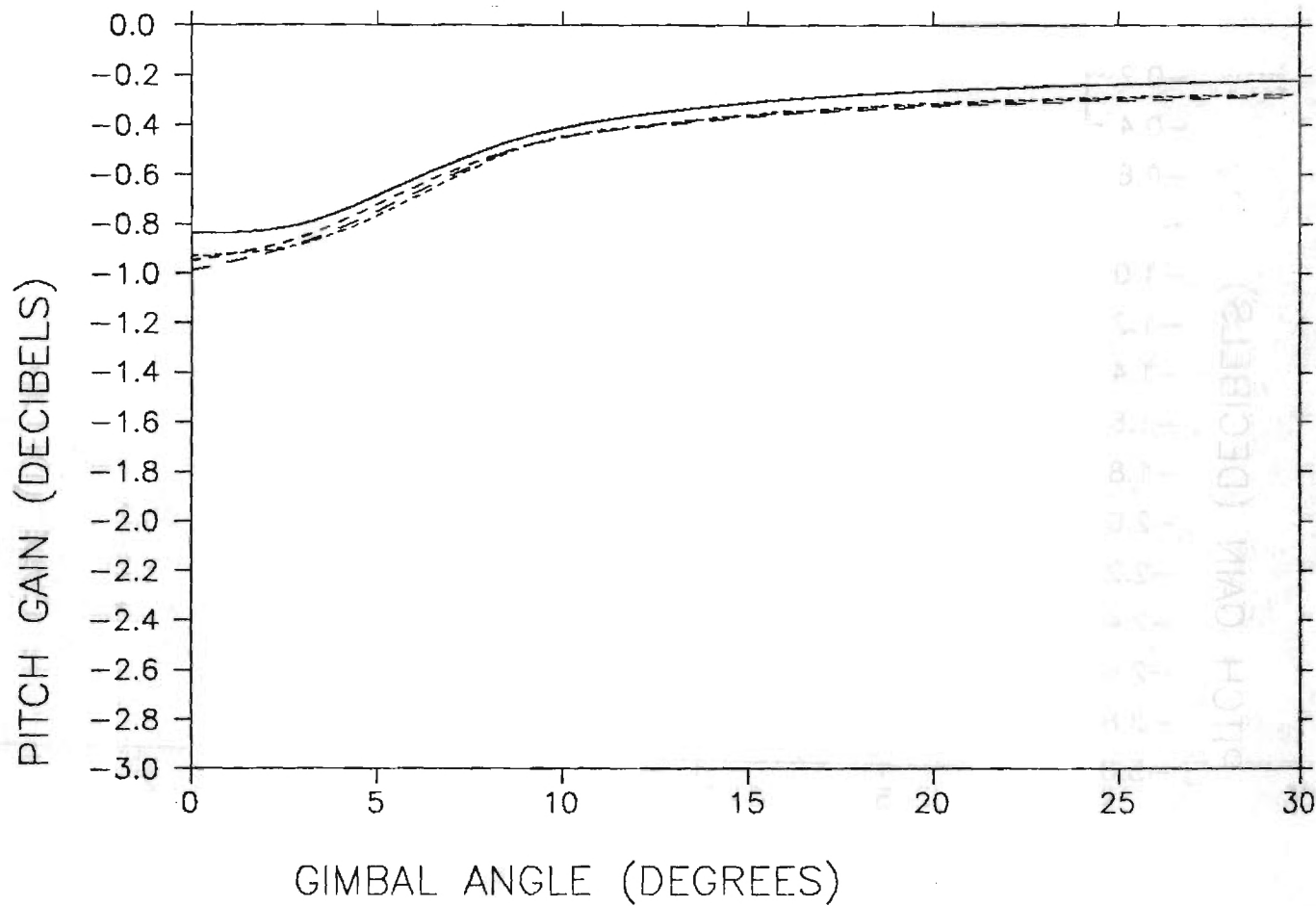
" $R=30'$, 100dB

" $R=20'$, 100dB



LEGEND

2-Point, $R=\infty$
 " 100dB, $R=40'$
 " $R=30'$
 " $R=20'$



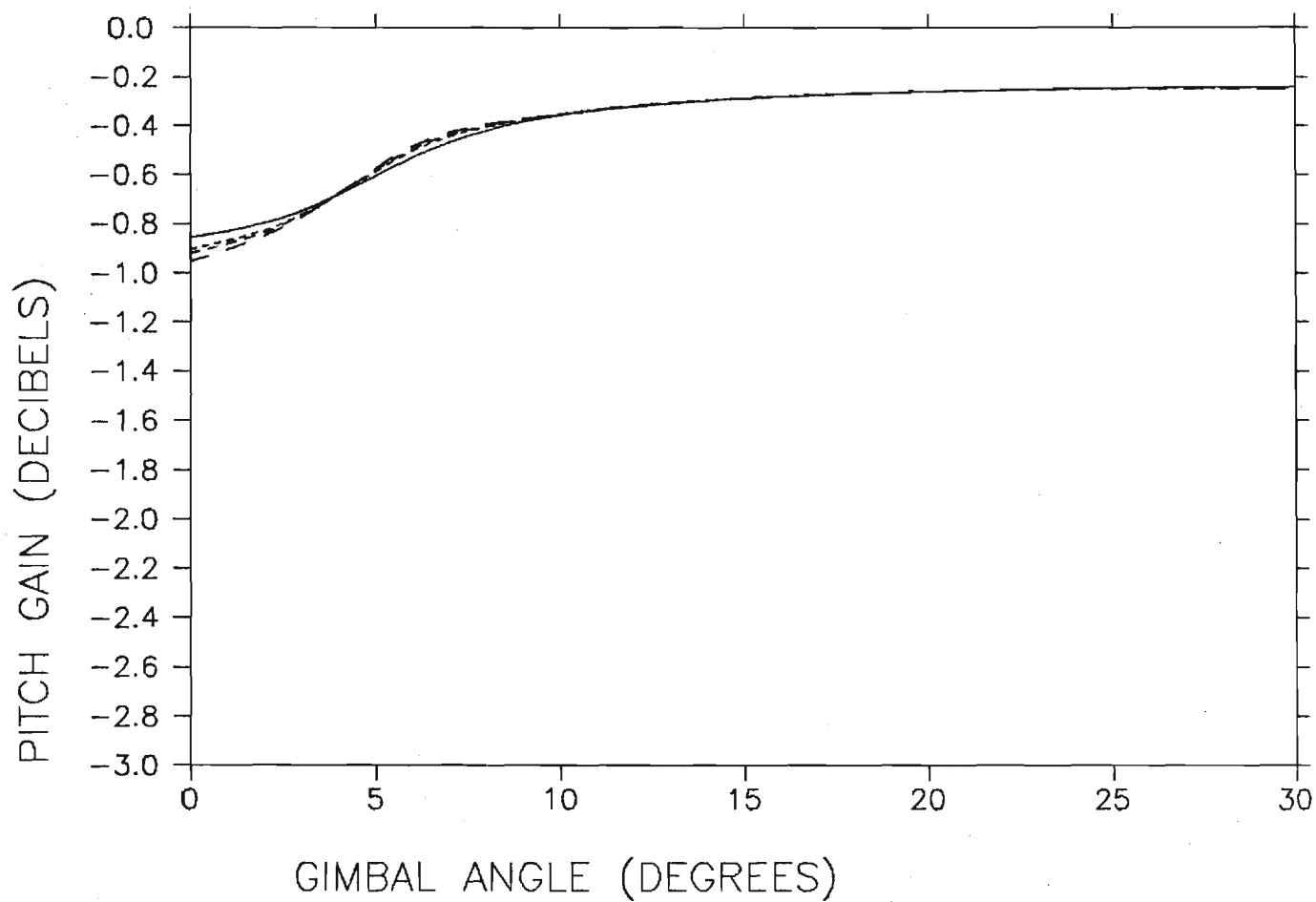
LEGEND

1-POINT, $R=\infty$

" $R=40'$, 100dB

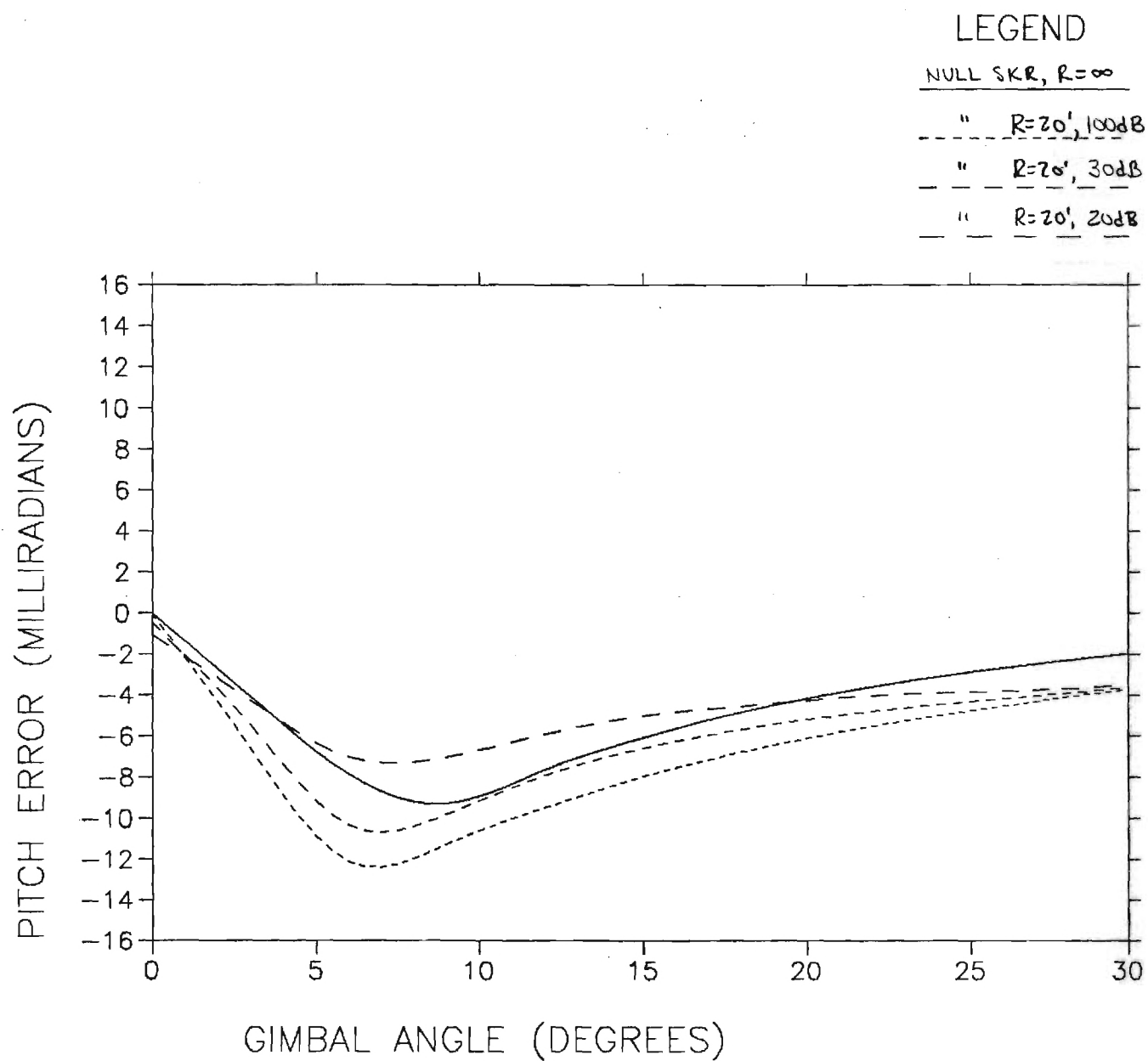
" $R=30'$, 100dB

" $R=20'$, 100dB



APPENDIX G

EFFECTS OF REFLECTIONS ON BSE ALGORITHMS



PITCH FGHZ, LET2, 20 FT, 20DBREF, 16X16 AUT, .500 SUB., .250 ABL. 7-17-83

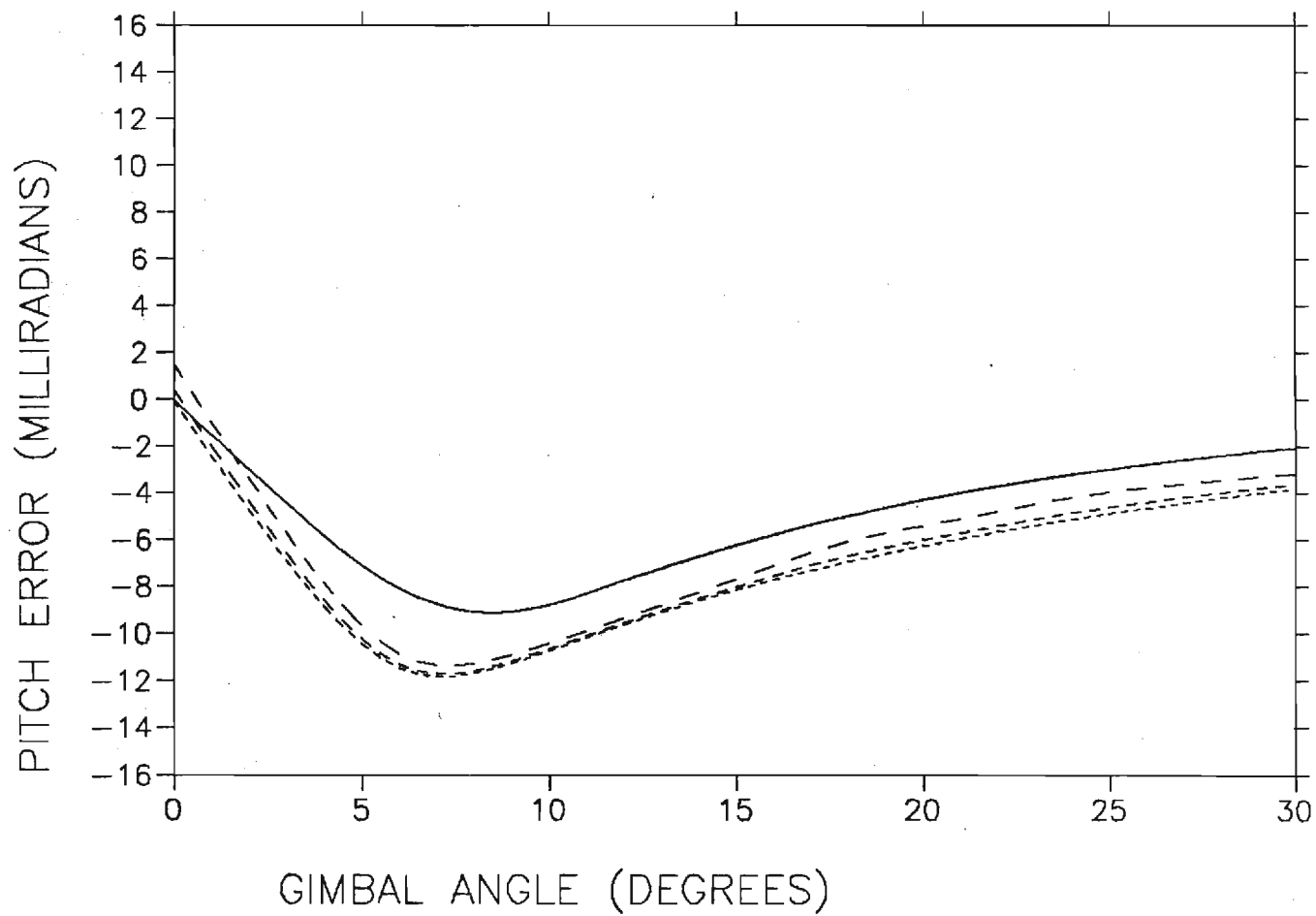
LEGEND

Z-POINT, $R=\infty$

" $R=20'$, 100dB

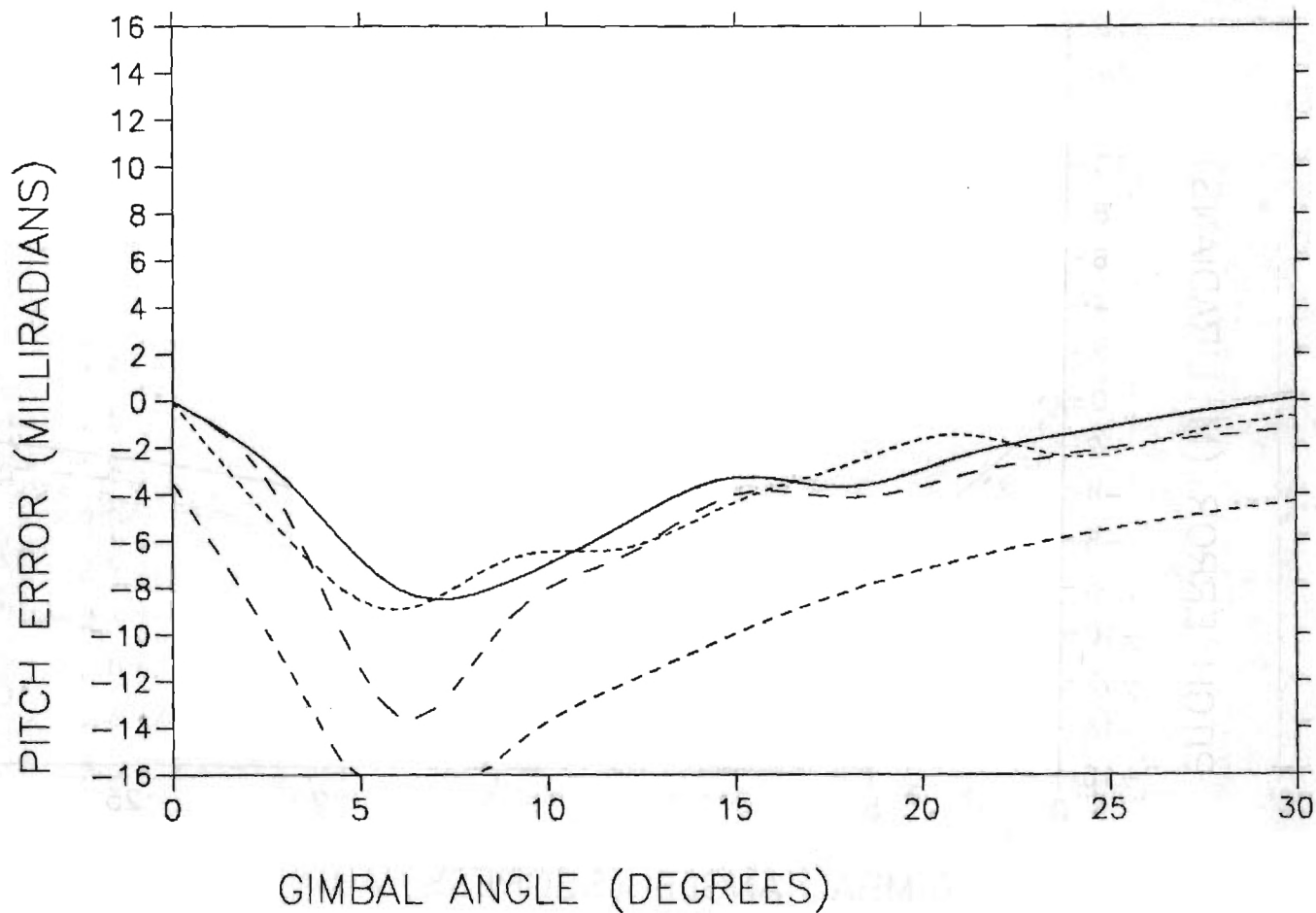
$R=20'$, 30dB

$R=20'$, 20dB



LEGEND

- 1-POINT, $R=\infty$
- 1-POINT, $R=20'$, 100dB
- 1-POINT, $R=20'$, 30dB
- " $R=20'$, 20dB



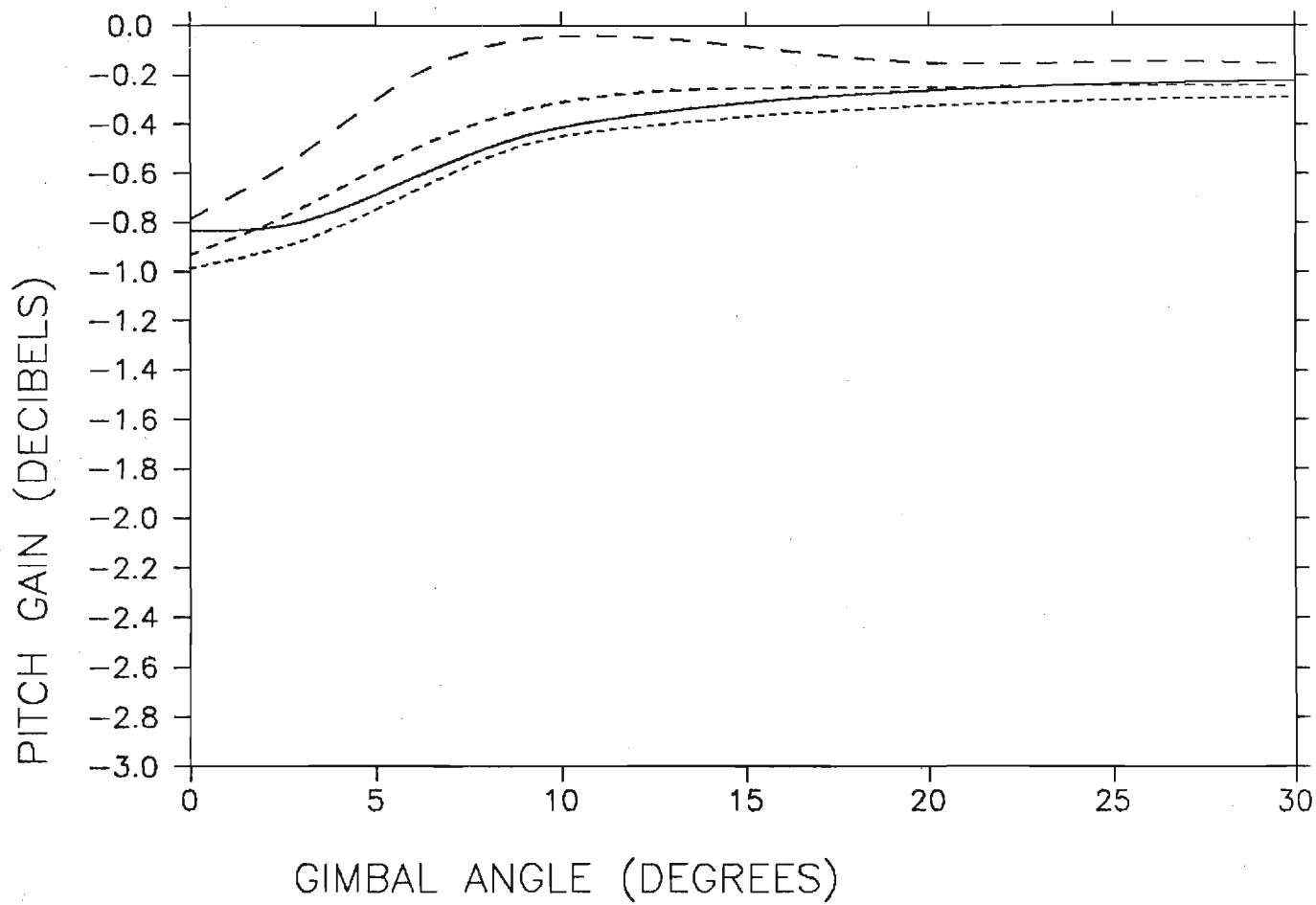
LEGEND

NULL SKR, $R=\infty$

" $R=20'$, 100dB

" $R=20'$, 30dB

" $R=20'$, 20dB



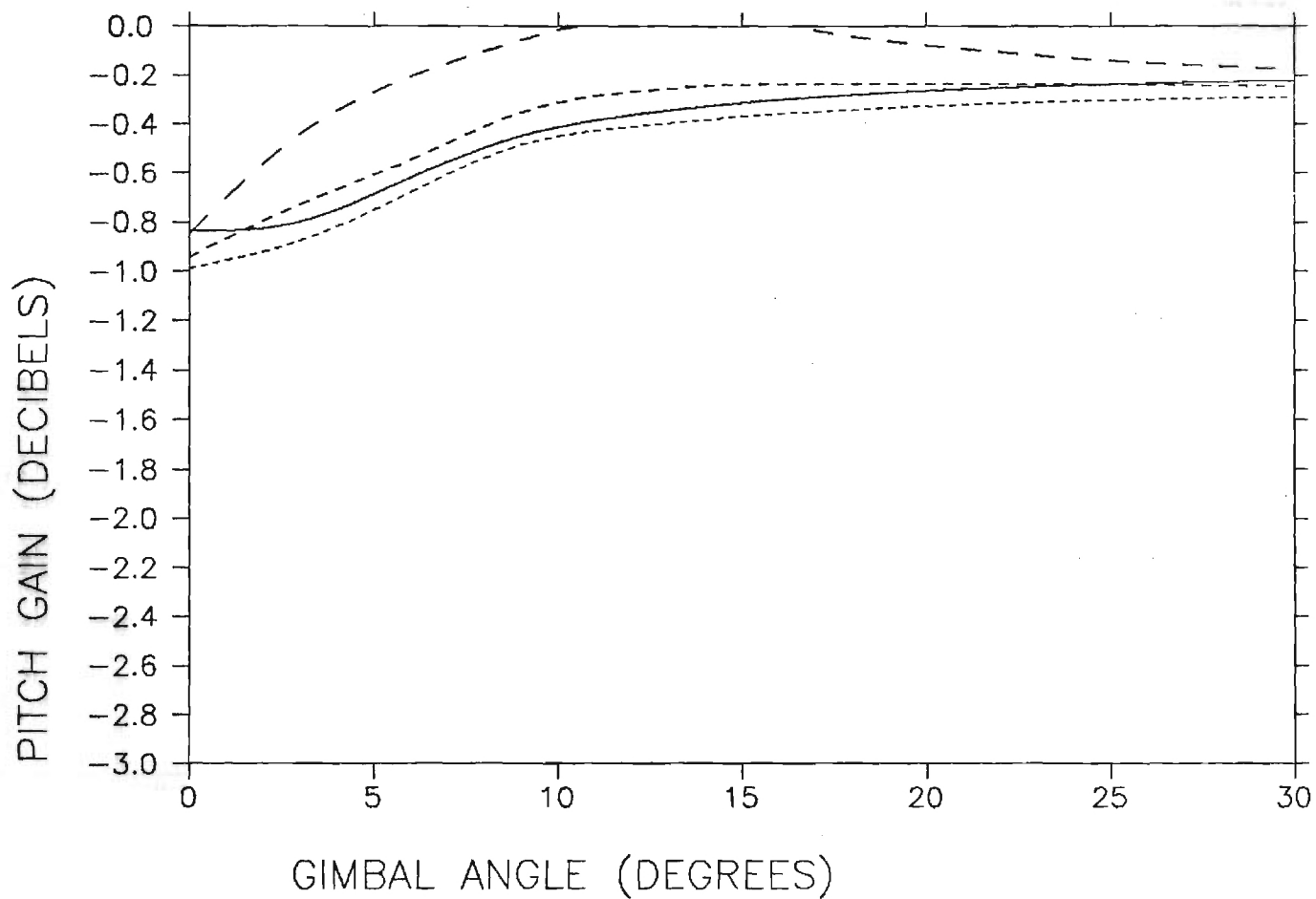
LEGEND

Z-Point, $R=\infty$

" $R=20'$, 100dB

" " 30dB

" " 20dB



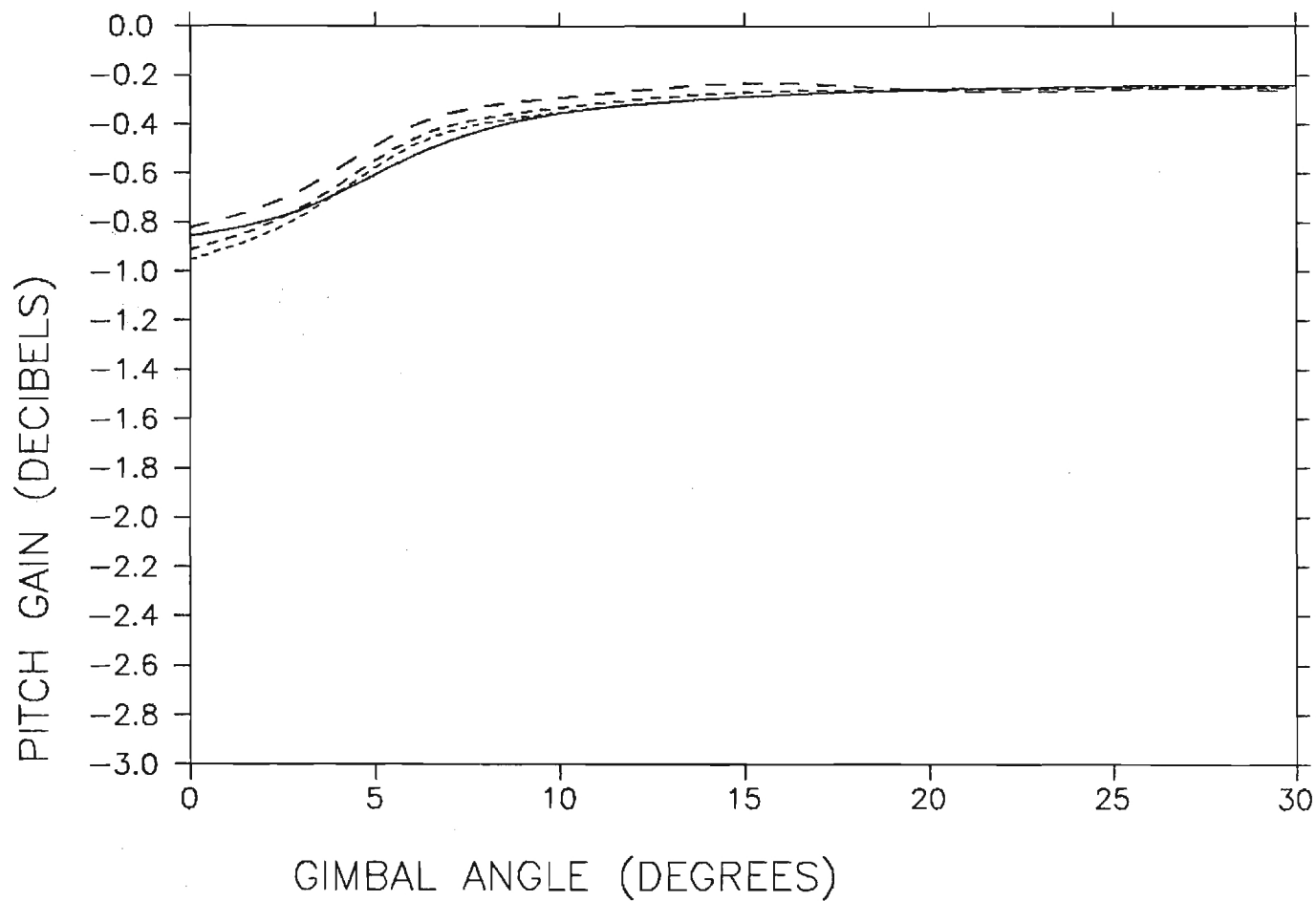
LEGEND

1-Point, $R=\infty$

" $R=20'$, 100dB

" $R=20'$, 3dB

" $R=20'$, 20dB





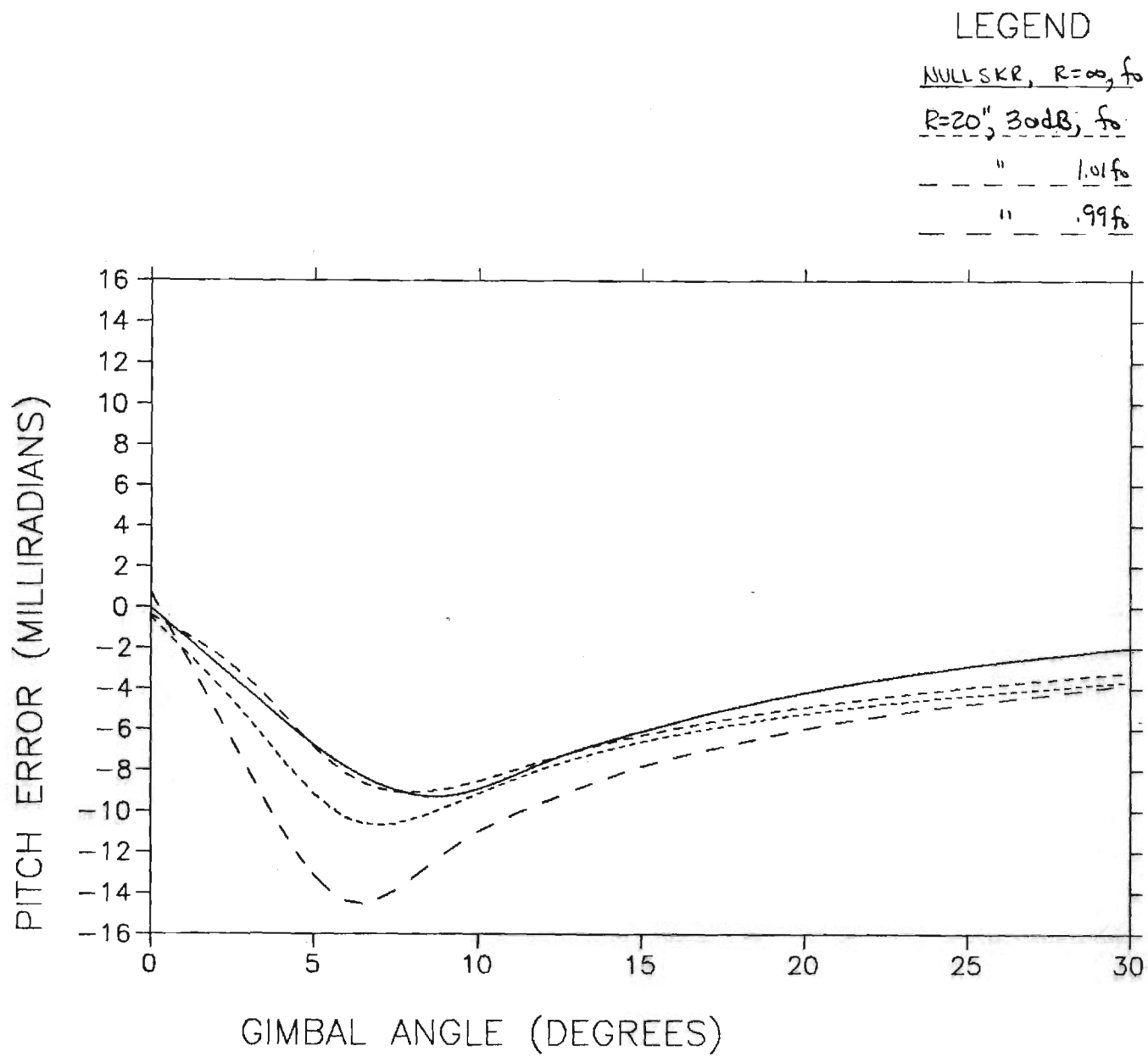
0 1 2 3 4 5 6 7 8 9 10 11 12 13 14 15 16 17 18 19 20 21 22 23 24 25 26 27 28 29 30 31 32 33 34 35 36 37 38 39 40 41 42 43 44 45 46 47 48 49 50 51 52 53 54 55 56 57 58 59 60 61 62 63 64 65 66 67 68 69 70 71 72 73 74 75 76 77 78 79 80 81 82 83 84 85 86 87 88 89 90 91 92 93 94 95 96 97 98 99

PLUCK (CM) (DECIBELS)



APPENDIX H

EFFECTS ON FREQUENCY ON BSE ALGORITHMS



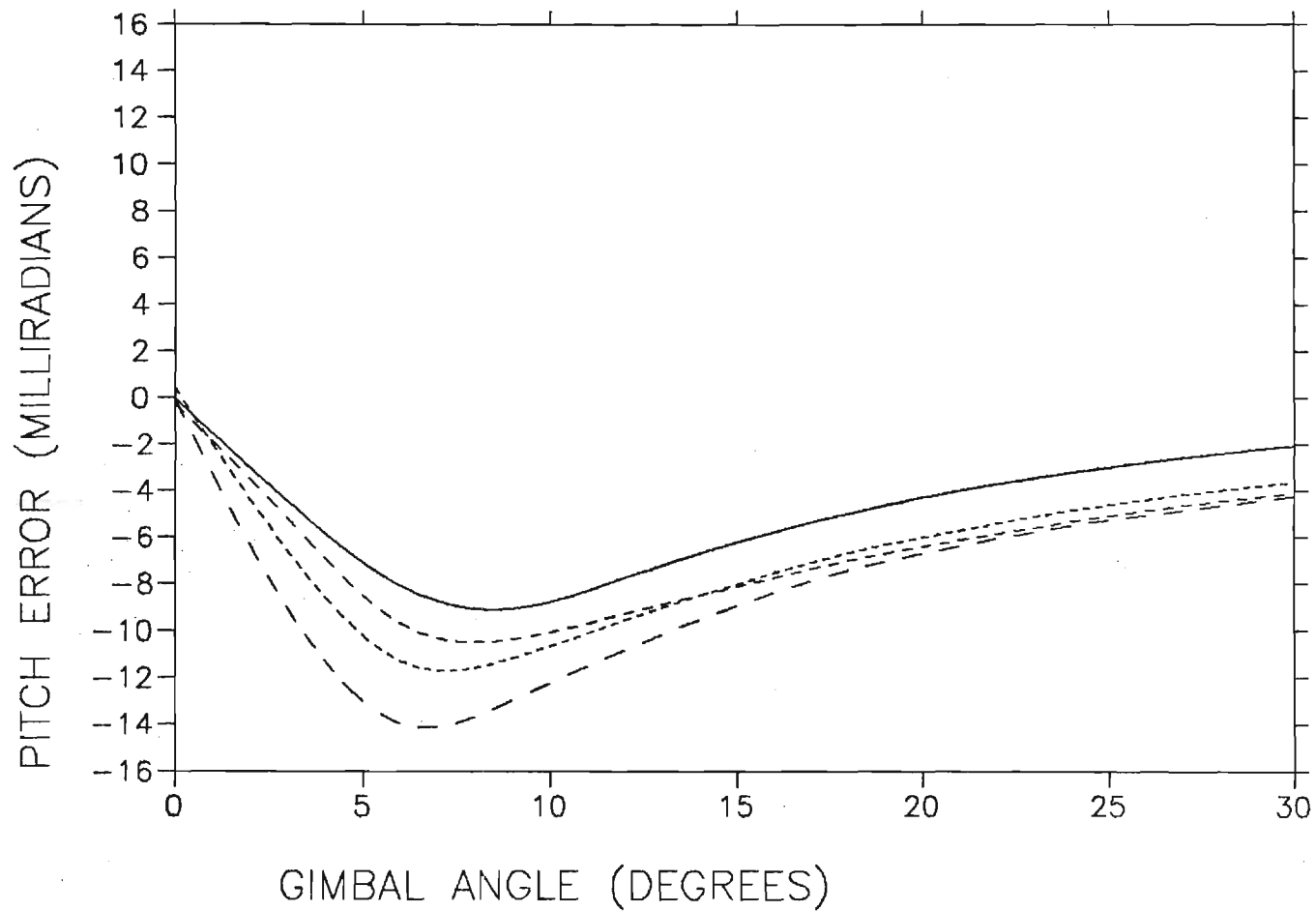
LEGEND

2-Point, $R=\infty$, f_0

" $R=20', 30d8, f_0$

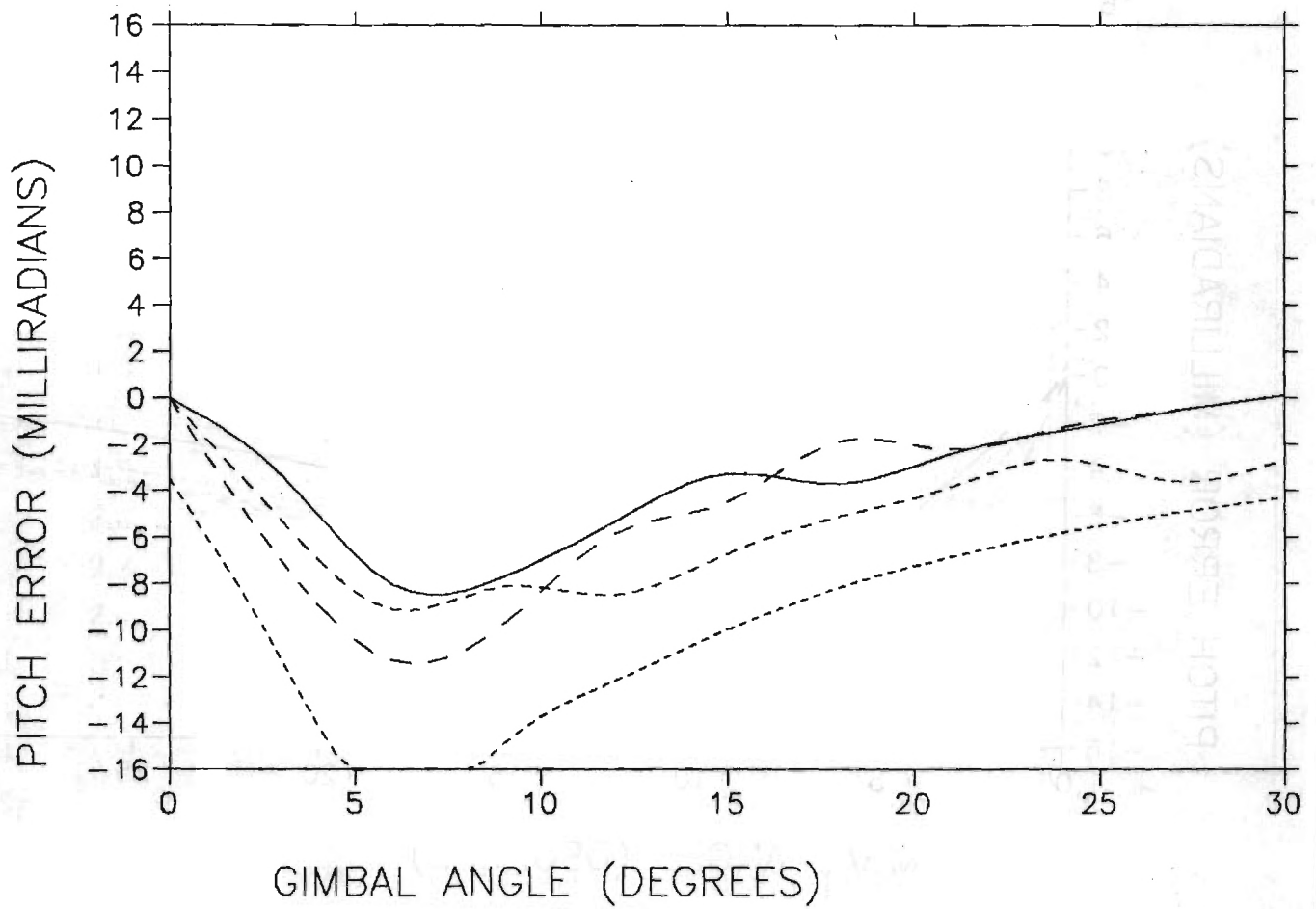
" $1.01f_0$

" $.99f_0$



LEGEND

1-Point, $R=\infty$, f_0
 " $R=20'$, 30dB, f_0
 " $1.01f_0$
 " $.99f_0$



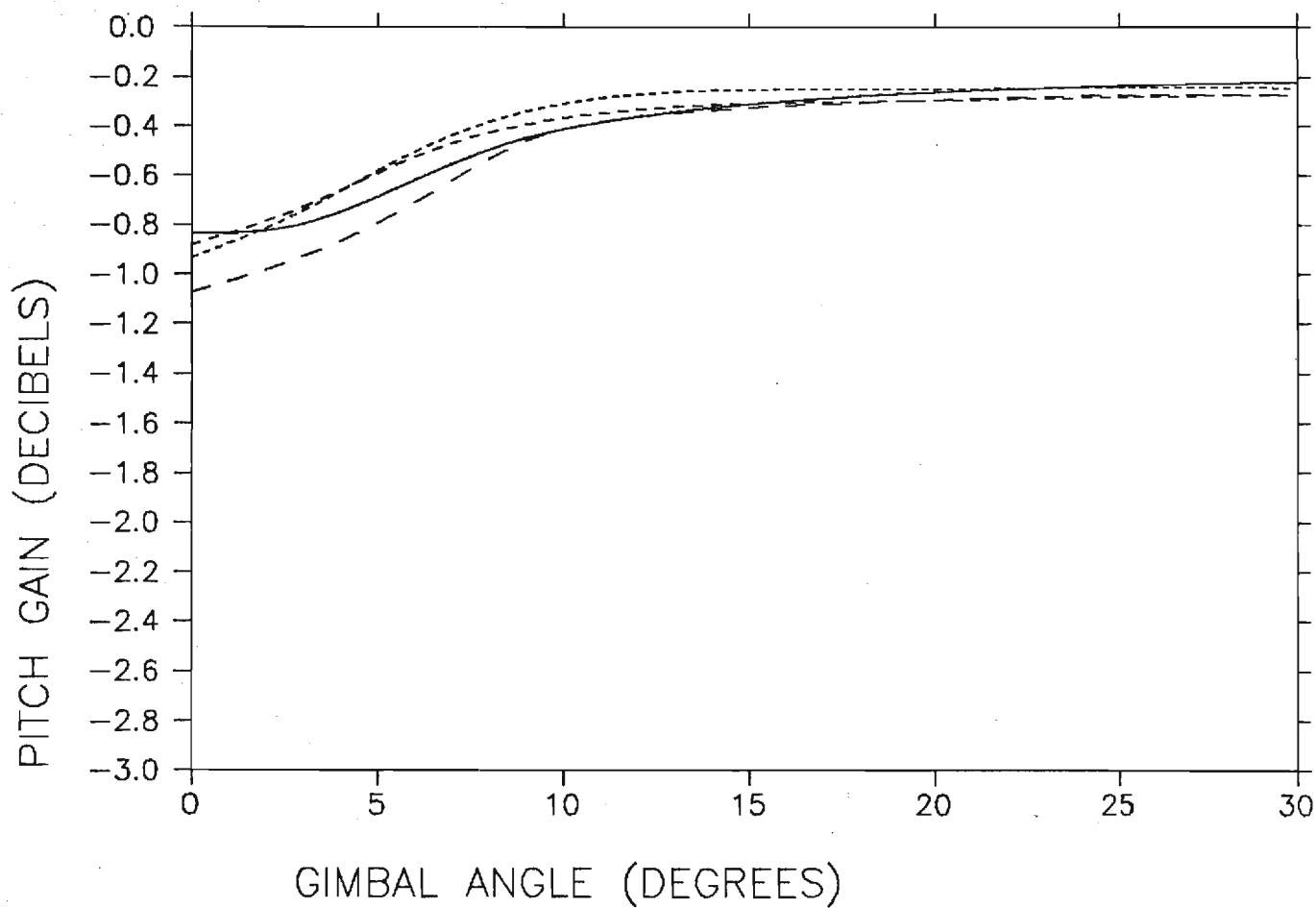
LEGEND

NULLSKR, $R=\infty$, f_0

" $R=20'$, 30dB, f_0

" $1.01 f_0$

" $.99 f_0$



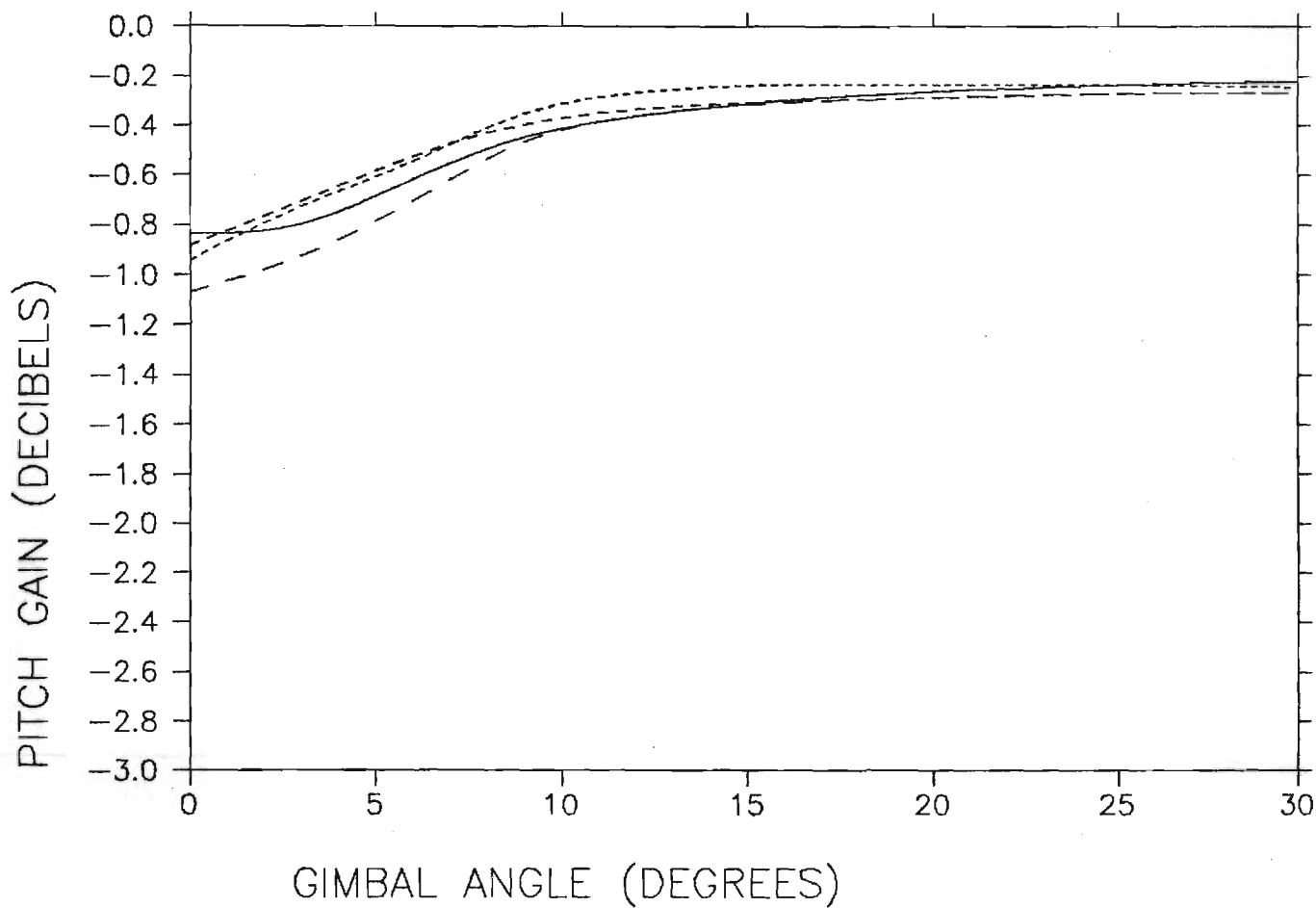
LEGEND

Z-Point, $R=\infty$, f_0

" $R=20'$, 3dB , f_0

" $1.0 f_0$

" $.99 f_0$



LEGEND

1-Point, $R=\infty$, f_0

" $R=20$, 20dB, f_0

" $1.01f_0$

" $.99f_0$

